IDENTIFICATION OF LEFT VENTRICULAR MASS QTL IN THE STROKE-PRONE SPONTANEOUSLY HYPERTENSIVE RAT

This being a thesis submitted for the degree of Doctor of Philosophy in the Faculty of Medicine, University of Glasgow

©Kirsten Gilday B.Sc. Hons (University of Glasgow), M.Sc. (University of Glasgow)

University of Glasgow
Division of Cardiovascular & Medical Sciences
BHF Glasgow Cardiovascular Research Centre
126 University Place
Glasgow
G12 8TA

Oct, 2006

DECLARATION

I declare that this thesis has been written entirely by myself and has not been submitted previously for a higher degree. The work recorded has been carried out by me under the supervision of Professor Anna Dominiczak and Dr Delyth Graham, unless stated otherwise in acknowledgements.

.....

KIRSTEN GILDAY

ACKNOWLEDGEMENTS

I would like to express my sincere appreciation to my supervisors Dr Delyth Graham and in particular Professor Anna F Dominiczak, for their constant support, guidance and help throughout the course of my study for this thesis.

I would also like to thank Dr Barrie Condon and the technical staff at 7T MRI unit, Garscube. I am also very grateful to Drs Martin McBride and Wai Kwong Lee for their teaching in molecular techniques and advice throughout and Dr John McClure for statistical direction and help in analysing large volumes of data.

Finally and most importantly, this thesis would not have been possible without the constant support and encouragement from my family, in particular my husband, without whom I would not have been able to accomplish a higher education.

CONTENTS

		PAGE
DECLARATION		**ii**
ACKNOWLEDGEMENTS		**iii**
CONTENTS		**iv**
LIST OF TABLES		**vii**
LIST OF FIGURES		**ix**
ABBREVIATIONS		**xii**
SUMMARY		**xv**
1	**CHAPTER 1 INTRODUCTION**	
1.1	COMPLEX CARDIOVASCULAR TRAITS	1
1.1.1	BLOOD PRESSURE: REGULATION AND MAINTENANCE	3
1.1.2	HUMAN ESSENTIAL HYPERTENTION	6
1.1.3	LEFT VENTRICULAR HYPERTROPHY (LVH)	11
1.2	EVIDENCE FOR GENETIC EFFECTS	14
1.2.1	MENDELIAN FORMS OF HYPERTENSION	14
1.2.2	MENDELIAN FORMS OF CARDIAC HYPERTROPHY	18
1.2.3	HUMAN STUDIES OF HYPERTENSION	20
1.2.4	HUMAN STUDIES OF LVH	22
1.3	EXPERIMENTAL ANIMAL MODELS	25
1.3.1	ANIMAL MODELS OF CARDIOVASCULAR DISEASE	25
1.3.2	MOUSE MODELS FOR CARDIOVASCULAR DISEASE	25
1.3.3	RAT MODELS OF HYPERTENSIVE CARDIOVASCULAR DISEASE	26
1.3.4	THE STROKE-PRONE SPONTANEOUSLY HYPERTENSIVE RAT	27
1.3.5	STUDIES IN ANIMAL MODELS	29
1.3.6	GENDER DIFFERENCES	33
1.4	GENETIC MARKERS/MAPS	35
1.4.1	GENOME WIDE QTL ANALYSIS	35
1.4.2	COMPARATIVE GENOME ANALYSIS	39
1.4.3	CANDIDATE GENE ANALYSIS	39
1.4.4	CONGENIC STRAIN AND SUBSTRAIN PRODUCTION	40

1.5	GENE EXPRESSION PROFILING	41
1.5.1	MICROARRAY ANALYSIS AND QUANTITATIVE RT-PCR	41
1.6	HIGH FIDELITY PHENOTYPING	45
1.6.1	HAEMODYNAMIC PROFILING	45
1.6.2	CARDIAC IMAGING TECHNIQUES	46
1.7	AIMS OF THE STUDY	48
2	**CHAPTER 2**	
	METHODS	
2.1	GENERAL LABORATORY PRACTICE	51
2.2	ANIMAL STRAINS	51
2.2.1	F_1 and F_2 PRODUCTION	52
2.2.2	CONGENIC STRAINS	52
2.3	PHENOTYPIC ANALYSIS	55
2.3.1	TAIL CUFF PLETHYSMOGRAPHY	55
2.3.2	RADIO-TELEMETRY	55
2.3.3	BODY AND CARDIAC MEASUREMENTS	56
2.3.4	ECHOCARDIOGRAPHY	56
2.3.5	MAGNETIC RESONANCE IMAGING (MRI)	57
2.4	GENETIC ANALYSIS	59
2.4.1	DNA EXTRACTION	59
2.4.2	POLYMERASE CHAIN REACTION (PCR)	61
2.4.3	GEL ELECTROPHORESIS USING AGAROSE GELS	62
2.4.4	GEL ELECTROPHORESIS USING POLYACRYLAMIDE GELS AND AUTORADIOGRAPHY	62
2.4.5	FLUORESCENT PCR AND ABI DNA SEQUENCER ANALYSIS	64
2.5	QTL ANALYSIS	64
2.5.1	JOINMAP VERSION 3.0	65
2.5.2	MAPMANAGER QTX VERSION B20	66
2.5.3	WINDOWS QTL CARTOGRAPHER VERSION 2.5	67
2.6	QUANTATITIVE RT-PCR	68
2.6.1	RNA EXTRACTION	68
2.6.2	DNAse TREATMENT OF RNA	69
2.6.3	QUALITY ASSESSMENT OF RNA	69
2.6.4	TWO STEP RT-PCR (TAQMAN)	69
2.7	SEQUENCING OF CANDIDATE GENES	71
2.7.1	CLEANING PCR PRODUCT	71
2.7.2	SEQUENCING PCR PRODUCT	72
2.8	MICROARRAY	73
2.8.1	TISSUE PREPARATION	73
2.8.2	TARGET HYBRIDISATION	74
2.8.3	FLUIDIC STATION AND PROBE ARRAY SETUP	75

2.8.4	DATA ANALYSIS	77
3	**CHAPTER 3**	
	IDENTIFICATION OF LEFT VENTRICULAR MASS QTL IN SHRSP	
3.1	INTRODUCTION	79
3.2	METHODS	82
3.2.1	EXPERIMENTAL ANIMALS AND GENETIC CROSSES	82
3.2.2	GENOTYPING, IMPROVED GENETIC LINKAGE MAP AND QTL ANALYSIS	83
3.3	RESULTS	99
3.4	DISCUSSION	98
4	**CHAPTER 4**	
	COMPARATIVE MAPPING AND IDENTIFICATION OF CANDIDATE GENES	
4.1	INTRODUCTION	104
4.2	METHODS	106
4.2.1	COMPARATIVE MAPPING	106
4.2.2	PHARMACOLOGICAL INTERVENTION	106
4.2.3	RNA EXTRACTION AND cDNA SYNTHESIS	106
4.2.4	REAL-TIME PCR QUANTIFICATION	107
4.2.5	SEQUENCING CANDIDATE GENES	107
4.2.6	SEQUENCE ANALYSIS	110
4.2.7	SNP GENOTYPING	110
4.3	RESULTS	110
4.4	DISCUSSION	126
5	**CHAPTER 5**	
	MRI AS A METHOD FOR *IN VIVO* LV QUANTIFICATION AND GEOMETRY	
5.1	INTRODUCTION	133
5.2	METHODS	135
5.2.1	EXPERIMENTAL ANIMAL STRAINS	135
5.2.2	ECHOCARDIOGRAPHIC LEFT VENTRICLE DETERMINATION	135
5.2.3	ANIMAL PREPARATION FOR MRI IMAGING	138
5.2.4	MRI ASSESSED LV DETERMINATION AND CALCULATIONS	140
5.2.5	*POST MORTEM* EVALUATION	140
5.3	RESULTS	142
5.4	DISCUSSION	147
6	**CHAPTER 6**	
	PRODUCTION OF CONGENIC STRAINS	
6.1	INTRODUCTION	155
6.2	METHODS	157
6.2.1	CONGENIC STRAIN PRODUCTION	157

6.2.2	TAIL-TIPPING AND DNA EXTRACTION	159
6.2.3	PCR AND GENOTYPING	159
6.2.4	DESIGN OF MICROSOFT ACCESS DATABASE	159
6.2.5	PHENOTYPE MEASUREMENTS	160
6.3	RESULTS	160
6.4	DISCUSSION	164
7	**CHAPTER 7**	
	GENOME WIDE EXPRESSION ANALYSIS	
7.1	INTRODUCTION	173
7.2	METHODS	175
7.2.1	EXPERIMENTAL ANIMALS, DIETARY MANIPULATION AND PHENOTYPIC MEASUREMENTS	175 175
7.2.2	RNA EXTRACTION AND MICROARRAY EXPERIMENT	175
7.2.3	MICROARRAY DATA ANALYSIS	176
7.3	RESULTS	176
7.4	DISCUSSION	211
8	**CHAPTER 8**	
	GENERAL DISCUSSION	215
	REFERENCES	219
	APPENDICES I-V	252

LIST OF TABLES

		Page
Table 1.1:	Key regulatory hormones and neurotransmitters involved in the regulation and maintenance of blood pressure	8
Table 1.2:	The JNC-7 guidelines for blood pressure classification	9
Table 1.3:	Mendelian forms of hypertension, mutations and molecular mechanism involved in blood pressure modulation	16
Table 1.4:	Disease genes involved in Familial Hypertrophic Cardiomyopathy (FHC)	20
Table 1.5:	Genetically inbred hypertensive rat strains in common use for cardiovascular research	28
Table 3.1:	Polymorphic microsatellite marker oligonucleotide sequences	82
Table 4.1:	PCR and sequencing primers for *Dbp*	109
Table 4.2:	PCR and sequencing primers for *Corin*	110
Table 4.3:	Pairwise analysis of candidate genes	114
Table 5.1:	MRI summary data for animals	146
Table 6.1:	Background heterogeneity in backcross strains generated	164
Table 7.1:	Differentially expressed genes mapping to chromosome 14	184
Table 7.2:	Networks identified from RP analysis for each sample group comparison	185
Table 7.3:	List of 119 genes identified from highest significant network	190
Table 7.4:	Two-way ANOVA strain-salt interaction	210

LIST OF FIGURES

	Page
Figure 1.1: Illustration of the polygenic, multifactorial nature of a complex trait	2
Figure 1.2: Diagram outlining the sequence of events during a heartbeat	4
Figure 1.3: The rate at which a viscous fluid flows through a cylindrical shaped pipe	5
Figure 1.4: Diagrammatic outline of the RAS regulatory cascade in blood pressure regulation	7
Figure 1.5: Organ damage resulting from elevated blood pressure	10
Figure 1.6: Outline of sarcomere organisation	12
Figure 1.7: Left ventricular geometric patterns, consequences of different combinations of pressure and/or volume overload	13
Figure 1.8: Choices of analysis for quantitative trait locus mapping	39
Figure 1.9: Cartoon representing the basic principals behind the production of congenic strains	43
Figure 2.1: Diagram depicting congenic strain production	54
Figure 2.2A: Representative echocardiogram	59
Figure 2.2B: Correlation of echocardiograph estimated LVM and post mortem evaluation	59
Figure 2.3A: Short axis view image of 1mm slice through the heart in diastole	61
Figure 2.3B: Short axis view image of 1mm slice through the heart in systole	61
Figure 2.4: An example of output from GeneMapper v3.7	66
Figure 2.5: Diagram of the GeneChip® Probe Array	77
Figure 3.1: A representative agarose gel of 47 F_2 animals genotyped with marker *D14Arb17*	86
Figure 3.2A: Chromosome 14 map generated by Clark *et al.* (1996)	87
Figure 3.2B: Improved genetic linkage map generated using JoinMap 3.0	87
Figure 3.3A: CMI QTL confirmed using simple interval mapping analysis – males and females	89
Figure 3.3B: CMI QTL analysed using composite interval mapping analysis – males and females	89
Figure 3.3C: CMI QTL identified using multiple marker analysis – males and females	89
Figure 3.4A: LVMI QTL analysed using simple interval mapping analysis – males and females	90
Figure 3.4B: LVMI QTL analysed using composite interval mapping analysis – males and females	90
Figure 3.4C: LVMI QTL identified using multiple marker analysis – males and females	90
Figure 3.5A: CMI QTL analysed using simple interval mapping – males	91
Figure 3.5B: CMI QTL analysed using composite interval mapping – males	91

Page

Figure 3.5C: CMI QTL identified using multiple marker analysis – males 91
Figure 3.6A: LVMI QTL analysed using simple interval mapping – males 92
Figure 3.6B: LVMI QTL analysed using composite interval mapping – males 92
Figure 3.6C: LVMI QTL identified using multiple marker analysis – males 92
Figure 3.7A: PRA QTL identified using simple interval mapping analysis – males 93
Figure 3.7B: PRA QTL analysed using composite interval mapping – males 93
Figure 3.7C: PRA QTL identified using multiple marker analysis – males 93
Figure 3.8A: Single factor ANOVA analyses of LVMI (*D14Wox14*) – males 94
Figure 3.8B: Single factor ANOVA analyses of LVMI (*D14Got33*) – males 94
Figure 3.9A: Single factor ANOVA analyses of LVMI (*D14Wox14*) – females 95
Figure 3.9B: Single factor ANOVA analyses of LVMI (*D14Wox14*) – females 95
Figure 3.10: Graph showing SBP and LVMI values for male rats 97
Figure 3.11: Analysis of the Y chromosome effect in male data subset 98
Figure 3.12: Graph showing SBP and LVMI values for male rats separated by Y chromosome origin 99
Figure 4.1: Comparative map for rat chromosome 14 112
Figure 4.2A: Plot of CT values for *Corin* and housekeeping reference gene 115
Figure 4.2B: Relative multiplex PCR efficiency plot 115
Figure 4.3: CT values for *β-actin* 117
Figure 4.4A: Ct values for *Dbp*, *Corin* and *GAPDH* 118
Figure 4.4B: Relative PCR efficiency plots 118
Figure 4.5: TaqMan gene expression in aorta – *Corin* 119
Figure 4.6: Taqman gene expression in heart – *Corin* 120
Figure 4.7: TaqMan gene expression in heart – *Dbp* 121
Figure 4.8A: Pharmalogical intervention study – SBP 122
Figure 4.8B: Pharmalogical intervention study – LVMI 122
Figure 4.9A: Pharmacological effects on Corin 123
Figure 4.9B: Pharmacological effects on Dbp 123
Figure 4.10: Raw data output from SeqScape version 2.1 125
Figure 4.11: Graphical representation rat *Dbp* gene structure 126
Figure 4.12 Illustration of Vitamin D biosynthesis pathway 130
Figure 5.1 Graphic illustration of SP.WKYGla2a congenic strain 137
Figure 5.2: Representative radiotelemetry data for SBP 138
Figure 5.3: Echocardiograph image output 140
Figure 5.4A MRI Pilot images – sagittal 142
Figure 5.4B MRI Pilot images – transverse-coronal 142
Figure 5.5: Series of typical short axis transverse sections 144
Figure 5.6: Comparison of MRI, echocardiography and *post mortem* (PM) for LVM in 16 week old males 145
Figure 5.7 Linear regression analysis of LVM 147

Page

Figure 5.8A Comparison of echocardiographic statistical evaluation 149
Figure 5.8B: Linear regression analysis plot 150
Figure 5.9A: RWT calculated from MRI images at end diastole 151
Figure 5.9B: RWT calculated from echocardiographic images 151
Figure 6.1: Cartoon of congenic breeding strategy 159
Figure 6.2: Conceptual relationship schema 162
Figure 6.3: Search GUI for the breeding database 163
Figure 6.4: A diagram of chromosome 14 showing QTL1 and QTL2 166
Figure 6.5A: Single factor ANOVA analysis of LVMI – *D14Wox14* 167
Figure 6.5B: Single factor ANOVA analysis of LVMI – *D14Got33* 167
Figure 6.6A: Analysis of SBP in SHRSPGlaBX4 and SHRSP strains 168
Figure 6.6B: Analysis of LVMI in SHRSPGlaBX4 and SHRSP strains 168
Figure 6.7: Analysis of body weights in SHRSPGlaBX4 SHRSP strains 169
Figure 7.1A: A two-way factor design template 177
Figure 7.1B: Examples of various effects that can be identified by ANOVA 177
Figure 7.2: Diagram key for Ingenuity Pathway Analysis data output. 178
Figure 7.3 Haemodynamic and post mortem parameters 179
Figure 7.4 Non-linear Sammon Plot 180
Figure 7.5 Manhattan distance metric plot 181
Figure 7.6A: Venn diagrams of pairwise comparisons (strain) 183
Figure 7.6B: Venn diagrams of pairwise comparisons (salt) 183
Figure 7.7 Overlapping network analyses 189
Figure 7.8A: V-myc myelocytomatosis viral oncogene homolog network pathway 193
Figure 7.8B: V-myc myelocytomatosis viral oncogene homolog network pathway 194
Figure 7.8C: V-myc myelocytomatosis viral oncogene homolog network pathway 195
Figure 7.8D: V-myc myelocytomatosis viral oncogene homolog network pathway 196
Figure 7.9A: Transforming growth factor β1 network pathway 197
Figure 7.9B: Transforming growth factor β 1 network pathway 198
Figure 7.9C: Transforming growth factor β 1 network pathway 199
Figure 7.9D: Transforming growth factor β 1 network pathway 200
Figure 7.10A: V-fos murine osteosarcoma viral oncogene homolog (FOS) 201
Figure 7.10B: V-fos murine osteosarcoma viral oncogene homolog (FOS) 202
Figure 7.10C: V-fos murine osteosarcoma viral oncogene homolog (FOS) 203
Figure 7.10D: V-fos murine osteosarcoma viral oncogene homolog (FOS) 204
Figure 7.11A: Cyclin dependant kinase inhibitor 1A 205
Figure 7.11B: Cyclin dependant kinase inhibitor 1A 206
Figure 7.11C: Cyclin dependant kinase inhibitor 1A 207
Figure 7.11D: Cyclin dependant kinase inhibitor 1A 208
Figure 7.12: Representation of two-way ANOVA results for strain-salt interaction 209

LIST OF ABBREVIATIONS AND SYMBOLS

2-D	Two dimensional
3-D	Three dimensional
AII	Angiotensin II
ACE	Angiotensin converting enzyme
AGT	Angiotensinogen
AME	Apparent mineralocorticoid excess
ANOVA	Analysis of variance
ANP	Atrial natriuretic peptide
ASE	American Society of Echocardiography
AT_2	Angiotensin II receptor
AVI	Audio visual image
AWT	Anterior wall thickness
BAC	Bacterial artificial chromosome
BN	Brown Norway rat
BNP	Brain natriuretic peptide
BP	Blood pressure
BW	Body weight
BX	Back cross
°C	Degrees centigrade
cDNA	Complementary DNA
CD	Compact disc
cM	centiMorgan
Cm	Centimetre
CMI	Cardiac mass index
CMR	Cardiac magnetic resonance
CT	Cycle threshold
cRNA	Complementary RNA
Dahl R	Dahl salt resistant rat
Dahl S	Dahl salt sensitive rat
DBP	Diastolic blood pressure
Dbp	Vitamin D binding protein
dNTP	Deoxinucleotide
ddNTP	Dideoxinucleotide
DNA	Deoxyribonucleic acid
ECG	Electrocardiogram
EDD	End diastolic dimension
ESV	End systolic volume
EDV	End diastolic volume
FDR	False discovery rate
FHC	Familial hypertrophic cardiomyopathy
FHH	Fawn-hooded hypertensive rat
F_1	First filial progeny

F_2	Second filial progeny
g	grams
GH	Genetically hypertensive rat
GRA	Glucocorticoid remediable aldosteronism
HW	Heart weight
kg	Kilogram
LEW	Lewis rat.
LH	Lyon hypertensive rat
LN	Lyon normotensive rat
LV	Left ventricle
LVEF	Left ventricular ejection fraction
LVH	Left ventricular hypertrophy
LVM	Left ventricular mass
LVMI	Left ventricular mass index
LV+S	Left ventricle + septum
MAP	Mean arterial pressure.
Mg^{+2}	Magnesium
mg	Miligrams
MHS	Milan hypertensive rat
mHz	Megahertz
ml	Millilitre
mm	Millimetre
mmHg	Millimetres of mercury
MNS	Milan normotensive rat.
mRNA	Messenger RNA.
MR	Magnetic resonance
MRI	Magnetic resonance imaging
ms	Millisecond
PCR	Polymerase chain reaction.
PM	*Post mortem*
PWT	Posterior wall thickness
QTL	Quantitative trait locus (loci)
RAS	Renin angiotensin system
RF	Radio frequency
RFLP	Restriction fragment length polymorphism
RH	Radiation hybrid
RHR	Renal hypertensive rat
RNA	Ribonucleic acid
RNAi	Ribonucleic acid interference
RMA	Robust multi-chip analysis
RP	Rank product
RT-PCR	Real time polymerase chain reaction
RWT	Relative wall thickness
Sabra H	Sabra hypertensive rat
Sabra N	Sabra normotensive rat
SBP	Systolic blood pressure
SD	Standard deviation of the mean

s	Second
SEM	Standard error of the mean
SHR	Spontaneously hypertensive rat
SHRSP	Stroke-prone spontaneously hypertensive rat
SNP	Single nucleotide polymorphism
SNS	Sympathetic nervous system
SD	Sprague Dawley
SS	Spontaneously hypertensive stroke-prone rat homozygote
SV	Stroke volume
TE	Echo time
TR	Repetition time
UTR	Untranslated region
WKY	Wistar-Kyoto rat
WKHA	Wistar-Kyoto hyperactive rat
WS	Wistar-Kyoto rat/spontaneously hypertensive stroke-prone rat heterozygote
WW	Wistar-Kyoto rat homozygote

SUMMARY

Left ventricular hypertrophy (LVH) is accepted as an important independent predictor of adverse cardiovascular outcome; the aetiology includes a number of well-recognized causes but there is considerable interest in the genetics underlying cardiac hypertrophy. Data from several twin studies indicates that left ventricular mass index (LVMI) has a significant genetic basis that is most likely polygenic. Given the heterogeneity of the human condition, there has been little progress made towards identification of the genes involved, in this now common disease state. As an adjuvant to current human studies, inbred animal models have been developed which in turn have led to the identification of quantitative trait loci (QTL), via investigation using a genome wide strategy. This generally involves high fidelity phenotyping of large segregating F_2 populations, derived by crossing inbred strains of sufficiently differing phenotype and subsequent genotyping using a wide selection of polymorphic microsatellite markers spread across the entire rat genome.

The research described in this thesis incorporated an improved analysis of a previous genome wide scan, to confirm and identify QTL containing determinants of left ventricular hypertrophy in the Glasgow SHRSP x WKY F_2 cross. This genome wide scan was carried out in 134 F_2 hybrids (male: female = 65:69). Systolic and diastolic blood pressure was measured by radio-telemetry at baseline and after a 3 week 1% salt challenge in addition to heart rate, motor activity and pulse pressure. Other phenotype data included body weight, heart and LV weight and plasma renin activity. QTL affecting a given phenotype were mapped relative to an improved genetic linkage map for rat chromosome 14, with the aid of JoinMap 3.0, MapManager QTXb and Windows QTL Cartographer software. The original method of single marker analysis was used initially to test previous and newly acquired genotype data and confirm the cited LVMI QTL on rat chromosome 14. More stringent and complex statistical approaches were integrated in analysis resulting in detection of a second QTL for LVMI at marker *D14Got33* and a single QTL for cardiac mass at marker *D14Wox14*.

The identification of QTL, although a fundamental process, is only the initial step towards the end objective of gene identification. The next logical step is the physical capture and confirmation of QTL with the production of congenic strains and substrains. In this thesis, the process of verifying the chromosome 14 QTL began with the generation of congenic strains, using a marker assisted 'speed' congenic strategy, previously validated in rats by our group. This was achieved by backcross breeding two inbred rat strains (SHRSP X WKY) and introgression of marker delineated regions of chromosome 14, from one background into the recipient genome and vice versa. Complete homozygosity of the background genetic markers (n=168) was achieved after 4 backcross generations. In the time line allowed, it was not possible to achieve a fixed congenic line however based on data provided from QTL analysis it was possible to generate and analyse preliminary phenotype data from backcross 4 males on the SHRSP background. The initial readings from this pilot study provide physical evidence that substituting a portion of WKY chromosome 14 with SHRSP results in a reduced LVMI, despite equivalent systolic blood pressure.

An essential component of a successful QTL and congenic strategy is an accurate and reliable method of phenotyping. Simple *post mortem* measurement of heart and LV weight is satisfactory for end evaluation, but this method does not permit continuous or longitudinal studies in the animal. Echocardiography provides an inexpensive and accurate means to investigate LVMI *in vivo* however reproducibility of data can be poor and reliability of LVMI estimation varies between strains, primarily due to differences in heart shape. A current 'gold standard' method of cardiac imaging in the human clinical setting is magnetic resonance imaging (MRI). Although this technique has been used successfully for several years in therapeutic and diagnostic applications, the scope of MRI in small animals has not been fully investigated. With this aim, MRI was used to measure LVM and cardiac function in SHRSP, WKY and a chromosome 2 congenic strain (SP.WKYGla2a) with a significantly reduced systolic blood pressure. The *in vivo* use of MRI in this study provided 3-D images, which allowed for an accurate, highly reproducible and superior method of LVM estimation, applicable in a rat model of hypertension and cardiac hypertrophy. Furthermore, MRI was shown to be a sensitive technique, able to

discern subtle changes in ventricle shape, size and relative wall thickness (RWT) in small subject groups, not possible by simple *post mortem* or 2-D echocardiographic evaluation; a significant difference in RWT between the congenic strain and SHRSP was demonstrated for the first time.

In addition to QTL analysis, supplemental tools of investigation such as comparative mapping provide an inexpensive and relatively easy method of isolating large conserved regions of synteny between species. While this is still a relatively young field of research, it does provide insights into evolutionary aspects of gene hierarchy and provides a means of selecting genes of positional interest for further investigation. Candidate genes (*Corin* and *Dbp*) with shared synteny between rat, mouse and human were identified within LVMI QTL borders (on chromosome 14) for rat. It is important, however to conduct studies to confirm a functional role of candidate genes in cardiac hypertrophy. With the use of real time polymerase chain reaction (RT-PCR), cardiac mRNA was quantified and differential expression of candidate genes in parental strains was confirmed. The impact of blood pressure on these genes was further tested using mRNA taken from heart, after antihypertensive pharmalogical intervention. Despite a reduction in SHRSP blood pressure to equivalent WKY levels, the results of this study did not reflect a change in candidate gene expression comparable with WKY.

A two-factor microarray study of cardiac tissue in 21 week old SHRSP and WKY +/- salt was also undertaken in order to examine strain differences between SHRSP and WKY, as well as the effect of environmental stimuli on genotype. The high volume of data generated from this investigation required several filtering applications to reduce the number of significant differentially expressed genes. This was achieved initially by normalising the data for variation affects and partition clustering of groups into genetic profiles. Secondly, two different analytical approaches were used to determine genes of significance for follow up study on chromosome 14 regions of interest, in addition to genes determined as 'interacting' between strain and environment. The majority of genes identified as differentially expressed between strains were contractile proteins such as actin (*Acta1, Acta2, Actβ*), myosin heavy chain (*Myh6, Myh7*) and related proteins such as tropomyosin

alpha (*1pm1α*). Genes identified as differentially expressed post 3 week 1% salt challenge were mainly cell signaling kinases, growth factor receptors (*Egfr*) and transcriptional regulators (*Hes1, Hop*). Five genes were identified within the QTL regions on chromosome 14, of which two are functionally associated with cardiac hypertrophy; *Egfr* and *Hop*. The results from this microarray study offer several candidate genes for continued investigation in addition to providing a base of data in which to add further datasets, e.g. a chromosome 14 congenic.

In summary, this thesis describes the detailed investigation of the underlying genetic components and improved phenotypic analysis of left ventricular hypertrophy in the stroke prone spontaneously hypertensive rat, focussing in particular on the identification of candidate genes within an implicated region on rat chromosome 14.

CHAPTER 1
INTRODUCTION

1.1 Complex Genetic Cardiovascular Traits

Cardiovascular disease (CVD) is the main cause of death in the UK accounting for 39% of all deaths (British Heart Foundation Statistics, 2005). The major forms of CVD are coronary heart disease (CHD) and stroke with around half of all deaths from CVD attributed to CHD and about a quarter from stroke. In the last decade, the number of men living with CHD has increased to 7.4% of the adult population, from 6% and from 4.1% to 4.5% in women. These statistics indicate that there are now approximately 2.6 million people in the UK facing life with heart disease (British Heart Foundation Statistics, 2005). The cardiovascular disease epidemic has progressed from Western civilizations to the developing countries and despite healthcare advances the percentage of all deaths attributable to cardiovascular causes are estimated to rise from 25% in 1990 to 40% in 2020 (Reddy, 2004). The risk factors relating to cardiovascular disease extend from hypertension, insulin resistance and type 2 diabetes, obesity and hyperlipidaemias through traits such as metabolic syndrome and atherosclerosis to disease phenotypes including myocardial infarction, heart failure, stroke, left ventricular hypertrophy, peripheral vascular disease, and renal failure (Dominiczak & McBride, 2003).

Most cardiovascular diseases are complex, multifactorial, polygenic disorders, exhibiting the simultaneous effects of several genetic and environmental influences (Figure 1.1). A complex genetic trait can be described as a trait in which a simple one-to-one relationship between genotype and phenotype, as in classic Mendelian inheritance does not exist (Lander & Schork, 1994). The genetics of multifactorial diseases in human populations are particularly difficult to dissect due to the multiplicity of genes involved in complex phenotypes. Gene-gene (epistatic), gene-environment (ecogenetic) interactions, gender, discrete effects of each gene and heterogeneity within human populations are all factors influencing complex diseases (Stoll *et al.*, 2000). Despite these difficulties, identifying and understanding the principal genes underlying polygenic diseases can lead to improved methods of predicting inherited susceptibility and provide opportunities for the development of genome specific treatments (Lifton, 1995).

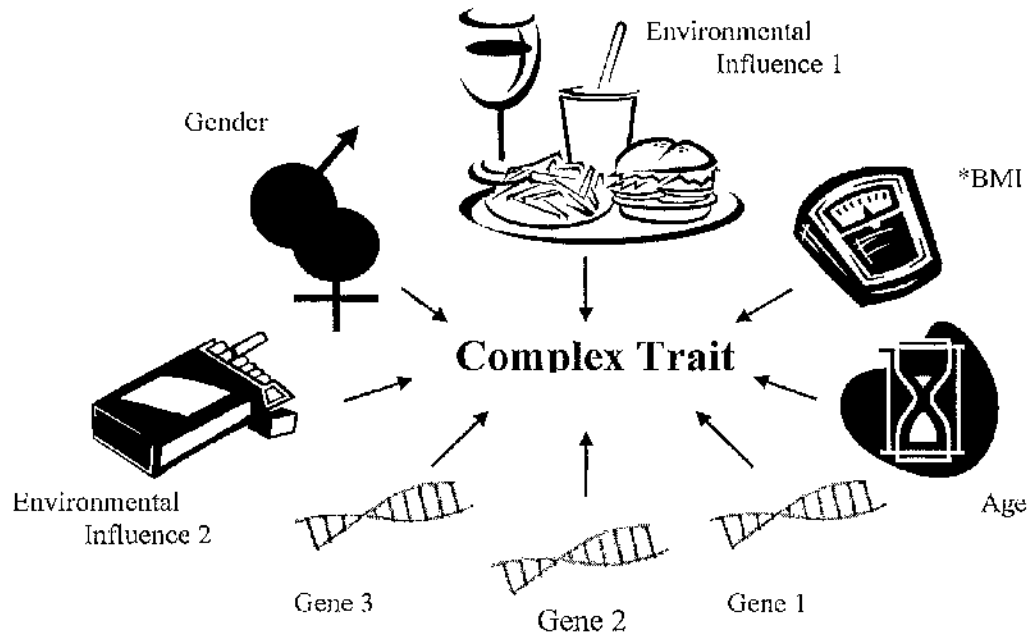

Figure 1.1 Illustration of the polygenic, multifactorial nature of a complex trait. *BMI - body mass index (Adapted from Lifton, 1995).

1.1.1 Blood pressure: regulation and maintenance

Blood pressure is the hydrostatic force blood exerts against the vascular walls and is determined by the amount of blood ejected from the heart and the resistance of arterioles to blood flow (Schork, 1997). Ventricular contraction (systole) ensures continuous flow to the periphery with forward propulsion of blood during ventricular relaxation (diastole). A sequence illustration of events during the cardiac cycle is shown in Figure 1.2. The physical relationships between the factors governing pressure and flow in a circulatory system are defined by Poiseuille' Law, which describes how flow relates to perfusion pressure, radius, length, and viscosity. However, flow in the body does not necessarily conform quantitatively to this relationship, which assumes long, straight tubes (not blood vessels), a Newtonian fluid (e.g., water, not blood which is non-Newtonian) and steady, laminar flow conditions. Nevertheless, this equation serves to demonstrate the dominant influence of vessel radius on resistance and flow (Figure 1.3).

Hormonal mechanisms act in concert with neuronal controls to regulate blood pressure via several methods, including vasoconstriction, vasodilation and alteration of blood volume. The reflex control of blood pressure is mediated by the medulla and to a higher degree by the hypothalamus, which acts neurally through the medulla, hormonally via vasopressin and consciously by creating a thirst drive (Burnstock 1986). A decrease in blood pressure results in sympathetic nervous system (SNS) activation leading to increased contractility of the heart (β_1-receptors) and vasoconstriction of both the arterial and venous side of the circulation (α-receptors). Stimulation of the parasympathetic system works in opposition to the SNS by slowing heart rate and causing vasodilation through release of acetylcholine (Benarroch, 1993). Whilst, all regulatory components influencing blood pressure are important, the renin angiotensin system (RAS) is considered a key modulator of blood volume, arterial pressure and sodium balance, the physiology of which continues to be a major source of investigation (Helmer, 1965; Meyer, 1965; Dzau, 1988). Figure 1.4 outlines the RAS; Table 1.1 summarizes the principal hormones and neurotransmitters involved in blood pressure regulation.

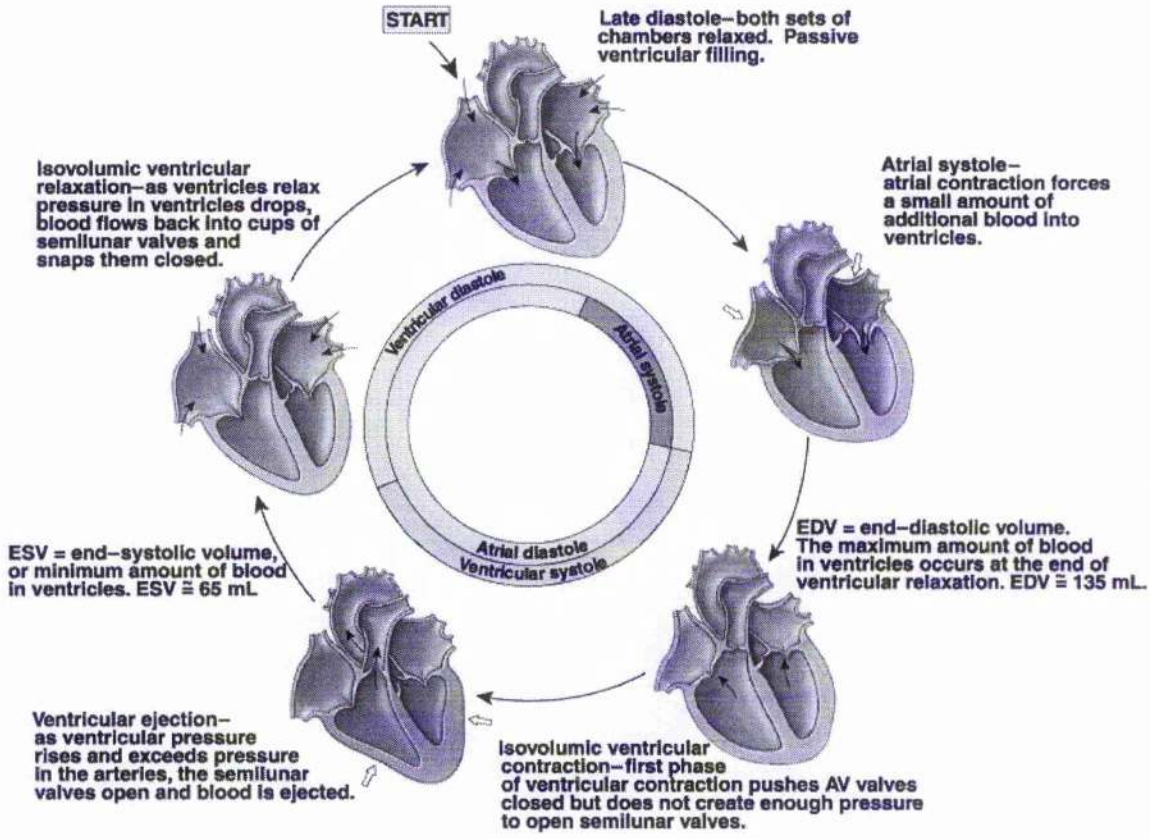

Figure 1.2 Diagram outlining the sequence of events during a heartbeat (taken from Berne & Levy, 1997).

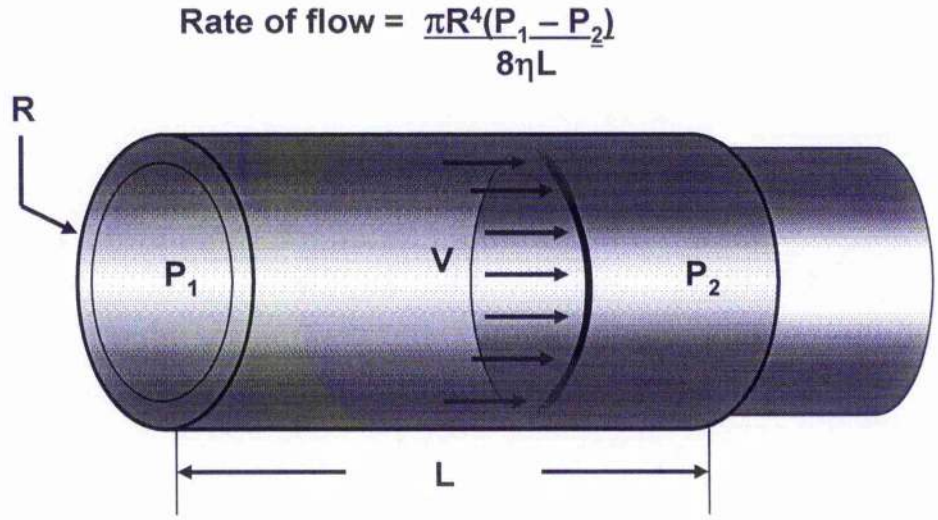

Figure 1.3 The rate at which a viscous fluid flows through a cylindrical shaped pipe. Poiseuille' Law, for laminar flow rate, where the velocity of blood in a smaller vessel is larger than that in a larger vessel with the same flow. R=radius, V=velocity, η=blood viscosity, L=length, P=pressure; increase radius, increase blood flow (adapted from Berne & Levy, 1996)

Atrial natriuretic peptide (ANP) was first identified 25 years ago as a cardiac peptide involved in the regulation of blood pressure (de Bold *et al.*, 1981). A physiologically inactive precursor to ANP, specifically pro-ANP, is stored and secreted from the atria and ventricle (Ogawa *et al.*, 1991) to high blood pressure. ANP acts to reduce water, sodium and adipose loads on the circulatory system, thereby reducing blood pressure and is an important regulator of homeostasis in the body. Recently a newly characterised serine protease, *Corin* was identified as the pro-ANP converting enzyme (Yan *et al.* 1999; Wu & Wu, 2003) involved in cleaving pro-ANP to the cardiac active hormone.

1.1.2 Human Essential Hypertension

The provision of a blood pressure level at which adequate tissue perfusion is maintained reflects the countless interactive neural, hormonal and circulatory systems and sub-systems (Schork, 1997). Hypertension refers to the maintenance of excessively high blood pressure (Pickering, 1965; Swales, 1994), which applies to elevations in mean arterial pressure, diastolic pressure, or systolic pressure and is often defined as a diastolic pressure of 90 mmHg or above, or a systolic pressure of 140 mmHg or above (Table 1.2) (Mikhail & Cope, 2004). Although without obvious symptoms, hypertension can have severe effects on a number of important tissues in the body including the heart, kidney and brain (Figure 1.5). In most individuals (90-95%) presenting with hypertension, the cause is unknown - essential (or primary) hypertension. In the remaining 5-10% of subjects with hypertension, it is secondary to renal disease, endocrine disorders, or other identifiable causes - secondary hypertension. As the core determinants of essential hypertension are unidentified, the efficacy of any preventative therapeutic measures is hampered (Dominiczak & Lindpaintner, 1994).

Blood pressure has a unimodal distribution in the general population with a strong positive and continuous correlation between blood pressure and cardiovascular disease

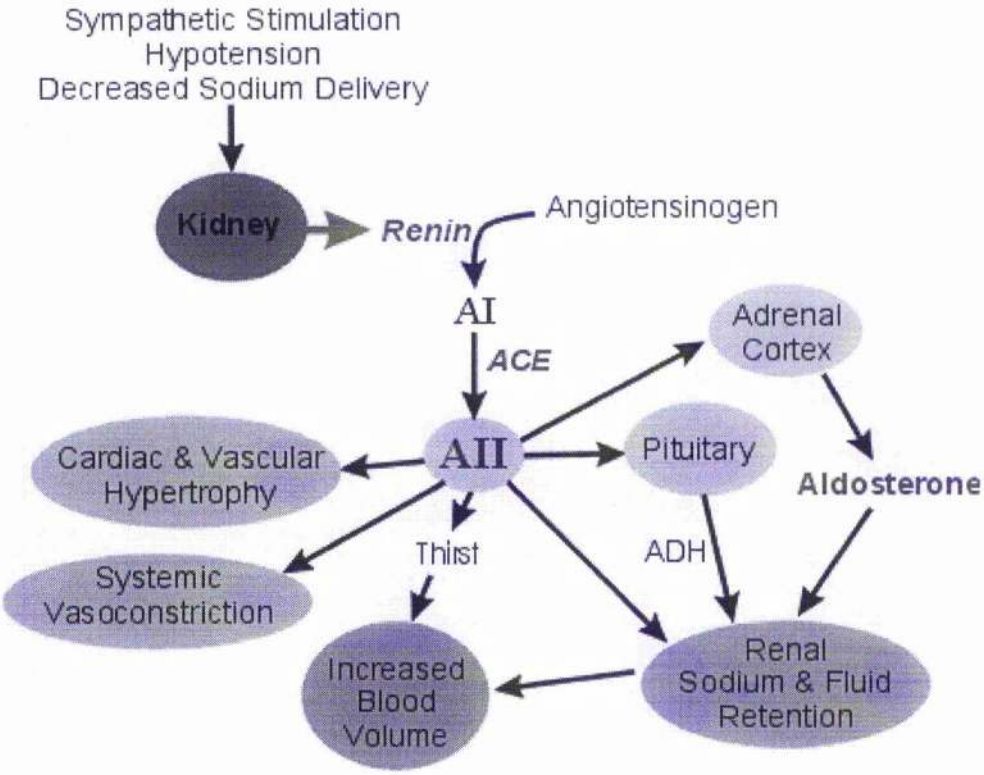

Figure 1.4 A diagrammatic outline of the RAS regulatory cascade in blood pressure regulation. The RAS pathway is common to many tissues however the most notable occurrence of this pathway is in the kidney. Sympathetic stimulation, renal artery hypotension, and decreased sodium delivery to the distal tubules stimulate the release of renin from the kidney, which then acts upon a circulating substrate, angiotensinogen. Proteolytic cleavage of angiotensinogen results in formation of the deca-peptide angiotensin I (AI). The vascular endothelium, particularly in the lungs, secrete angiotensin converting enzyme (ACE), which cleaves two amino acids from AI to form the octa-peptide, angiotensin II (AII) (modified from Zaman *et al.*, 2002).

Table 1.1. Key regulatory hormones and neurotransmitters involved in the regulation and maintenance of blood pressure

Neuronal/Hormonal Regulator	Site of Production/Secretion	Function
Renin and angiotensin	Kidney	Production is stimulated by decreased blood pressure (hypotension). Blood pressure modulation via control of blood volume, also stimulate production of aldosterone from the adrenal cortex (which also decreases urinary fluid and electrolyte loss from the body).
Natriuretic peptides: atrial natriuretic peptides (ANP) brain natriuretic peptides (BNP)	Atria (ANP) Ventricles (BNP)	Play a role in the regulation of blood pressure homeostasis and salt and water balance via diuretic, natriuretic and vasorelaxant effects.
Catecholamines: adrenaline, noradrenaline and dopamine	Adrenal Gland	Secreted in response to sympathetic nervous system stimulation and act rapidly to increase cardiac output and cause vasoconstriction.
Acetycholine	Cholinergic nerve (e.g. vagus)	Act to depress cardiac activity by slowing heart rate and causing vasodilation.
Vasopressin	Posterior Pituitary	An important hormone regulator of water balance.

Taken from Espiner *et al.*, 1995; Rubattu & Volpe, 2001.

Table 1.2. The JNC-7 guidelines for blood pressure classification

Blood pressure Classification	*SBP (mmHg)	†DBP (mmHg)
Normal	<120	<80
Prehypertensive	120-139	80-89
Stage 1 Hypertension	140-159	90-99
Stage 2 Hypertension	≥160	≥99

*SBP- systolic blood pressure

†DBP- diastolic blood pressure

Adapted from Mikhail & Cope, 2004.

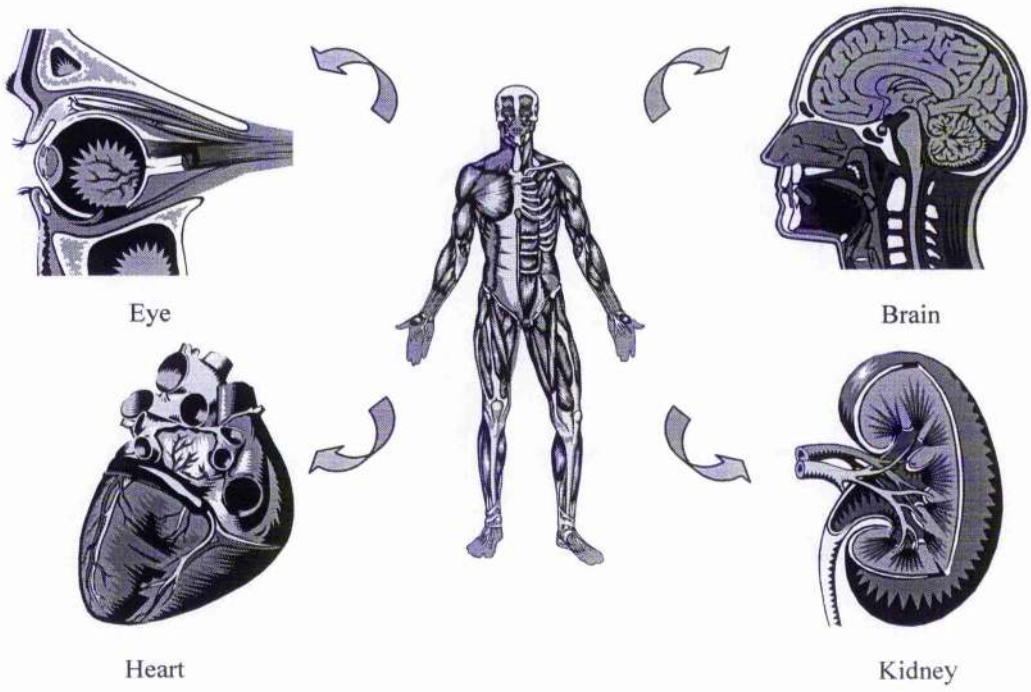

Figure 1.5 Organ damage resulting from elevated blood pressure – Injury to the brain due to haemorrhage or thrombosis, causing stroke. The vasculature of the kidney can become dramatically constricted restricting urine output and causing proteinuria. The heart can become hypertrophied and compromised in function, leading to heart failure. Hypertensive rentinopathy is a further complication of extremely high blood pressure where blood vessels in the eye become blocked or rupture, causing damage to the surrounding eye tissues.

risk and mortality, even in the normotensive range (Merlo *et al.*, 2004). Oldham *et al.* (1960) proposed that high blood pressure is an extreme of normal blood pressure distribution, which suggests that hypertension is influenced by several independently segregating genes, each exerting subtle effects on blood pressure. This hypothesis was quickly extended to five or six individual genes, contributing approximately 30% - 50% of observed variation in blood pressure in the general population (Ward, 1983).

1.1.3 Left Ventricular Hypertrophy

The cardiac muscle responds to chronically increased volume (preload) or pressure (afterload) by compensatory growth of the myocardium (Messerli, 1983). Ventricular hypertrophy is an adaptation by the ventricle that enables the heart to manage increased stress (Figure 1.6). At the cellular level, this involves a swelling of the myocyte cross-sectional area (hypertrophy), with the actual number of myocytes increasing (hyperplasia) when the heart reaches a critical weight of approximately 500g (Linzbach, 1960) or 7.5g/kg bodyweight (Dickhuth *et al.*, 1985). The process of hypertrophy is also linked to a cellular shift in expression of adult contractile proteins, to foetal isoforms (Durand *et al.*, 1999).

If the precipitating stress is volume overload, the ventricle responds with the addition of new sarcomeres in-series with existing sarcomeres resulting in ventricular dilation while maintaining normal sarcomeric lengths, thus wall thickness increases proportionally with chamber radius - eccentric hypertrophy (Koren *et al.*, 1991). In the case of chronic pressure overload, the chamber radius may not alter; however the wall thickness greatly increases as new sarcomeres are added in parallel to existing sarcomeres - concentric hypertrophy (Koren *et al.*, 1991) (Figures 1.6 & 1.7). This latter type of hypertrophy is capable of generating greater forces and higher pressures, while the increased wall thickness maintains normal wall stress however, over time the ventricle becomes "stiff" (i.e., compliance is reduced) and consequently less able to relax resulting in impaired filling and diastolic function (Gaasch *et al.*, 1976).

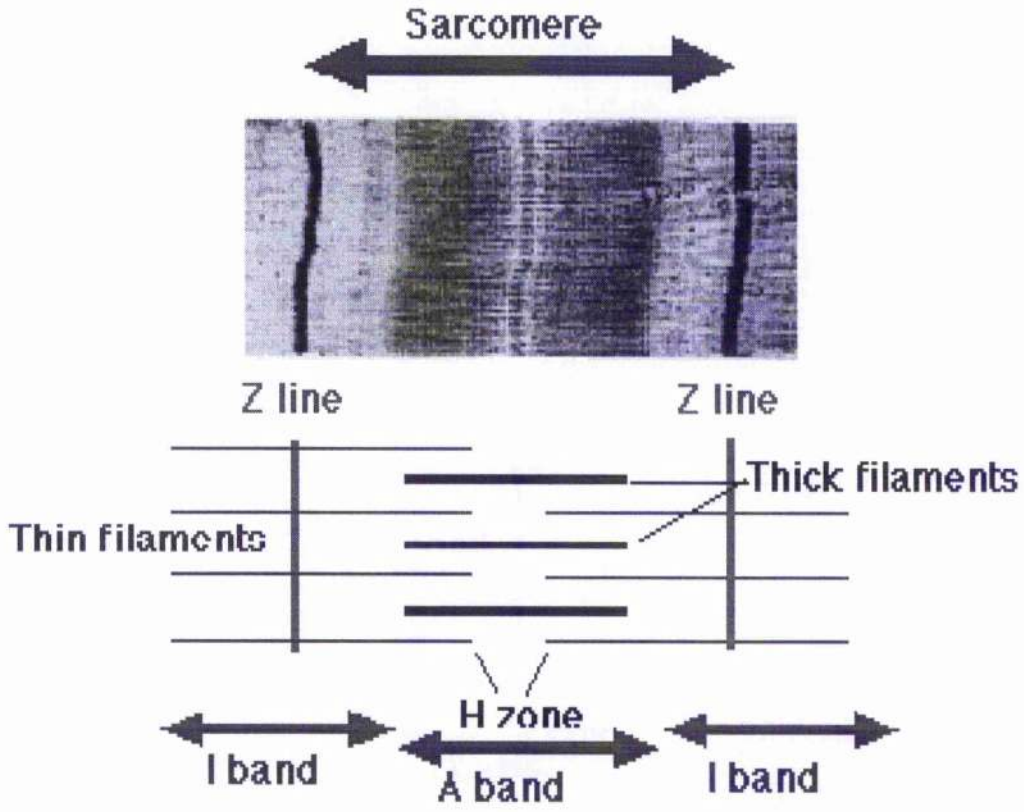

Figure 1.6 In contrast to skeletal muscle, cardiac muscle has a number of unique features that reflect its function of pumping blood. The myofibrils of each cell (cardiac muscle is made of single cells, each with a single nucleus) are branched and the branches interlock with those of adjacent fibres by adherens junctions. These strong junctions enable the heart to contract forcefully without ripping the fibres apart. Cardiac muscle is striated. Each cardiac muscle cell contains sarcomeres with sliding filaments of actin and myosin. Sarcomeres represent the minimal contractile unit of a muscle. Sarcomeres in a myofibril shorten resulting in shortening of the myofibril and in turn, the muscle fibre (electron micrograph, Porter & Bonneville, 1973).

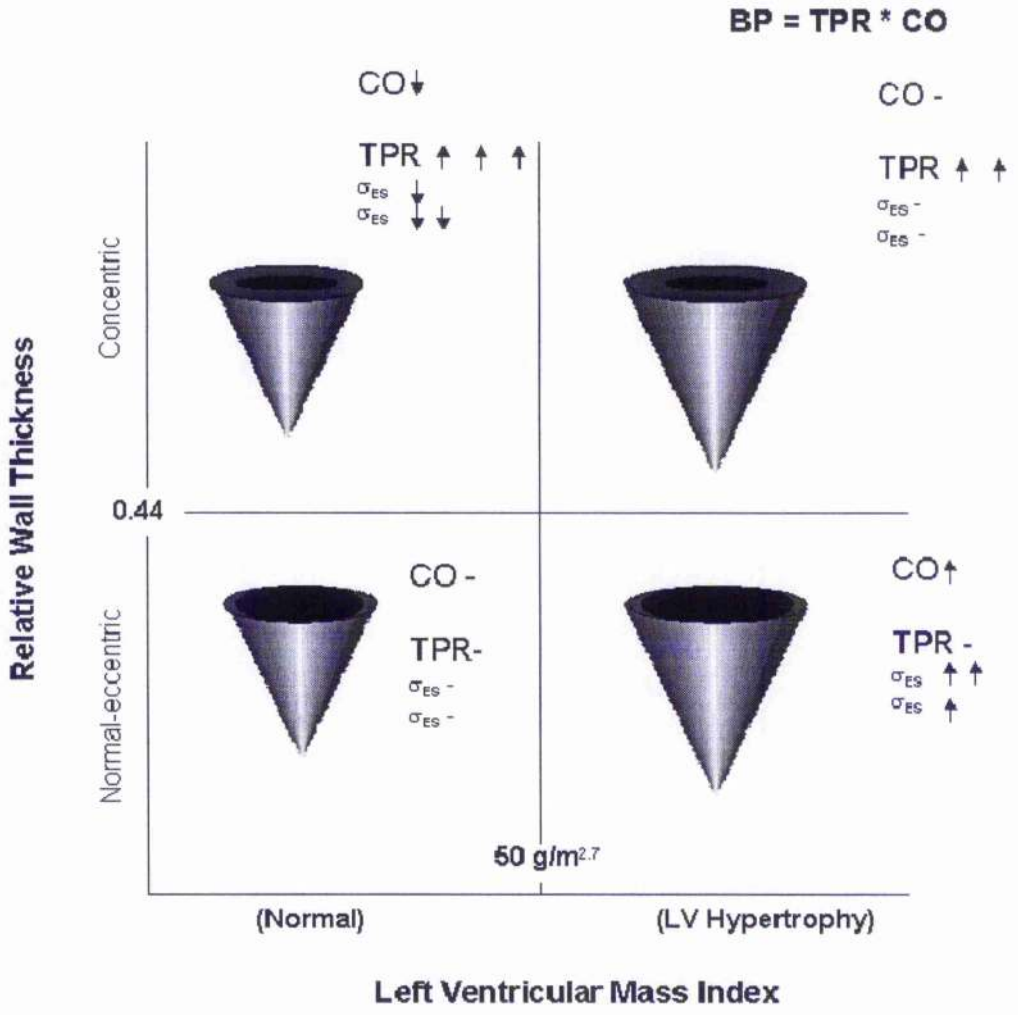

Figure 1.7 Left ventricular (LV) geometric patterns, consequences of different combinations of pressure and/or volume overload. Left ventricular mass index (LVMI) describes left ventricle mass relative to height; relative wall thickness (RWT) refers to LV wall thickness/LV radius. (Bottom left), the normal condition with normal LVMI, normal RWT, normal cardiac output (CO), total peripheral resistance (TPR) and end-systolic ($_{ES}$) and end-diastolic ($_{ED}$) wall stress (σ). (Top left) concentric LV remodelling and (bottom right), eccentric LV hypertrophy. (Top right) concentric LV hypertrophy. (adapted from Ganau *et al.*,1992).

Systemic perfusion is maintained until the development of ventricular dysfunction, leading to heart failure, myocardial infarction or arrhythmia (Pfeffer *et al.*, 1982; Devereux & Roman, 1995; Frohlich, 2001).

There is an approximate 60% increase in the incidence of coronary heart disease in men and 45% in women for every 50g rise in left ventricle mass (LVM), therefore left ventricular hypertrophy (LVH) is considered an important independent risk factor for cardiovascular morbidity and mortality (Kannel *et al.*, 1970; Levy *et al.*, 1990; Devereux *et al.*, 1994; Dominiczak *et al.*, 1997; Schillaci *et al.*, 2000). The intrinsic factors adding to risk (i.e. the pathophysiologic mechanisms by which hypertrophic remodelling of the myocardium contributes to cardiovascular related death) remain unknown (Devereux & Roman, 1995; Frohlich, 2001). One cause may be increased prevalence of ischaemic damage - enlarged myocardium leads to higher oxygen consumption while at the same time reducing coronary blood flow reserve, resultant in impaired blood delivery to the affected region (Schwartzkopff & Strauer, 2000).

Although elevated blood pressure is an important determinant of LVH (Kannel, 1983) the intensity of blood pressure load does not always correspond to the degree of hypertrophy observed in humans (Dominiczak *et al.*, 1997), indicating a more complex relationship than a simple dose-response effect. The distribution of cardiac mass within populations of unselected normotensive or hypertensive individuals appears to be largely continuous (Nunez *et al.*, 1996), with some studies reporting no indication of cardiac hypertrophy in 50% of hypertensive subjects (Devereux *et al.*, 1987).

1.2 EVIDENCE FOR GENETIC EFFECTS

1.2.1 Mendelian Forms of Hypertension

Evidence to support essential hypertension and LVH as a genetically determined disease is based on observations of a number of rare syndromes which display a Mendelian

inheritance pattern indicative of a monogenic disorder. Although these syndromes are uncommon, considerable effort has been spent to identify the genes responsible. There are several reasons for this; firstly, the effects of segregation of single alleles in families can be easily distinguished, thereby simplifying the molecular genetic analysis necessary. Secondly, these disorders often result in a severe disease state allowing for easier phenotypic selection. Finally, it is anticipated that the biochemical pathways and genes involved in these severe forms may also be implicated in the cardiovascular disease states more commonly seen in the general population. It then follows that understanding these disorders may not only be of value to the affected families but could also provide more broadly applicable diagnostic and therapeutic tools (Karet & Lifton, 1997).

There are currently at least six monogenic or Mendelian forms of human essential hypertension known to harbour mutations which impose large effects on blood pressure levels and are characterised by affecting sodium and water reabsorption in the kidney -- Glucocorticoid remediable aldosteronism (GRA), apparent mineral corticoid excess (AME), Liddle's syndrome, Gordon's syndrome, hypertension accelerated by pregnancy and hypertension with brachydactyly (see table 1.3) (Lifton, 1996).

a) Glucocorticoid-remediable aldosteronism (GRA) - a rare autosomal dominant form of primary aldosteronism in which aldosterone secretion is solely under the control of adrenocorticotropic hormone (ACTH). GRA is caused by a chimeric gene in which the ACTH- responsive 5'-promoter of the 11beta-hydroxylase gene is fused to coding sequences of the aldosterone synthase gene resulting in ectopic expression of aldosterone synthase activity in zona fasciculata cells of the adrenal cortex under the regulation of ACTH, with consequent hyperaldosteronism and suppression of angiotensin II-stimulated aldosterone production in the zona glomerulosa (White, 1988). Affected subjects have variable elevated plasma aldosterone levels in conjunction with suppressed plasma renin activity (PRA) and secrete high levels of

Table 1.3. Mendelian forms of hypertension, mutations and molecular mechanism involved in blood pressure modulation

Syndrome	Mutation	Mechanism
Glucocorticoid remediable aldosteronism (GRA)	Chimeric gene of aldosterone and 11-β-hydroxylase	Aldosterone synthase gene expression hormone instead of angiotensin II
Liddle's syndrome	Gain of a function mutation, of β and γ subunit of epithelial sodium channel (ENaC)	Reduction in ENac clearance and increased channels of ENac activity
Gordon's syndrome Psuedohypoaldosteronism typeII (PHA II)	Mutations in WNK1 and WNK4 genes	Increase reabsorption of chloride in the distal renal tubule
Apparent mineralcorticoid excess (AME)	Homozygous loss of function mutation of 11-β-hydroxysteroid dehydrogenase type 2	Reduced conversion of cortisol to cortisone
Hypertension accelerated by pregnancy	Missense mutation in the ligand binding domain of the mineralocorticoid receptor	Activation of receptor by progesterone
Hypertension with brachydactyly	Syndrome mapped to 12p11.2-12.2	Unknown, but complex chromosome rearrangement reported

Adapted from Dominiczak *et al.*, 2004

18-oxocortisol, produced in negligible amounts in unaffected individuals (Sutherland *et al.*, 1966, Ulick *et al.*, 1990). Using 18-oxocortisol secretion as a phenotype, linkage to a genomic segment of chromosome, 8 harbouring CYP11B2 (aldosterone synthase gene) has been established (Lifton *et al.*, 1992). This gene is 95% identical in DNA sequence to another involved in steroid biosynthesis, the 11beta-hydroxylase gene (CYP11B1), which also lies on chromosome 8 (Lifton *et al.*, 1992).

b) Apparent mineral corticoid excess (AME) - an autosomal recessive form of Mendelian hypertension associated with defects in steroid metabolism. Inactivating mutations in the renal isozyme of the 11beta-hydroxysteroid dehydrogenase (HSD11B2) gene, which normally converts cortisol to cortisone, create hypertension by failing to provide affected subjects with protection against the potent mineralocorticoid effect of cortisol (Mune *et al.*, 1995).

c) Liddle's syndrome - an autosomal dominant form of hypertension related to abnormalities in renal ion transport and clinically characterised by the suppressed secretion of aldosterone, suppressed PRA and hypokalaemia (Shimkets *et al.*, 1994). Initially linked to a short segment of human chromosome 16, subsequent research identified that constitutive over-activation of the aldosterone-regulated epithelial sodium channel (expressed in the renal nephron) arises from a mutation in the b subunit (SCNN1B) of this channel (Shimkets *et al.*, 1994) and/or a mutation truncating the carboxy terminus of the gamma subunit (SCNN1G) of the channel (Hansson *et al.*, 1995). Both lead to hypertension via increased renal salt and water absorption independent of mineralocorticoid action.

d) Gordon's syndrome or pseudohypoaldosteronism type II (PHA-II) - an autosomal-dominant disorder that features hyperkalemia and hyperchloremic metabolic acidosis, together with hypertension and hypercalciuria. Two genes WNK1 and WNK4 located in human chromosomes 12 and 17, respectively, are responsible for PHA-II. Immunohistochemical analysis revealed that WNK1 and WNK4 are predominantly expressed in the distal convoluted tubule and collecting duct.

Physiological studies have shown that WNK4 down-regulates the activity of ion transport pathways expressed in these nephron segments, such as the apical thiazide-sensitive Na^+-Cl^- cotransporter and apical secretory K^+ channel ROMK, as well as up regulates paracellular chloride transport and phosphorylation of tight junction proteins such as claudins. In addition, WNK4 downregulates other Cl^- influx pathways such as the basolateral Na^+-K^+-$2Cl^-$ cotransporter and Cl^-/HCO_3^- exchanger. WNK4 mutations behave as a loss of function for the Na^+-Cl^- cotransporter and a gain of function when it comes to ROMK and claudins. These dual effects of WNK4 mutations fit with proposed mechanisms for developing electrolyte abnormalities and hypertension in PHA-II and point to WNK4 as a multifunctional regulator of diverse ion transporters (Gamba, 2005).

e) Hypertension caused by gain-of-function mutation in the mineralocorticoid receptor - this missense mutation causes constitutive mineralocorticoid receptor activity and altered receptor specificity, so that progesterone and other steroids lacking 21-hydroxyl groups become mineralocorticoid receptor agonists. Pregnancy causes an extreme elevation of already increased blood pressure (Geller *et al.*, 2000).

f) Hypertension with brachydactyly - mapped to a region on the short arm of chromosome 12 (12p) (Chitayat *et al.*, 1997). Affected persons are shorter than unaffected individuals and not exhibit volume expansion-induced hypertension. The underlying mechanism of the hypertension is unknown. This syndrome has been described in several families; the hypertension follows an autosomal dominant mode of inheritance and cosegregates 100% with short stature and type E brachydactyly (Chitayat *et al.*, 1997).

1.2.2 Mendelian forms of Cardiac Hypertrophy

There are several inherited disorders associated with cardiac hypertrophy independent of secondary stimuli such as hypertension (Nunez *et al.*, 1996). Much of the

knowledge of familial hypertrophic cardiomyopathy (FHC), a genetically heterogeneous autosomal dominant disorder linked to cardiac contractile proteins (outlined in Table 1.4) is the result of molecular genetic studies (Ahmad, Seidman & Seidman, 2005). These genes encode components of the myofibril and so it has been proposed that sacromere disorganisation may play a role in the pathogenesis of the disease with impairment of correct protein packaging into functional macromolecular structures due to the abnormal protein (Nunez *et al.*, 1996). Whilst classic FHC causes death at an early age, several studies have shown that some FHC causing mutations are compatible with a long lifespan (Watkins *et al.*, 1993; Anan *et al.* 1994). In 1995 Maron *et al.* reported the prevalence of echocardiographically defined hypertrophic cardiomyopathy was as high as 0.2% in a large cohort of apparently young healthy adults selected from a community-based general population. It follows that carriers of mutations of the FHC type may be more common in the general population than previously appreciated.

All of the rare mutations discussed so far, corroborate beyond doubt that genetic defects can result in human cardiovascular disease. The question now stands as to whether these same genes play a role in the more common forms of each disease. The next logical step is to investigate their impact on clinical outcome by studies in the heterogeneous general population.

1.2.3 Human Studies of Hypertension

There are several lines of evidence in support of a genetic component contributing to the aetiology of human essential hypertension. Epidemiologic studies have revealed highly significant familial segregation of blood pressure. Individuals with essential hypertension are twice as likely as normotensive individuals to have a parent who is hypertensive and hypertension is 2-8 fold more common in the offspring of hypertensive parents than in the offspring of normotensive individuals (Perera *et al.*, 1972; Ibsen, 1984). Monozygotic twins (identical genetic profiles) demonstrate higher blood pressure correlations than dizygotic twins (50% genetically identical) (Feinleib *et al.*, 1977). Correlations are similarly high for first degree relatives such as sib-sib and child-parent

Table 1.4. Disease genes involved in Familial Hypertrophic Cardiomyopathy (FHC)

Gene	FHC Locus	Protein	Expression in Adult Striated Muscle
MYH7	14q11.2-q12	Myosin heavy chain polypeptide 7 (β-MyHC)	Cardiac muscle and slow-twitch skeletal muscle
MYH6	14q12	Myosin heavy chain polypeptide (α-MyHc)	Cardiac muscle and slow-twitch skeletal muscle
MYL3	3p21.2-3p21.3	Myosin light chain polypeptide 3 (MLC-1s/v)	Cardiac muscle and slow-twitch skeletal muscle
MYL2	12q23-q24.2	Myosin light chain polypeptide 2 (MLC-2s/v)	Cardiac muscle and slow-twitch skeletal muscle
TNNT2	1q3	Troponin T2 (cTnT)	Cardiac muscle
TNNI3	19p13.2-q13.2	Cardiac troponin I (cTnI)	Cardiac muscle
TPM1	15q22	Tropomyosin α (α-TM)	Cardiac muscle and slow-twitch skeletal muscle
MYBPC3	11p11.2	Myosin binding protein 3, cardiac (cMyBP-C)	Cardiac muscle
ACTC	15q14	α cardiac actin	Cardiac muscle
TNNC1	3p21-p14	Cardiac troponin C	Cardiac muscle
TTN	2q31	Titin	Cardiac muscle and slow-twitch skeletal muscle

Adapted from Ahmad, Seidman & Seidman, 2005

pair than for more distant relatives. Whilst these findings estimate 20-40% of blood pressure variation is attributable to genes (Annest *et al.*, 1979; Mongeau, 1989), the results also imply the multifactorial nature of essential hypertension. Blood pressure does not segregate in families in a way consistent with Mendelian transmission as spouses of hypertensive individuals also show significant correlations despite sharing no genetic component (Mongeau *et al.*, 1986). A range of other factors have been shown to impact on blood pressure levels, including high salt, low calcium and low potassium intake, limited physical exercise, exposure to noise and stress, age, gender and body mass and demographics (Horan & Lenfant, 1990). It is likely that an increase in blood pressure is only observed when genetically determined susceptibility is a factor, indicating a relationship between environment/demographic factors and certain allelic variants. A classic illustration of genetic heterogeneity is the consistent response of blood pressure to dietary salt intake; sensitivity or resistance to blood pressure increasing effects of salt intake have been demonstrated in both normotensive and hypertensive human subjects (Weinberger, 1996).

The prevalence and onset of hypertension in men and women is disparate, with males at greater risk for cardiovascular disease than pre-menopausal females (Kannel *et al.*, 1995). Although the underpinning mechanisms responsible for the sexual dimorphism of blood pressure control are not clear, there is significant evidence that androgens, such as testosterone, play an important role in gender-associated differences in blood pressure regulation. Studies using ambulatory blood pressure monitoring techniques in children have shown blood pressure increases in both boys and girls with age however, after the onset of puberty, boys exhibit higher blood pressure than age-matched girls (Bachmann *et al.*, 1987; Harshfield *et al.* 1994). Harshfield *et al.* (1994) noted higher systolic blood pressures of approximately 4 mmHg in boys aged 13 to 15 years, rising to differences of 10 to 14 mmHg at 16 to 18 years of age. In addition, women with polycystic ovary syndrome (characterized by elevated testosterone levels), experience hypertension, which further emphasises the importance of androgens and blood pressure regulation.

In women, menopause is characterized by increases in blood pressure (Kannel *et al.*, 1995; August & Oparil, 1999), with the incidence of hypertension in women doubling post menopause, leading to the suggestion that the loss of female gonadal steroids caused by menopause is a risk factor for post-menopausal hypertension (Staessen *et al.*, 1989; Marcus *et al.* 1994). Additionally, oestrogen has been shown to stimulate nitric oxide (NO) production (Weiner *et al.*, 1994; Goetz *et al.*, 1994) and may be protective of blood pressure increases in pre-menopausal women. However, since oestrogen replacement therapy has not been shown to decrease blood pressure, it is doubtful that the effect of estrogen on NO is the protective mechanism acting to lower blood pressure in pre-menopausal women (Akkad *et al.*, 1997; Pripp *et al.*, 1999).

Tingleff *et al.* (1996) examined the role of both hypertension and gender in the prevalence of an additional cardiovascular risk factor (LVH) with reference to a normotensive group across several age clusters. They demonstrated rates of 14% (males) and 20% (females) in normotensive subjects. Higher percentages of LVH (25% and 26% respectively) were apparent in hypertensive subjects. Therefore, the conclusions drawn from this study predict the probability of observed variance in LVH is not entirely attributable to haemodynamics, but is also subject to both unidentified genetic and non-genetic determinants (Nunez *et al.*, 1996).

1.2.4 Human Studies of LVH

The quantitative distribution of cardiac mass within human populations supports the view that any heritable effects are likely to be polygenic. However, there is a deficit of strong data supporting the extent and importance of inherited variability, in response of the heart and hypertrophic stimuli, such as hypertension (Nunez *et al.*, 1996). As many studies comprise of hypertensive families investigated with respect to blood pressure rather than cardiac hypertrophy, this is not unexpected. Twin studies can provide persuasive data for the heritability of cardiac mass in humans (Nunez *et al.*, 1996).

In a large twin study by Verhaaren *et al.* (1991), involving 254 pairs of 11-year old Caucasian school children, univariate analyses documented that genetic variance in boys (63%) and girls (71%) explained a significant proportion of LVM variability. The group determined that genes controlling LVM included those regulating LVM only and other genes concerned were common to both LVM and body weight. After removing the effect of weight and sexual maturity by regression methods, the influence of genetic effect continued to be important in determining LVM. Bivariate genetic analyses of their data demonstrated that genes common to LVM and weight significantly influence the covariation of these variables and that > 90% of the correlation of these traits is due to common genes. This study served to demonstrate that LVM was genetically determined in childhood and further emphasised the existence of several genes acting to modify cardiac mass including the multifactorial effect of environment and demographics.

Swan *et al.* (2002) determined the degree of LVM heritability and tested the association of three candidate genes (G protein beta-3 subunit, aldosterone synthase, and beta-1 adrenoceptor genes) in an adult population-based twin study. Their analysis demonstrated the genetic determination of various aspects of LV structure in middle-aged adults, with LVM shown to have approximately 50% heritability unexplained by any known confounding elements. They were able to demonstrate significant heritability indicative of an underlying genetic effect, in that correlations in monozygotic twins was greater than dizygotic twins, for LVM, LV diastolic dimensions, left atrial size, and LV systolic function. However, although there appeared to be a heritable component contributing to LV mass in this adult twin population, the group failed to show any association with the candidate genes assessed.

More recently, Sharma *et al.* (2006) used a large prospective twin database to establish heritability of LVM; a total of 376 normotensive Caucasian twin pairs (182 monozygotic and 194 dizygotic) aged 25-79. In this study, heritability estimates suggested that the genetic variance of LVM is 59%, with no common overlapping environmental effects identified between subjects, suggesting LVH has a substantial genetic basis that is likely to be polygenic. The results from this group, forms one of the largest normotensive twin pair

studies to date and adds further weight that development of LVH is independent of a blood pressure effect and is influenced by several underlying genetic components.

Similar to the observed blood pressure increases in menopausal women, there is a growing population of post menopausal women with target organ damage such as LVH (Gordon *et al.*, 1978; Stober *et al.*, 1985; Colditz *et al.*, 1987). Hinderliter *et al.* (2002) evaluated cardiovascular changes related to menopause, in a cohort of both pre- and post-menopausal women of similar age, race, weight, and blood pressure. The group showed that despite similar blood pressures, post-menopausal women had a higher indexed peripheral resistance and a lower cardiac index than pre-menopausal women. In association with this greater haemodynamic load, post-menopausal women also showed evidence of early concentric left ventricular remodelling, determined by increased relative wall thickness, in comparison to pre-menopausal women. This study further highlights the association of the menopause with both haemodynamic changes and left ventricular remodelling, in agreement with previous research (Pines *et al.*, 1996; Schillaci *et al.* 1998), however the results from these studies do not offer any insight into the mechanistic processes contributing to LVH as a consequence of the menopause.

In addition to gender, ethnicity and socioeconomic status has been shown to be predictive epidemiologic indicators in LVH. This is probably due in part to both demographics and elevated risk of hypertension associated with individuals of African descent. The results of the Evans County, GA heart study showed an almost 4-fold increase in the incidence of LVH in Black individuals versus White individuals (Arnett *et al.*, 1992). Even after adjusting for age, systolic blood pressure, weight, and change in weight/change in blood pressure, Black men still had an Odds Ratio for LVH of 3.0 (Arnett *et al.*, 1996). More recently, Rodriguez *et al.* (2004) produced data from a population-based sample of 1916 subjects living in Northern Manhattan, USA. The group showed that LVM varied according to race (blacks 48.9 g/m2.7, Hispanics 48.4 g/m2.7, whites 45.6 g/m2.7) in hypertensive and normotensive subjects, with an inverse association between mean LVM and socioeconomic status for the total cohort. These results suggest that both low social status and race are independent factors contributing to LVM in a heterogeneous population

and further indicate that, in consideration of the independent risk associated with LVH, the socio-economic aspects as well as the pathology of disease should be a target of treatment and prevention (Rodriquez *et al.*, 2004).

1.3 EXPERIMENTAL ANIMAL MODELS

1.3.1 Animal Models of Cardiovascular Disease

Animal models, in particular rodents, offer numerous advantages for genetic research. The low cost, ease of handling and breeding, access to sophisticated measurements, short generation time, complete environmental control and large litters all function to eliminate some of the complexity inherent in human studies (Lovenberg, 1987). This has been further extended with the production of inbred genetically homogeneous rodent models of hypertensive cardiovascular disease including congenic lines, transgenic animals and recombinant inbred strains. Each of these models are designed to express a variety of phenotypes, including spontaneous hypertension, salt sensitivity, LVH, stress sensitivity, stroke and susceptibility to end-organ damage (Dominiczak & Lindpaintner, 1994).

1.3.2 Mouse Models of Cardiovascular Disease

Currently the mouse is the preferred mammalian system for genetic manipulation. This is mainly due to the extensive knowledge of the mouse genome, with over 10 000 genetic markers including in excess of 6000 microsatellite sequences that are critical to genetic studies (Hoit & Walsh 1998; Mouse Sequencing Consortium, 2004). To date, a number of diverse modifications of the mouse genome have resulted in mice with both cardiac hypertrophy and altered cardiovascular function. These studies include loss/gain of function analysis using cardiomyocyte ligands and receptors, G proteins, signal transduction pathways, calcium cycling proteins, sarcomeric or structural proteins and or

sub-cellular components. Of particular note, *in vivo* studies involving transgenic mice emphasize the application of transgenic mouse models as an effective analytical tool to investigate molecular alterations of specific genes in the whole animal. Nonetheless, in order to understand the processes and genes involved in the development and pathogenesis of disease, it is necessary to study mammalian physiology and pathophysiology rather than the single gene approach. For this reason the production and use of animal strains permissive to the investigation of several candidate genes *in situ*, is central to the initial investigation of complex polygenic diseases.

1.3.3 Rat Models of Hypertensive Cardiovascular Disease

Cardiovascular disease has been widely investigated in rat models, with more than one model representing a genetic aetiology. The number of rat strains commonly in use (Table 1.5) offers a useful parallel to the multiplicity of human cardiovascular disease. Each of these rat strains has distinctive pathophysiological features linked to disease development and bears a similarity to disorders found in subgroups of hypertensive subjects worthy of independent genetic investigation, including left ventricular hypertrophy and stroke (Ganten, 1987). The Spontaneously Hypertensive Rat (SHR) is the most commonly employed model of cardiovascular disease, with over 4000 published articles in the last 10 years. In particular, developments of rat models derived from the SHR are now widely used for hypertension related diseases (Yamori & Swales, 1994).

A common used approach in developing inbred models of hypertensive cardiovascular disease has been to measure blood pressure in a large number of out-bred animals and then selectively breed those with the highest blood pressures (Kurtz *et al.*, 1994). In each successive generation, offspring with the highest blood pressures are brother X sister mated to produce an inbred strain. After 20 generations of brother X sister mating, the offspring should be homozygous at >99% of loci and therefore all animals within the strain are nearly isogenic (Rapp, 1983). This resolves problems of aetiological heterogeneity observed in humans, while also producing large number of progeny. Moreover, under conditions of standardised animal husbandry, the ability to control environmental factors

offers the prospect of investigating more complex genetic interactions than is possible in even the most closely managed clinical trials (Dominiczak & Lindpaintner, 1994).

1.3.4 The Stroke Prone Spontaneously Hypertensive Rat

In 1963, Okamota and Aoki produced a colony of spontaneously hypertensive rats (SHR) by selective in-breeding of individual normotensive Wistar-Kyoto (WKY) rats with elevated blood pressure from the Animal Center Laboratory, Kyoto University Faculty of Medicine, Japan (Yamori & Lovenberg 1987). Typical lesions often associated with human hypertensive cardiovascular disease, including cerebral (infarction, haemorrhage), myocardial (infarction, fibrosis) and nephrosclerotic (benign, malignant) were all observed in SHR after three months of age and potentiated the use of SHR as a model of the human condition (Okamoto & Aoki, 1963).

In 1971, SHR were separated into 3 main substrains, at which time it was confirmed the incidence of spontaneous cerebrovascular disease was different among them; high in substrain A (80%) and low in substrains B and C (50%), despite similarity of blood pressure measurement the 3 substrains. Suspecting the involvement of independent genetic factors in the pathogenesis of stroke, Okamoto and co-workers selectively bred substrain A by maintaining offspring from SHR dying from stroke, resulting in the generation of a stroke-prone spontaneously hypertensive rat, or SHRSP (Okamoto *et al.*, 1974).

The SHRSP displayed a rapid onset of hypertension after birth in comparison to SHR and by twelve weeks of age had a systolic blood pressure of 230mmHg. The SHRSP had a high tendency to naturally develop cerebrovascular lesions, particularly in the antermedial and occipital cortex and the basal ganglia with over 90% of all males suffering stroke while on a Japanese diet of high salt, low potassium and protein (Nagaoka *et al.*, 1976). In contrast to regular SHR strains, which were known to be resistant to salt, the SHRSP were found to be salt sensitive (Yamori *et al.*, 1981).

Table 1.5 Genetically inbred rat strains in common use for cardiovascular research

Name of Strain	Origin of Strain	SBP (mmHg)
Spontaneously Hypertensive Rat (SHR)	Kyoto, Japan	200
Stroke-Prone Spontaneously Hypertensive Rat (SHRSP)	Kyoto, Japan	230
Milan Hypertensive Rat (MHS)	Milan, Italy	175
Dahl Salt-Sensitive Rat (Dahl S)	Brookhaven, USA	170
Lyon Hypertensive Rat (LH)	Lyon, France	180
Sabra Hypertensive Rat (SBH)	Jerusalem, Italy	185
Genetically Hypertensive Rat (GH)	Dunedin, New Zealand	185
Fawn Hooded Hypertensive Rat (FHH)	The Netherlands	150
Wistar Kyoto Rat (WKY)	Kyoto, Japan	120
Dahl Salt Resistant Rat (Dahl R)	Copenhagen, Denmark	125
Sprague Dawley (SD)	Hoechst, Frankfurt	110

Given the distinctive traits of the SHRSP, the strain was distributed within a selection of high profile research groups for use in study of hypertension and stroke. This circulation, prior to complete in-breeding (F_{20} required at least), resulted in significant genetic heterogeneity between different colonies (Matsumoto *et al.*, 1991; Samani *et al.* 1989; Nabika *et al.*, 1991). Whilst this does not affect the use of SHRSP as an experimental model for study, it does call for an awareness of the source of the SHRSP, SHR or WKY, when making comparisons of results obtained by different research groups.

There are several pathophysiological similarities between hypertensive cardiovascular disease in SHRSPs and humans, which encourage the use of SHRSPs in genetic research. For example, male SHRSPs have higher blood pressures than females, in common with human essential hypertension (Yamori *et al.*, 1976). Whilst the most preponderant site for stroke in SHRSP is the cortical region (69.8%), the basal ganglia, is next highest (24.5%) in common with humans. Indeed, a branch of the middle cerebral artery (the lenticulostriate artery) is responsible for basal ganglia lesions in both the SHRSP and humans. In addition to hypertension and stroke, the SHRSP also displays cardiac hypertrophy and LVH.

It then follows that a suitable in-bred model of human hypertensive cardiovascular disease in which to begin analysis of the genetic determinants of hypertension, left ventricular hypertrophy and cerebrovascular disease, is the SHRSP. However, as indicated by the studies of Mendelian forms of human hypertension, any success in dissecting out common underlying determinants is dependant on strong, defined and uniform phenotyping. For this reason, an error free, high fidelity method of blood pressure and left ventricle mass measurement and assessment of cardiac function is essential.

1.3.5 Studies in Animal Models

The use of experimental animals offers a useful supplementary to genetic study in humans. These animal models not only preserve the polygenic nature of the disorder but are not compounded by genetic heterogeneity and are easily subject to a controlled

environment (Dominiczak & Lindpaintner, 1994). Additionally, the use of animal models affords the applicability of high fidelity phenotyping. Indeed, crude biometric estimates from breeding experiments in various hypertensive rat strains have shown the number of independent genes affecting blood pressure control to be between two and six (Rapp, 1983). This moderately low number of loci implies the feasibility of identifying these genes as well as gene(s) independently influencing left ventricular hypertrophy in such models (Harrap, 2002).

Traditionally genetic research using inbred hypertensive rat strains was undertaken in a solely comparative fashion using a control reference strain (Lander & Schork, 1994). An assortment of biochemical, anatomic and histological characteristics, were used as phenotypic parameters for this approach, with >100 differences determined (Dominiczak & Lindpaintner, 1994). However, in all likelihood this variance is probably unrelated to the pathogenesis of hypertension and has evolved as a corollary of random allelic fixation (genetic drift), during the process of selective breeding and inbreeding (Rapp, 1983).

In order to address some of these issues, Rapp (1983) devised a set of criteria, applicable to quantifiable differences between normotensive and hypertensive strains. The most prevailing of these being the requirement that the trait under investigation (or the intermediate phenotype) must cosegregate in an F_2 backcross population of rats derived from a cross between phenotypically divergent strains thus, allowing random associations to be distinguished from evidence of a causal relationship (Rapp, 1983, Dominiczak & Lindpaintner, 1994). A case in point is noradrenaline induced oscillatory activity and increased lymphocyte potassium efflux, shown to cosegregate with blood pressure in the SHRSP (Dominiczak & Lindpaintner, 1994). Unfortunately, there is still the question as to whether the cosegregating trait signifies a primary, causative factor or is simply a secondary effect of hypertension.

There are several examples of cosegregation analysis studies, notably four independent rat F_2 populations have been tested for cosegregation between a polymorphic marker on the renin gene and blood pressure. In one study, using a cross between the Dahl salt-sensitive

(hypertensive) and salt-resistant (normotensive) strains, a co-dominant effect of the hypertensive allele on blood pressure was shown (Rapp, 1989), although in a SHRSP-Wistar-Kyoto (WKY) cross, no such effect could be established (Lindpaintner, 1991). The third study, performed on a cross between SHR and Lewis rats, observed an association relating the presence of the hypertensive renin allele and blood pressure in animals heterozygous at the renin locus (Dominiczak & Lindpaintner, 1994). Yu (1998) identified co-segregation of the renin allele with higher systolic blood pressure in male rats aged 8-24 weeks and in females aged 12-24 weeks, in a cross between SHR and WKY rats. In this study, the SHR renin allele was also associated with higher mean arterial pressure in older rats and co-segregated with body weight males rats aged 12-24 weeks, but not with females, indicative of both an age and gender effect.

In considering if the same genes involved in blood pressure regulation also influence cardiac hypertrophy, Zhang (1996) analysed a cosegregating F_2 population of SHR and WKY strains. The group provided evidence of a chromosomal region close to the ANP locus determining mean blood pressure, although found no indication that the same region influenced heart weight. These results suggest that blood pressure and heart weight may be independently controlled by different genetic mechanisms in the SHR. Several years later, Masciotra (1999) carried out cosegregation analysis in genetic crosses of WKY-derived hyperactive (WKHA) and WKY and WKY-derived hypertensive (WKHT) and SHR strains to assess increased ventricular mass and association with expression of the ANP gene. The abundance of ventricular ANP mRNA and peptide was shown to correlate inversely with LVM, in contrast to the positive correlation observed with α-myosin heavy chain mRNA (Masciotra, 1999). Data from the equally hypertensive SHR and WKHT strains showed LVM was larger in SHR than in WKHT, yet ventricular ANP mRNA was significantly less in SHR than in WKHT. These results provide evidence that low ventricular ANP gene expression can be linked genetically to high cardiac mass independently of blood pressure and are consistent with the hypothesis that ANP may offer protection against hypertrophy.

Results from studies using transgenic mice over expressing ANP suggest ANP gene expression is inversely related to cardiac growth, with transgenic animals exhibiting lower heart weight and blood pressure than wild type mice. Conversely, transgenic mice with homozygous disruption of the pro-ANP gene (Nppa) or the natriuretic peptide receptor (NPR-A) exhibit significant cardiac enlargement, proportionally disparate with observed increases of blood pressure in these models (John *et al.* 1995; Kishimoto *et al.*, 2001; Knowles *et al.* 2001). More recently, Mori *et al.* (2004) investigated the effect of ANP deficiency in response to volume overload and observed exaggerated increased heart and LV weight in response to volume overload, which was not prevented by normalization of blood pressure (Mori *et al.*, 2004) .

However, raised circulating levels of ANP and pro-ANP are associated with (i) reduced ventricular systolic and diastolic function; (ii) presence of left ventricular hypertrophy (and possibly geometric form); and (iii) severe myocardial infarction (Sagnella, 1998). Recently, Tran *et al.* (2004) demonstrated upregulation of the pro-ANP convertase *Corin* gene in hypertrophic cardiomyocytes and failing myocardium. Conversely Lanenickel *et al.* (2004) demonstrated downregulation of atrial *Corin* mRNA expression in an experimental heart failure model. Although these data are conflicting, they do indicate an important role for both ANP and *Corin*, in the hypertrophic response.

In 2005, Chan *et al.* produced a *Corin* knockout mouse model, which compared to wild type animals exhibited spontaneous hypertension (increased after dietary salt manipulation), and cardiac and LV hypertrophy. The effects of hypertrophy in this model eventually led to a decline in heart function over time, characterised by a reduced fractional shortening in animals aged 35 weeks. However, the group also established that *Corin* was not a fundamental requirement to ensure embryonic development or postnatal survival, as *Corin* deficient mice developed normally with no abnormal pathology noted in other major organs such as the brain, kidneys, lung, liver and spleen.

In another study using angiotensin II (ATII) knockout mouse, it was established that the AT_2 receptor is essential for cardiac hypertrophy induction from pressure overload

(Senbonmatsu *et al.*, 2000; Ichihara *et al.*, 2001). These results contradict earlier findings employing AT_2 antagonists, which showed antigrowth effects exerted by the AT_2 receptor (Booz and Baker, 1996). Furthermore, a different strain of ATII knockout mice generated independantly did not exhibit any difference in cardiac hypertrophy development after pressure overload however vascular hypertrophy was enhanced in these mice (Brede *et al.*, 2001). Accordingly, a transgenic mouse over-expressing the AT_2 receptor in the heart was less susceptible to AT_1-mediated actions compared to controls (Masaki *et al.*, 1998) and developed less fibrosis after ATII infusion (Kurisu *et al.*, 2003), whereas hypertrophy induction was equal (Sugino *et al.*, 2000). ATII induced fibrosis was reduced in these animals by a mechanism involving the kallikrein kinin system (Kurisu *et al.*, 2003), which has been shown to have antihypertrophic and antifibrotic actions in the heart by the use of tissue-kallikrein overexpressing transgenic rats (Silva *et al.*, 2000). These findings together not only suggest a possible role for ATII as a physiologic modulator of cardiac hypertrophy, independent of a blood pressure effect but also the utility of experimental animals in cardiovascular research.

There is also an accumulating body of evidence to suggest a role for steroid hormones in cardiovascular disease, such as vitamin D (Zitterman, 2006). Abnormal vitamin metabolism, through deficiency of the active form of 1,25-dihydroxyvitamin D3, and acquired vitamin D resistance through a uraemic state, have been shown to be important in end stage renal disease (Andress, 2005). Vitamin D deficiency has long been known to affect cardiac contractility, vascular tone, cardiac collagen content, and cardiac tissue maturation. Recent studies using vitamin D receptor deficient mice as a model demonstrate a crucial role of vitamin D in regulation of the RAS (Xiang *et al.*, 2003). Additionally, there is emerging evidence linking treatment with vitamin D to improved survival on haemodialysis and improvement in cardiac function.

1.3.6 Gender Differences

The differences in blood pressure levels documented in human studies, between males and females, have also been reported in various animal models (Masubuchi *et al.*,

1982; Ganten *et al.*, 1989). In hypertensive rat strains, many investigators have found increased systolic blood pressure in SHR males in comparison to age matched females (Masubuchi *et al.*, 1982; Ganten *et al.*, 1989). Similar gender differences in the development of hypertension are also found in Dahl salt sensitive rats, SHRSP and the New Zealand genetically hypertensive rat (Ashton & Balment, 1991). A number of groups have reported blood pressure differences in SHRSP and SHR rat strains, consistent with a Y chromosome effect (Ely & Turner, 1990; Hilbert *et al.*, 1991; Jacob *et al.*, 1991). Concordant with these findings, Davidson *et al.* (1995), using a genetic cross between WKY and SHRSP, established that male offspring originating from a SHRSP progenitor, had significantly higher average systolic, diastolic, and mean arterial pressures at baseline compared with male F_2 hybrids from a WKY grandfather. There are, however conflicting reports with regards the effect of the Y chromosome in other rat SHR strains, for example studies using the Charles River SHR (SHR/crl) strain of rat (Vincent *et al.*, 1994, Ely & Turner, 1995) show no Y chromosome effect on systolic blood pressure.

Studies carried out in female SHR support the view that female hormones do not play a protective role against development of blood pressure similar to levels noted in male SHR. Ovariectomised female SHR at 4 to 5 weeks of age does not result in higher blood pressures than in intact females at 18 to 20 weeks of age (Reckelhoff, 1998; Reckelhoff, 2000). However, androgen treatment of ovariectomized female SHR causes an increase in blood pressure that is dose dependent (Reckelhoff, 1999), suggesting lack of testosterone may protect female SHR from the higher blood pressure found in males rather than female hormones. Similarly, studies have shown castration of male SHR results in reduced blood pressure, to the equivalent level of female SHR (Chen & Meng, 1991; Reckelhoff, 1998). The combined results of these studies are unclear as to the role of the Y chromosome in blood pressure regulation and the question still remains whether there is a cost to being male or simply a consequence to not being female.

Similar to gender associated effects observed in animal models of hypertension, a study by Vincent *et al.* (1996) illustrates the involvement of sex chromosome loci and heart weight in LH rats using reciprocal back-crosses between Lyon hypertensive (LH) and Lyon

normotensive (LN) rats. In populations where all rats carry an LH X chromosome, left ventricular weight was shown to be significantly higher than in groups where only 50% of rats carried the chromosome. Based on these results, they suggest that relative left ventricular weight in this animal model is genetically determined (estimated at 41%) with partial contribution by a locus on the X chromosome that is independent of blood pressure.

1.4 GENETIC MARKERS/MAPS

1.4.1 Genome Wide Quantitative Trait Loci Analysis

A quantitative trait is a trait that is continuously distributed within a population and is measurable by phenotypic variation due to genetic and/or environmental effects. Quantitative trait loci (QTL) are specific chromosomal region(s) which contain genes that have a significant effect on this variation and are generally identified by comparing the linkage (degree of covariation) of polymorphic molecular markers and phenotypic trait measurements. Much of genetic variation underlying disease susceptibility and morphology is, however complex. The ultimate goal of complex trait dissection is identification of the actual genes central to the trait and an understanding of the cellular roles and functions of these genes *in vivo*. Theoretically, by scanning the entire genome (genome-wide scan) in search of putative QTL, genes not previously implicated in pathways related to trait variation can be detected. Thus, QTL analysis is a phenotype driven means of identifying genomic regions that contain polymorphisms affecting the distribution of a measurable trait in a mapping population.

Genetic linkage is measurable by the recombination fraction (number of recombinants observed divided by the total number of meiotic events (progeny). If loci are unlinked (whether on different chromosomes or distanced on the same chromosome), approximately half of the progeny will be recombinants (50%). If genes are linked (less than 50%) parental combinations will predominate and in the case of closely linked genes (where no recombination has occurred) the percentage equals 0%. As the frequency of recombination between two loci is a function of physical distance on a chromosome, the recombination fraction may be converted into distance and expressed as centiMorgan (cM), where one cM represents 1% likelihood of recombination, corresponding to approximately 1-2 million base pairs of the mammalian genome (Lindpaintner, 1992).

Gene-gene and gene-environment interactions add to difficulty of QTL identification and detection. An important development in complex trait analysis is the use of

molecular/genetic markers, which are used to construct detailed genetic linkage maps. The accuracy and precision of locating these loci is partly dependant on the density of the linkage map created; the higher the map density, the more precise the location of the putative QTL. However, heritability of the trait, genetic nature (dominant, recessive or additive) and the number of genes involved also affect the likelihood of success in QTL mapping. For any given QTL, the mapping resolution depends on the number of recombination events in the mapping population as well as the type of population studied.

Progress in human QTL mapping is more slow-moving than in animal counterparts, mainly due to the constraints involved in human analyses, for example ethical considerations, recruitment of data subjects and limitations presented by outbred, heterogeneous population strata. Therefore, the use of experimental inbred animals is frequently the first step in QTL-mapping and so will be the focus of this section. Statistical associations between the markers and quantitative traits are established through statistical approaches ranging from simple techniques, such as analysis of variance (ANOVA), to models that include multiple markers (composite interval mapping) and interactions (epistasis). The advantages of experimental designs and statistical genetic approaches to efficiently map QTL in experimental line-crosses are numerous.

Simpler statistical approaches to QTL detection are methods that assess differences in phenotypic means for single-marker genotypic classes (single marker analysis), however this type of analyses focus on detecting individual markers rather than genomic regions. A more sophisticated method of QTL analysis, which relies on the estimated order of markers and map distances, is interval mapping. The additional information gained from understanding the relationships between markers is essential to QTL methodologies aiming to locate QTL, as the linear arrangement of markers into linkage groups, produces a genetic map for locating QTL relative to marker intervals (or statistically related sets of markers). In addition to providing a structure in which to search for QTL, the estimated genetic map allows for the approximation of missing marker information by using flanking marker genotypes to infer information for missing marker genotypes. The intervals defined by ordered pairs of markers are searched in increments (for example, 2 cM), and

statistical approaches are used to test the likelihood that a QTL is present at the location within the interval or not. It is important to note that interval mapping, statistically tests for a single QTL at each increment across the ordered markers in the genome. Results of the tests are expressed as LOD (logarithm of the odds) scores, which compare the evaluation of the likelihood function under the null hypothesis (no QTL) with the alternative hypothesis (QTL at the testing position) for the purpose of locating probable QTL.

Jansen (1993) and Zeng (1994) independently proposed the combination of interval mapping with multiple regression analysis – composite interval mapping. This approach tests for QTL at an interval, whilst using other markers as covariates to control for other QTL outside this defined window of analysis, thus reducing residual variance. The criticism of this method is the limitation to one-dimensional scans across the genetic map, which is challenged at times by the multiplicity of several interacting QTL effects (Piepho, 2001). Examples of analyses using these three QTL analysis techniques are depicted in Figure 1.8. Clearly, the quality of genome coverage by molecular markers (i.e. even distribution of markers) can also critically affect the chances of success in any mapping project, therefore it is important to achieve even spacing of markers before undertaking any QTL analysis (Rapp, 1991).

Hilbert *et al.* (1991) and Jacob *et al.* (1991) independently completed a genome wide QTL analysis in search of hypertension genetic determinants in a $SHRSP_{Heidelberg}$ x WKY F_2 cross. Three chromosomal loci with LOD scores of over 3.0 were identified, leading to the mapping of locus (BP1 or BP/SP-1) on rat chromosome 10, where the candidate gene angiotensin converting enzyme (ACE) is positioned. A second locus (BP2) was mapped to a second locus by Jacob *et al.* (1991) to chromosome 18 and linked to baseline diastolic blood pressure with a significant LOD score of 3.23, whilst Hilbert *et al.* (1991) mapped an X-linked locus contributing to high blood pressure. Subsequent, blood pressure QTL have been identified in the $SHRSP_{Izumo}$ (Nara *et al.*, 1993; Nabika *et al.*, 1997) on chromosomes 1 (basal blood pressure) and 3 (basal and salt-loaded blood pressure).

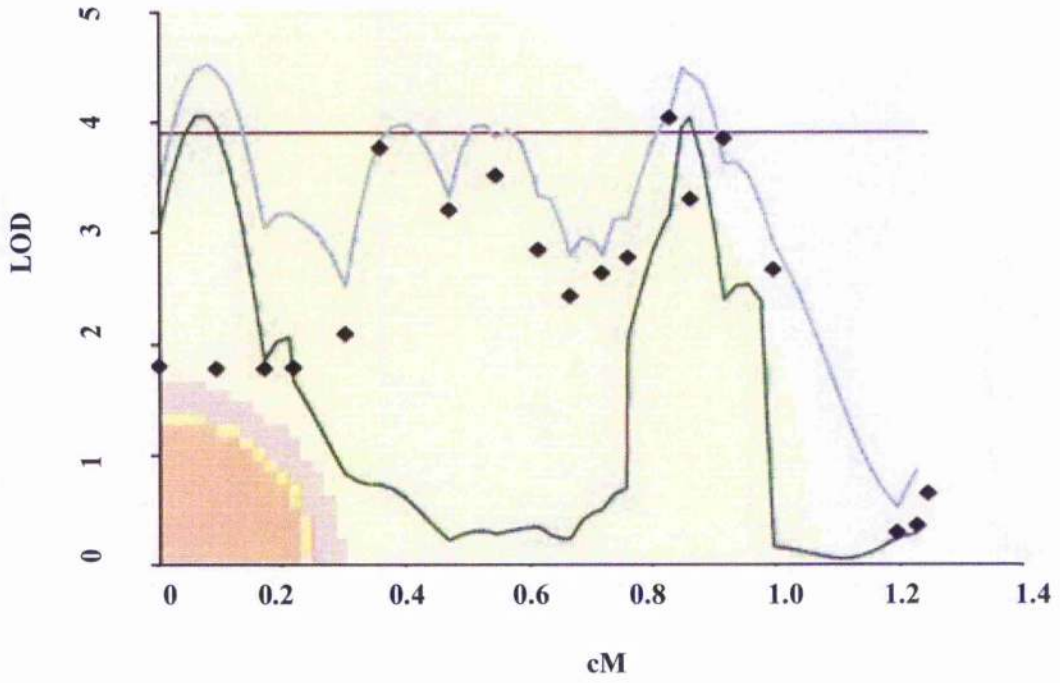

Figure 1.8 Choices of analysis for quantitative trait locus mapping - QTL analysis carried out using several different approaches: single-marker analysis using a t-test (black diamonds); interval mapping (blue line); and composite interval mapping (green line). The red line represents the 95% significance level on the basis of 1,000 permutations of the phenotypic data. Single-marker t-tests identify one significant marker, interval mapping locates four maximum QTL locations on the LOD profile, and composite interval mapping finds two significant QTL. Differences between single-marker analysis, interval and composite interval mapping result from using an estimated genetic map. The difference between interval mapping and composite interval mapping is the result of composite interval mapping's use of a 'window' or genomic region that allows other effects that are outside the window, but associated with the quantitative trait, to be eliminated from the analysis point under consideration. The benefit of defining a window is that the variation associated with the point of analysis is confined to the QTL effects within the window and not outside this field of view, thereby reducing the effects of linked and 'ghost' QTL.

As various groups have also identified the same loci in other experimental crosses, this result suggests that they are of general significance in rats. Since a QTL allele may have differing effects when bred onto a different genetic background (Rapp & Deng, 1995), genetic mapping results need not be consistent among different crosses and for that reason is exemplar of the polygenic nature of hypertension.

1.4.2 Comparative Genome Analysis

The suggestion that genomic organisation may be evolutionarily conserved between species was postulated in the early 1900s (Castle and Wachter 1924; Haldane 1927). Studies linking banding conservation and chromosome painting (ZOO-FISH) have since shown that considerable stretches of DNA are conserved in mammalian species as divergent as drosophila and humans (Nash and O'Brien 1982; Sawyer and Hozier 1986; Scherthan *et al.* 1994; Weinberg and Stanyon 1995). Although these studies showed a degree of genome commonality between species, precise high resolution gene order was only achieved through genetic/physical mapping. Several groups have established that gene order tends to be conserved between mammals (Oakey *et al.* 1992; Stubbs *et al.* 1994), which in turn has lead to the concept of constructing and using maps based on genetic sequence and map information between multiple species (Nadeau 1989; Lyons 1997). Comparative genomics was successfully applied in cardiovascular research, by Julier *et al.* (1998) and Baima *et al.* (1999) with the identification of a region involved in blood pressure regulation on rat chromosome 10 and a susceptibility locus for human hypertension on human chromosome 17q.

1.4.3 Candidate Gene Analysis

Candidate gene analysis is a key step in current strategies used for disease gene identification and is used widely to investigate the genetics of hypertension and cardiovascular disease, with case-control association analyses among the most common study design (Dominiczak *et al.*, 1994). Selection of a candidate gene generally requires prior understanding of the physiologic pathways acting to influence the disease state (Dominiczak & Lindpaintner, 1994) and therefore is based either on the known or

suspected function of the gene, sequence homology with other known gene(s) interaction of the protein product with another protein or tissue specificity of gene expression. In the post genomic era, investigating genetic variation by sequence comparison of candidate genes is becoming an increasingly important and feasible tool to study phenotypic variation.

In addition, detection of single nucleotide polymorphisms (SNPs, pronounced "snips") has permitted the identification of groups of SNPs that move simultaneously in families and populations; haplotype blocks, characterized by a relatively small number of SNPs (tag-SNPs). Regardless of these major advances and constantly improving genetic markers, the problems concerning statistical power remain an issue. With these difficulties forefront, prospective studies should take account and include a sufficient sample size to detect small genetic effects and gene-gene and gene–environment interactions. One such study is the UK Biobank, who potentially may be one of the best DNA resources available for candidate gene studies in cardiovascular and other complex traits. Other approaches to tackle candidate genes is to limit investigations to positional candidate genes currently emerging from genome wide scans or alternatively reproduce the QTL containing region in a whole organism.

1.4.4 Congenic Strains and Substrain Production

The initial screening of the genome yields only approximate locations of QTL, therefore it becomes necessary to confirm and refine these locations. One strategy is the use of congenic strains (Figure 1.9), in which a chromosomal segment from one strain (recipient) is selectively replaced through breeding, by the homologous portion of the same chromosome from another strain (donor). If the preferred phenotype, for example cardiac hypertrophy, of the congenic strain is significantly different from the recipient strain, it is then assumed that this particular chromosomal fragment contains a QTL contributing to this phenotype. Congenic strains are traditionally developed through a series of backcrosses - the donor strain (which contains the genomic region of interest) with the recipient inbred strain, together with selection for progeny heterozygous for the desired region in each backcross generation (Wakeland *et al.*, 1997). Essentially, this leads to a

'dilution' of the donor genome into the recipient genome, with continuous maintenance of the QTL. The introgressed region is fixed homozygous by intercrossing and the resulting congenic strain has a genetic background identical to that of the recipient inbred strain with the exception of the introgressed region.

Whilst the protocol for breeding congenic strains is straightforward, the main constraint of this strategy is time limitation, with at least 2 ½ - 4 years required to achieve background purity. Continual additions of microsatellite markers to rat maps provide an opportunity to reduce this time constraint with the application of a 'speed congenic' approach. This requires analysis of polymorphic marker loci distributed throughout the genome, in order to allow specific selection of male progeny carrying the target genomic region, whilst also retaining the lowest background heterozygosity throughout the remaining genome, at each successive backcross generation. Selective breeding with these 'best' males accelerates the elimination of unwanted donor genome, thereby reducing the number of backcross generations required to successfully construct a congenic strain to typically 4 - 5 backcrosses.

1.5 GENE EXPRESSION PROFILING

1.5.1 Microarray analysis and real time RT-PCR

Gene expression profiling at the RNA level has been significantly facilitated by microarray analysis and quantitative real-time-PCR (RT-PCR). Microarray analysis is a powerful technique for high-throughput, large-scale profiling of gene expression allowing investigation of several thousand genes simultaneously, both in diseased and non-diseased tissues and/or cell lines. Although RT-PCR analysis provides precise quantification over a wider dynamic range of expression levels, this technique is not suited for simultaneous

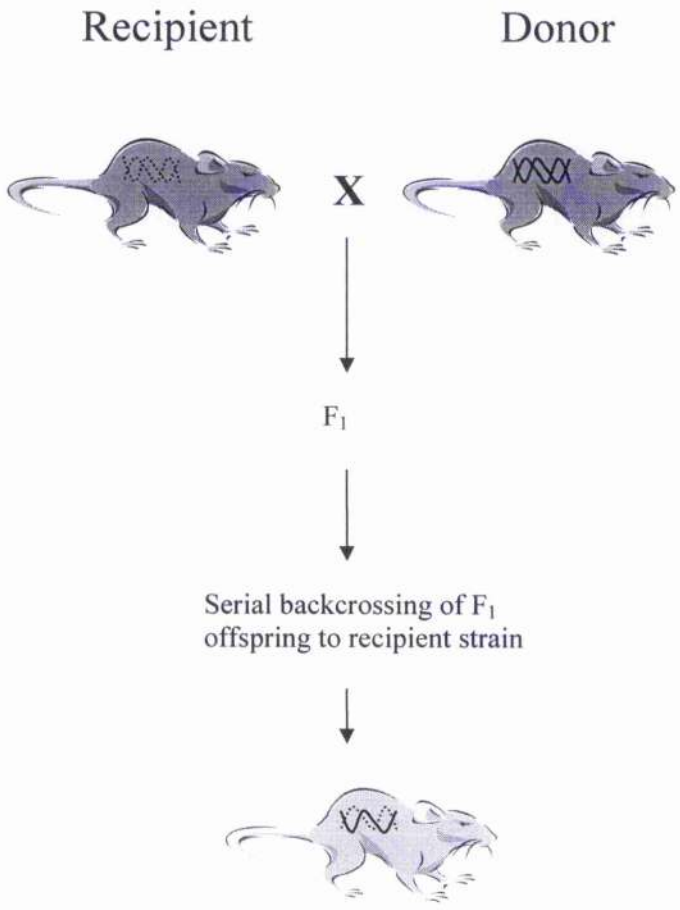

Figure 1.9 A cartoon representing the basic principals behind the production of congenic strains. Selective introgression of a chromosomal region from a donor to a recipient strain. Typically, the production of a congenic line can take between 8-10 serial backcrosses, to ensure elimination of background heterozygosity (adapted from McBride *et al.*, 2003).

analysis of large numbers of genes, genome wide. Therefore, array analysis is often used as a tool for screening target genes that are differentially expressed between biological samples, and quantitative RT-PCR allows for precise quantification and validation of the microarray results.

Although microarray is most commonly equated with DNA microarray, the history of microarray began with oligopeptides in the context of immunoassays (Etkins, Chu & Micallef, 1989). In the late to mid-eighties, the concept was tendered that sensitivities of immunoassays could be dramatically increased using chemiluminescent and fluorescent substances even when the reaction is localised in "microspots" distributed on an inert solid support. Several years later, Pease *et al.* (1994) reported the development of densely packed arrays of oligonucleotide probes. These probe arrays, termed DNA chips, were used for hybridization to target DNA sequences. The scope of microarray has since been extended to include other biologically important entities, such as protein, carbohydrate and RNA interference (RNAi) microarray and has enabled a paradigm shift in research biology from the traditional hypothesis-driven research to a more data-driven research.

From inception, microarray technology has expanded into several supplementary tracks. One of the most widely used approaches, first developed by Stanford University and sold commercially by sources such as Agilent, uses complimentary DNA (cDNA) clones as probes (Schena *et al.*, 1996). The most frequently used competing method developed by Affymetrix employs the use of short, 25mer DNA oligonucleotides as probes that are chemically synthesized using sequence information from genomic databases (Lipshutz *et al.*, 1999). More recently, Illumina has provided an assay for multiplex SNP genotyping for high-throughput genetic analysis of large populations using a bead array platform. Arrays are made of beads located on silicon slides, which are multi-channel pipette compatible for loading multiple samples onto a single silicon slide. This format allows many samples to be processed in parallel and differs from Affymetrix, which operates a single channel approach i.e. a single sample per chip (Shen *et al.*, 2005).

Numerous groups have used microarray technology to aid gene identification at the genetic and physical level, and are agreed that gene order is relatively unchanging, with conserved synteny between mammalian species. Aitman *et al.* (1999) identified a gene responsible for defective fatty acid metabolism in the SHR strain (Cd35) using cDNA microarrays and rat chromosome 4 congenic animals. McBride *et al.* (2003) investigated differential gene expression in whole kidney RNA isolates from parental SHRSP, WKY and congenic strain (hypertensive background, introgression of WKY chromosome 2 segment). By taking advantage of the genotypic similarities and differences between the congenic and parental strains, they were able to reduce the number of differential genes under investigation and identify glutathione S-transferase mu-type 1 (Gstm1), a positional and physiological candidate gene involved oxidative stress.

Recently, Kong *et al.* (2005) considered gene expression in Dahl salt-sensitive rats, during physiological hypertrophy, pathological hypertrophy, and heart failure. They noted increased expression of stress response genes (e.g., heat shock proteins) and inflammation-related genes (e.g., pancreatitis-associated protein and arachidonate 12-lipoxygenase) in the pathological processes but not in physiological hypertrophy. Expression differences in ANP and BNP were also evident dependant on specific conditions, indicating that these genes may influence cardiac pathological hypertrophy or simply be markers for hypertrophic response and heart failure. This study demonstrates gene regulations specific to distinct hypertrophic stimuli and provides evidence of gene alterations as well as significantly altered pathways during various forms of cardiac hypertrophy.

DNA microarrays have also been used to define comprehensive gene expression profiles in SHR strains aged between 12 and 20 months, during the development of LVH and in the transition to diastolic heart failure (Jaana *et al.*, 2005). Consistent with previous reports, the group observed a progressive LVH and a thickening of LV walls leading to diastolic heart failure with preserved systolic performance. The relatively small number of known altered genes (ninety two) corresponds with previous observations indicating that more genes alter in response to acute rather than chronic overload. Many of the genes identified are known contributors of LVH and heart failure in SHR. A key finding from the study by

Jaana *et al.* was a lack of immediate gene expression shift when diastolic dysfunction progressed to diastolic heart failure. Instead, significant changes in gene expression developed over time and were associated with hypertrophic process and development of heart failure. In addition, upregulation of several inhibitors of proteolytic enzymes (tissue inhibitor of metalloproteinase-1, plasminogen activator inhibitor-1) and cysteine endoproteases (cathepsin K and cathepsin S) suggests dynamic regulation of matrix degradation and deposition during the LV remodelling process in hypertrophic heart failure (Jaana *et al.*, 2005) in this hypertensive rat strain.

The studies discussed thus far, serve to demonstrate the inherent genetic complexity of hypertension and LVH, which involves a complicated pattern of altered gene expression between hypertensive rat strains of varying ages and sex. Although the collective data is difficult to interpret, the results emphasize the complex genetic nature of hypertension and LVH and illustrate the importance of the genetic cross studied and almost certainly the conditions and method of phenotyping.

1.6 HIGH FIDELITY PHENOTYPING

1.6.1 Haemodynamic Profiling

The goal of any genetic mapping experiment is to detect and localise the genetic elements responsible for the variation in a phenotype of interest. Therefore, careful selection of the type of species examined, cross, sex, parental strains and methods used for measuring the phenotype is crucial to the design of the mapping experiment. Traditionally, genotyping and phenotyping strategies have been evaluated in terms of their power to detect a genetic effect, which depends on the size of the genetic effect and the phenotypic information collected in the experiment. In general, a researcher has little control over the former, but phenotype and genotype strategies can be designed to extract maximum information, subject to cost or other constraints.

There are various ways in which to determine haemodynamic parameters in experimental animals. The most common system currently employed for monitoring blood pressure in conscious rats and mice is the tail cuff (Bunag, 1983; Bunag, 1991; Van Vliet *et al.*, 2000). Another, less common but more invasive method, is the exteriorized catheter, which feeds a pressure transducer located outside the cage. There are however, considerable drawbacks associated with these procedures, which in many respects make each of these techniques undesirable as a wholly exact means of obtaining pressure measurements (Van Vliet *et al.*, 2000). Recent studies have shown measurements of physiological variables, such as heart rate, and body temperature and activity, from freely moving animals by using an implantable radiotelemetry transmitter is more efficient, reliable, less labour intensive and permits continuous monitoring of blood pressure (allowing for diurnal variation analysis) (Hess, Clozel & Clozel, 1996; Van Vliet *et al.*, 2000). Several groups have validated radiotelemetry as a quantitative method for acquisition of blood pressure data in both mice and rats (Brockway, Mills & Azar, 1991; Hess, Clozel & Clozel, 1996). More recently, non-invasive techniques for the evaluation of functional and dynamic processes such as cardiac function and ventricular remodelling are increasingly preferred, in particular when serial measurements is required on living animals during development, genetic manipulation and/or in response to pharmacological or surgical interventions.

1.6.2 Cardiac Imaging Techniques

High spatial and temporal resolutions are required to preserve signal fidelity when imaging small mammals, which poses a problem on a technical level. Several groups have developed cardiovascular imaging modalities suitable for rodent applications, with ultrasound techniques such as echocardiography currently the most widely used. With constant advances in medical imaging diagnostics, magnetic resonance imaging (MRI) is a non-invasive exact technique which offers new insights into cardiac remodelling processes. These non-invasive methods are convenient, easy to apply and have been used successfully to detect and evaluate numerous cardiovascular phenotypes in small mammals such as mice and rats.

Cardiac echocardiography is a non-invasive procedure that makes use of ultrasonic waves directed over the chest wall to obtain a graphic record of the heart's position and size, motion of the walls, or internal parts such as the valves (Feigenbaum, 1996). Sonar or diagnostic ultrasound was initially a crude, two-dimensional scanning technique, with A-mode examinations merely offering a location and amplitude of the returning ultrasonic signal. But it was Edler and Hertz (Edler and Hertz, 1954) who are accredited with the first use of cardiac echocardiography as the method is currently applied.

In validation studies, M-mode echocardiography has been shown to measure LVM with reasonable accuracy ($r > or = 0.90$ versus *post mortem* values) in rats ranging in body size and age, however reproducibility of these results can vary due to several factors including respiratory depression caused by anaesthesia, the position and shape of the heart (dense bone matter can obscure view) and quick heart rate averaging 350-400bpm (de Simone *et al.*, 1990; Devereux *et al.*, 1994; Slama *et al.*, 2005). Recent research indicates that the level of LVM measured in humans by M-mode echocardiography is a stronger predictor of subsequent morbid events and death than blood pressure or other conventional risk factors, except age (Devereux *et al.*, 2003). For these reasons, accurate, quick and reproducible evaluation of LVM in experimental animals is important to the study of cardiovascular research with respect to identification of genetic components involved in the pathogenesis of LVH and the development of pharmacological agents which prevent or reverse the phenotype.

Over the past ten years, magnetic resonance imaging (MRI) has rapidly progressed from a purely anatomical imaging technique to one that reports on a wide variety of tissue functions (Higgins *et al.*, 1988; Gibbons & Araoz, 2005). Cardiac magnetic resonance (CMR) is currently the ideal method of choice for precise measurements of ventricular volumes, function and left ventricular mass in humans (Watzinger *et al.*, 2005). This is due to high spatial resolution, excellent delineation of endocardial and epicardial borders, good image quality and ability to reconstruct the heart shape in three dimensions. Results are not only independent of geometrical assumptions but are highly reproducible and accurate (Bastarrika *et al.*, 2005). CMR is particularly useful in research, as it is highly sensitive to small changes in ejection fraction and mass, and a relatively small number of

subjects are required for study. Also, due to the excellent reproducibility of data, temporal follow-up of any individual in the clinical setting is a more realistic possibility.

Irrespective of current imaging fashions, *in vivo* assessment of cardiac morphology and function in experimental animals using ultrasound imaging techniques such as echocardiography suffer from high signal to noise ratio. High fidelity, non-invasive imaging methods such as CMR offer desirable option to evaluate and monitor even fractional changes in heart weight and function in order to characterize fully the influence of pharmacological and/or surgical interventions and genetic manipulation.

Validation of MRI to measure cardiac function and mass has been shown in mice with numerous MR studies performed using transgenic animals (Franco *et al.*, 1999; Woodman *et al.* 2002; Schlieper *et al.*, 2004). More advanced techniques like perfusion imaging, delayed enhancement or tag imaging are now emerging (Waller *et al.*, 2000; Zhou *et al.*, 2003). Nevertheless, more effort is required to standardize acquisition protocols such as obtaining a reliable cardiac trigger, type of anaesthesia used, acquisition time and more uniform method of data analysis. In this respect, more improved 'gold standard' methods to measure cardiac parameters are necessary. Regardless of this, the results generated so far from CMR, indicate that this technique can be applied to various aspects of cardiac research using small animals.

1.7 AIMS

In a previous genome wide scan using an F_2 cross, our group identified a QTL for heart weight on chromosome 14 in a Glasgow colony of SHRSP. The overall aim of this study was to improve the current genetic linkage map of rat chromosome 14 to confirm this QTL and combined with high fidelity phenotyping identify QTL determinants of left ventricular mass in the SHRSP.

In order to achieve this aim, it was necessary to carry out the following steps:

I. Confirm QTL previously identified using an improved genetic map and genotyping. Construct congenic strains using speed congenic strategy, in both directions, i.e., by (A) transferring a large region of chromosome 14 from the SHRSP to the WKY genetic background and looking for an increment in phenotype and (B) transferring the 'minus' allele from the WKY to the SHRSP and looking for a decrement in phenotype.

II. High fidelity phenotyping using echocardiography and MRI to detect differences in LV geometry and mass in congenic and parental strains.

III. Comparative mapping to identify candidate genes in the QTL region and differential expression analysis in parental and congenic strains using, microarray and RT-PCR gene expression assay techniques.

IV. Direct sequencing of candidate genes to supplement genetic mapping and gene expression analysis and identify any single nucleotide polymorphisms (SNPs) in both exonic and upstream gene regions that may be of important functional relevance in relation to phenotype.

CHAPTER 2
METHODS

2.1 GENERAL LABORATORY PRACTICE

Reagents and equipment used were of the highest quality commercially available. During all laboratory procedures, laboratory coat and powder-free latex gloves were worn. Reagents deemed hazardous were dealt with appropriately as described in the Control of Substances Hazardous to Health regulations by the wearing of laboratory spectacles, facemasks and use of a fume hood (Holliday, Fielding & Hocking, Ltd., UK). Appendix I lists the suppliers of all chemicals and reagents used and protocols followed in the preparation of solutions.

Standard laboratory glass wear was washed in Decon 75 detergent, rinsed with distilled H_2O and dried in a 37°C oven. Reagents were weighed using a Mettler P2000 balance (up to 3 decimal places) or a Mettler AT250 balance (up to 5 decimal places) both obtained from European Instrument Sales. The pH of solutions was obtained using a CO720 digital pH meter (WPA Cambridge, UK), which was calibrated on a regular basis with solutions of pH7.0 and 4.0 prepared from buffer tablets (Sigma, Europe). Volumes between 0.1 µl and 5,000 µl were dispensed using appropriate Gilson pipettes (Gilson Medical Instruments, USA) and pipette tips (Alpha Laboratories Ltd, UK). Unless stated otherwise, autoclaved distilled H_2O was used to prepare aqueous solutions. To dissolve solute in appropriate solvents a HB502 stirrer with hot plate capabilities was used (Barlow-world Scientific Ltd., UK). Centrifugation of up to 14,000 rpm was used for small samples (maximum of 2,000 µl) using a Centrifuge 5420 (Eppendorf, UK). Larger samples were centrifuged using an IEC centra-GP8R centrifuge (Life Sciences International Ltd, UK).

2.2 ANIMAL STRAINS

All animals were housed under controlled environmental conditions. Temperature was maintained at 21°C, 12-hour light/dark cycles were from 7am to 7pm and rats were fed standard rat chow (rat and mouse No.1 maintenance diet, special diet services) and H_2O provided ad libitum. Offspring were weaned after 3 weeks of age when they were sexed,

ear-tagged (National Band and Tag Co., USA) and caged (maximum 3 animals per cage) according to sibling group and sex.

All procedures carried out on experimental animals were in accordance with the Animals (Scientific Procedures) Act 1986 under the project licence held by Prof. A.F. Dominiczak. Inbred colonies of the SHRSP and WKY strains have been maintained in Glasgow by brother-sister mating since 1991, when 6 males and 7 females of each strain were given as a gift by Dr. D.F. Bohr from the Department of Anatomy and Cell Biology at the University of Michigan, USA. Prior to this, the colonies were maintained as inbred for over 15 years in the National Institutes of Health, Bathseda, USA. Maintenance of the colony integrity as well as the hypertensive and normotensive phenotypes was achieved by selecting SHRSP adult breeders with blood pressure values between 170-190 mmHg (males) and 130-150 mmHg (females), and WKY adult breeders with blood pressure values between <140mmHg (males) and <130mmHg (females). Routine microsatellite screening was used to confirm homozygosity of all loci within groups of animals from each strain, selected at random.

2.2.1 F_1 and F_2 Strain Production

An F_2 cohort was previously produced in 1996 from two reciprocal F_1 genetic crosses. One male SHRSP was mated with 2 WKY females (in cross 1) and 1 male WKY was mated with 2 SHRSP females (cross 2) to produce the F_1 generation. Three F_1 males and 6 females were then mated from each cross to produce an F_2 generation. Reciprocal crosses were produced in order to ensure representation of the Y chromosome from both hypertensive and normotensive strains.

2.2.2 Congenic Strain Production

The traditional development of a congenic strain requires 8-12 backcross generations and therefore takes over 4 years. To reduce the time taken to produce congenic strains a speed congenic approach was implemented (Figure 2.1). By using this breeding

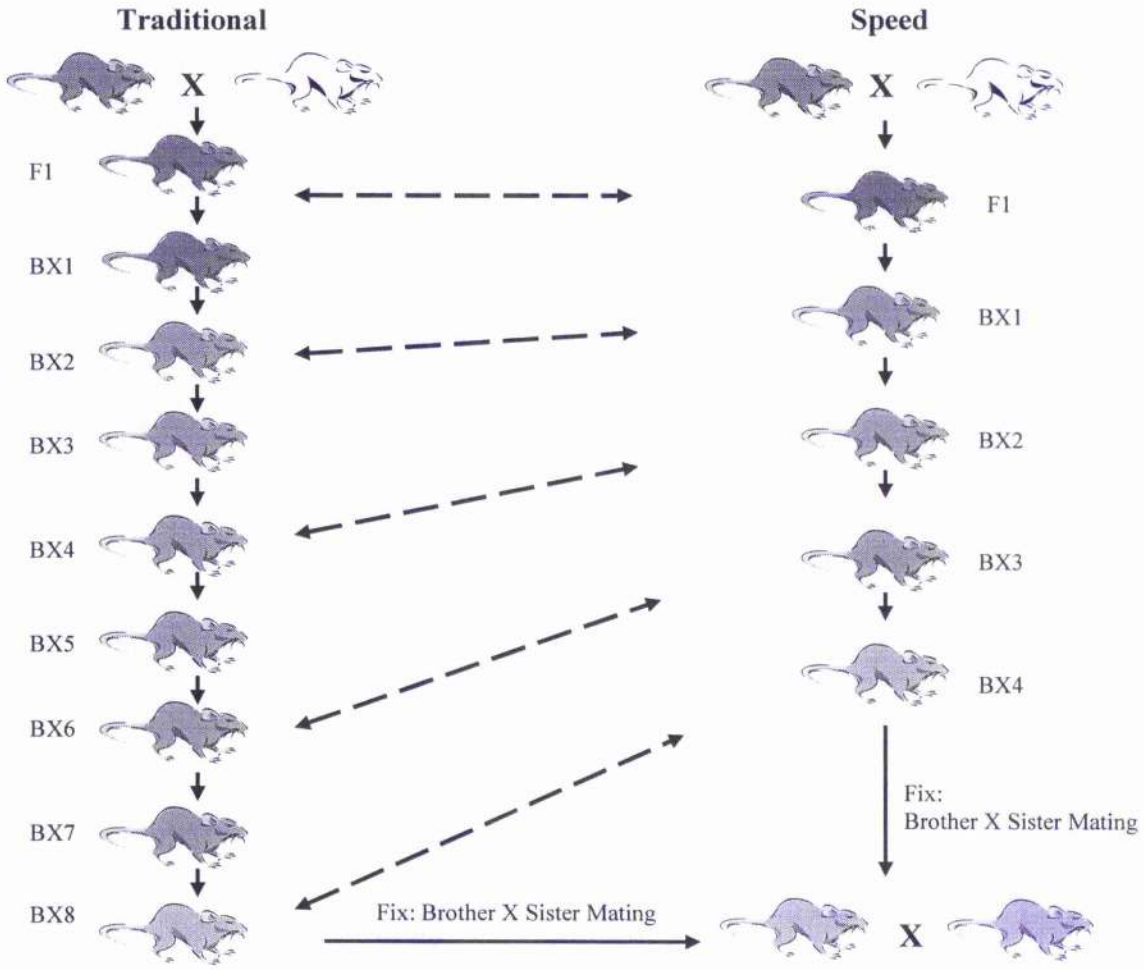

Figure 2.1 Diagram depicting congenic strain production. The traditional method of eight backcrosses (BX) versus the speed strategy previously used to produce rodent congenic strains (Markel *et al.*, 1997; Jeffs *et al.* 2000). The dashed arrows indicate the theoretical backcross stage at which background heterozygosity is the same.

strategy, the transfer of regions indicated in the genome-wide scan as QTL for LVMI on rat chromosome 14, was initiated. Regions of rat chromosome 14 were transferred from the donor SHRSP strain to the genetic background of the recipient WKY and vice versa within 4 to 5 backcross generations (Figure 2.1).

The F_1 population was generated by mating 1 SHRSP male with 2 WKY females (cross 1) and mating 1 WKY male with 2 SHRSP females to produce the reciprocal lines (cross 2). The first backcross consisted of F_1 generation males mated with females of the recipient background strain. Thirteen microsatellite markers were genotyped throughout the chromosome 14 region as well as 168 background microsatellite markers spanning the rest of the genome. Background markers were selected based on optimal coverage of the rat genome (Clark *et al.* 1996, Jeffs *et al.* 2000), using a variety of rat genome databases available on-line - Ratmap: The Rat Genome Database, Sweden at http://ratmap.gen.gu.se/; The Whitehead Institute Center for Genome Research Rat Mapping Project, Boston, USA at http://www.genome.wi.mit.edu/rat/public/ and the Wellcome Trust Centre for Human Genetics Genetic Linkage Maps of the Rat Genome, Oxford, UK at http://www.well.ox.ac.uk/~bihoreau.

The "best" males were selected at this stage for use in the next round of backcrossing. These animals are defined as having heterozygosity of the donor strain genotype at the QTL region on chromosome 14 (as indicated by the genotypes of the chromosome 14 microsatellite markers) and least heterozygosity of donor alleles in the genetic background (indicated by the genotypes obtained from the background microsatellite markers). This procedure was repeated for 4-5 backcrosses, until all the background microsatellite markers showed no contamination of the donor genome. At this stage one male and one female with heterozygosity at the QTL of interest were mated to fix the QTL region in a homozygous state. These fixed congenic strains are maintained through intercross brother-sister mating.

2.3 PHENOTYPIC ANALYSIS

2.3.1 Tail-cuff Plethysmography

This procedure was performed on rats heated to 30°C, wrapped in a cloth, and an inflatable cuff placed on their tail along with a piezoceramic transducer (Hartmann & Braun type 2) for pulse detection. The pressure in the cuff could be controlled in 1mmHg steps over a 300mmHg range and the resulting pulsation detected by the transducer was amplified and filtered before being displayed on computer using IBM compatible software. This signal was visualised as a function of pressure and an estimation of the systolic pressure was marked. An average of twelve readings were taken for each rat per sitting and a mean value was calculated around a standard deviation of approximately 10mmHg, 3 sittings were taken for each rat and the average of all three sittings was taken for the true systolic blood pressure value for that age.

2.3.2 Radio-telemetry

To directly measure systolic pressure, diastolic pressure, mean arterial pressure, heart rate and motor activity the Dataquest IV telemetry system (Data Sciences International, USA) was utilised. Prior to implantation of the radio transmitter, calibrations were verified to be accurate within 3mmHg. Each transmitter could be used a maximum of three times following re-sterilisation in Terg-A-Zyme, an enzyme activated powdered detergent (Alconox Inc, USA).

Implantation was performed using halothane (2.5-3%) anaesthetised animals at 12 weeks of age, under standard sterile conditions. Temporary externalisation of intestines allowed access to the abdominal cavity where silk sloops were placed at the aorta below the renal arteries and around both iliac arteries. The sloops were held to temporarily occlude blood flow to the area and an incision if approximately 1mm diameter was made in the aorta using a 21 G needle, just above the bifurcation point of the iliac. The catheter of the transmitter was then inserted into the hole, against the flow of pressure and held in place

with a sterilised cellulose patch (Data Sciences International, USA) and Vet Bond biological glue (Data Sciences International, USA). Sloops were removed from the arteries and intestines were returned to the abdominal cavity and the transmitter was sutured to the abdominal wall.

Each animal was placed in an individual cage, placed over a receiver which was connected to a computer for data acquisition. Haemodynamic data was obtained every 5 minutes for 10 seconds. As stabilisation of measurements postoperatively required 7 days, day 7 to day 42 were considered as baseline measurements. From day 43, until sacrifice on day 64, 1% NaCl was administered in their drinking H_20 (salt-loaded period).

2.3.3 Body and Cardiac Measurements

The body weight of each rat was measured using a CT200V portable balance (Ohaus Corporation UK). Cardiac weight was measured using a Mettler AT250 balance after removal and blotting on tissue paper to remove excess blood. Both atria and right ventricle were removed prior to weighing of left ventricle and septum. Ratios of heart weight to body weight (cardiac mass index; CMI) and left ventricle plus septum weight to body weight (left ventricular mass index; LVMI) were determined and expressed as mg/g to correct for differences in body size.

2.3.4 Echocardiography

All animals were examined using a Medison Sonoace SA8800 (Diagnostic Sonar, Livingston, UK) interfaced with a JVC Super-VHS video recorder for continuous monitoring and recording of moving images. The transducer was a 7.5MHz, 128 line phase-array system, with an adjustable 60° imaging angle and a 2cm footprint with an imaging depth of up to 7.5cm and an accuracy of 10% in distances between 1-60mm.

Animals were sedated by intraperitoneal injection of Hypnorm (approx. 0.1-ml of Hypnorm per 100gram body weight) and the chest was shaved. Ultrasound gel was used to dispel

any pockets of air trapped in the fur. The rat was positioned to lie in the left lateral position, short-axis 2-dimentional B-mode and corresponding M-mode images were obtained through the left parasternal window at the level of the papillary muscles. Images were adjusted in order to obtain the optimal dynamic range of the displayed image (Figure 2.2a). Data from six consecutive cardiac cycles from each M-mode tracing was used in the following equation for the calculation of left ventricular mass –

$$\text{LV mass} = 0.8\{1.04[(\text{EDD} + \text{PWT} + \text{AWT})^3 - \text{EDD}^3]\} + 0.6.$$

Where PWT = Posterior wall thickness (mm); AWT = Anterior wall thickness (mm); EDD = End diastolic dimension (mm).

Each echo examination consisted of 3-5 sets of images from both B-mode and M-mode and lasted for 5-10 minutes. The M-mode images were selected based on good edge definition when both the anterior and posterior cardiac walls were clearly visible, and when there was a regular cardiac cycle with very little change in the dimensions between beats. Within 24 hours of echocardiographic examination, animals were transported to 7T MRI unit in Garscube for a cardiac magnetic resonance imaging (MRI) scan.

2.3.5 Magnetic Resonance Imaging

Cine MRI was performed on a 7 T-Biospec (Bruker, Germany) using an ECG-triggered FLASH-sequence. For rat imaging a rat size whole body coil was used as a transmitter and a surface coil as a receiver, with the animal placed in a small cradle and lightly anesthetised with halothane gas administered in nitrous oxide/oxygen (70:30). An ECG- fast gradient echo (FLASH) cine sequence was used. A flip angle of 30 - 40 degrees, echo time of 1.1ms and repetition time of 3.2ms was used. A total of 12 frames per heart cycle was obtained, resulting in a total acquisition time (TAT) for one cine sequence of 4 minutes depending on heart rate (TAT = 128 phase encoding steps X averaging steps X length of one heart cycle).

a)

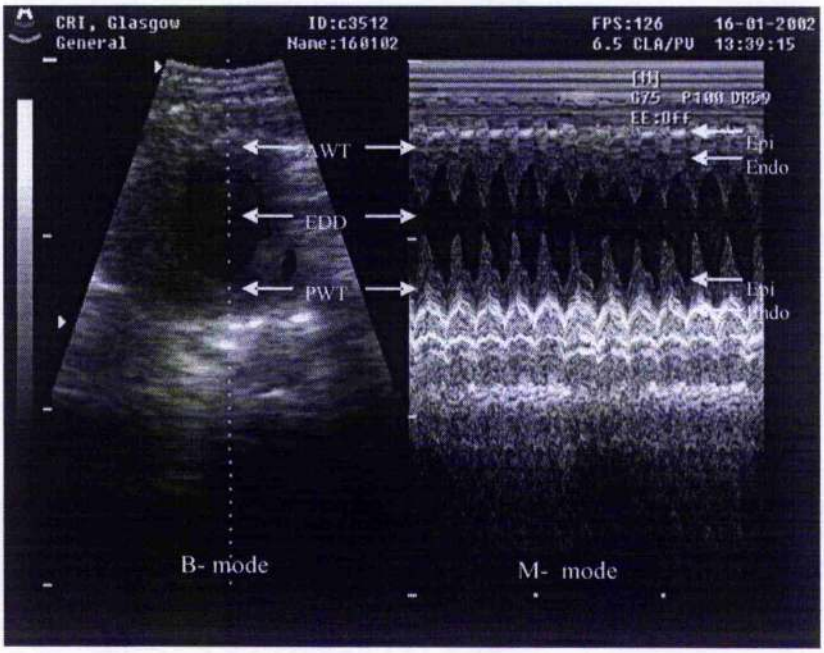

b)

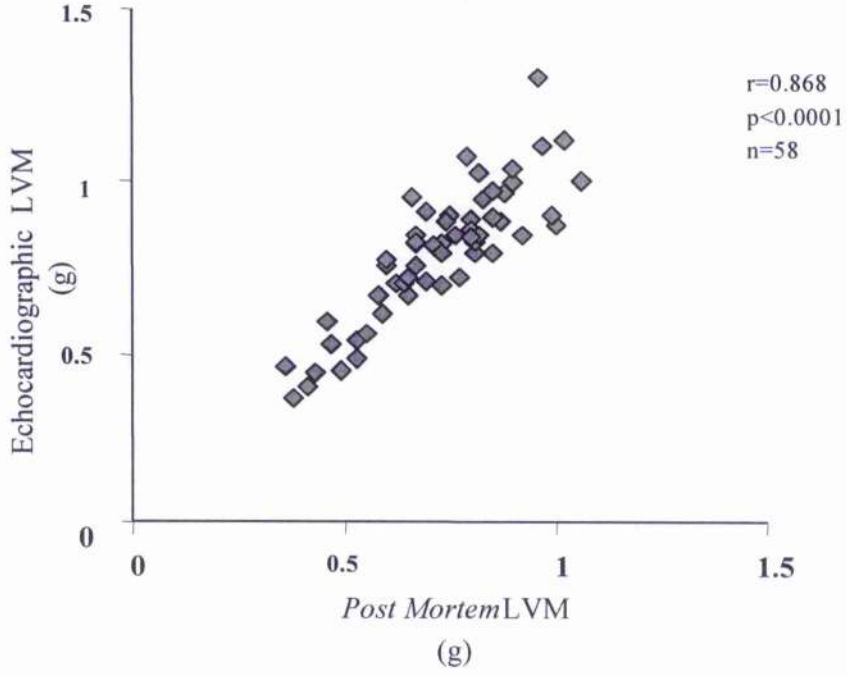

Figure 2.2 (a) Representative echocardiogram. Anterior wall thickness (AWT), end diastolic dimension (EDD) and posterior wall thickness (PWT), as well as epicardial (epi) and endocardial (endo) boundaries is indicated. **b)** Correlation of echocardiograph estimated LVM and *post mortem* evaluation (n=58).

Measurements were averaged four times to increase signal-to-noise ratio with a total of 12 – 16 contiguous ventricular short axis slices of 1 mm thickness required to achieve coverage of the entire heart. Total scan time was 1 ½ - 4 hours. The acquisition matrix used was 256 X 192, with a spatial resolution in a plane of 195 X 260. A field of view of 3 – 4 cm in plane resolution was 230 – 310 mm, scaled to 5.12 pixels / mm. Data was visualized and analysed using ImageJ acquired from http://rsb.info.nih.gov/ij/ (see Figure 2.3a-b). Estimation of LVM was calculated as follows –

LVM = (epicardial boundary – endocardial boundary) x 0.1 (slice thickness) x 1.05 (myocardial density)

2.4 GENETIC ANALYSIS

2.4.1 DNA Extraction

Genomic DNA was extracted from tissue using the Nucleon extraction kit for soft tissue (Tepnel life sciences, UK). Tissue was defrosted and ≤0.25g was added to 2.5ml of reagent A, and homogenised using the conventional rotor–stator homogenizer polytron PT2100 (Kinematica, Luzern, Switzerland). The solution was centrifuged at 1300g for 10 minutes and the supernatant discarded. Cell lysis was undertaken by adding 0.5ml of Reagent B to the pellet and vortexing briefly. De-proteinisation was performed by adding 150µl of sodium perchlorate and inverting at least seven times by hand. Chloroform (0.5ml) was added and mixed by inversion to emulsify the phases. To this 150µl of Nucleon resin was added and mixed by rotation for 5 minutes. The solution was centrifuged at 350g for 1 minute. The upper phase was removed into a microfuge tube to which 2 volumes of cold absolute ethanol was added. This was centrifuged at 4000g for 2 minutes to pellet the DNA and the supernatant removed. Cold 70% ethanol (1ml) was added, the sample was re-centrifuged and supernatant discarded. The pellet was air-dried for 10 minutes to ensure removal of all ethanol. The DNA was re-dissolved in 50µl of TE/ H_2O and stored at 4°C

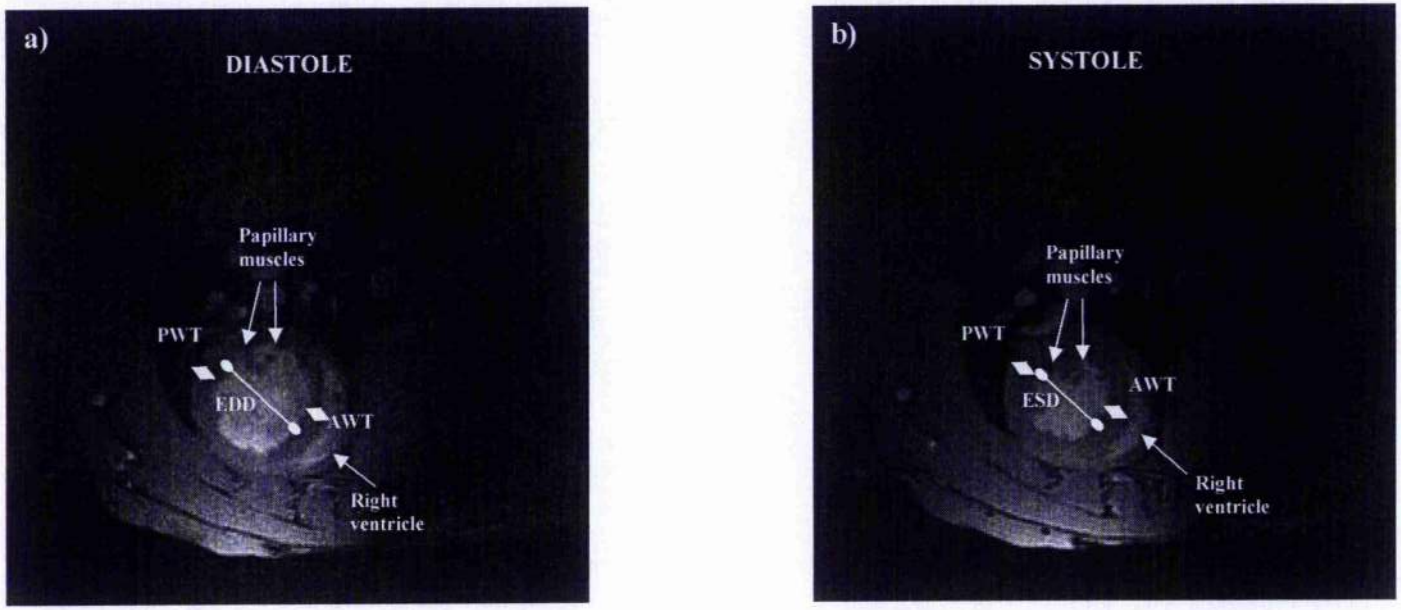

Figure 2.3 Short axis view image of 1mm slice through the heart in (a) diastole and (b) systole. A Bruker 70/30 USR Biospec system with a 32mm diameter surface coil was used for image acquisition with the following parameters: single slice flash cine; TE=1.8ms; TR=14ms; Averages=6; field of view=50x50mm; image matrix=256x192mm; flip angle=30°. The entire volume of the heart was scanned by moving 1mm between acquisitions from the base of the heart to the apex. Between 12 -16 images were taken throughout the cardiac cycle for each slice. Posterior wall thickness (PWT), anterior wall thickness (AWT) and end diastolic dimensions (EDD) are detailed with papillary muscles and right ventricle indicated by white arrows.

All DNA extracted was quantified using a NanoDrop® ND-1000 UV-Vis Spectrophotometer (Nanodrop Technologies, USA). With the sampling arm open, 2µl of the extracted DNA was dropped onto the lower measurement pedestal. The sampling arm was closed and a spectral measurement was initiated using the operating software. The optical density of the sample was determined in triplicate at 260nm and 280nm against a blank calculated for each sample. The ratio of the absorbance at 260:280nm was a measure of the purity of the sample. A ratio of between 1.8 and 2.0 was considered ideal and these samples were diluted to a concentration of 20ng/µl and stored at 4°C. Ratios above 2.0 and below 1.8 indicated contamination by phenols or proteins and these samples were discarded.

2.4.2 Polymerase Chain Reaction

Polymerase chain reaction (PCR) is an *in vitro* method of specific nucleic acid amplification using oligonucleotide primers designed to hybridise to the opposite nucleic acid strand and flank the target region of interest. Originally described by Saiki *et al.* (1985) the protocol involves a series of template denaturation, primer annealing and elongation of annealed primers by a thermostable recombinant Hotstart Taq DNA polymerase, which results in exponential accumulation of a specific fragment. The primer extended amplicon synthesised in one cycle serves as template in the next series resulting in a doubling of target DNA with each consecutive cycle. Thus 20 cycles of PCR yields around a million-fold increase in copy number.

Owing to the large number of samples to be genotyped, 96-well skirted ABgene Thermo-Fast plates (Abgene, UK) were used in an MJ Research tetrad thermocycler PTC225 (Genetic Research Instrumentation Ltd.). Each reaction was set up by first aliquoting 5µl of each DNA sample (20ng/ µl) into a 96-well skirted PCR plate using a multichannel pipette (ensuring no cross contamination). Once all samples were added to the plate, a mastermix (including 1.0µM of each primer, hotstart Taq DNA polymerase, 10X buffer and H_2O) was added to each well and a adhesive PCR sealing sheet (Abgene, UK) was used to cover the plate and prevent evaporation.

2.4.3 Gel Electrophoresis using Agarose

If polymorphic differences between the WKY and SHRSP alleles where in the order of 10-15bp for a given marker, high resolution agarose gels were prepared to resolve the products and facilitate genotyping the animals. Approximately 400ml of 1X TBE buffer was added to a 1L beaker with 4g of agarose powder and stirred rapidly with a teflon stir bar. The agarose solution was heated in a microwave oven on high power for 3 minutes. While the agarose solution was cooling, ethidium bromide was added to a final concentration of 0.2μg/ml, the solution cooled to 50-60°C and poured into a gel casting tray containing the appropriate combs.

After the gel was poured, the agarose was allowed to set and reach room temperature (approximately 40 minutes). Approximately 10μl of PCR product mixed with 2X formamide loading buffer was loaded onto the gel and run against a DNA size ladder marker at 120V for 2 hours (according to the size difference of alleles) to allow for separation and resolution. Gels were then scored by two independent observers.

2.4.4 Gel Electrophoresis using Polyacrylamide Gels and Autoradiography

Polymorphic markers with allelic differences <10bp (between SHRSP and WKY) were resolved by polyacrylamide gel electrophoresis using standard denaturing sequencing gels, blotting onto a nylon membrane and visualised by autoradiography. An 8% polyacrylamide gel was prepared using the SequaGel sequencing system solutions (National Diagnostics, UK). Polymerisation was initiated with 60μl of TEMED (Sigma Aldrich, USA) and 700μl of 10% ammonium persulfate (APS). After the addition of these reagents the gel was poured immediately. A small volume of the gel mixture was left in the beaker to test for setting (approximately 1 hour). Once set, the gel was placed into a vertical STS-45 standard thermoplate sequencer gel electrophoresis unit (Kodak International Biotechnologies Inc, UK) with both buffer reservoirs filled with 1X TBE. A 60 well comb (Kodak International Biotechnologies Inc, UK) was inserted into the top of the gel and the gel pre-run at 2000V (40mA, 70W)

for approximately an hour to heat it to around the optimum temperature for loading of 55°C. Alternatively, a temperature probe was used and fixed into the glass plate to allow the gel reaching automatically the optimum temperature when a Power Pac 3000 power supply (Bio-Rad, USA) was used.

Prepared PCR samples were denatured at 94°C for 4 minutes prior to loading and 7µl of each sample was loaded in the gel. The orientation was annotated to enable genotyping. The time for the optimum separation between the different PCR products was calculated as follows to allow for optimum gel usage: products of approximately 100bp were run until the slowest component of the loading dye had ran down the gel 30cm, products of approximately 150bp were 40cm, and those of approximately 200bp were 50cm.

After electrophoretic separation, the gel was cooled and the glass plates split. A 28 x 28 cm Hybond-N^+ nylon membrane (Amersham Biosciences, UK) was placed on the gel, followed by two pieces of absorbing paper, the gel-free glass plate, and weights to allow southern blotting overnight. Once blotting was completed, the membrane was carefully removed and placed in a tray with 500ml of 0.4M sodium hydroxide for 20 minutes, followed by 2 x 10 minute washes in 2X SSC (300mm sodium chloride; 30mm sodium citrate, pH 7.0), during which the membrane was shaken. The membrane was placed in a hybridisation tube (Stuart Scientific Co. Ltd, UK). The forward primer was radiolabelled with [α-^{32}P] dCTP, and the reaction completed as follows: 12.5µl of distilled water, 4µl of terminal transferase buffer (Promega, UK), 1µL of forward primer, µl of [α^{32}P]dCTP, and 0.5µl of terminal deoxynucleotidyl transferase (TDT) followed by incubation at 37°C for 30 minutes and 10 minutes at 68°C to stop the reaction. Once the reaction was completed, a pre-hybridisation solution was prepared (24ml sterile water; 12ml 20X SSC; 4ml 10X SDS; 0.1g powdered milk to prevent non-specific binding) and the radiolabelled primer added. This mixture was poured into to the hybridisation tube containing the membrane for hybridisation at 55°C for 2 hours or at 42°C overnight. On completion of hybridisation, the membrane was washed twice with 1L of post-hybridisation solution (0.2% SDS; 2X SSC), dried between two pieces of absorbent paper, wrapped in Saran wrap (Dow Chemical Company, Europe) and placed in a special cassette (Bio-Rad, USA) against an imaging screen K (Bio-Rad, USA). This screen reduced the exposure required with normal film up to ten times due

to its increased sensitivity to ^{32}P. An image was acquired using the Molecular Imager FX System (Bio-Rad, USA) which scanned the screen with a dual wave-length laser. To re-probe the membrane with different primers, the membrane was washed twice in boiling 0.4% SDS followed by two washes in 2X SSC.

2.4.5 Fluorescent PCR

Using the PCR method described above, polymorphism of microsatellite markers can be read a non-radioactive PCR protocol. The 5'-end of the forward primer was labelled with a fluorescent dye (FAM, TET, PET and NED dyes) and subsequently analysed with an automated ABI 3730 DNA sequencer (Applied Biosystems, USA). The PCR reaction was carried out in a total volume of 20µl as before but with the following reagents: 5µl of DNA template (100ng), 2µl of 10X buffer (Qiagen, USA) containing tris-HCL, KCL, $(NH_4)_2SO_4$, and 15mm $MgCL_2$ pH 8.7; 1µL of polyoxyethylene (Life Technologies Inc., UK); 200 µM of each dATP, dCTP, dGTP, and dTTP; 0.5 µl of each labelled primer (MWG Biotech, USA) and 0.4U HotStart Taq polymerase (Qiagen, USA) and GeneScan 500 ROX size standard (Applied Biosystems, USA). Further optimisation was required for some primers where annealing temperatures varied from 50°C to 68°C in increments of 1°C to find optimal conditions for amplification. The fluorescent PCR fragments were pooled according to size and fluorescent label used. The use of several fluorescent dyes allows high throughput analysis of different markers even if allele size is similar. Each marker can be identified according to the fluorescent tag by the DNA sequencer and analysed using GeneMapper v3.7 software (Applied Biosystems, USA). Figure 2.4 is an example of the data output from GeneMapper.

2.5 QTL ANALYSIS

2.5.1 JoinMap 3.0

JoinMap 3.0 was used to calculate a genetic linkage map for chromosome 14 based on the genotype datasets. A new project was created and a locus genotype file containing

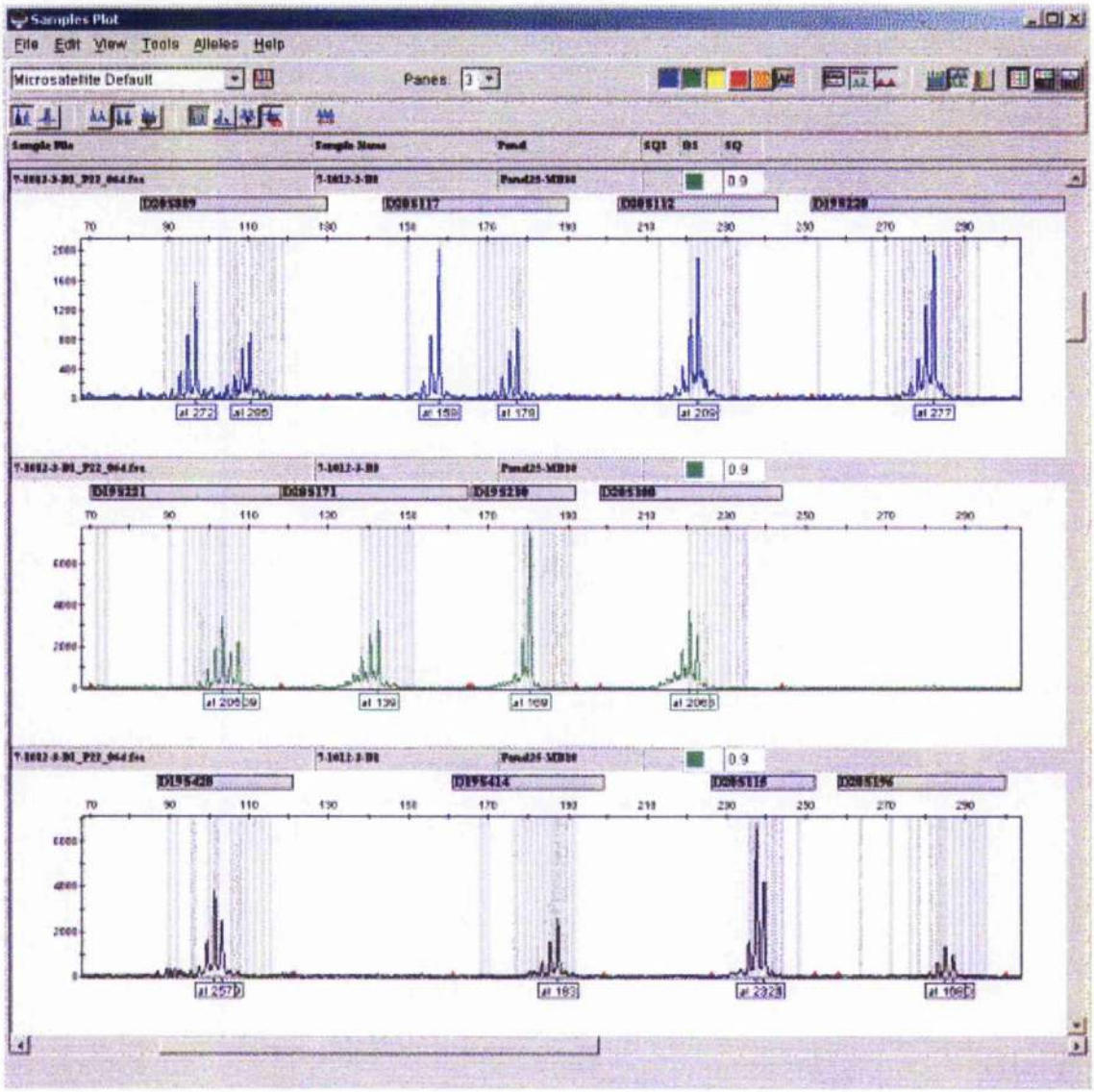

Figure 2.4 An example of output from GeneMapper v3.7. Allele sizes are input, with corresponding tagged fluorescent dye. From this, the output from the 3730 DNA analyser can be visualised and genotypes assigned.

genotype codes were prepared in order to generate locus genotype frequencies and calculate linkage groups. Loci were determined to be significantly associated at the current LOD threshold with at least one member of a group. The map calculated was based on the selected set of loci. The mapping procedure was a process of building a map by adding loci one by one, starting from the most informative pair of loci. For each added locus the best position is searched and a goodness-of-fit measure is calculated. When the goodness-of-fit reduces too sharply (too large a jump), or when the locus gives rise to negative distances, the locus is removed again. This was continued until all loci had been handled at least once.

2.5.2 MapManager QTXb20

Map Manager QTXb20 provides two functions, which can be used for QTL detection; marker regression and interval mapping. Marker Regression specifically tests the association of the trait values with the genotypes of single loci and can be applied to multiple chromosomes. Interval mapping checks the same dataset for QTL when markers are spaced >20cM apart.

$$b = (X^T X)^{-1} X^T y$$

Where b represents a vector, which gives the estimated constant term and a regression coefficient estimate for each locus, X^T indicates the transpose of matrix X, and X-1 indicates the inverse of X.

Interval mapping was performed by QT>Interval Mapping command. The target locus was replaced by a position in a target interval (Lander & Botstein, 1989; Knapp & Bridges., 1990; Haley & Knott, 1992; Markel *et al.*, 1996). The expected effect of a hypothetical QTL at this location was estimated from the genotypes at marker loci flanking the interval. QTX allows a choice of mapping functions: Haldane, Kosambi, or Morgan.

Composite interval mapping (Jansen, 1993; Zeng, 1993) adds background loci to simple interval mapping. The design matrix X is expanded to include a column for each background locus, with the genotype of that locus expressed in the code appropriate for an additive model. QTX always includes the effect of background loci according to an additive model, even in intercrosses, in which there would be a possibility of using different models for each background locus.

Permutation tests were performed on the dataset to establish empirical significance thresholds for significance of QTL mapping results (Churchill & Doerge, 1994; Doerge & Churchill, 1996). QTX uses the same routines for a permutation test as for interval mapping, but it permutes the trait values among the progeny before calculating the X matrix and fitting the regression. This permutation destroys any relationship between the trait values and the genotypes of the marker loci. The regression model was fitted for the permuted data at all positions in the genome and the maximum likelihood ratio statistic (LRS) and p value is recorded. This procedure was repeated one thousand times, giving a distribution of LRS values expected if there were no QTL linked to any of the marker loci and was represented as threshold values – suggestive, significant and highly significant.

The LRS was converted to the conventional base-10 LOD score by dividing the value by 4.61 (twice the natural logarithm of 10). Confidence intervals were estimated by bootstrap analysis (Visscher *et al.*, 1996), which creates multiple bootstrap datasets by randomly choosing individuals with replacement from the original dataset. Each bootstrap dataset was used for QTL mapping, and the location of the strongest QTL for each set recorded. These locations are summarized in a histogram showing the size of the region in which the QTL is expected.

2.5.3 Windows QTL Cardographer 2.5

Locus data and genotype/trait data is imported into Windows QTL Cartographer (WinQTLCart) from Map Manager QTXb20 as exported map.inp and cross.inp files. The datasets are also saved as text files to check locus, genotype and trait information.

Results are displayed in graphical and statistical view windows with calculation of a chromosome map/ QTL map based on the dataset input.

2.6 QUANTITATIVE RT-PCR

2.6.1 RNA Extraction

Total RNA was extracted from tissue using RNeasy Maxi kit (Qiagen, UK) Frozen tissue was placed in 5ml of RLT buffer (containing 10µl of β-mercaptoethanol) and quickly homogenized using a conventional rotor–stator homogenizer polytron PT2100 (Kinematica, Luzern, Switzerland) until the sample was uniformly homogeneous (usually 45–60seconds at 20,000rpm). The lysate was then transferred to a sterile 50ml falcon tube containing 15ml of nuclease free H_2O (Ambion Europe Ltd) and 250µl of 20mg/ml proteinase K (Qiagen, UK). The cocktail was incubated in a hybaid mini hybridization oven at 55°C for 20 minutes. Following proteinase K digestion, the sample was centrifuged at 5000g for 6 minutes until formation of a small pellet at the bottom of the tube. The clear supernatant was transferred to a fresh 50ml falcon tube and mixed with 11ml cold absolute ethanol.

Approximately 12ml of the sample was loaded onto an RNeasy Maxi column, placed in a fresh 50ml falcon tube and centrifuged at 5000g for 5 minutes. The flow through was discarded and the procedure repeated several times until the entire clear supernatant sample has been passed through the column. 15ml of RW1 buffer was then added to the RNeasy column and centrifuged at 5000g for 5 minutes and the flow through discarded. 10ml of RPE buffer diluted with 4 volumes of absolute ethanol was added to the RNeasy column and centrifuged at 5000g for 2 minutes and the flow through discarded. Approximately 10ml of RPE buffer diluted with 4 volumes absolute ethanol was added to the RNeasy column and centrifuged at 5000g for a further 15 minutes until the membrane on the column was dry. The column was transferred to a fresh 50ml collection tube and total RNA was eluted by pipeting 800µl of nuclease free H_2O directly onto the column and centrifuged at 5000g for 6 minutes. To obtain a higher concentration of RNA, a second elution step was performed using the first eluate.

All RNA extracted was quantified using the NanoDrop® ND-1000 UV-Vis Spectrophotometer (Nanodrop Technologies, USA). With the sampling arm open, 2µl of RNA was pipetted onto the lower measurement pedestal. The sampling arm was closed and a spectral measurement was initiated using the operating software. The sample column automatically sets between the upper and lower measurement pedestals and the spectral measurement was taken and output as a concentration in ng/µl and a ratio of the absorbance at 260:280nm. A ratio between 1.9 and 2.2 was considered ideal.

2.6.2 DNAse Treatment of RNA

In order to prevent any contaminating DNA providing false positive results, total purified RNA was treated using DNA-free (Ambion) to digest DNA. 44µl of RNA was pipetted into a 0.5ml RNase free microfuge tube (Ambion, UK) with 0.1 volume (5µl) of 10x DNaseI buffer and 1µl of DNaseI then vortexed to mix. The mixture was incubated at 37°C for 30 minutes. Following incubation, 5µl of resuspended DNase inactivation reagent was added and the mixture vortexed every 20 seconds for 2 minutes. In order to pellet the DNase inactivation reagent, the RNA was centrifuged at 10,000g for 1.5 minutes and then transferred to a clean 0.5ml RNase free microfuge tube.

2.6.3 Quality Assessment of RNA

RNA was assessed for quality using an agilent bioanalyzer 2100. Approximately 1.5µl of total RNA was spotted onto a specialised agilent chip and RNA was quality check referenced with18S and 28S ribosomal RNA. Samples were rejected if the fluorescent amplitude of the RNA measured lower than average for total RNA and ribosomal RNA.

2.6.4 Two Step RT- PCR Taqman

The technique consists of two parts: synthesis of cDNA from RNA by reverse transcription, and amplification of a specific cDNA by polymerase chain reaction (PCR). The method requires very little RNA and differs from Northern blotting because it is somewhat tolerant of degraded RNA, as long as the RNA is intact within the region

of interest. First strand cDNA was synthesized using RT-for PCR kit (BD Biosciences, USA). Approximately 1µg of DNase treated RNA was pipetted into an RNase free 0.5-ml microfuge tube and diluted to a total volume of 13.5µl with DEPC-treated H_2O and 1µl of oligo (dT) primers. The reaction mixture was then heated to 70°C for 2 minutes then placed on ice immediately. 6.5µl of a reagent master mix composed of 4µl 5X reaction buffer, 1µl dNTP (10mm each), 0.5µl recombinant RNase inhibitor and 1µl of Moloney Murine Leukemia Virus (MMLV) reverse transcriptase was added per reaction, vortexed and incubated at 42°C for 60 minutes on an MJ DNA engine tetrad (PTC 225). To stop the cDNA synthesis reaction and to destroy any DNase activity, the reaction was heated to 94°C for 5 minute then diluted to a final working volume of 100µl.

RT-PCR was performed using the ABI prism 7900HT Sequence Detection System and Taqman Gene Expression Assay probes (Applied Biosystems, USA). Housekeeping genes, Glyceraldehyde-3-phosphate-dehydrogenase (GAPDH) and β-Actin were selected as controls. Consistent expression of the selected endogenous controls was then verified in the sample set (heart, liver and aorta). The endogenous control normalizes differences in the amount of cDNA loaded into PCR reaction wells, therefore endogenous control expression must be uniform across all samples in the study. Comparison of the housekeeping gene expression of several samples was used as a test of uniform expression of the endogenous control. Gene expression of endogenous controls should vary only slightly, therefore any statistical differences in gene expression across the samples tested was taken as an unstable housekeeping gene in the tissue type analysed and the housekeeping gene was rejected as an endogenous control.

The endogenous control and target assays must have identical PCR efficiency in order to obtain a comparative cycle threshold (CT) value. To ensure the target gene(s) and endogenous control had identical PCR efficiency, a series of serial dilutions of the cDNA sample was carried out. A constant CT difference across a range of at least 3 logs (1000-fold) of initial template concentration was used to verify identical PCR efficiency in the target gene(s) and the endogenous housekeeping gene.

The PCR step for the multiplex assay was carried out in a 96-well format using PCR reaction mix components – 1 µl of 20x Taqman Gene Expression Assay probe, 4µl of cDNA diluted in 5µl of H_2O and 10µl of Taqman 2x Universal PCR Master Mix. All reaction mix components were vortexed prior to use and mixed by pipeting. Each reaction was replicated 3 times and the reaction plate was covered with an optical adhesive cover and pulse centrifuged at 10 000g for 5 seconds. The reaction plate was then placed in the sequence detector and the thermal cycling conditions were set using the standard run conditions of 40 cycles with a 95°C denature step for 1 second and 60°C extension for 20 seconds.

Data was analysed using the comparative CT method, which involves comparing the CT values of the sample(s) of interest with a control or calibrator RNA from normal tissue. The real-time PCR system is based on the detection and quantitation of a fluorescent reporter (Lee, 1993; Livak, 1995). This signal increases in direct proportion to the amount of PCR product in a reaction. By recording the amount of fluorescence emission at each cycle, it is possible to monitor the PCR reaction during exponential phase where the first significant increase in the amount of PCR product correlates to the initial amount of target template. The CT values of both the calibrator and the samples of interest were normalized to a pre-selected endogenous housekeeping gene with identical amplification efficiency to the target gene. The comparative CT method is also known as the $2^{-[delta][delta]}$ CT method, where

$$[delta][delta]C_t = [delta]C_{t,sample} - [delta]C_{t,reference}$$

$[delta]CT_{,sample}$ is the CT value for any sample normalized to the endogenous housekeeping gene (target CT – endogenous CT) and $[delta]CT_{,reference}$ is the CT value for the calibrator also normalized to the endogenous housekeeping gene.

2.7 SEQUENCING CANDIDATE GENES

2.7.1 Cleaning PCR Product

PCR fragments were cleaned using an AMPure Purification Kit (Agencourt Bioscience, USA). AMPure was added according to PCR reaction volume (36µl for

20µl PCR reaction). The AMPure resin binds to fragments >100bp. The solution was vortexed and centrifuged for 1 sec at 2000g then allowed to incubate at room temperature for 5 minutes. The reaction was then incubated at room temperature for a further 10 minutes on the SPRI magnet plate (Agencourt Biosciences, USA). The plate was then tipped to remove the cleared solution. 200µl of 70% ethanol (Sigma Aldrich, USA) was added and to allow precipitation of fragments. The solution was discarded after 30 sec by inverting the plate, which was left to air dry for 35 minutes at room temperature. Once all ethanol had evaporated, 40µl of distilled water was added to the reaction, which was sealed using an adhesive PCR film lid (Abgene, UK), vortexed and centrifuged for 1 sec at 2000g. Cleaned products were then transferred to a fresh skirted 96-well PCR plate (Abgene, UK).

2.7.2 Sequencing of Candidate Genes

Sequencing of the clean PCR products required use of BigDye Terminator v3.1 sequencing kits (Applied Biosystems, UK). The 20µl sequencing reaction contained 0.5-1.0µl of template, 3.2 pmol of primer (forward or reverse), 3.75µl of 5x sequencing buffer, 0.5µl of ready reaction mix and autoclaved distilled H_2O. The sequencing reaction program was as follows: 45 seconds at 96°C and 24 cycles of 25 seconds at 50°C and 4 minutes at 60°C. To remove unincorporated BigDye ddNTPs and primers the sequencing reaction was cleaned by CleanSeq Dye Terminator Removal Kit (Agencourt Bioscience, USA). 10µl of Cleanseq was added to 10µl of each sequencing reaction . 42µl of 85% ethanol was added and the reaction was centrifuged at 2000g for 1 sec. The PCR plate was placed on a SPRI magnet plate for 4 min until the solution was clear. The following steps occur on the SPRI magnet. The cleared solution was removed by inversion of the plate and 150µl of 85% ethanol added to each reaction and allowed to incubate for 30 secs. The plate was then inverted and centrifuged at 2000g for 1 sec to remove all ethanol and air dried for 35 minutes at room temperature. The cleaned sequencing products were then re-suspended in 40µl of nuclease free H_2O and transferred to a Thermo-Fast 96-well barcoded Detection Plate (Abgene, UK) and resolved on the 3730 DNA analyser using the manufacturers recommended run conditions, POP-7 polymer and a 36 cm capillary array. Data was analysed using

Sequence Analysis software version 5.0 and results compared to published sequence using BLAST

2.8 MICROARRAY

Affymetrix GeneChip® probe arrays are made using spatially patterned, light-directed, combinatorial chemical synthesis, and contain thousands of different oligonucleotides on a glass surface.

2.8.1 Target Tissue Preparation

Target preparation involves the preparation of biotinylated target RNA sourced from a total RNA sample obtained from whole heart (described in detail in *Chapter 2.6.1)*. Double-stranded cDNA was synthesized using a T7-$(dT)_{24}$ oligomer (5' –GGC CAG TGA ATT GTA ATA CGA CTC ACT ATA GGG AGG CGG – $(dT)_{24}$– 3') to prime first-strand cDNA synthesis, which was HPLC-purified. First strand cDNA synthesis reactions were carried out in 1.5ml polypropylene RNase-free tubes. Second strand cDNA was synthesized by adding reagents listed in Appendix I, to the first strand reaction tube (briefly centrifuged), which were placed on ice. The tube was tapped gently to mix the reagents and incubated at 16°C in a water-bath for approximately 2 hours. Approximately 2µl (10U) of T4 DNA Polymerase was added and incubated for 5 minutes at 16°C. 10µl of 0.5M EDTA was added to stop DNA synthesis and the mixture was stored at -20°C.

RNA transcripts were labeled using Enzo Bioarray HighYield RNA Transcript Labelling Kit; all reagents were supplied with the kit except DEPC-treated, sterile, de-ionized water. The following reaction components were added in order to RNase-free microfuge tube: Template DNA (variable volume to give 1µg of cDNA), deionised water (variable to give a total reaction volume of 40µl), 10X HY Reaction Buffer (vial 1)(4µl), 10X biotin labelled ribonucleotides (vial 2)(4µl), 10X DTT (vial 3)(4µl), 10X RNase inhibitor mix (vial 4)(4µl) and 20X T7 RNA polymerase (vial 5)(2µl). After a brief centrifugation to collect all reagents at the base of the tube, it was immediately placed in a 37°C water bath and left to incubate for 4-5 hours, gently mixing the

contents of the tube every 30-45 minutes. Following incubation the RNA produced either purified immediately or at –70°C. IVT products were purified using RNeasy Mini spin columns (Qiagen) to remove unincorporated NTPs to accurately determine the quantity of cRNA.

Depending on recovery, ethanol precipitation was required to concentrate cRNA. 0.5 volumes of 7.5M NH_4Ac and 2.5 volumes of absolute ethanol (stored at -20°C) were added to the sample, which was then vortexed. The solution was allowed to precipitate for one hour to overnight at -20°C prior to centrifugation at >12.000 x g for 30 minutes. The resulting pellet was washed twice with 0.5ml of 80% ethanol (stored at -20°C) and air dried before resuspension in 10-20µl of RNase-free water. Quantification of cRNA (cleaned IVT product) was done using a NanoDrop® ND-1000 spectrophotometer, as outlined previously (*Chapter 2.6.1*). An adjusted cRNA yield is calculated to include any unlabelled total RNA. The starting amount of total RNA (µg) can be multiplied by the fraction of cDNA used in the IVT and subtracted from the amount of cRNA measured after IVT (µg) to give an adjusted cRNA yield.

2.8.2 Target Hybridisation

Frozen stocks of GeneChip® eukaryotic hybridization control cocktail were heated to 65°C for 5 minutes to completely re-suspend cRNA before aliquoting. Target purification and hybridization, using a probe array (at room temperature) was carried out prior to use. As the hybridisation cocktail was heated to 99°C for 5 minutes, the array was wet by filling via one of the septa (see Figure 2.5) using an appropriate volume of 1X hybridisation buffer (standard array = 200µl, midi array = 130µl and mini array = 80µl) using a micropipettor and corresponding tips. When filling the probe array cartridge, two pipette tips are used; one for filling and the second to allow air venting from the hybridisation chamber. After incubation at 99°C, the hybridisation cocktail was heated to 45°C for 5 minutes using a heat block and then spun at maximum speed in a microcentrifuge for 5 minutes to remove any insoluble material from the hybridisation mixture. The buffer solution was removed from the probe array cartridge and replaced with the appropriate volume (total fill volumes are: standard array = 250µl,

midi array = 160µl and mini array = 100µl) of clarified hybridisation buffer. Probe arrays were placed in a balanced configuration in the 45°C hybridisation oven for 16 hours.

2.8.3 Fluidic station and probe array setup

Probe information, fluidics protocols and experimental data were entered and then checked in the file locations window. The experiment name and probe array type were defined and other optional parameters entered, i.e. sample for reservoir A was changed to non-stringent wash buffer (wash buffer A) and intake buffer reservoir B to stringent wash buffer (wash buffer B) prior to priming (see Appendix I for preparation of buffers). After 16-hour hybridisation of the probe, the hybridisation cocktail was removed from the probe array and set aside in a microcentrifuge tube (stored at -20°C). The probe array temperature was reduced to room temperature before washing and staining. It was then filled completely (250µl) with non-stringent wash buffer. The GeneChip® fluidics station 400 was used to wash and stain the probe arrays, which was operated using the GeneChip® software. Priming of the fluidics station ensured that the lines connected to it were filled with the appropriate buffers and that the station was ready to run the protocols. The intake buffer Washing and staining for antibody amplification was then carried out using strepdavidin phycoerythrin (SAPE) stain solution. SAPE solution was prepared immediately prior to use and wrapped in foil to protect from light penetrance. For a 1200µl solution the following reagents were mixed together: 600µl of 2X Stain Buffer, 540µl water, 48µl of 50mg/ml acetylated bovine serum albumin (BSA), 12µl of 1mg/ml SAPE. These were divided into two aliquots of 600µl each to be used for stains 1 and 3 respectively. Antibody solution was prepared by mixing 300µl of 2X Stain Buffer, 266.4µl water, 24µl of 50mg/ml acetylated BSA, 6.0µl of 10mg/ml normal goat IgG and 3.6µl of 0.5mg/ml biotinylated antibody. The appropriate antibody amplification protocol was selected on the workstation to control the washing and staining of the probe array. The appropriate probe arrays were inserted into the designated modules in the fluidics station. The 600µl of SAPE solution in a microfuge tube was placed into the sample holder, ensuring that the sampling needle is in the tube with its tip at the bottom. When indicated, the next solution of 600µl of antibody stain solution was applied in the same manner. Again, this was then replaced

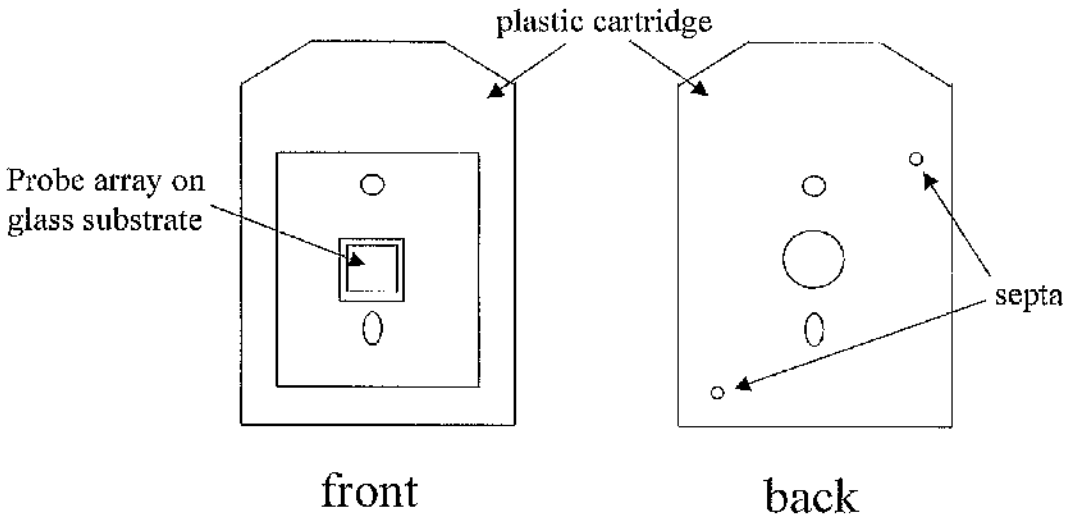

Figure 2.5 Diagram of the GeneChip® Probe Array.

with the last 600µl of SAPE solution. When the protocol was complete the software indicated to eject the cartridge containing the array. An empty microcentrifuge tube was placed on the sampling needle and the probe array checked for bubbles. If bubbles were present, the array was placed back into the cartridge and the station will drain and refill the array with the last buffer used. Once no bubbles were present the probe array was ready to be scanned, or could be kept in the dark at 4°C.

2.8.4 Data Analysis

Low-level normalization of data was carried out using the Robust Multichip Average (RMA) method (Irizarry *et al.*, 2003), which performs several operations including:

i. probe-specific background correction, to compensate for non-specific binding
ii. probe-level multichip quantile normalization to unify distributions across all chips
iii. robust probe-set summary of the log-normalized probe-level data by median polishing.

Cluster analysis was used to identify and classify samples on the basis of similarity, to minimize within-group variance and maximize between-group variance. Probe sets were identified as differentially expressed using the rank product (RP) method of analysis, a novel approach based on calculating RP from replicate experiments, providing a straightforward and stringent way to determine the significance level for each gene, which allows for flexible control of the false-detection rate (Breitling *et al.*, 2004). Genes were defined as differentially expressed with a $p < 0.05$ ($p<0.01$ and $p<0.1$ were also tested). Ingenuity Pathways Analysis (https://analysis.ingenuity.com) software was employed to gain functional and network information from RP data. Two-way analysis of variance (ANOVA) was used as an additional analytical method, to test for interactions between strain and environmental stimuli.

CHAPTER 3

IDENTIFICATION OF LEFT VENTRICULAR HYPERTROPHY IN SHRSP

3.1 INTRODUCTION

Current major strategies developed for gene identification in humans (linkage analysis in families segregating for rare Mendelian forms of cardiac hypertrophy and a candidate gene approach) are limited due to the complex, multifactorial and polygenic nature of the common disease form (Brand *et al.*, 1998). To some degree, a number of the inherent complexities encountered in the study of human subjects can be circumvented with the use of inbred rat models. The main advantages to using experimental animals are the ability to study large numbers of homogenous progeny under controlled environmental conditions and the application of standardised and uniform high fidelity phenotyping methods. The stroke prone spontaneously hypertensive rat (SHRSP) is one of the best animal models available for the study of cardiovascular disorders, as it is characterised by a number of vascular complications including left ventricular hypertrophy and salt-sensitivity in common with the human disease state (Okamoto & Aoki, 1963; Yamori, 1982). Indeed, several studies have confirmed the polygenic inheritance of left ventricular mass (LVM) with the use of inbred SHRSP (Tanase *et al.*, 1992; Clark *et al.*, 1996; Inomata *et al.*, 2005).

The main impetus to these investigations is the ultimate goal of gene identification. In the SHRSP, quantitative trait loci (QTL) are detected from the results of a complete genome wide scan in a segregating F_2 population, obtained by cross breeding the SHRSP with the normotensive reference strain Wistar Kyoto rat (WKY). As early as 1982, Tanase *et al.* demonstrated the heritability of heart weight in the rat and suggested the effect of genetic factors influencing cardiac mass is larger than that of blood pressure alone. From this study, the extent of genetic influence was estimated to be 45%-65% (by strain comparison) and 35%-60% (by cross analysis) (Tanase *et al.*, 1982). Following on from these results, genome wide scans carried out in a variety of inbred rat strains have led to the identification of QTL for LVM independent of blood pressure, on rat chromosome 17 (Pravenec *et al.*, 1995; Tsujita *et al.* 2000), chromosome 3 (Sebkhi *et al.*, 1999), chromosome 5 (Deschepper *et al.* 2001) and chromosome 2 (Innes *et al.*, 1998).

Pravenec *et al.* (1995) used recombinant inbred strains initially derived from the SHR and normotensive Brown Norway strain (HXB and BXH). In this genome wide scan, they found the genetic marker for dopamine 1A receptor (*Drd1A*) on chromosome 17 showed a high correlation for LVM irrespective of blood pressure values. Similarly, Tsujita *et al.* (2000) identified a blood pressure independent locus for left ventricular mass index (LVMI; LVM indexed to body weight) on chromosome 17 in an F_2 cross between SHR and the Lewis rat. This locus was not in the same region identified by Pravenec *et al.*, however it does illustrate the importance of strain differences and the requirement to examine a variety of strains. Innes *et al.* (1998) used 182 F_2 male animals derived from a cross between SHR and normotensive Donryu rats. The group identified a locus on chromosome 2 (lvm-1) with linkage to relative LVMI but showed no evidence of linkage to mean arterial pressure. These results further indicate that LVM is influenced by parameters other than blood pressure in hypertensive rat crosses and the genetic factors relating to cardiac mass may not be the same genes controlling blood pressure. In order to investigate this hypothesis further, several studies have been carried out in normotensive rat crosses. Sebkhi *et al.* (1999) examined 126 F_2 male rats obtained from a normotensive WKY and Fischer 344 rat cross. They identified a QTL on chromosome 3, accounting for 16.5% of the total variance of LV weight. This QTL was also found to be significantly linked to total heart weight. Deschepper *et al.* (2001) investigated LVM using a normotensive cross between the WKY and WKHA (WKY hyperactive) rat. From this study, they identified 2 contiguous QTL on chromosome 5, with linkage to either LVM or ANP, suggesting a possible correlation between ANP levels and LVM in normotensive animals. However, in order to support this hypothesis, further investigation to discount other physiological factors relating to ANP levels and the biochemical pathways involved in both normotensive and hypertensive strains is required.

QTL analysis itself can have a number of limitations with several factors influencing results, for example, the population under investigation, polymorphic marker loci and number, missing genotype/phenotype data, the location, number and interaction of QTL and of course human error. For these reasons, more refined statistical approaches to QTL mapping have been developed. Broadly speaking, there are three different types of

statistical analysis that can be used in the search for QTL: single-marker tests, interval mapping and composite interval mapping. The advantage of composite interval mapping methods is that they accommodate multiple QTL. However, none of the current available methods can accommodate fully the complexity of multifactorial traits that arise from gene-gene and gene-environment interactions.

With multiple traits and multiple environmental factors involved in a QTL mapping experiment, the estimation of pleiotropic effects and QTL-environment interactions is fundamental as is the understanding and estimation of the structure and genetic make-up of quantitative traits. With the advent of well-saturated genetic maps, it is possible to single out major structural components of the genetic architecture of quantitative traits and estimate the associated parameters. Multiple interval mapping is a well adapted statistical approach to identify and estimate these parameters, which include QTL number, genomic positions, effects and interactions of significant QTL and their input on genetic variance. Published studies over the last decade have provided a large number of newly developed microsatellite markers, which have vastly improved the density of the rat genetic linkage map (Jacob *et al.*, 1995; Pravenac *et al.*, 1996; Bihoreau *et al.* 1997; Brown *et al.*, 1998). These markers, together with refined statistical analysis should allow a more complete mapping of heart weight in the SHRSP.

Previously, our group identified two blood pressure QTL on rat chromosome 2, a single QTL for pulse pressure on rat chromosome 3 and a suggestive QTL for LVMI on rat chromosome 14, using F_2 genome wide analysis of a $SHRSP_{Gla}$ x WKY_{Gla} cross (Clark *et al.*, 1996). The aims of this study were to perform an improved QTL analysis scan in both male and female F_2 hybrids produced from this cross, using phenotypic data collected from the previous F_2 genome wide scan (detailed in Appendix II; Clark *et al.*, 1996) and an improved genetic linkage map for rat chromosome 14.

3.2 METHODS

3.2.1 Experimental Animals and Genetic Crosses

Inbred colonies of SHRSP and WKY rats have been established at the University of Glasgow since 1991. Two reciprocal crosses were previously produced in 1996, 1 male SHRSP was mated with 2 WKY females (cross 1) and 1 male WKY was mated to 2 SHRSP females (cross 2). From the F_1 generation of each cross, 3 males and 6 females were brother-sister mated to produce F_2 rats (57 in cross 1 with a male: female ratio of 28:29 and 83 in cross 2 with a male: female ratio of 37:46). Phenotypic data was previously obtained for 140 F_2 (male: female = 65: 75) rats at 21 weeks of age, including radiotelemetry data (SBP, DBP, heart rate and activity) over a 5-week baseline period and after a 3- week salt challenge (1% NaCl in drinking water) (Clark *et al.*, 1996). Gravimetric measurements of cardiac mass index (CMI; heart weight to body weight ratio) and left ventricular mass index (LVMI; left ventricle mass relative to body weight) were calculated from *post mortem* values (see *Chapter 2.3.3*), following a 3-week 1% salt loading period. Liver DNA used for analysis was extracted and stored at -20°C (see *Chapter 2.4.1*).

3.2.2 Genotyping, Improved Genetic Linkage Map and QTL Analysis

A total of 24 new microsatellite markers in addition to the original 5 previously used by Clark *et al.*, (1996) were screened and 8 of these were found to be polymorphic between SHRSP and WKY. Genotyping was performed by PCR amplification of DNA around all 13 microsatellite markers for chromosome 14 (Table 3.1). The PCR primers for typing the microsatellite markers were obtained from MWG Biotech, UK and have been previously published by the Welcome Trust Centre for Human Genetics (http://www.well.ox.ac.uk/). PCR products were separated by agarose gel electrophoresis, analysed using bioanalyzer (Bio-rad, USA) and scored by two independent operators, unaware of the phenotypic data.

Genotype results gained from these additional genetic markers were added to data previously collected and mapped relative to each other using JoinMap 3.0 (Van Ooijen and Voorrips, 2001). The genetic linkage map generated by JoinMap 3.0 was used to analyse genotype and phenotype data for QTL on rat chromosome 14. Software packages used to analyse QTL included Windows QTL Cartographer and MapManager QTXb40. In order to account for missing genotype and trait data, several QTL analyses were performed, including interval mapping, composite interval mapping and multiple marker mapping using both software packages. Data was permutated 10000 times in order to obtain a more robust dataset and set significant threshold levels unique to the trait under analysis. The likelihood ratio statistic (LRS) was converted to the conventional base-10 LOD score, which varied for each trait analysed.

3.2 RESULTS

Raw genotype data acquired for this study is listed in Appendix II as well as the raw phenotype data used to re-analyse LVMI QTL on rat chromosome 14. Twenty four markers were tested in addition to the five used in the original genome wide scan (Clark *et al.*, 1996), of which eight markers were polymorphic and agarose gel resolvable. Figure 3.1 is an example of PCR fragments amplified from F_2 DNA using a polymorphic marker (*D14arb17*) and visualised using a 1% agarose gel. Figures 3.2a-b illustrates an improved genetic linkage map for rat chromosome 14, generated by genotyping F_2 DNA samples (n=134) for 13 polymorphic microsatellite markers. Initially, LOD scores and pairwise recombination frequencies between markers was calculated, however due to a region of approximately 20 centiMorgans (cM) between *D14rat41* and *D14rat110*, two distinct genetic linkage groups were created. Linkage group 1, comprised of 12 microsatellite markers (excluding *D14Rat110*) was integrated and recombination values converted to genetic distances using the Kosambi mapping function. This improved rat chromosome 14 genetic linkage map is in correct orientation and corresponds well with physical distances cited on online databases (http://www.ensembl.org;).

Table 3.1 Polymorphic microsatellite marker oligonucleotide sequences.

Marker	Left Sequence	Right Sequence
D14Rat54	AGGCGTGCACACACATAAAC	TTGCCCAGAGTATAGGCCTG
D14Rat75	GCACACTGCAGTGAGACAAA A	TGACCCTTCAGTTGCAAATTC
D14Wox18	GAGTTTTCTTGCTGTCCAGAT T	TCAGAATCCCTATGCCTTTAG
D14Wox10	TCCTTTGGTGATGATTAATAT CAC	ATAAGGATTCTCAGATGCAAATG
D14Wox8	AAGCATAGCAGTGAATTGGT G	TTCATCATCCTTTCATAAAGGC
D14Arb17	ACTGAGGAATGCTGTGCTGA GG	TAACTGGGAGTAGGTGACTTGG
D14Mgh3	CAAGCACACCGTAGTAGAGG G	AATGGCTAGCTATCTATTGTGCG
D14Wox12	CCAACTGCTATGACACCAGG	AACTGGGAGTAGGTGACTTGG
D14Wox14	ACTTGATTACACACACAAAC ACAGA	CTTTGCTTTCTTTTAGCCATTT
D14Got33	TCGATCACATTTGCTGTGAG	AGACAAATCAGGCAACCCTTG
D14Rat41	TTTGCAAACTCATCCCCCT	TGCCCTTGAGAGGAGATAATG
D14Rat24	GCAGAGGGGAGAGGTAATAA	AAGCCTGCTCCACTCCAC
D14Rat110	AACATTGTCTTGCTTAGCCTC A	CTCCACCCACACACCACG

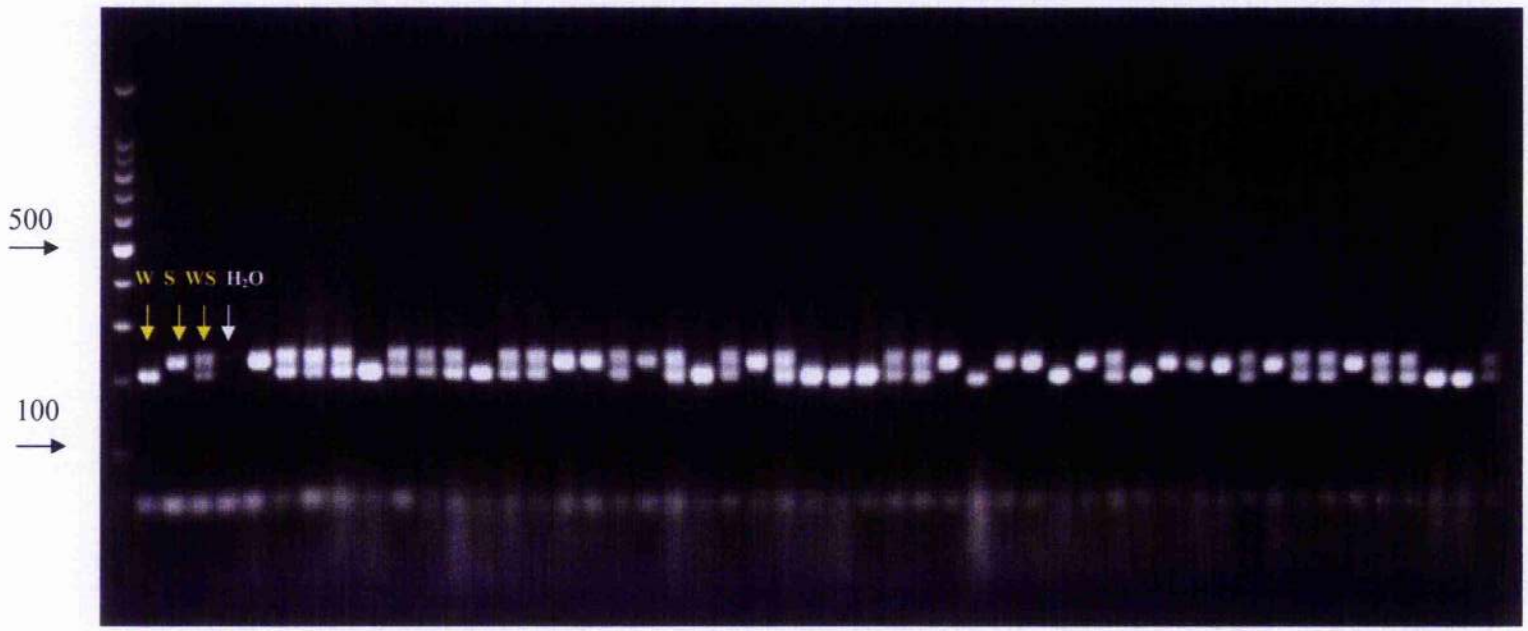

Figure 3.1 A representative agarose gel of 47 F_2 animals genotyped with marker *D14Arb17*. A 100bp marker is shown in lane 1; black arrows are included to highlight 100bp and 500bp bands. The parental samples are loaded in lanes 2-4 and are annotated in yellow with corresponding coloured arrows and the control water blank is indicated with a white arrow. From this agarose gel, animals are genotyped W, S or WS according to the band size and number. The row of bright bands below the 100bp marker size, are primer dimer artefacts.

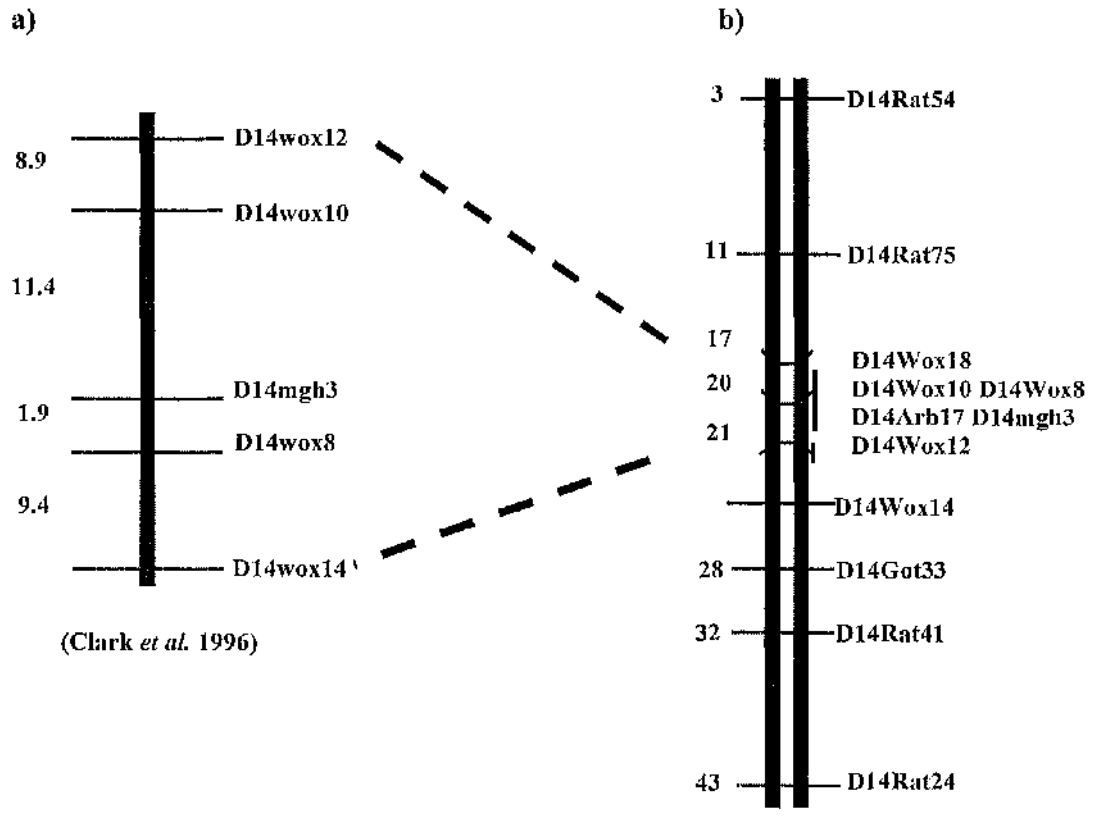

Figure 3.2 (a) Chromosome 14 map generated by Clark *et al.* (1996). Microsatellite markers correspond to a region of approximately 10cM, as defined by the addition of further polymorphic microsatellite markers. **(b)** Improved genetic linkage map generated using JoinMap 3.0 and 8 additional polymorphic microsatellite markers; *D14rat110* is not shown on this linkage map as this marker forms a linkage group unlinked to the 12 markers shown.

In order to confirm the suggestive QTL for LVMI, previously identified by Clark *et al.* (1996), simple interval mapping was used to analyse the entire F_2 group including males and females (n=134) for all traits. A QTL for CMI was identified, LOD = 4.0 (Figure 3.3a) and a QTL for LVMI, LOD = 2.8 (Figure 3.4a). Clark *et al.* (1996) reported a possible gender bias specific for males therefore the 69 females were removed from techniques; composite interval mapping and multiple interval mapping (Figures 3.3b, 3.3c, 3.4b, 3.4c, 3.5b, 3.5c, 3.6b, 3.6c, 3.7b, 3.7c).

In each dataset, analysis was initially performed using the simple statistical approach of interval mapping. With the application of more complex QTL analyses, generally the QTL region was more defined. Figures 3.3-3.7 illustrate the increasing complexity of the QTL region as more sophisticated statistical analysis methods are used. For example, in Figure 3.3a, a broad QTL peak for LVMI is visualised by simple interval mapping. Re-analysis using a composite interval mapping strategy results in a reduced QTL spread (Figure 3.3b). Further analysis using multiple interval mapping (Figure 3.3c) produces two distinct QTL peaks linked to markers *D14Wox14* (QTL1) and *D14Got33* (QTL2). For this reason, the likelihood-ratio statistic (LRS) and therefore logarithm of the odd score (LOD) varied for each trait analysed, however the location of the QTL was consistent regardless of the model tested. Furthermore, the suggestive QTL identified for PRA by simple interval mapping analysis is lost when re-analysed by more composite statistical methods (Figure 3.7). There were no QTL identified for any trait by subsequent analysis in the female subset of animals, suggesting a possible gender specific effect for CMI and LVMI observed only in males.

Variance in LVMI between heterozygote (WS) and homozygote (WW, SS) genotypes was examined using single factor (one-way) ANOVA, for polymorphic marker loci underlying the peak of LVMI QTL1 (*D14Wox14*) and QTL2 (*D14Got33*) in groups separated by sex. The results shown in Figures 3.8a-b (male) and 3.9a-b (female) respectively indicate both *D14Wox* and *D14Got33* loci affect LVMI in a recessive manner in males only.

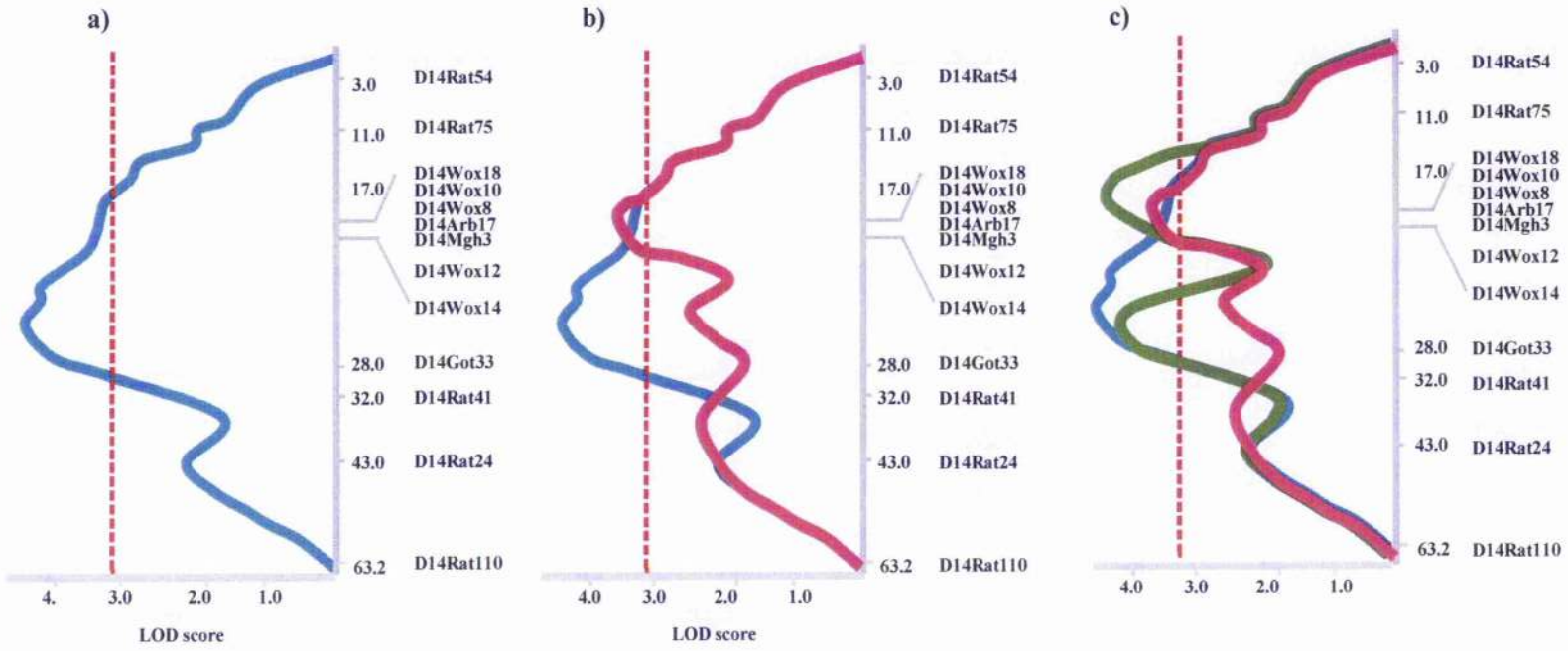

Figure 3.3 Rat chromosome 14 linkage map and CMI localisation for a F_2 population derived from SHRSP x WKY (males and females). Distances between markers are shown in cM. The red broken line denotes a significant LOD threshold, determined by 10,000 permutations of the data. **(a)** CMI QTL confirmed using simple interval mapping analysis (solid blue line), LOD = 4.0. **(b)** CMI QTL analysed using composite interval mapping (solid pink line), LOD = 3.5. **(c)** CMI QTL identified using multiple marker analysis (solid green line) (i) LOD = 4.0 (ii) LOD = 3.8 (P=0.0001, P=0.0002 respectively)

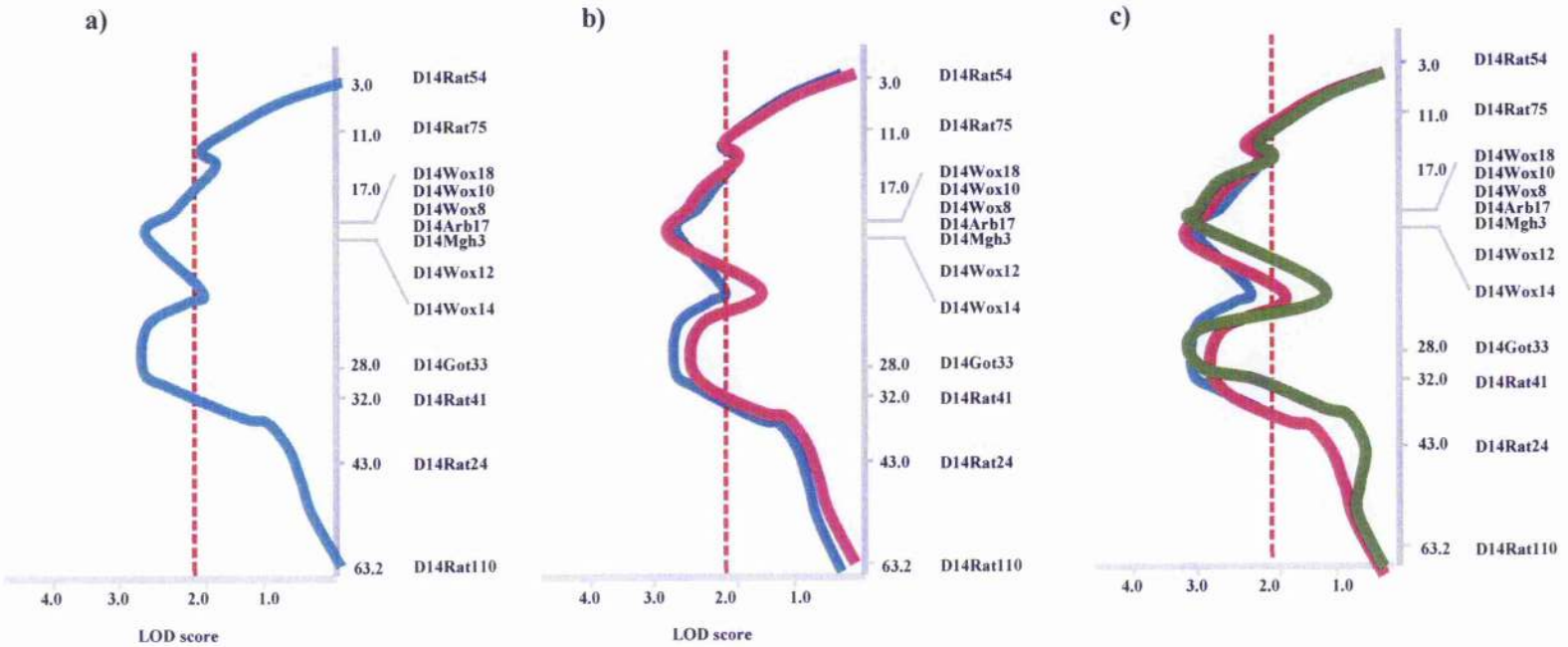

Figure 3.4 Rat chromosome 14 linkage map and LVMI localisation for a F_2 population derived from SHRSP x WKY (males and females). Distances between markers are shown in cM. The red broken line denotes a significant LOD threshold, determined by 10,000 permutations of the data. **(a)** LVMI QTL confirmed using simple interval mapping analysis (solid blue line), LOD = 2.8. **(b)** LVMI QTL analysed using composite interval mapping (solid pink line), LOD = 2.8. **(c)** LVMI QTL identified using multiple marker analysis (solid green line) (i) LOD = 2.9 (ii) LOD = 2.9 (P=0.02, P=0.001 respectively)

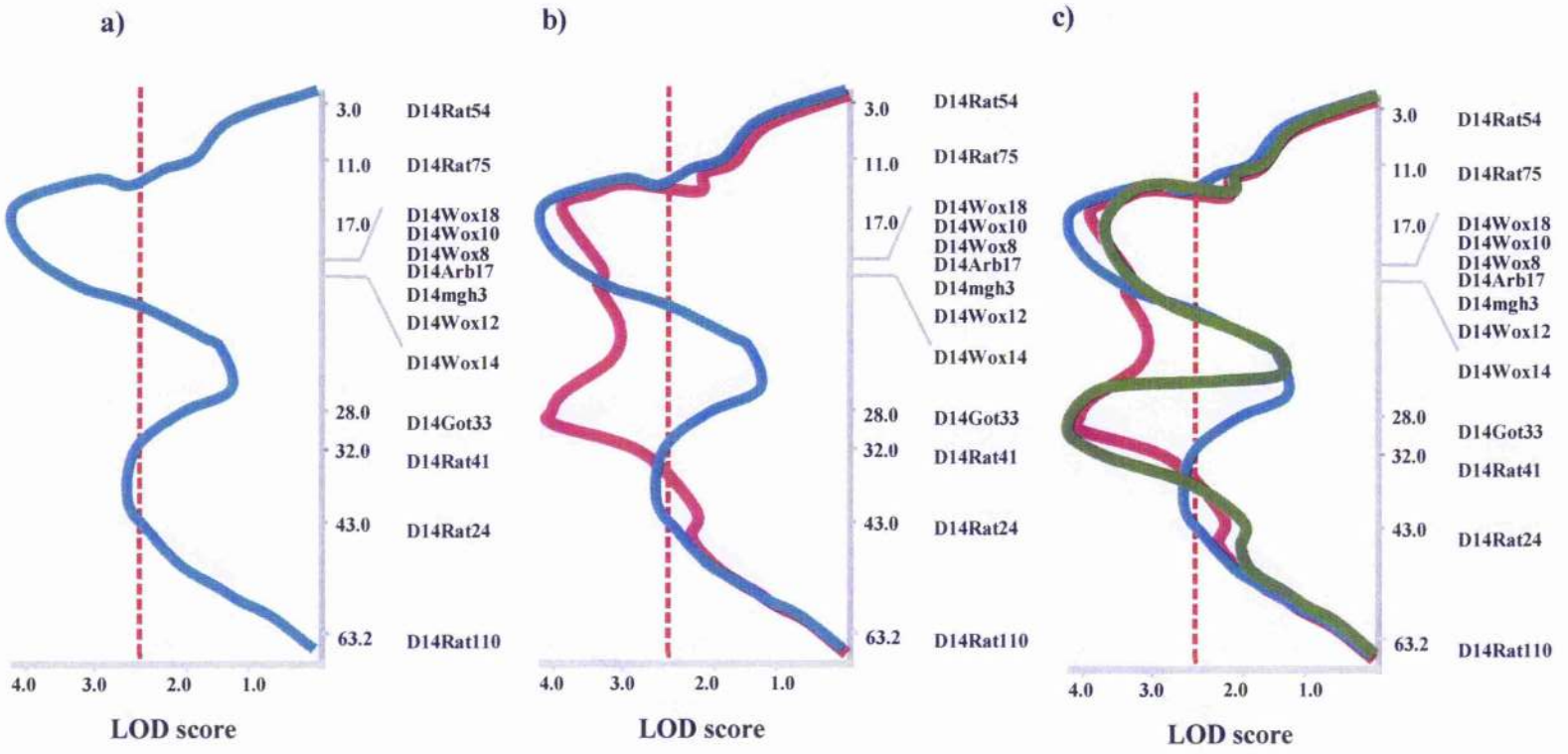

Figure 3.5 Rat chromosome 14 linkage and localisation for CMI in a F_2 population derived from SHRSP x WKY (males only). Distances between markers are shown in cM. The red broken line denotes a significant LOD threshold, determined by 10,000 permutations of the data. **(a)** CMI QTL confirmed using simple interval mapping analysis (solid blue line), LOD = 4.1. **(b)** CMI QTL analysed using composite interval mapping (solid pink line), LOD = 4.0. **(c)** CMI QTL identified using multiple marker analysis (solid green line) (i) LOD = 3.7 (ii) LOD = 4.0 (P=0.0002, P=0.0003 respectively)

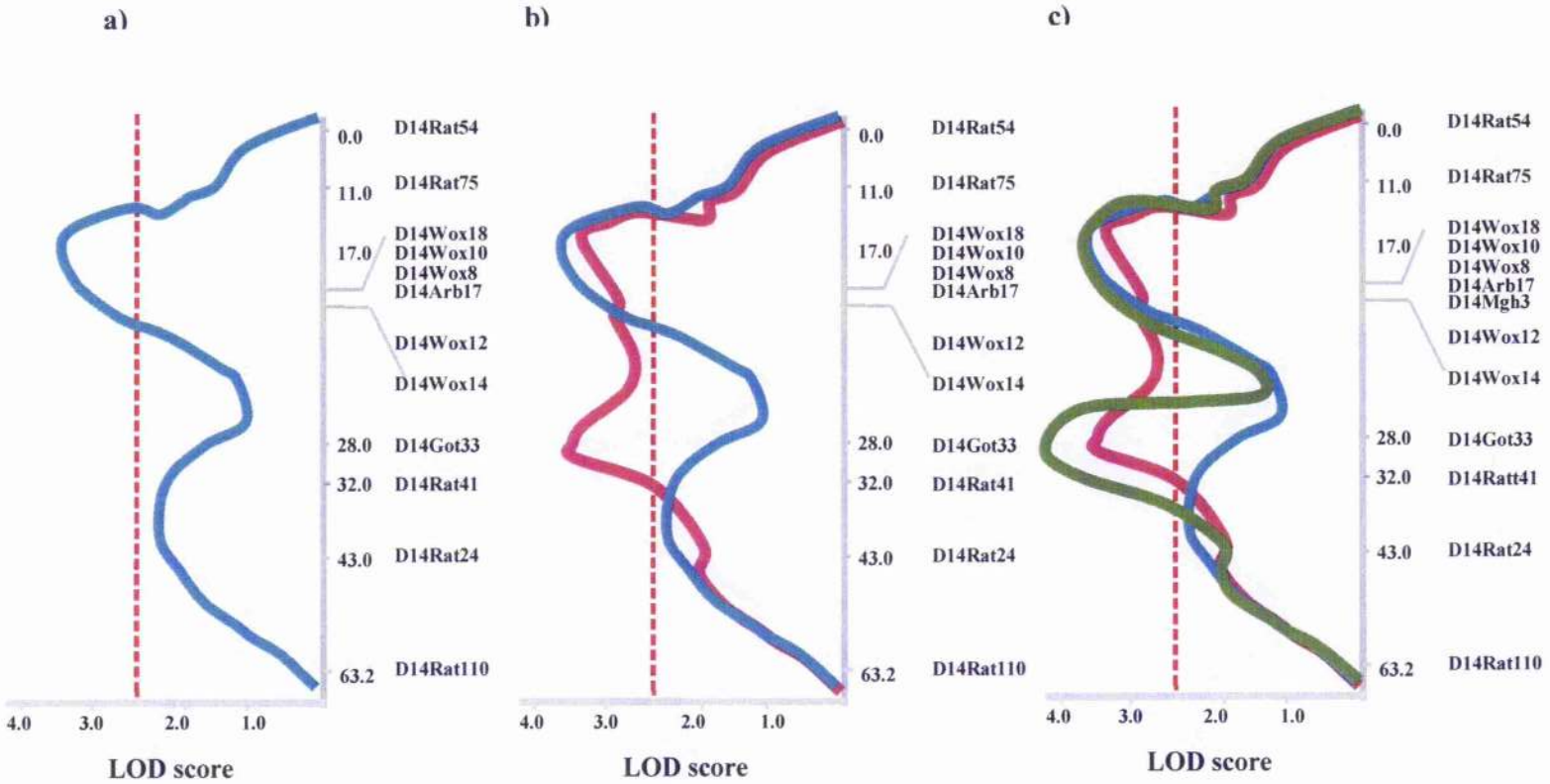

Figure 3.6 Rat chromosome 14 linkage map and LVMI localisation for a F_2 population derived from SHRSP x WKY (males only). Distances between markers are shown in cM. The red broken line denotes a significant LOD threshold, determined by 10,000 permutations of the data. **(a)** LVMI QTL confirmed using simple interval mapping analysis (solid blue line), LOD = 3.7. **(b)** LVMI QTL analysed using composite interval mapping (solid pink line), LOD = 3.5. **(c)** LVMI QTL identified using multiple marker analysis (solid green line) (i) LOD = 3.7 (ii) LOD = 4.0 (P=0.0001, P=0.00001 respectively)

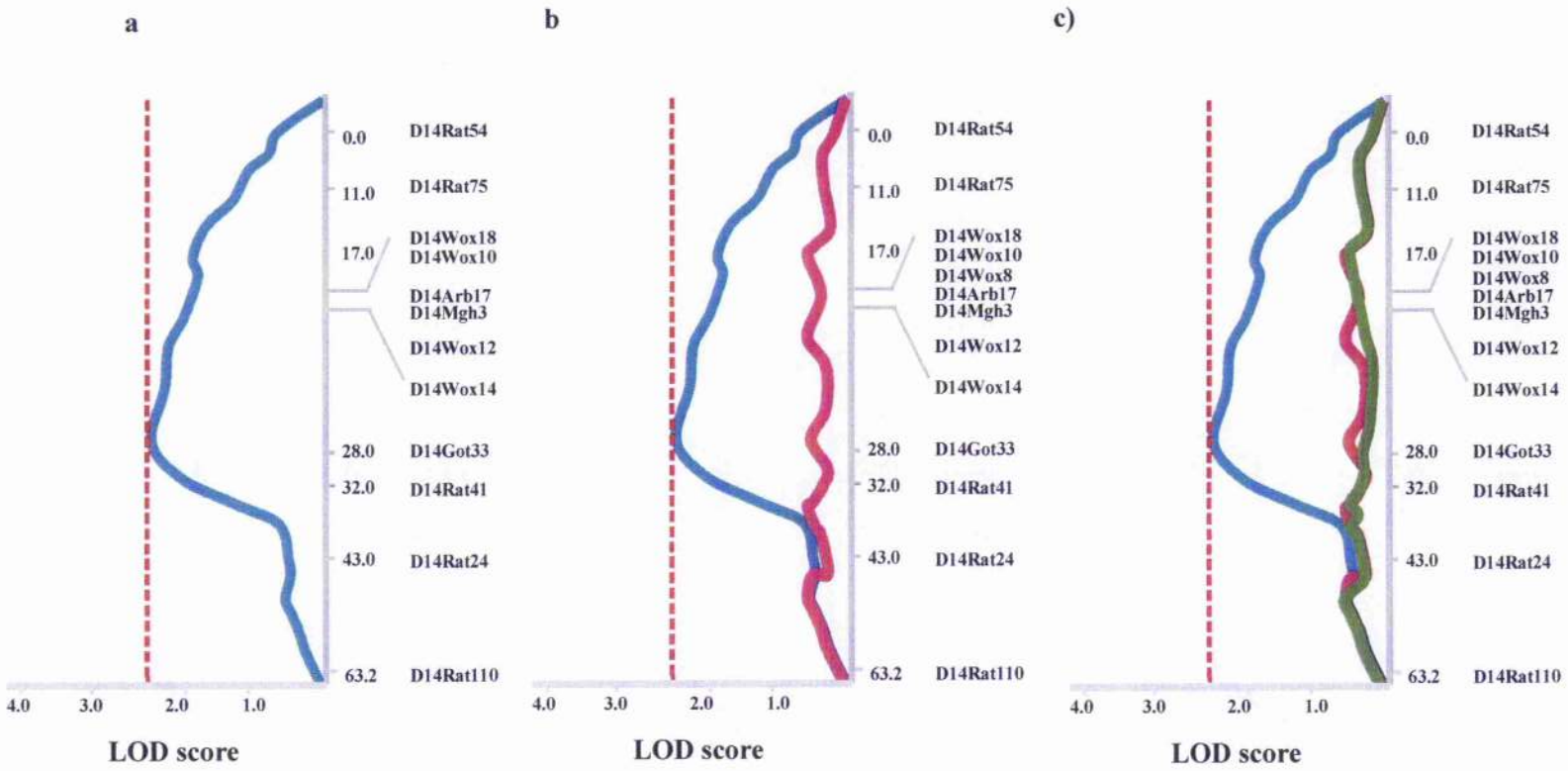

Figure 3.7 Rat chromosome 14 linkage map and plasma renin activity (PRA) localisation for a F_2 population derived from SHRSP x WKY (males only). Distances between markers are shown in cM. The red broken line denotes a significant LOD threshold, determined by 10,000 permutations of the data. **(a)** PRA QTL identified using simple interval mapping analysis (solid blue line), LOD = 2.8. **(b)** PRA QTL analysed using composite interval mapping (solid pink line), LOD = 0.2. **(c)** PRA QTL identified using multiple marker analysis (solid green line) (i) LOD = 0.2 (P=0.45)

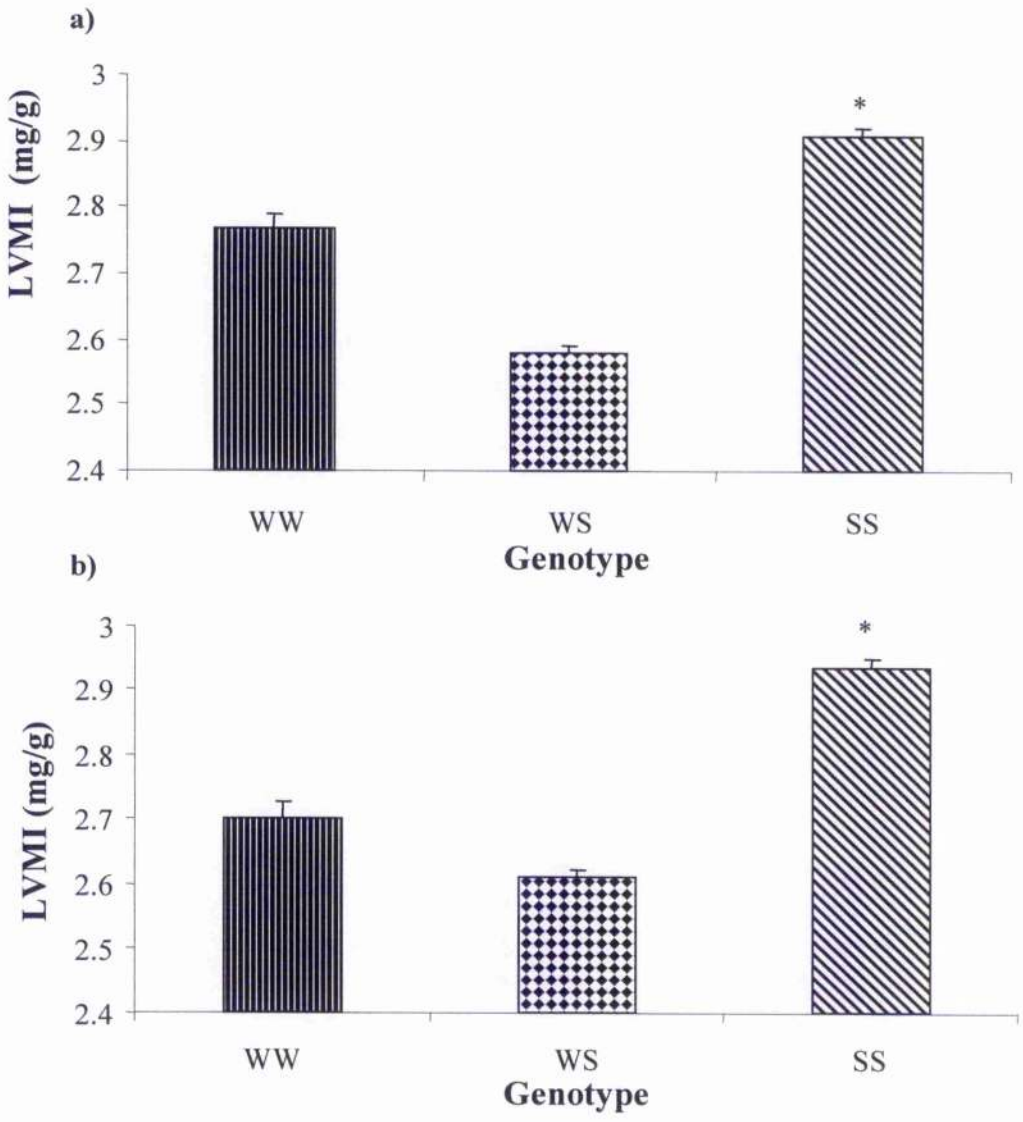

Figure 3.8 Single factor ANOVA analyses of LVMI in males at polymorphic marker loci **(a)** *D14Wox14* between heterozygote (WS, n=27) and homozygotes (WW, n=10; SS, n=26) and **(b)** *D14Got33* between WS (n=30), WW (n=12) and SS (n=21). Between WW and SS there is a significant difference in LVMI of 1.44 (*, $P<0.0001$) and 1.22 (*, $P<0.001$) at markers *D14Wox14* and *D14Got33* respectively. As WW and WS rats have equivalent LVMI, both marker loci affect LVMI in a recessive manner. There is no statistical difference in LVMI between WW and WS at both polymorphic loci. Data shown is mean ±SEM, *post hoc* Bonferroni adjustment.

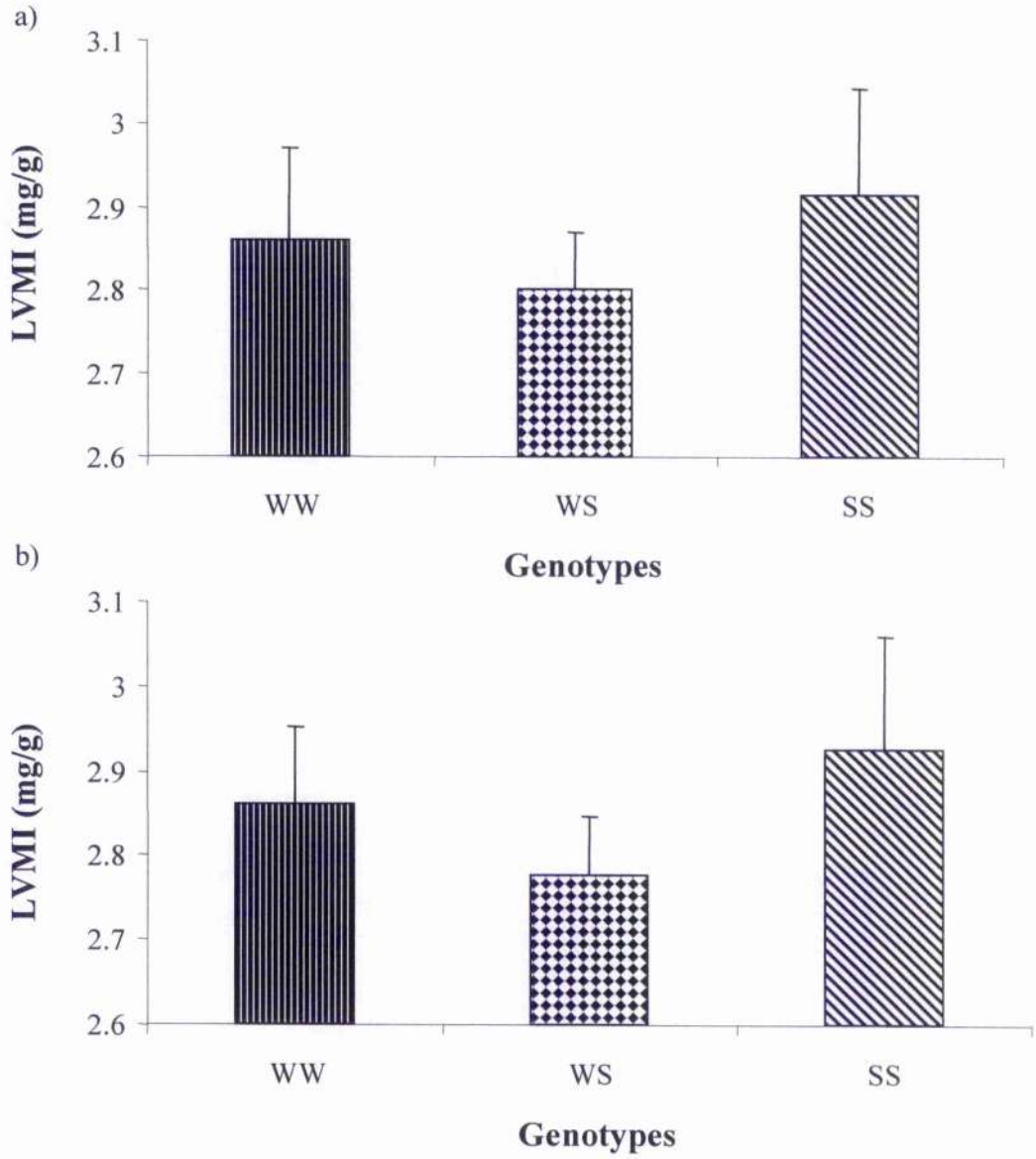

Figure 3.9 Single factor ANOVA analyses of LVMI in females at polymorphic marker loci **(a)** *D14Wox14* between heterozygote (WS, n=30) and homozygotes (WW, n=16; SS, n=19) and **(b)** *D14Got33* between heterozygote (WS, n=30) and homozygotes (WW, n=19; SS, n=18). There is no statistical difference in LVMI between the three genotypes WW, WS and SS at both polymorphic loci. All data shown is mean ±SEM.

with no corresponding QTL identified in the female subgroup, thus confirming a sex difference between males and females.

F_2 data was further analysed by linear regression to test the null hypothesis, LVMI in males is independent of SBP (after 3-week 1% salt loaded period), shown in Figure 3.10. There is a suggested relationship between SBP and LVMI; SBP accounted for between 21%-27% of observed variance in LVMI, determined by R^2 linear regression. In Figure 3.10, SHRSP homozygotes (labelled 'S') tend to have higher LVMI compared to animals with genotypes "W" (WKY homozygote) or 'H' (WKY/SHRSP heterozygote); the percentage variation explained by the *D14Got33* genotype is estimated between 11% and 19%. By fitting a regression model with LVMI as the response and SBP as the predictor and including SHRSP homozygous as a factor, resulted in significant coefficients for both SBP (coefficient±SE=0.010±0.002, $P=1.2\times10^{-6}$) and SHRSP homozygous (0.233±0.067, P=0.001); these regression lines are also plotted on Figure 3.10. There was no evidence that the relationship between SBP and LVMI was different for SHRSP homozygotes compared to animals with other genotypes (i.e. there is no evidence that the slope of the SHRSP homozygotes' regression line differed from the slope for the other animals; coefficient±SE=-0.0024±0.0037, P=0.519).

Statistical interpretation within the male subgroup was broadened to include student t-test analyses of Y chromosome origin (SHRSP grandfather versus WKY grandfather) and LVMI and SBP (after 3-week 1% salt loading period). From the data, the SHRSP derived Y chromosome segregates with an increased LVMI and SBP (Figures 3.11, 3.12) confirming previous findings by Davidson *et al.* (1995) with respect to blood pressure. Figure 3.11 shows the mean LVMI values separated by Y chromosome origin and a regression analysis plot is shown in Figure 3.12. From the data, males with a SHRSP grandfather have both larger LVMI and increased SBP compared to males with a WKY grandfather. In both cases this difference is statistically significant when compared using a unpaired t-test (LVMI difference=0.35mg/g, 3.7×10^{-6}; SBP difference=18.8mmHg, $P=3.2e\times10^{-5}$). The Y chromosome effect percentage variation on LVMI and SBP is approximately 29% and 27% respectively.

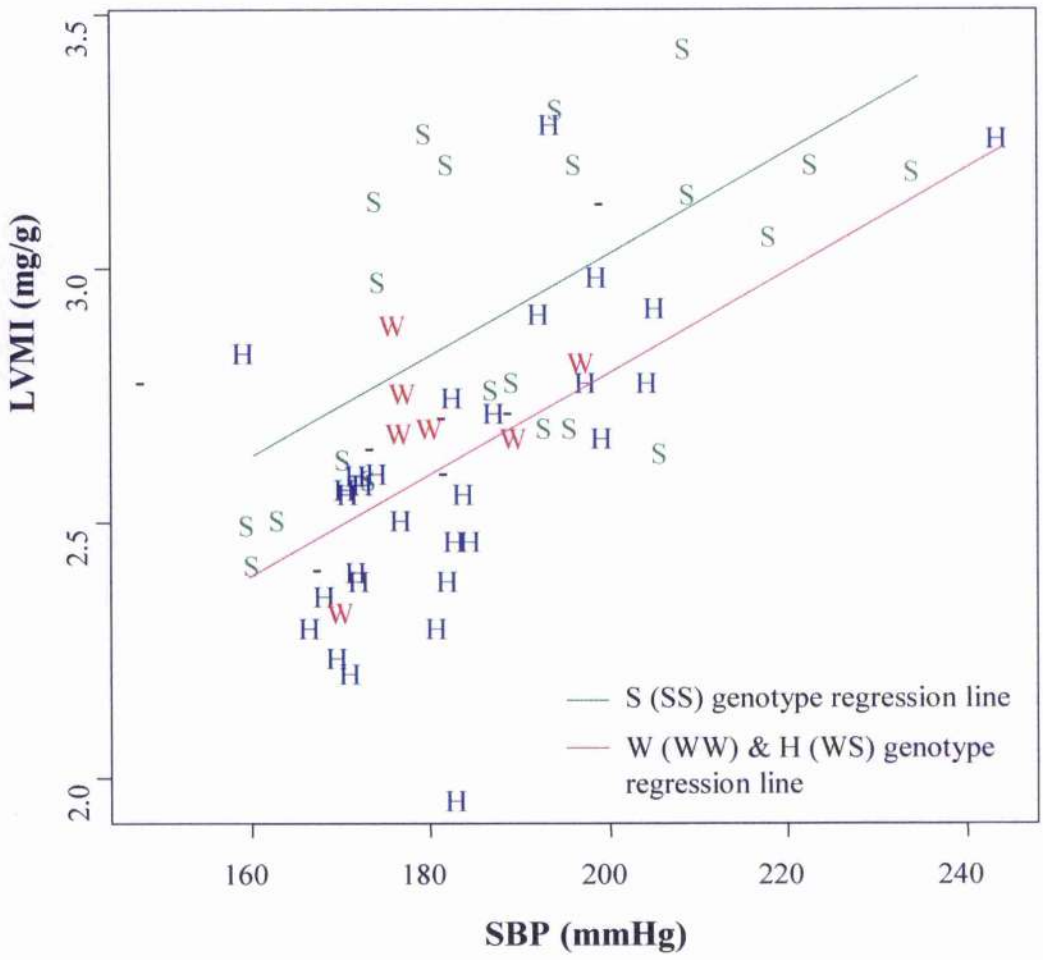

Figure 3.10 Graph showing SBP and LVMI values for male rats. The *D14Got33* genotype is shown: 'S' = SHRSP homozygous, 'W' = WKY homozygous and "H" = WKY/SP heterozygous; missing genotypes are shown as '-'. Regression lines for the model of LVMI using SBP (coefficient±SE=0.010±0.002, $P=1.2\times10^{-6}$) and the SHRSP homozygous factor (0.233±0.067, P=0.001) as regressors are shown; adjusted R^2= 0.47, F=25.81 with 2 and 54 d.f., $P=1.4\times10^{-8}$.

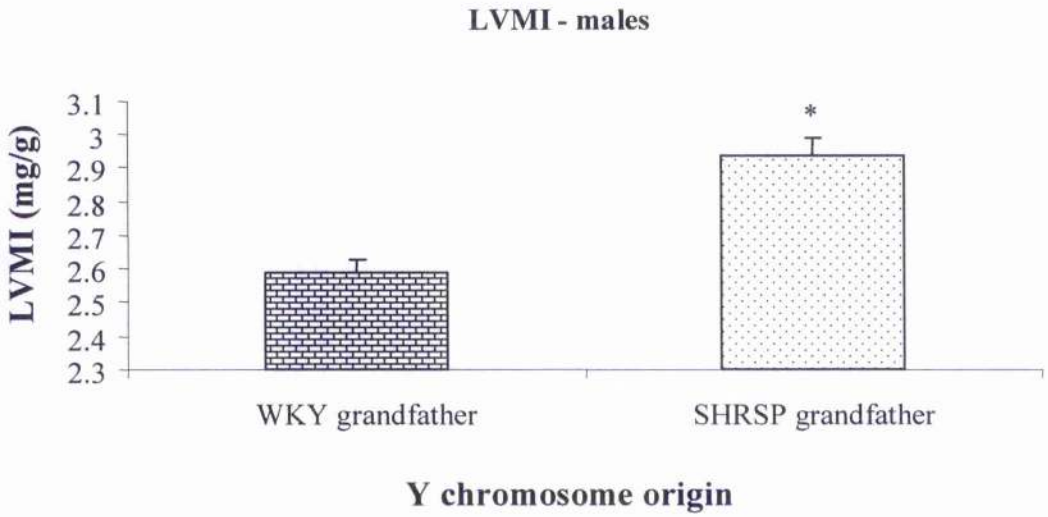

Figure 3.11 Analysis of the Y chromosome effect in male data subset. Animals are grouped according to Y chromosome origin: WKY grandfather (n=37) and SHRSP grandfather (n=28). LVMI was highest in males derived from SHRSP progenitor with a difference of 0.35mg/g ($P=3.7x10^{-6}$, F=27.27). Data shown is mean ±SEM using unpaired student t-test.

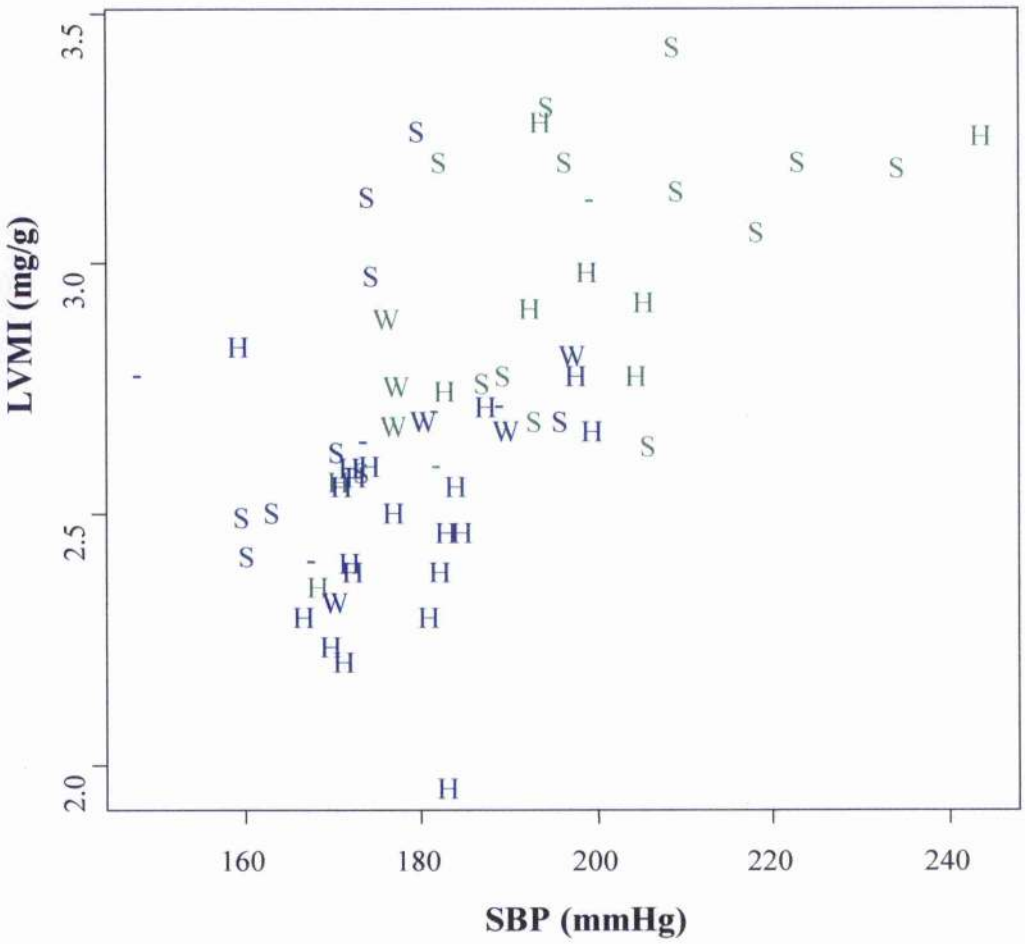

Figure 3.12 Graph showing SBP and LVMI values for male rats separated by Y chromosome origin. The D14Got33 genotype is shown: "S" = SHRSP homozygous, "W" = WKY homozygous and "H" = WKY/SHRSP heterozygous; missing genotypes are shown as "-". Animals with SHRSP grandfathers are coloured green and those with a WKY grandfather are coloured blue. Unpaired student t-test analysis F=27.27, P=3.7×10^{-6}, n=65).

3.3 DISCUSSION

With the addition of a further eight microsatellite markers, the number of polymorphic loci was increased from five to thirteen, resulting in a more improved coverage of rat chromosome 14 and a genetic linkage map spanning 63cM in the correct orientation, in comparison to the previous map generated (Clark *et al.*, 1996). In this study, a QTL for LVMI (QTL1) in males, identified by Clark *et al.* (1996) was confirmed and additional QTL for LVMI (QTL2) and CMI were identified using a dense genetic linkage map and three independent analysis methods.

Regardless of how the data was interrogated, a consistent single QTL linked to marker *D14Wox14* was identified and segregated with LVMI. The application of more complex and strict conditions identified a second QTL for both LVMI and CMI linked to *D14Got33*, which was not previously identified in the original F_2 genome wide scan carried out by Clark *et al.* (1996) and at the time of writing this thesis there were no other cited QTL for CMI or LVMI on rat chromosome14.

Continued analysis of the data to include all traits, using simple interval mapping, identified an additional QTL for PRA. However, this QTL was completely lost after re-analysis using both composite interval and multiple interval mapping approaches. These findings would suggest that application of a stringent and more refined statistical approach can reduce or completely eliminate artefacts associated with QTL identification, however these results also raise questions regarding gender within an inbred population and how sex can mask the effect of QTL leading to a complete loss or reduction of effect due to the simplicity of the statistical approach used. A further point to note with regards the results of this study is the gender bias toward males for the identified LVMI QTL. Comparisons between LVMI and linked polymorphic marker loci *D14Wox14* and *D14Got33* within the male and female subgroups showed statistical relevance in the male subset only. There was a higher standard error of the mean (SEM) in LVMI within the female group compared to the males,

which may be a result of population size or simply higher intra-group variability, although SEM by itself is difficult to interpret.

Many compounding factors can affect QTL analysis, for example the number and interaction of QTL. LOD score–based (likelihood ratio statistic) methods were used by Lander & Botstein (1989) to define an approximated confidence interval of an estimated QTL position; "support interval" mapping. Jiang and Zeng (1995) also used the likelihood ratio statistic approach to test hypotheses such as close linkage vs. pleiotropy. Consequently, the actual drop-off required in the likelihood ratio statistic to define support intervals varies with both each study and QTL. This problem becomes further complicated when other markers are fitted in a model, in addition to the markers flanking the interval under investigation. In particular, when extra markers are added to a genetic linkage map, a sharp rise or conversely fall, in the likelihood ratio curve at some marker loci is often observed. Assuming the QTL exists, increasing the complexity of the statistical analysis and applying a more stringent criterion, can therefore result in a more refined model of the QTL. This study demonstrates that application of composite statistical analysis methods result in more delimited QTL, including the identification of an additional QTL (QTL2) and the reduction of a suggestive QTL, for PRA.

It is has previously been established that male SHRSP have higher blood pressure in comparison to females (Davidson *et al.*, 1995), therefore to test the variance of LVMI with SBP (after 3-week 1% salt challenge) as a variable, stepwise linear regression analysis of the data was performed. The results for genotypes WKY/SHRSP heterozygote and SHRSP homozygote at markers underlying the peak of QTL2 showed a statistical relationship between LVMI and blood pressure, indicating that LVMI is influenced by blood pressure, but genotype is not linked to blood pressure, as there is no blood pressure QTL identified on rat chromosome 14 in this study. This relationship is not surprising given that a correlation with blood pressure and LVMI has previously been shown in SHR and other rat models (Cicila *et al.*, 1999; Rapp, 2000; Aiello *et al.*, 2004).

The same analysis in the WKY homozygote genotype showed a trend towards a blood pressure effect and LVMI, but this did not reach a level of significance and may simply be due to a lack of power due to a lower number of animals in this subgroup. From Figure 3.10 differences within the genotypes groups are also apparent, most notably half of the SHRSP homozygotes seem to have higher LVMI compared to almost all the animals with the other genotype groups. This difference leads the linear regression model with the binary factor "SHRSP homozygote" to find a significant increase in LVMI for animals which are SHRSP homozygotes. However, the bimodal nature of the SHRSP homozygote genotype suggests that there may be some other factor(s) involved. This could be due to operator differences in data acquisition or seasonal/time differences as animals used in the study were bred over one year period.

Another possibility for the observed gender effect is a Y chromosome/autosome interaction. When the data was analysed using linear regression, there is a SHRSP derived Y chromosome effect with respect to LVMI and SBP. These results do not necessarily implicate an epistatic Y chromosome-autosome interaction, as SBP is a dependant variable and previous data by Davidson *et al.* (1995) confirmed SBP in the SHRSP is influenced by loci on the Y chromosome. It is also important to note that there was no significant linkage between genotypes underlying the QTL2 peak and SBP and that LVMI variance is greater than that of blood pressure effects alone, which account for between 21%-27% variance in this study.

Recently, Inomata *et al.* (2005) carried out genome-wide screenings in two F_2 populations bred from the SHRSP X WKY (110 male and 110 female rats) and SHR X WKY (151 male rats; 1% salt loading), which showed consistent linkage to cardiac mass on rat chromosome 3, in the vicinity of D3Mgh16 (LOD = 4.0 to 6.6 across the F_2 populations). The QTL was defined in a relatively narrow region <25 cM in both F_2 cohorts and despite confounding factors such as differences in haemodynamic overload and dietary manipulation (with or without salt-loading), was highly reproducible. In addition, the group identified a high degree of gender specific linkage from their data, with the genetic

percentage impact on QTL variance in both sexes estimated to 23% (males) and 17% (females).

Deschepper *et al.* (2005) mapped the progeny of an F_2 inter-cross between normotensive WKY and WKHA rats, showing male-specific linkage between locus Cm 24 and LVMI. Genome wide expansion of their analysis detected additional loci, all linked to LVMI in a sex-specific manner, regardless of the autosomal location - a locus (Lvm-8) on chromosome 5 (LOD=3.4), two loci (Lvm 13; LOD=4.5 and Lvm 9; LOD=2.8) on Chromosome 17, and on chromosome 12 (Lvm 10; LOD=4.2). These results indicate that LVMI in normotensive rats is influenced by genes separate to those controlling blood pressure, with the suggestion that these genes may also act in a gender-specific manner possibly via sex-specific gene-gene-protein interactions.

Altogether, these studies provide further evidence that genes underlying LVMI QTL influence heart weight in both hypertensive and normotensive rat strains and support the hypothesis that sexual dimorphic effects are important with regards genetic susceptibility of cardiac hypertrophy. In conclusion, this current study is notable for the use of several statistical applications for localisation of LVMI QTL on rat chromosome 14, though these analyses only refine the region of interest and do not reduce the QTL peak to the inclusion of a single gene. The outcome of this statistical breakdown resulted in confirmation and identification of QTL for LVMI and CMI in SHRSP X WKY cross, which showed no linkage with genotypes underlying the QTL2 peak and SBP in SHRSP or WKY F_2 animals. In particular, the relative prevalence of sexual dimorphic QTL was highlighted in males, which may be masked in data produced by groups performing analyses exclusively in male only populations. Whilst no obvious physiological candidate genes have been identified within the QTL regions, there are a number of positional candidates with functional relevance to the phenotype which will be discussed in detail in results Chapter 4. In spite of this and due to the large area delimited by QTL regions, the generation of congenic strains is required in order to either confirm or refute the putative QTL and further dissect the region further (*Chapter 6*).

CHAPTER 4

COMPARATIVE MAPPING AND IDENTIFICATION OF CANDIDATE GENES

4.1 INTRODUCTION

The candidate gene approach focuses on specific genes, based on some a priori knowledge regarding loci or system(s), which at a functional level may be expected to show significant differences in animal models. Comparative mapping efforts, whereby regions of conserved synteny in different species are investigated and combined with QTL analysis data, can provide candidate genes of interest within a specific region, in the absence of gene profiling data. This strategy has several advantages such as lower cost, ease of use and the relatively high number of candidate genes identified. There are several disadvantages however, including the limitations of gene mapping resources and restrictions in available knowledge and understanding of gene function, which is required when filtering candidate genes to take forward to quantitative expression analysis. In order to maximise the potential of comparative mapping, QTL with shared commonality between rodent strains should also be seen as important candidate loci for the disease under investigation.

One such example of this is the QTL identified on rat chromosome 10, which provides a paradigm and highlights the importance of conserved regions of synteny between chromosomes. This particular QTL was reported in several rodent crosses, including - SHRSPHd x WKYHd cross, (Jacob *et al.*, 1991; Hilbert *et al.*, 1991) Dahl S x MNS cross, (Deng *et al.*, 1991; Deng *et al.*, 1995) Dahl S x LEW cross, (Garrett *et al.*, 1998) GH x BN cross, (Harris *et al.*, 1995) and SHR x WKY cross (Zhang *et al.*, 1996). In addition, Julier *et al.* (1997) investigated both the QTL region on rat chromosome 10 and a homologous region of conserved synteny on human chromosome 17. The same region has also been linked to a monogenic disorder, pseudohypoaldosteronism type II or Gordon's syndrome, in a subset of families (Mansfield *et al.*, 1997). In 1999, Baima *et al.* confirmed these data in another population of patients with essential hypertension and further clarified the region of interest. These studies (Julier *et al.*, 1997; Baima *et al.*, 1999) provide classic evidence of the proof of concept that a QTL identified in a rodent species can be translated directly to a QTL in humans and set a precedent for similar studies for other cardiovascular QTL.

Once a positional candidate gene has been identified, it is important to investigate functional roles both *in vitro* and in the whole animal at different stages in development in order to assess how the gene(s) impact on the phenotype of interest. There are a number of investigative approaches to this. For example, at the molecular level expression of specific genes in a target tissue can be examined using techniques such as real-time PCR with pharmacological intervention and dietary manipulation studies as well as protein analysis at the physiological and biochemical level. Pharmacological intervention studies involving antihypertensive drugs allow a route for investigation of candidate gene expression in response to chemotherapy and provides some insight into both biochemical pathways/interactions and pharmacogenetics in experimental animal models. A recent example of this comes from Zhou *et al.*, (2006) who demonstrated the long-term regulation of cardiac K^+ channel gene expression could be controlled by the gene activation of AT_1 receptors, by angiotensin II.

Identified QTL regions still contain a large number of potential candidate genes and in the absence of high-throughput genotyping methods, comparative mapping techniques rely on bioinformatic methods such as data mining to reduce the number of potential gene candidates. In this study, the primary objective was to narrow the QTL region further by mapping conserved regions of synteny between the rat, mouse and human. In doing so, putative genes of interest can be identified and taken forward for further analysis including tissue specific mRNA quantification and sequencing. Additionally, the functional role of candidate genes was investigated by gene expression analysis at different stages in the development of hypertension. Furthermore, the impact of pharmacological intervention on the expression of candidate genes identified will be investigated with the use of drugs previously demonstrated to affect blood pressure and LVM via different mechanisms.

4.2 METHODS

4.2.1 Comparative Mapping

Data mining using online databases was carried out and data used to build comparative maps for mouse, rat and human (http://www.ensembl.org; http://www.ncbi.nih.gov; http://www.softberry.com/). Regions of synteny were mapped concordantly and known genes identified within defined regions of synteny between the chromosomes of rat, mouse and human.

4.2.2 Pharmacological intervention

AT_1 receptor antagonist (olmesartan) and a vasodilator + diuretic combination (hydralazine + hydrochlorothiazide) were administered to 16-wk old SHRSP males (n=9) over a 4 week period by mixing with banana custard baby food. Daily doses - olmesartan (20mg/kg/day; n=3), hydralazine (16mg/kg/day; n=3) + hydrochlorothiazide (16mg/kg/day; n=3) (Sigma, UK). Control animals were fed vehicle only (WKY, n=3; SHRSP n=3). Blood pressure measurements were recorded on a weekly basis by tail cuff plethysmography. Hearts were removed at sacrifice for RNA extraction (n=3 per group) and quantitative analysis as follows.

4.2.3 RNA extraction and cDNA synthesis

Liver, aorta and whole hearts were removed at sacrifice from SHRSP and WKY animals: ages 6 weeks (n=3 respectively), 16 weeks (n=3 respectively), 21 weeks (n=3 respectively) and 21 weeks after 1% dietary salt manipulation (n=3 respectively). In addition, heart tissue was removed from animals receiving pharmacological intervention treatment. The heart was blotted and weighed; the LV was dissected free from right ventricle and atria and weighed. LVMI was calculated from LVM indexed to body mass (mg/g). The liver was sliced and aorta left intact. All tissues were snap frozen using liquid nitrogen. RNA was extracted as described in *Chapter 2.6.1* using Qiagen RNeasy Maxi kit

(heart and liver) and Qiagen RNeasy mini kit (aorta). Single stranded cDNA was synthesised using 1µg of total RNA and the Advantage RT for PCR kit from Clontech.

4.2.4 Real-time PCR Quantification

With the purpose of identifying differential gene expression patterns between SHRSP and WKY parental strains, tissue from aorta and whole heart were examined from animals aged 6wk (prior to the onset of significant hypertension), 16wk (when significant hypertension is established), 21wk and 21wk ('S', 3 week, 1% salt in drinking water). Additionally, heart RNA was examined from animals in the drug intervention study. RNA was quantified by real-time PCR (RT-PCR) using TaqMan® Gene Expression Assays (Applied Biosystems, Foster City, CA) as detailed in *Chapter 2.6.4*. A concern with the use of certain housekeeping genes in RT-PCR, is non specific binding of contaminating DNA, which can interfere with the measure of fluorescence from both target and control gene probes, therefore DNA digestion was carried out on all RNA samples prior to use. In order to assess the possibility of relative quantification, singleplex and multiplex reactions were tested to examine PCR efficiency for both the gene(s) of interest and appropriate housekeeping gene. All gene expression PCR was carried out on an ABI prism 7900HT Sequence Detection System using a 96-well plate format.

4.2.5 Sequencing Candidate genes

Candidate genes were sequenced from PCR products obtained from genomic DNA extracted from 3 SHRSP, 3 WKY, 1 Brown Norway (BN) and 3 (WKY/SHRSP) heterozygote rats' liver tissue using the method described in *Chapter 2.4.1*. The inclusion of heterozygote DNA was to provide further confirmation of SNPs identified, as heterozygote animals will possess both alleles. Forward and reverse primers were designed in house to cover exon/intron boundaries as well as 5' flanking regions of the genes, to include approximately 1500 bases upstream of the initiating methionine codon of the open reading frame. Primer sequences used to sequence *Dbp* and *Corin* are listed in Tables 4.1 & 4.2 respectively.

Table 4.1 PCR and sequencing primers for *Dbp*.

Primer	Sequence (5'-3')	BP#	GC%	Coverage
*Dbp*_01F	ACCACTTTACAACTTGAAGCGGG	23	47.8	Exon 1
*Dbp*_01R	GGAAACAGAAATGCGCAGTTGT	22	45.5	
*Dbp*_02F	CAATTCTCCCTCCCACATTGG	21	52.4	Exon 2
*Dbp*_02R	TGGGTGAGGCTGTGAAGGAA	20	55	
*Dbp*_03F	AAGGGCATCTGAACACACTCTGA	23	47.8	Exon 3
*Dbp*_03R	TCAAGGTTTTATGCATCCCCAG	22	45.5	
*Dbp*_04F	TTCAAGCATCAGGAAGCCCTG	21	52.4	Exon 4
*Dbp*_04R	CTACCGGATCATAGCATGGCTC	22	54.5	
*Dbp*_05F	GTATTTGCCAGGACGTGCTTCA	22	50	Exon 5
*Dbp*_05R	TGTGGTGATGGAGCACGTTTAG	22	50	
*Dbp*_06F	GATACTTGACCTTTCCCGAGTGC	23	52.2	Exon 6
*Dbp*_06R	GCCTTGTAGCCATGACATTGCT	22	50	
*Dbp*_07F	GCTCTCACAGACCGATAGCAATG	23	52.2	Exon 7
*Dbp*_07R	GAATCGCAGTGGGGACTAAAATC	23	47.8	
*Dbp*_08F	CAACATGAAGTGGAGAACTC	20	45	Exon 8
*Dbp*_08R	CCAGTGGTTCTCAATCTTC	19	47.4	
*Dbp*_09F	ACCCACCTCAAGTGGAATTTTG	22	45.5	Exon 9
*Dbp*_09R	TCTGGGAATGGAGTTGTTGGTC	22	50	
*Dbp*_10F	AAGTGTCTACTATCGCTATTGGAC	24	41.7	Exon 10
*Dbp*_10R	TGCATGTGTGTTTTTTACAGAGCC	24	41.7	
*Dbp*_11F	TTGTTGGACAAGTAGAGGAC	20	45	Exon 11
*Dbp*_11R	GGTTTGGAGCAAGAAGATAG	20	45	
*Dbp*_12F	TTGCTGAGTCCCCTGAAAAC	20	50	Exon 12
*Dbp*_12R	CTTCTCTGTATCTGCAACATGGGT	24	45.8	
*Dbp*_up_01F	GACACCAGCTATTTACTGTC	20	45	Up – 750
*Dbp*_up_01R	AGAAAGCTGCCTCCAGCAATG	21	52	
*Dbp*_up_02F	CCCAAGGGAAAGAAGATCATGG	22	50	Up 750 - 1500
*Dbp*_up_02R	AACGCTGTGGTTCCTGAACTGT	22	50	

All primers were designed in house using reference sequences taken from Ensembl database (http://www.ensembl.org). F refers to a forward strand primer and R refers to a reverse strand primer (reverse primers are in reverse complement format). Base pair number (BP), G (guanine)/C (cytosine) percentage and primer coverage is listed.

Table 4.2 PCR and sequencing primers for *Corin*.

Primer	Sequence (5'-3')	BP#	GC%	Coverage
CRN01F	CTTGGAGTCGGAGGCTCGGAC	21	47.8	Exon 1
CRN01R	TTACCATAGAGCTCCAGATGTCTC	23	45.5	
CRN02F	CAATTCTCCCTCCCACATTGG	20	52.4	Exon 2
CRN02R	TGGGTGAGGCTGTGAAGGAA	20	55	
CRN03F	TTCCTCCTGCTTGTGCTCATC	20	47.8	Exon 3
CRN03R	CTTGTCCACACAGTCATGGTC	21	45.5	
CRN04F	GTGGAATGCAGAAGTGGACAG	22	52.4	Exon 4
CRN04R	GTGCTCCCATTGAGATTCTC	20	54.5	
CRN05F	CAAATTCTGCCCTACCACAGCAC	23	50	Exon 5
CRN05R	GGCGTCGCTGTTATTCTCAGTG	22	50	
CRN06F	GATACTTGACCTTTCCCGAGTGC	23	52.2	Exon 6
CRN06R	GCCTTGTAGCCATGACATTGCT	22	50	
CRN07F	GCTCTCACAGACCGATAGCAATG	23	52.2	Exon 7
CRN07R	GAATCGCAGTGGGGACTAAAATC	23	47.8	
CRN08F	CAACATGAAGTGGAGAACTC	20	45	Exon 8
CRN08R	CCAGTGGTTCTCAATCTTC	19	47.4	
CRN09F	ACCCACCTCAAGTGGAATTTTG	22	45.5	Exon 9
CRN09R	TCTGGGAATGGAGTTGTTGGTC	22	50	
CRNup_01F	GACACCAGCTATTTACTGTC	20	45	Up – 750
CRNup_01R	AGAAAGCTGCCTCCAGCAATG	21	52	
CRNup_02F	CCCAAGGGAAAGAAGATCATGG	22	50	Up 750 - 1500
CRNup_02R	AACGCTGTGGTTCCTGAACTGT	22	50	

All primers were designed in house using reference sequences taken from Ensembl database (http://www.ensembl.org). F refers to a forward strand primer and R refers to a reverse strand primer (reverse primers are in reverse complement format). Base pair number (BP), G (guanine)/C (cytosine) percentage and primer coverage is listed.

PCR (20μl) product was purified to facilitate elimination of dNTPs and primer oligonucleotides. Sequencing reactions were performed, cleaned and run on an ABI 3730 (Applied Biosystems, UK) as described previously in *Chapter 2.7.2*

4.2.6 Sequence analysis

Candidate gene sequences were analysed using Seqscape version 2.1 (Applied Biosystems, USA), which is designed for reference-based analysis such as mutation detection and analysis, SNP discovery, validation and sequence confirmation. Data was input in text file format and sequences aligned against a reference sequence dataset downloaded from Ensembl database (http://www.ensembl.org). Detection of SNPs was carried out manually with two independent observers and automatically, using Seqscape console commands. Short sequences including SNPs were then re-aligned against reference databases of transcription factors and corresponding binding sites with commercially available software TFSearch© (Yutaka Akiyama, 2002), rVista version 2.0 and GeneQuest version 5.05 (Dnstar, USA).

4.2.7 SNP Genotyping

Re-genotyping of F_2 animals was carried out by sequencing DNA of each animal using primers designed against a named SNP identified from candidate gene sequencing. As all animals used to produce the F_2 progeny are inbred, linkage disequilibrium of SNPs identified in candidate genes will be high therefore only one SNP was used for genotype analysis.

4.3 RESULTS

Comparative mapping strategies aim to identify putative candidate genes based on conserved regions of synteny between species. Figure 4.1, is an illustration of a comparative map based on data from identified orthologous regions between rat chromosome 14, mouse and human. Mouse chromosome 5 and human chromosome 4

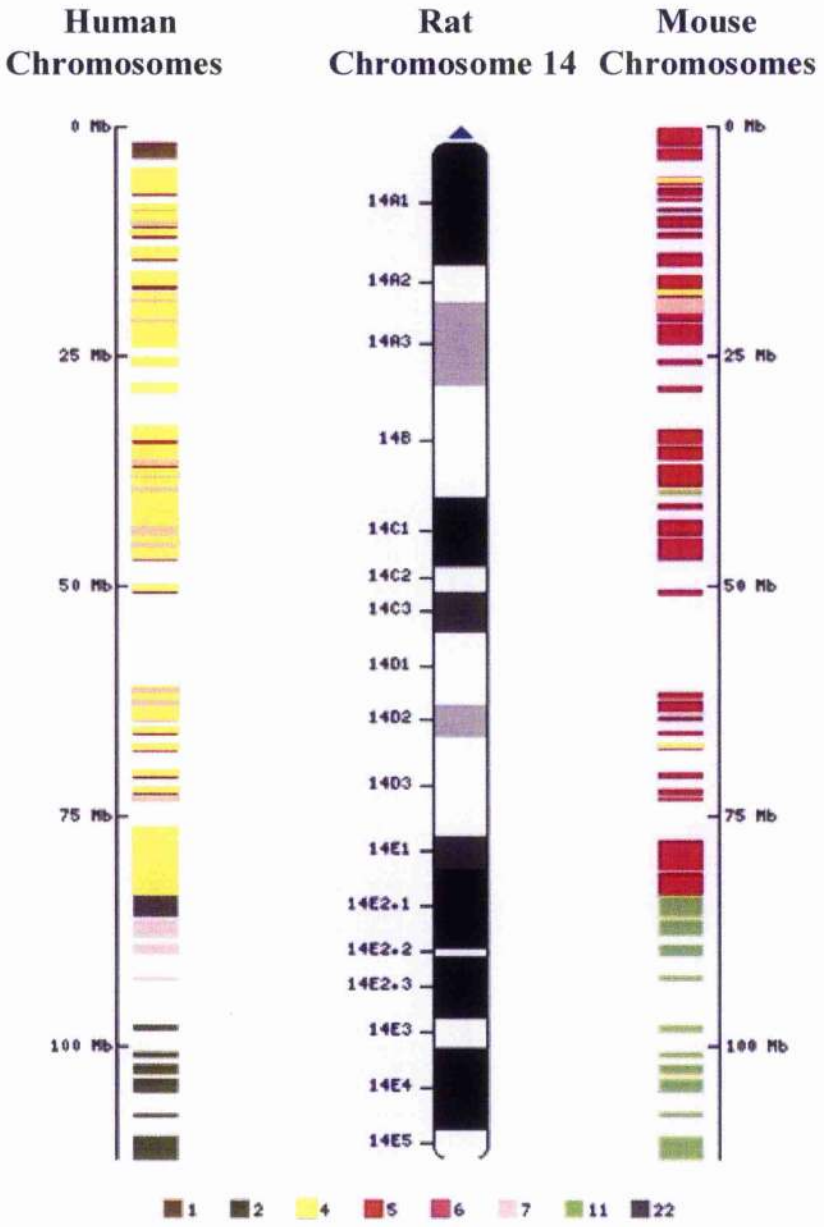

Figure 4.1 Comparative map for rat chromosome 14 (centre). Regions of common synteny between the mouse and human are colour coded, with corresponding chromosome indicated. Chromosomes identified in mouse are 5, 11, 4 and 7. Chromosomes identified in human are 4, 2, 7, 22 and 1.

approximated to QTL regions identified in *Chapter 3*. Selection of two candidate genes was based on a combination of cross-referencing literature with available online databases for functional relevance to cardiac hypertrophy and narrowing the regions of interest to the underlying QTL peaks; listed in Appendix III. In addition, data from a previous microarray study carried out by our group (McBride *et al.*, 2003) in kidney tissue was used as an initial reference to gauge differential expression of putative candidate genes of interest.

The selected genes were then tested by pairwise display to check for sequence percentage homology, using a simple model designed by Jukes and Cantor (1969) to adjust for the number of differences observed between sequences. This corrective formula, D=-3/4ln (1-(4p/3)), explains the relation between the percent difference and the genetic distance (the fraction of expected substitutions) between sequences. If the genetic difference 'D' is increased between sequences, the percentage of dissimilarity will also increase. Table 4.3 details the pairwise alignment scores obtained from NCBI Homologene, for candidate genes *Corin* and *Dbp* in human, mouse and rat. From the data, it can be seen that *Dbp* has a more highly conserved inter species amino acid sequence homology (92.3%) than *Corin* (83%) and a relatively shorter evolutionary genetic distance; D= 0.157-0.162 in *Dbp* compared to D=0.187-0.193 for *Corin*.

Both candidate genes were further investigated using relative quantification real time PCR (RT-PCR), which allows for detection of changes in steady-state mRNA levels across multiple samples relative to an endogenous control, which is constitutively and uniformly expressed. Calculations are based on cycle threshold (CT) value comparisons at a constant level of fluorescence from the gene expression probes using a $2^{-\Delta\Delta CT}$ method assuming ≈100% PCR efficiency of reaction between the target and reference gene. Therefore, in order to quantify mRNA of a target gene relative to an endogenous control, efficiency of PCR is first examined in a multiplex reaction using mRNA from 16wk heart tissue. Figure 4.2a shows the relative CT values (y-axis) obtained for candidate gene *Corin* and reference housekeeping gene *β-actin*, plotted against the log of cDNA (x-axis) and Figure 4.2b illustrates the relative PCR efficiency plot for both genes. Expression of *β-actin* was identified as unstable in heart tissue with an unacceptable level of inter-strain variability

Table 4.3 Pairwise analysis of candidate genes

Species	Gene	aa%ID	nt%ID	D	Ka/Ks	Knr/Knc
H.sapiens						
	CORIN					
vs. M.musculus	*Corin*	83	83.5	0.187	0.128	0.786
vs. R.norvegicus	*Corin*	82.7	83	0.193	0.128	0.968
H.sapiens						
	DBP					
vs. M.musculus	*Dbp*	92.3	85.4	0.162	0.067	0.763
vs. R.norvegicus	*Dbp*	92.3	85.8	0.157	0.071	1

A pairwise score display gives a table of pairwise statistics for a 'Homologene' group, that includes percent amino acid (aa%) and nucleotide identities (nt%), the Jukes-Cantor evolutionary genetic distance parameter (D) (Jukes and Cantor; 1969), the ratio of non-synonymous to synonymous amino acid substitutions (Ka/Ks) for predicted proteins, and the ratio of radical to conservative changes in the transcript (Knr/Knc). Sequences input for HomoloGene processing comprise of the proteins from input organisms compared to one another (using blastp) and then paired and grouped, using a tree built from sequence similarity, where closer related organisms are matched first, and then further organisms added as the tree is navigated in the direction of the root. Protein alignments are mapped back to their corresponding DNA sequences, where distance metrics are calculated (e.g. molecular distance, Ka/Ks ratio). Sequences are paired using syntenic regions where applicable, with the remainder of sequences matched by application of an algorithm used to maximize the score globally, rather than locally, in a bipartite matching. Cutoffs on bits per position and Ks values are set to avoid improbable "orthologs" from being grouped together (NCBI HomologGene).

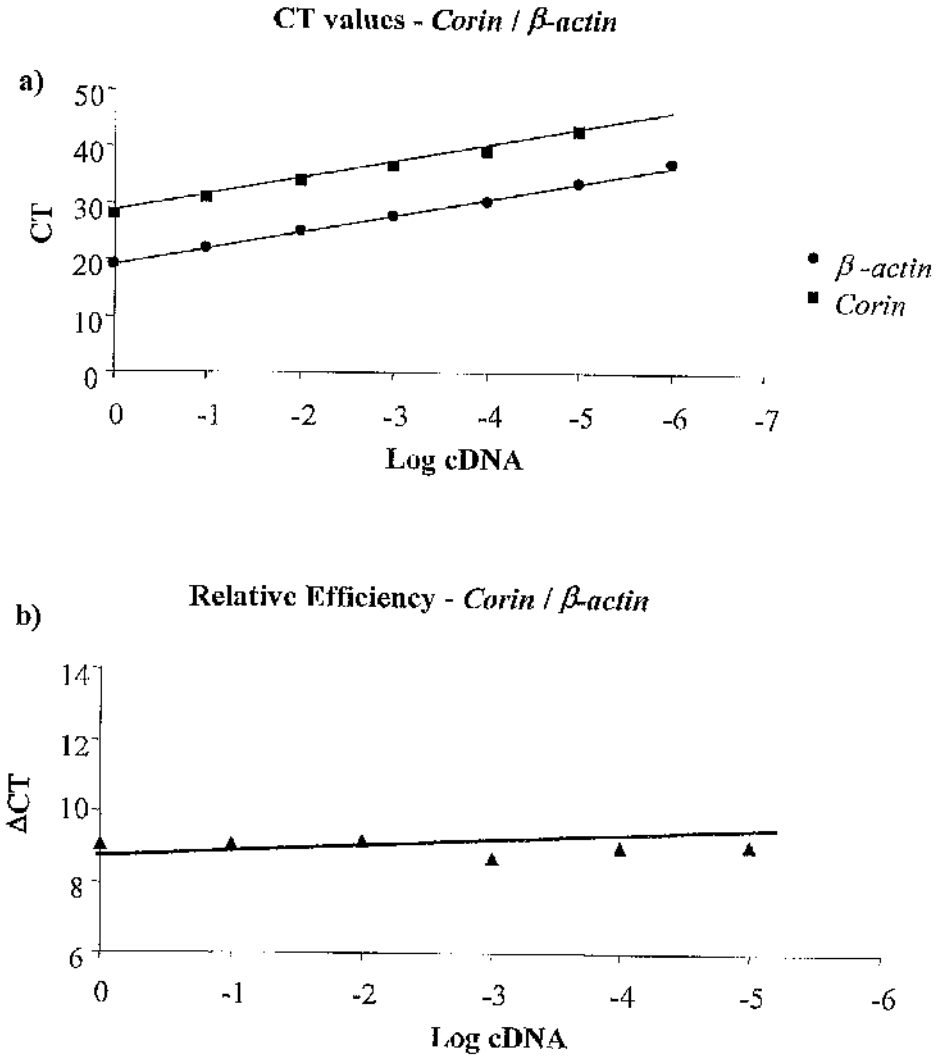

Figure 4.2 CT values for positional candidate gene corin. The CT and ΔCT (y-axis) is plotted against the log of cDNA (x-axis) and the equation calculated by linear regression analysis. **(a)** Plot of CT values for *Corin* and housekeeping reference gene *β -actin*. **(b)** Relative multiplex PCR efficiency plot of *Corin* and *β -actin*.

detected; a higher level of β-actin gene expression was observed in SHRSP in comparison to WKY (Figure 4.3). An alternative endogenous control was selected - Glyceraldehyde-3-phosphate dehydrogenase (*GAPDH*). Relative PCR efficiency of *Corin* and *Dbp* was then tested in a multiplex reaction with *GAPDH* as the endogenous reference housekeeping gene (Figure 4.4a-b). *GAPDH* remained stable in both strains and various tissues at different time points; tabulated in Appendix IV.

Gene expression analysis of *Corin* was examined in aortic and heart tissue and the results are shown in Figures 4.5 and 4.6. In aorta, gene expression does not vary between WKY groups, with a 6-fold increase observed in SHRSP at ages 16, 21 and 21 weeks (S). A different pattern of gene expression was noted in heart tissue with an initial 3-fold increase observed in SHRSP age 6 weeks, no significant difference between the strains at the 16 week time point and an approximate 6-fold increase in WKY versus SHRSP at age 21 week and 21 week (S). There was no significant difference in gene expression observed in SHRSP across all age groups, regardless of dietary salt manipulation.

It was not possible to assess *Dbp* gene expression in aortic tissue, as the level of gene expression in SHRSP was consistently below the threshold intensity of detection; Ct values for WKY are shown in Appendix IV. In Figure 4.6, at age 6 weeks *Dbp* gene expression in heart tissue is significantly increased in WKY by approximately 5-fold, rising to 6-fold at 16 weeks and 17-fold at 21 weeks in comparison to age matched SHRSP. After a 3 week 1% salt challenge, the level of gene expression observed in WKY drops from a fold change of 17 to 3. *Dbp* gene expression in SHRSP was consistently low across all age groups and dietary manipulation.

The results of pharmalogical intervention to reverse LVH in mature SHRSP are given in Figures 4.8a-b and 4.9a-b. The effects of olmesartan (AT_1 receptor antagonist) and combined hydralazine and hydrochlorothiazide (vasodilator and diuretic) on systolic blood pressure over a 4 week period are shown in Figure 4.8a. SBP is significantly reduced in SHRSP to levels comparable with age matched WKY in both drug treated groups. The effect on LVMI, of a 4 week drug regimen is described in Figure 4.8b.

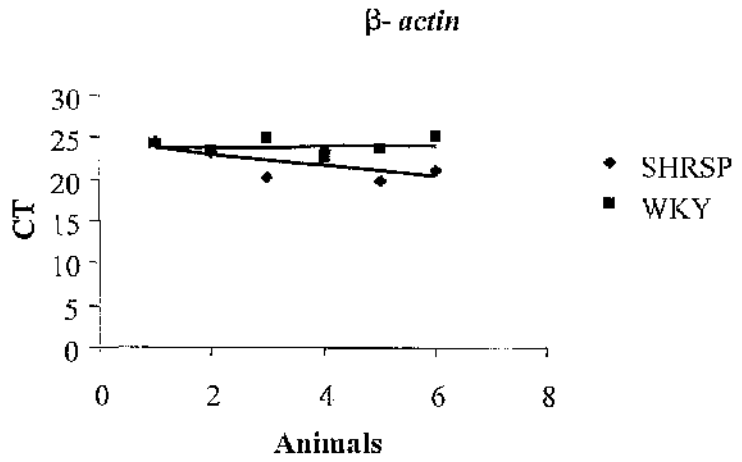

Figure 4.3 CT values for *β -actin*. There was significant inter-strain variability (P=0.01) for β -actin CT values in a multiplex reaction, with an increased expression of *β -actin* observed in SHRSP versus WKY heart tissue. Analysis by unpaired student t-test.

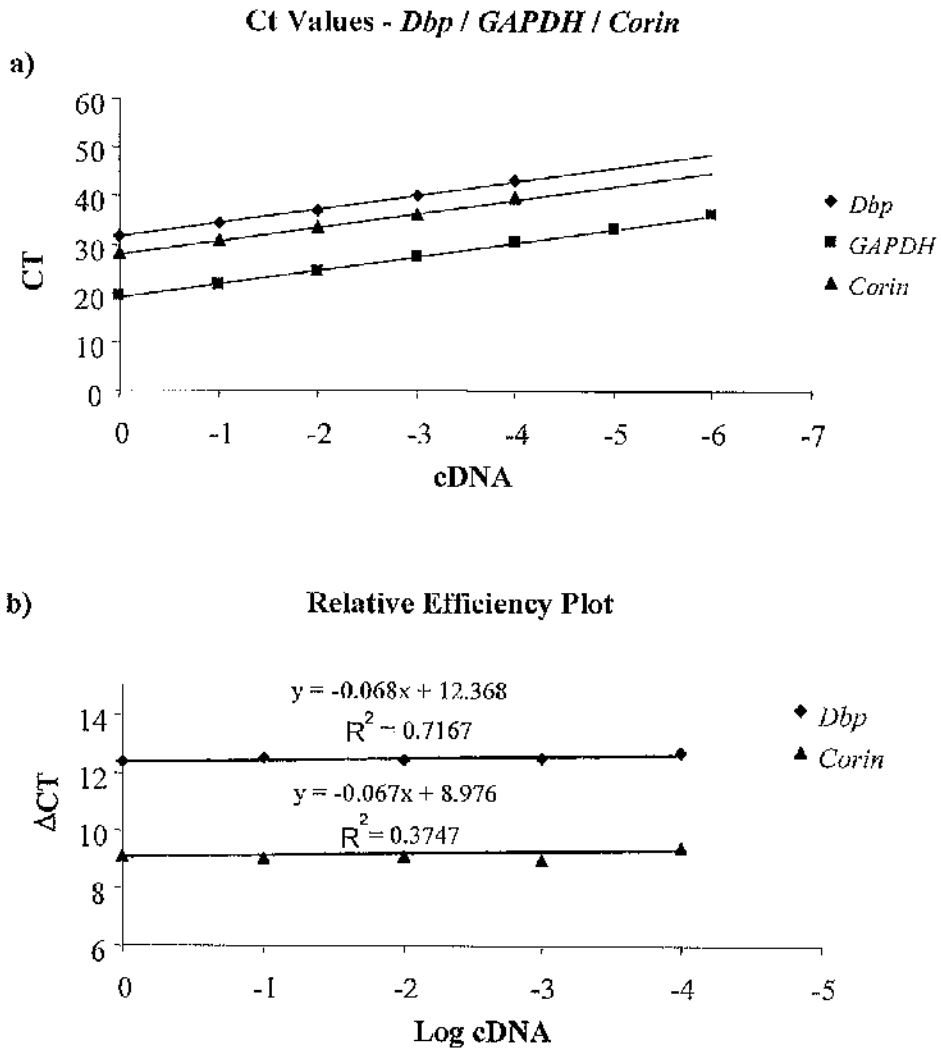

Figure 4.4 Ct values for *Dbp*, *Corin* and GAPDH. **(a)** Illustrates the relative Ct values for positional candidate genes *Dbp* and *Corin* with reference housekeeping gene *GAPDH*. **(b)** Relative PCR efficiency plots for both candidate genes in a multiplex reaction with housekeeping gene *GAPDH*.

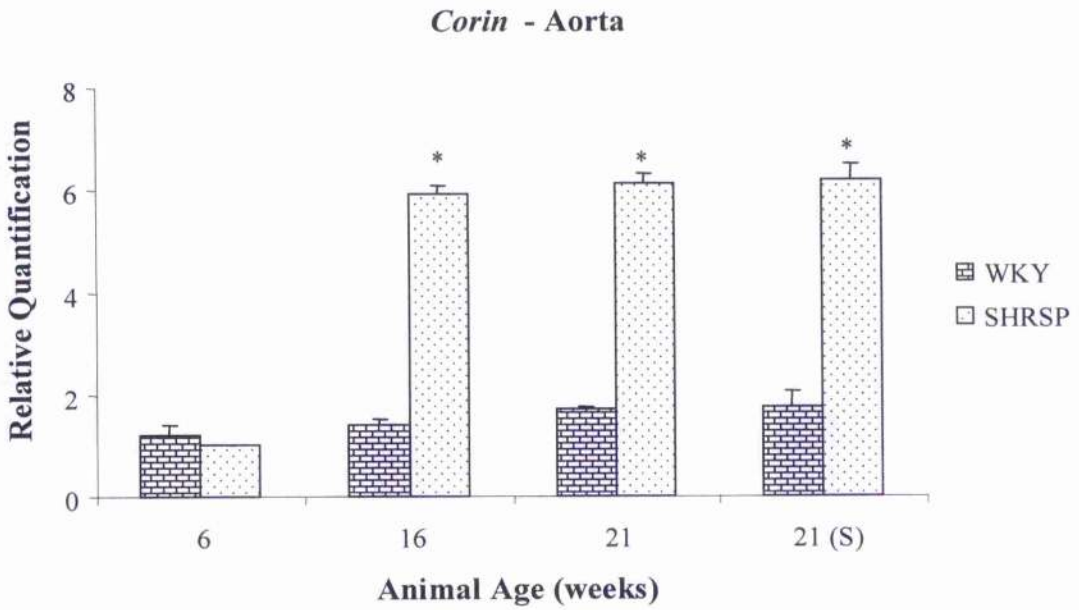

Figure 4.5 TaqMan gene expression in aorta - *Corin*. All data shown was normalised to SHRSP 6 weeks for $2^{-\Delta\Delta CT}$. At16 week, 21 week and 21 week (S) there was an approximate 6-fold increased gene expression in SHRSP compared to WKY (n=3, P=0.002; n=3, P=0.003, P=0.003 respectively). There was no significant difference observed in WKY strains across all age groups. All data shown is mean ±SEM, analysed by unpaired student t-test.

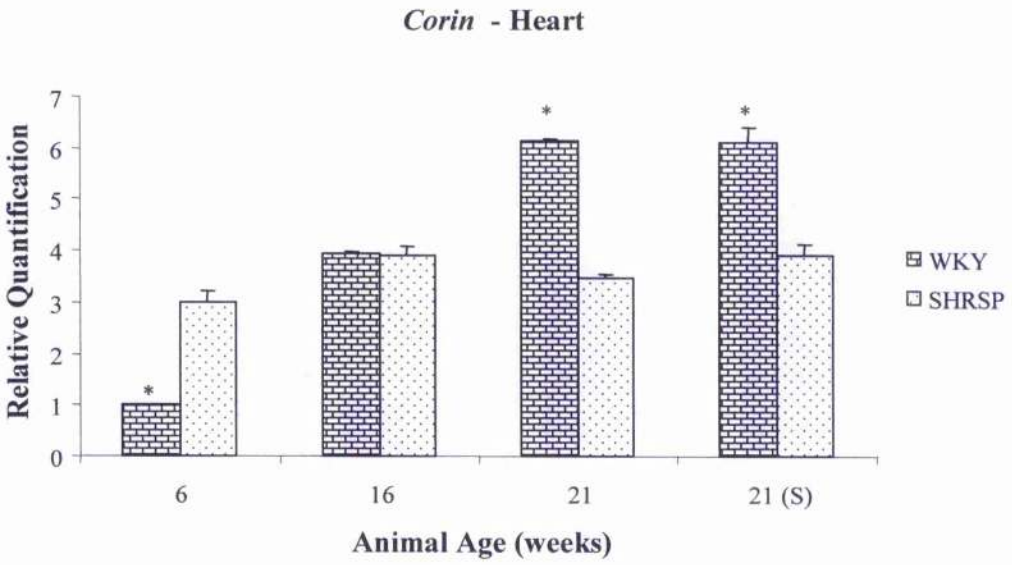

Figure 4.6 Taqman gene expression in heart - *Corin*. All data shown was normalised to WKY 6 weeks for $2^{-\Delta\Delta CT}$. In WKY, a significant increase of approximately 3-fold was noted at ages 21 week and 21 week (S) respectively (n=3, P=0.006; n=3, P= 0.005) with an approximate 3-fold decrease compared to SHRSP at 6 weeks of age. There was no significant difference detected between the strains at 16 weeks of age and no significant difference was noted in SHRSP across at any time point. Data shown is mean ±SEM analysis by unpaired student t-test.

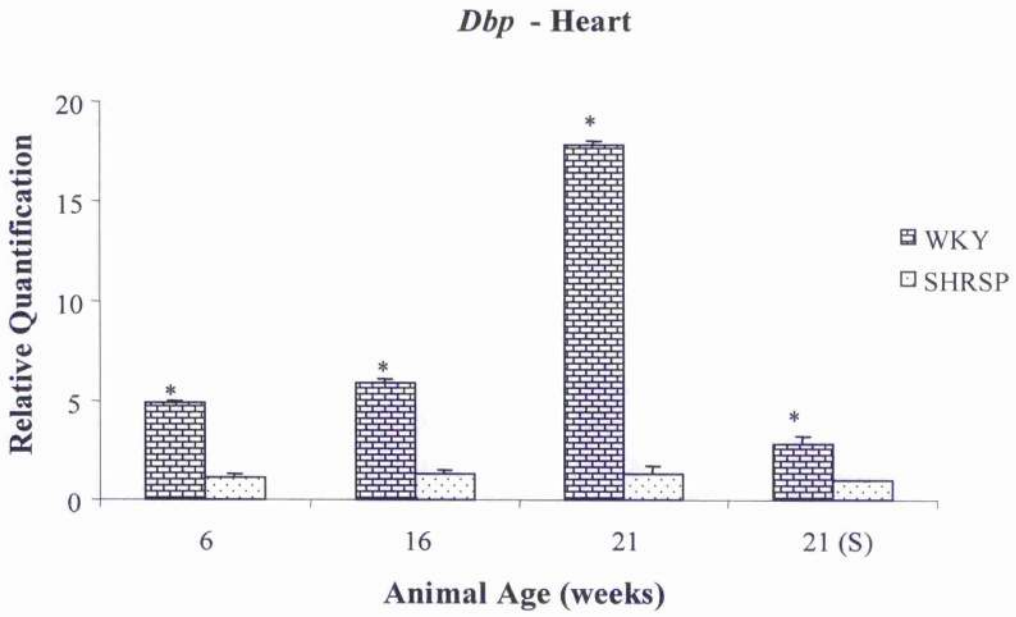

Figure 4.7 TaqMan gene expression in heart - *Dbp*. All data shown was normalised to SHRSP 21 weeks (S) for $2^{-\Delta\Delta CT}$. In WKY, at ages 6 week, 16 week and 21 week, *Dbp* gene expression was increased approximately 5-fold (P=0.0003), 6-fold (P=0.0004) and 17-fold ($P=3.2x10^{-7}$) respectively compared to age matched SHRSP. There was a drop in gene expression at 21-wk (S) in WKY to an approximate 3-fold increase versus 21 week (S) SHRSP (P=0.01). There was no statistical difference in *Dbp* gene expression in SHRSP across all time points. Data shown is mean ±SEM, analysis by unpaired student t-test.

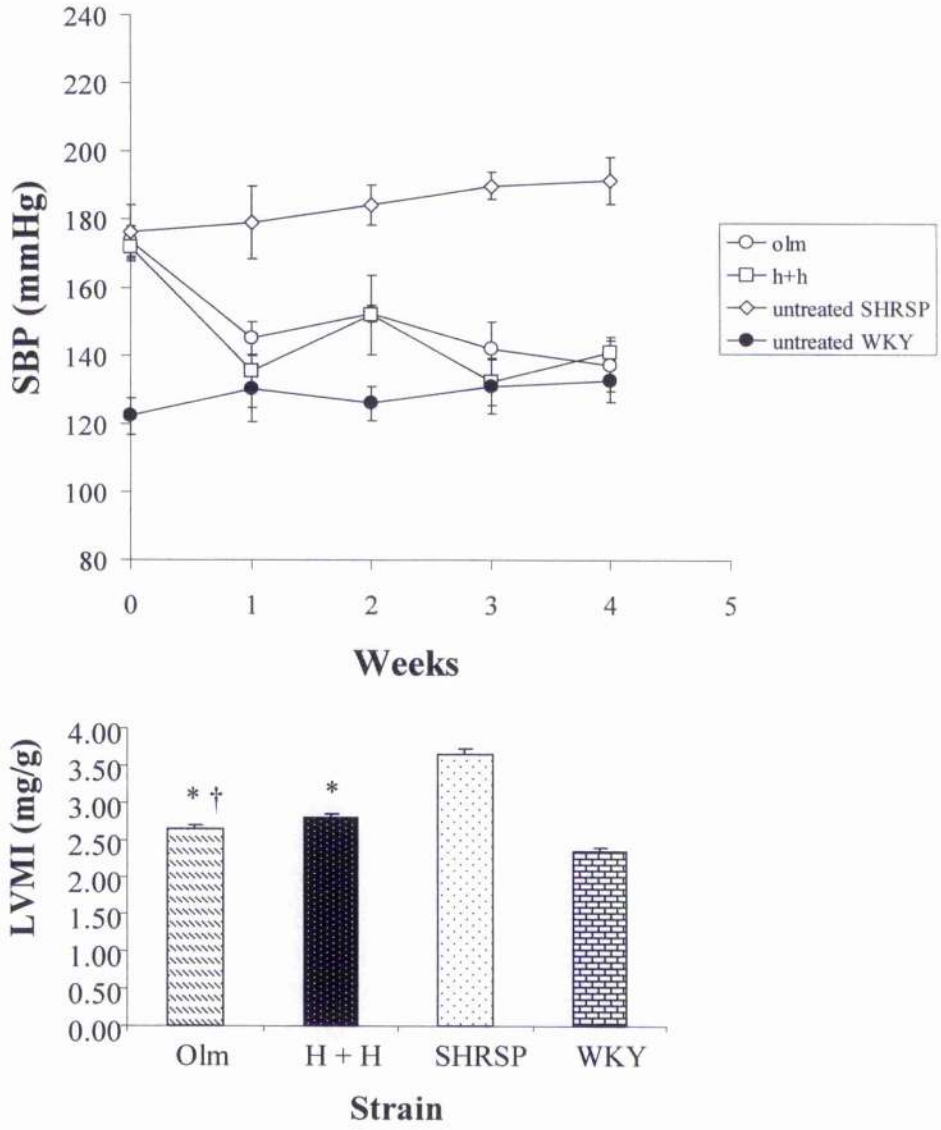

Figure 4.8 Pharmalogical intervention study. Olmesartan (Olm) or combinded hydralazine and hydrocholorothiazide (H+H) administered over 4 weeks. **(a)** Averaged weekly daytime SBP is significantly reduced in Olm (n= 7; *, P<0.001) and H+H (n=7; *, P<0.001) treated SHRSP versus untreated SHRSP (n=7). **(b)** Gravimetric LVMI is significantly reduced in Olm (n= 7, *P=0.001) and H + H (n=7, *P<0.01) treated SHRSP versus untreated SHRSP (SHRSP, n=7). LVMI was reduced further in Olm treated animals (†, P<0.05) versus the group receiving H+H. All data shown is mean ±SEM, single factor ANOVA with *post hoc* Bonferroni adjustment for multiple comparisons.

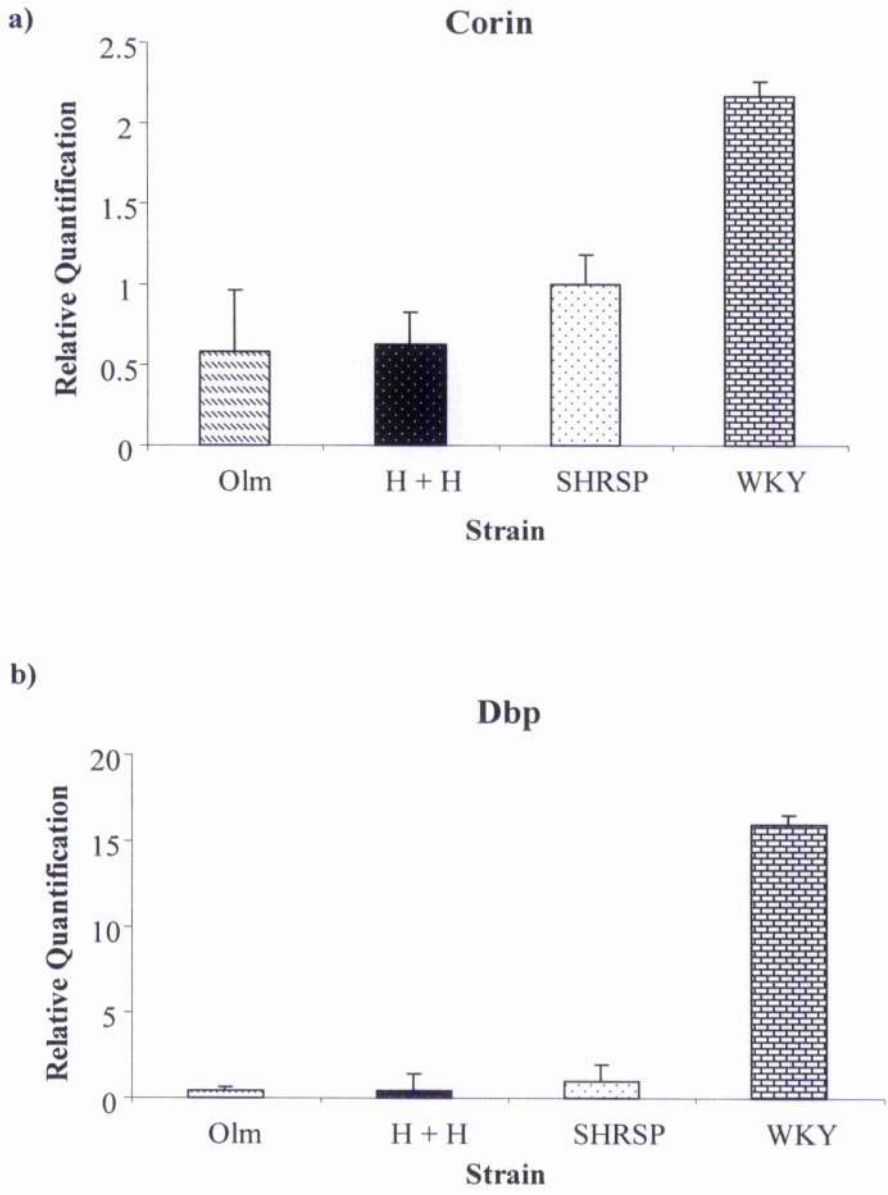

Figure 4.9 Pharmacological effects on gene expression in **(a)** *Corin* and **(b)** *Dbp*. All data shown was normalised to Olm treated SHRSP for $2^{-\Delta\Delta CT}$ (as this was the lowest expression group). There is no statistical difference in candidate gene expression in heart tissue of Olm (Olm, n=3) or hydralazine hydrochlorothiazide (H + H, n=3) treated SHRSP versus untreated SHRSP (SHRSP, n=3). Data shown is mean ±SEM, analysis by unpaired student t-test.

observed in AT_1 receptor antagonist group. Body weight and cardiac parameters are tabulated in Appendix VI. The effect of drug treatment on candidate gene expression levels is illustrated in Figures 4.9a-b. Although there is a trend towards a reduced expression of both genes in treated animals, this was not significantly different to the untreated SHRSP group.

Single nucleotide polymorphisms (SNPs) found within the promoter or coding region of a gene may explain differences in gene regulation, therefore sequencing was carried out on both candidate genes in SHRSP, WKY and BN liver DNA. There were no SNPs detected from sequencing the rat *Corin* gene in either exonic or upstream regions. In exons 3, 4, 5 and 13 of rat *Dbp*, synonymous SNPs were identified. A graphical representation of raw data output shown in Figure 4.10. All SNPs identified in rat *Dbp* (with the exception of one exon 4 SNP at position 14505) are novel. In addition to exonic polymorphisms, a SNP located at position -1244 was detected in the proximal 5' region. Analyses with transcription factor binding sites and promoter sequence software predicted an unusual TGTAAA motif located at position -1244, which may serve as a proxy TATA sequence. Figure 4.11 illustrates the structure of the rat *Dbp* gene and putative binding transcription factors based on sequence data. Further analysis of the predicted promoter region identified a cap signal for transcription initiation and several putative binding transcription factors – globin transcription factor 1 (*GATA1*), globin transcription factor 2 (*GATA2*), activator of nitrogen-regulated genes 2 (*NIT2*) and cyclic AMP response element binding protein (*CREB*).

Genotyping F_2 animals was repeated for the *Dbp*exon-4 SNP. Re-analysis with additional genotypes improved the QTL region marginally but not significantly. Linear regression analysis showed no difference between *Dbp*exon-4 SNP genotypes and *D14Got33* genotypes with respect to LVMI; P=0.679 for the difference in SS intercepts for *D14Got33* (0.233) and *Dbp*exon4 (0.195), therefore data is not shown. These data also demonstrate high linkage disequilibrium between *D14Got33* and *Dbp*exon4, which is expected in an inbred homogeneous population.

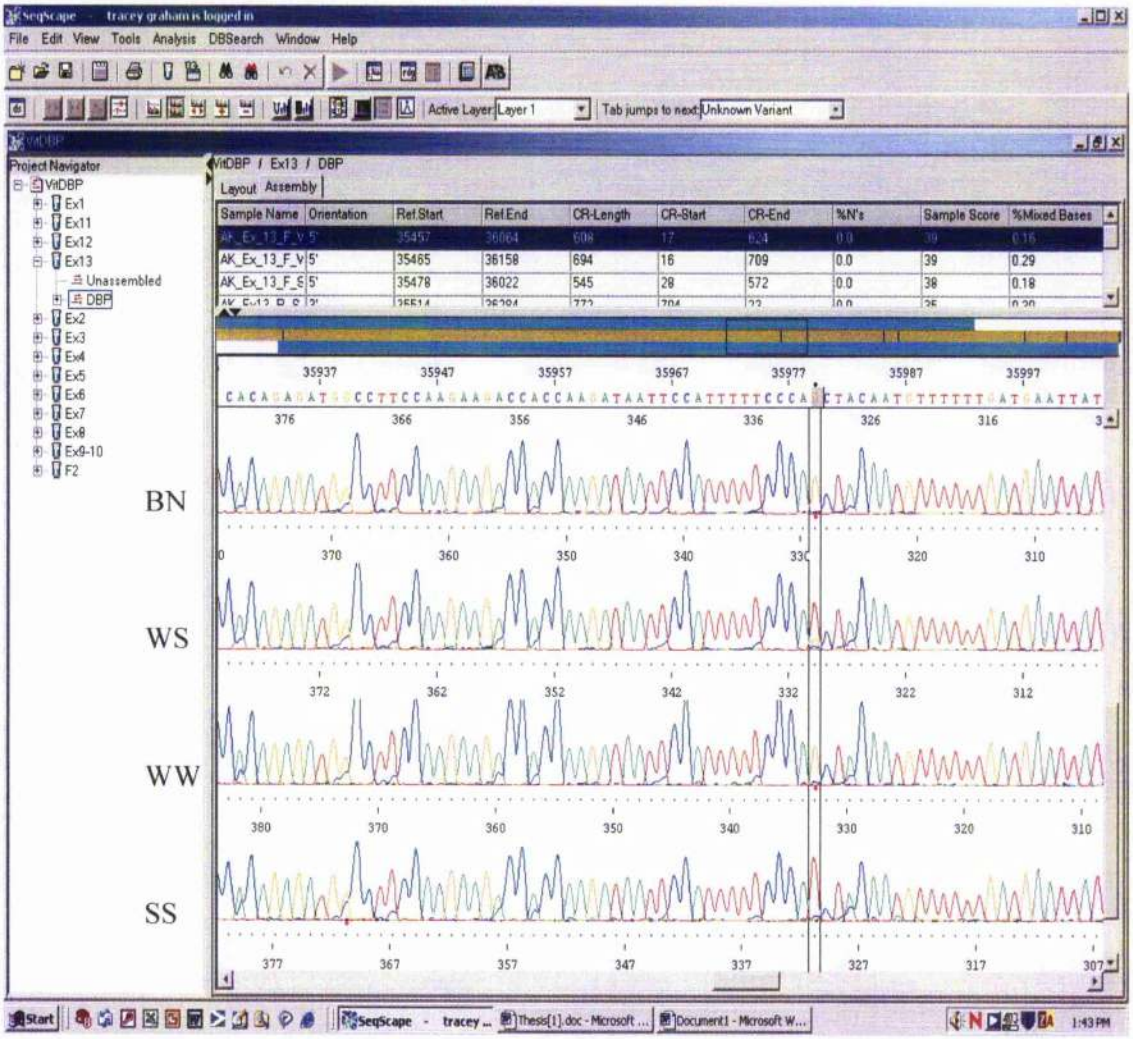

Figure 4.10 Raw data output from SeqScape version 2.1 sequencing analysis software. The data shown here is a SNP located in exon 13 of rat *Dbp*. The reference sequence for alignment is from Brown Norway (BN) rat sequence downloaded from Ensembl database. The SNP at position 35979 is highlighted by two black parallel lines with nucleotide substitution shown by colour changes from reference colour yellow (G) to red (T). Homozygote WKY (WW) and SHRSP (SS) are shown as yellow and red respectively; WKY/SHRSP heterozyote (WS) is obvious from the presence of both yellow and red colours.

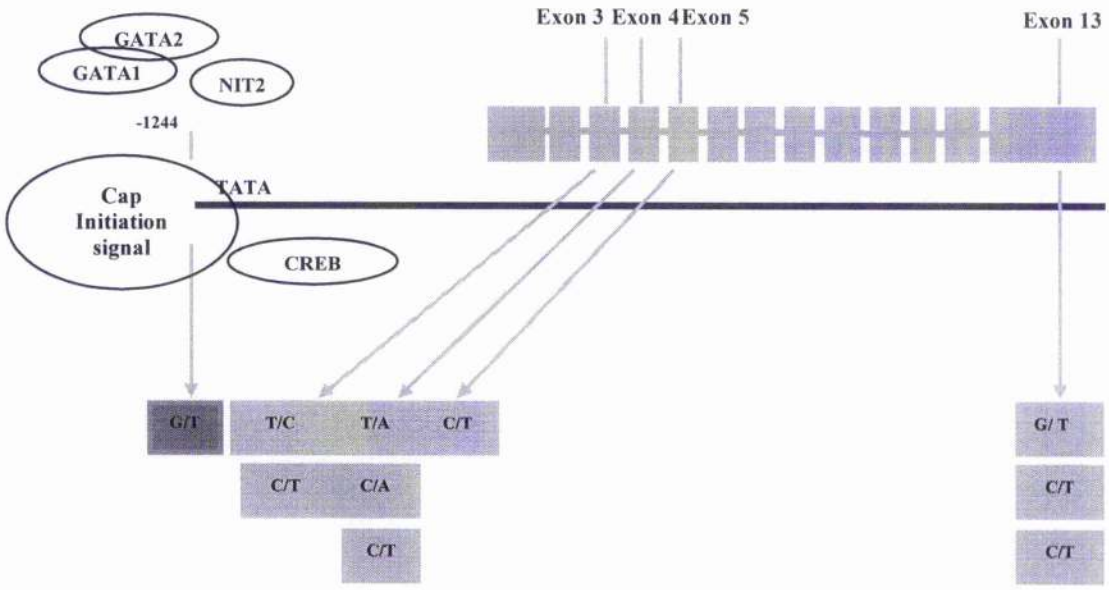

Figure 4.11 Graphical representation rat *Dbp* gene structure. SNPs were identified at position -1244, exons 3, 4, 5 and 13 (indicated by grey arrows). The putative TATA sequence, position of the cap initiation signal and promoter region, is shown in the 5' region of the gene. From cross-referencing bioinformatic databases, transcriptions factors *GATA1, GATA2, NIT2 and CREB* were identified. Synonymous exonic SNP nucleotide changes are shown in light grey boxes with the intronic SNP nucleotide changes shown in dark grey.

4.4 DISCUSSION

From this study, two positional candidate genes (*Corin* and *Dbp*) were identified based on comparative mapping of syntenic regions in mouse, rat and human. Subsequent pairwise analysis confirmed sequence homology between species. Differential gene expression patterns in SHRSP and WKY strains were detected in cardiac tissue and aortic tissue for *Dbp* and corin respectively, by RT-PCR. Further analysis of the candidate genes by sequencing identified 4 novel SNPs in *Dbp*, in particular a 5' SNP located at postion –1244, in a putative promoter sequence and thus transcription factor-binding site, with no SNPs identified in *Corin*.

Dbp also known as group-specific component of serum (Gc-globulin) is a member of a multigene family that includes albumin, α-fetoprotein and α-albumin/afamin (Cook & David, 1985) and is the major plasma carrier protein of vitamin D and binds monomeric G-actin, released during cell lysis or injury, thus preventing polymerisation to F-actin (Van Baelen, Boullion & De Moor, 1985; White & Cook, 2000). In this study, a highly significant drop in *Dbp* gene expression was observed in WKY 21-week (S) compared to 21-week, suggesting an inhibitory effect of dietary salt intake in WKY animals. In 2004, Thierry-Palmer *et al.* demonstrated, using the Dahl salt-sensitive (S) and salt resistant (R) rat, similar levels of protein-bound 25-hydroxyvitamin D (25-OHD) in urine, when rats are fed a low salt (0.3%) diet. However, in older S rats fed a high salt (3%) diet, lower plasma 25-OHD concentrations are found than in S rats compared to levels detected in R rats, with concentrations of PTH in S rats twice that of R rats (Thierry-Palmer *et al.*, 2004).

Although WKY is not classically defined as salt sensitive, the inhibitory effects of a sustained salt intake over a long period of time in this rat strain have not been studied. Furthermore, the relatively low levels of *Dbp* gene expression observed in SHRSP in this study may be indicative of low vitamin D status and consequentially an altered calcium homeostasis. Although the SHRSP was described in one study as a model of spontaneous osteoporosis in man (Yamori *et al.*, 1991), vitamin D status is yet to be fully investigated in this strain. Figure 4.12 illustrates the process of vitamin D production, transport and

metabolism. Sequencing of *Dbp* has led to the discovery of novel SNPs identified in exons 3, 4, 5 and 13 (which includes the 3' untranslated region; UTR) and a putative promoter site.

In 1991, Ray *et al.* sequenced the entire rat *Dbp* gene, which is approximately 35 Kbp and contains 13 exons with the transcription cap site located 62 bp upstream from the translation start codon (Ray *et al.*, 1991). From the sequencing data presented by Ray *et al.* (1991), it appears introns within the coding regions of the *Dbp* gene are highly conserved between other members of the albumin gene family (albumin and α-fetoprotein genes). The primary role of *Dbp* is the transport of vitamin D sterols, which are involved in calcium homeostasis along with calcitonin and parathyroid hormone (PTH). Calcium modulators have been shown previously to have vascular actions in rat and may be important in humans (Gairard *et al.*, 1994; Bukoski RD, Ishibashi K, Bian K, 1995; Levin & Li, 2005). In particular there is strong evidence for the role of vitamin D in the pathogenesis of cardiovascular disease from patients with end-stage renal disease (Foley *et al.*, 1998). In patients undergoing hemodialysis, 1α-vitamin D and the vitamin D analogue paricalcitol are highly effective in reducing the risk of death from cardiovascular disease (Shoji *et al.*, 2004; Teng *et al.*, 2005). In addition, there are several studies reporting an association between PTH and LVMI (London *et al.*, 1987; Bauwens *et al.* 1991), with a study by Hara *et al.* (1995) demonstrating a regression of ventricular hypertrophy and improvement in cardiac contraction after parathyroidectomy in 10 patients on maintenance haemodialysis, and similar results reported by Park *et al.* (1999) who used intravenous calcitriol. The possible functional role of calcium modulators is further, strengthened by *in vitro* studies, where PTH appears to have chronotropic, inotropic as well as hypertrophic effects on rat cardiomyocytes (Bogin *et al.*, 1981; Katoh *et al.*, 1981; Schulter *et al.*, 1995).

Dbp also known as group-specific component of serum (Gc-globulin) is a member of a multigene family that includes albumin, α-fetoprotein and α-albumin/afamin (Cook & David, 1985) and is the major plasma carrier protein of vitamin D and binds monomeric G-actin, released during cell lysis or injury, thus preventing polymerisation to F-actin (Van Baelen, Boullion & De Moor, 1985; White & Cook, 2000).

In this study, a highly significant drop in *Dbp* gene expression was observed in WKY 21-week (S) compared to 21-week, suggesting an inhibitory effect of dietary salt intake in WKY animals. In 2004, Thierry-Palmer *et al.* demonstrated, using the Dahl salt-sensitive (S) and salt resistant (R) rat, similar levels of protein-bound 25-hydroxyvitamin D (25-OHD) in urine, when rats are fed a low salt (0.3%) diet. However, in older S rats fed a high salt (3%) diet, lower plasma 25-OHD concentrations are found than in S rats compared to levels detected in R rats, with concentrations of PTH in S rats twice that of R rats (Thierry-Palmer *et al.*, 2004). Although WKY is not salt sensitive, the inhibitory effects of a sustained salt intake over a long period of time in this rat strain have not been studied. Furthermore, the relatively low levels of *Dbp* gene expression observed in SHRSP in this study may be indicative of low vitamin D status and consequentially an altered calcium homeostasis. Although the SHRSP was described in one study as a model of spontaneous osteoporosis in man (Yamori *et al.*, 1991), vitamin D status is yet to be fully investigated in this strain. Figure 4.12 illustrates the process of vitamin D production, transport and metabolism. Sequencing of *Dbp* has led to the discovery of novel SNPs identified in exons 3, 4, 5 and 13 (which includes the 3' untranslated region; UTR) and a putative promoter site.

The UTR of mRNAs can determine gene expression by influencing mRNA stability and translational efficiency, with recent reports demonstrating gene expression regulation by the differential use of alternative 3' UTR (Hughes, 2006). An example of this is demonstrated by Kloss *et al.*, (2005) who showed reduced expression of soluble guanylyl cyclase subunits was mediated by downregulation of the mRNA-stabilizing protein human-antigen R, emphasising the importance of 3' UTR binding proteins in mRNA stability. The regulation of PTH gene expression by Ca^{2+} is also post-transcriptional and affects mRNA stability mediated by the binding of protective trans acting factors to a cis acting instability element in the 3' UTR. Indeed, in hypocalcemia there is increased binding that protects

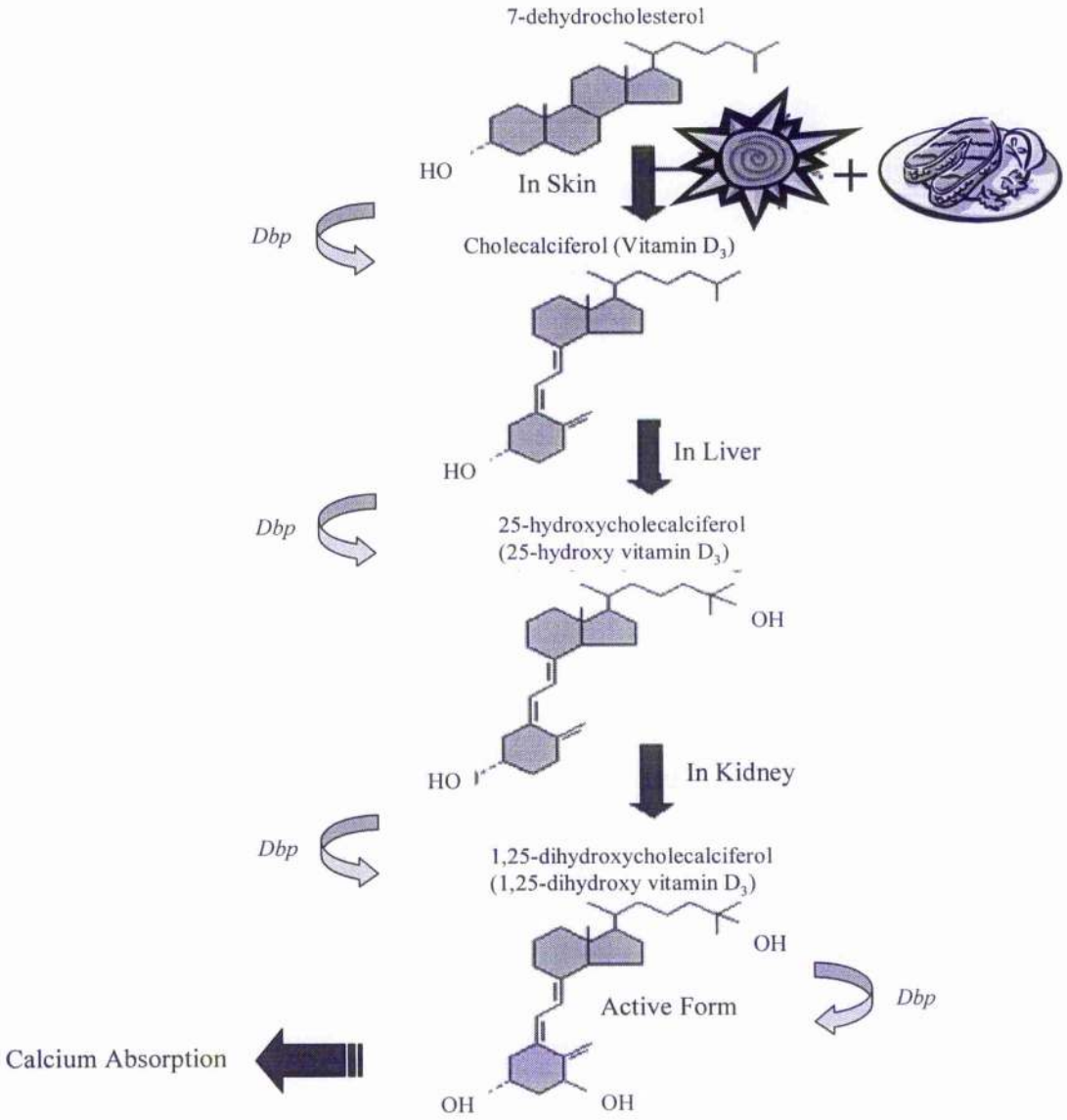

Figure 4.12 Illustration of Vitamin D biosynthesis pathway. Vitamin D is produced in the skin of mammals when light energy is absorbed by a precursor molecule 7-dehydrocholesterol and by dietary sources of Vitamin D (egg yolk and fish oils) Each of the various forms of vitamin D are lipophilic and are transported in blood bound to carrier proteins; the major protein is *Dbp*.

PTH mRNA from degradation by cytosolic ribonucleases resulting in higher levels of PTH mRNA, whereas in hypophosphatemia there is decreased binding, with a subsequent increased degradation of the PTH mRNA resulting in low levels of PTH mRNA (Naveh-Many *et al.*, 2002).

In this study, *Corin* gene expression in SHRSP heart tissue remains unchanged across all time points, in contrast to WKY where expression is increased with age and consequently body size. In aorta, gene expression increases in SHRSP as blood pressure rises, but remains unaltered in WKY. This observed difference may be the result of reduced and impaired atrial stretch in SHRSP, due to concentric remodelling of the left ventricle and could also explain why a different gene expression profile is seen in aortic tissue. The suggestion that a local release of *Corin* is important to ensure the required hypertrophic response is supported by Langenickel *et al.* (2003). Using an experimental model of heart failure, atrial *Corin* mRNA was decreased in parallel to a blunted ANP release upon stretch (Langenickel *et al.*, 2003) offering corroboration that *Corin* released upon atrial stretch may be a rate-limiting mechanism for ANP release *in vivo*. Lanenickel *et al.* (2004) also sequenced the *Corin* and determined a high degree of homology between rat *Corin*, mouse (93.6%) and human (85%); the latter confirmed by pairwise sequence homology in this study.

In order to investigate the significance of blood pressure reduction on candidate gene expression, pharmalogical intervention using three different classes of anti-hypertensive drugs was used to reverse the effects of high blood pressure in the SHRSP. It should be noted that although both drug treatments reduced SBP to an equivalent WKY level, this was not sufficient to reverse LVH, as LVMI was still significantly increased in drug treated animals compared to WKY. Although there appears to be slight downward trend in expression of both genes with drug treatment, the results were not significant. The overall lack of increased gene expression in SHRSP to equivalent WKY levels by anti-hypertensive treatment suggests that reduced gene expression observed in SHRSP is not simply a secondary response to elevated SBP, as there is no significant change in gene expression after SBP reduction. The results of this study are in contrast to findings of

Kaganovsky *et al.* (2001) who showed a positive correlation between levels of ANP granularity and myocyte size in SHR, which was significantly reduced after treatment with hydralazine. Similarly, Ohta *et al.*, (1995) demonstrated reduced ANP gene expression in 10-wk SHR heart after treatment with an AT1 receptor antagonist although they observed no suppression of ANP gene expression with the use of hydralazine.

To date, there is a reported single QTL on mouse chromosome 5 and QTL for blood pressure, heart rate and myocardial infarction susceptibility on human chromosome 4, which are syntenic to rat chromosome 14. There is currently no reported LVMI or CMI QTL on either mouse chromosome 5 or human chromosome 4. The identification of candidate genes based on comparative mapping is laborious as many genes within syntenic regions require screening as well as determination of functional impact on the phenotype of interest as well as proximal distance to the QTL. There is also a certain element of guesswork in identifying candidate genes from comparative mapping resources as the function of many genes is still unknown with numerous genes still uncharted in the rat. The combined strategies of congenic breeding with high throughput gene expression analysis methods, such as microarray should provide a more robust approach to candidate gene identification offering insight into the intricate network of molecular pathways.

CHAPTER 5

MRI AS A METHOD FOR IN VIVO LVM QUANTIFICATION AND ASSESSMENT OF LV GEOMETRY

5.1 INTRODUCTION

Over the past ten years, magnetic resonance imaging (MRI) has rapidly progressed from a purely anatomical imaging technique to one that reports on a wide variety of tissue functions. Cardiac magnetic resonance is currently the ideal method of choice for precise measurements of ventricular volumes, function and left ventricular mass in humans (Sola, White & Desai, 2006). This is due to high spatial resolution, excellent delineation of endocardial and epicardial borders, good image quality and ability to reconstruct the heart shape in three dimensions. For these reasons, results are not only independent of geometrical assumptions but are highly reproducible and accurate. CMR is particularly useful in research, as it is highly sensitive to small changes in ejection fraction and mass, and a relatively small number of subjects are required for study. In addition, due to the excellent reproducibility of data, temporal follow-up of any individual in the clinical setting is a more realistic possibility.

Following the release of the rat genome sequence there has been a forward, steady trend towards the use of the rat in cardiovascular research. In vivo assessment of cardiac morphology and function in rodents is hampered by both the small size and rapid action of the heart therefore high fidelity phenotyping techniques such as CMR are desirable to monitor even fractional changes in heart weight and function, in order to characterize fully the influence of genes and pharmacological and/or surgical interventions.

In 1990, Manning *et al.* investigated the capacity of electrocardiogram (ECG)-gated MRI to assess *in vivo* LVM in the rat in comparison to gravimetric dry weight values. In this study, healthy Sprague-Dawley and Fischer 344 were imaged pre and post volume overload induction by aortic leaflet disruption. The group demonstrated a high correlation between MRI-estimated LVM quantification and *post mortem* LVM values and showed a 40% increased mass in animals after aortic leaflet disruption. These preliminary results demonstrated both the feasibility and precision of MRI for *in vivo* assessment of LVM in the adult rat.

Following on from the work of Manning *et al.*, Laurent, Allergrini & Zierhut (1995) showed a difference in left ventricular remodelling and function between the renal hypertensive rat (RHR) and SHR, despite similar SBP and LVM, using cardiac MRI. Several years later, Al Shafei *et al.* (2002), developed a cine MRI technique to allow detection and characterization of chronic changes in myocardial tissue volume in the normotensive WKY rat. This was closely followed in 2003 with the application of single-shot ultrafast spin-echo (Parzy *et al.*, 2003), to determine and evaluate left ventricular hypertrophy in hypertensive rats.

More recently, MRI has become a valuable, non-invasive technique in the characterisation of pathological changes in the heart during the progression of disease and as a tool for the evaluation of new therapies in left ventricular hypertrophy (Nahrendorf *et al.*, 2003; Schalla *et al.*, 2004; Loganathan *et al.*, 2005). Further exploration of theses studies not only allows an understanding of the requirement for high fidelity phenotyping in experimental animals but also helps examine how animal models can be of clinical benefit to humans.

Nahrendorf *et al.* (2003) studied the feasibility of cine MRI for assessment of infarcted rat and mouse heart, compared to established methods previously used for the prediction and prevention of heart failure in patients. They did this by testing cine MRI in studies investigating interventions to alter the path of the remodelling process. MRI was used to establish left ventricular volumes and mass, myocardial infarct size and cardiac output and compared to left ventricle wet weight and conventional haemodynamic measurements for determination of cardiac output and LV volumes by electromagnetic flowmeter and pressure-volume curves. They were able to show a high concordance between LVM assessed by MRI and wet weight and in the MRI- and flowmeter measurements of cardiac output. From these initial results, it can be concluded that cine MRI is a valuable non-invasive diagnostic tool for use in rat and mouse to assess cardiac function, which may offer new insights into remodelling processes.

Collectively, these studies highlight the use of MRI as an invaluable, non-invasive technique to monitor changes in heart geometry and physiology (Loganathan *et al.*, 2005)

and demonstrate the viability and utility of MRI in the study of experimental animal models. Of course the translation of these investigations to the human clinical platform is invaluable from both a diagnostic and investigative standpoint.

This study aims to develop a MRI imaging protocol to compare 3-dimensional quantification of LVM with 2-dimensional conventional methods such as echocardiography and simple *post mortem* evaluation in SHRSP, WKY and SP.WKYGla2a (a congenic strain with a reduced SBP compared to SHRSP). In addition, it is anticipated that MRI evaluation will allow the detection of subtle differences and changes in heart physiology in these strains.

5.2 METHODS

5.2.1 Experimental Animal Strains

Inbred colonies of SHRSP and WKY rat strains have been maintained at the University of Glasgow since 1991 as described in section 2.2. The previously generated SP.WKYGla2a congenic strain (Jeffs *et al.*, 2000) has an approximate 65cM homozygous WKY region of rat chromosome 2, containing 2 blood pressure QTL (minimum boundary markers; *D2Wox13, D2Rat157)* introgressed into the SHRSP background; a graphical representation is shown in Figure 5.1. The strain is characterized by a reduced SBP in comparison to the SHRSP parental strain (approximately 20 mmHg), but is not normotensive (Figure 5.2).

5.2.2 Echocardiographic LV Determination

Thirty rats, ranging from 8 weeks to 21 weeks of age per strain group, were assessed by echocardiography (SHRSP n=10; WKY n=10; SP.WKY.Gla2a n=10) as described in *Chapter 2.3.3.* Posterior wall thickness and LV internal dimensions were

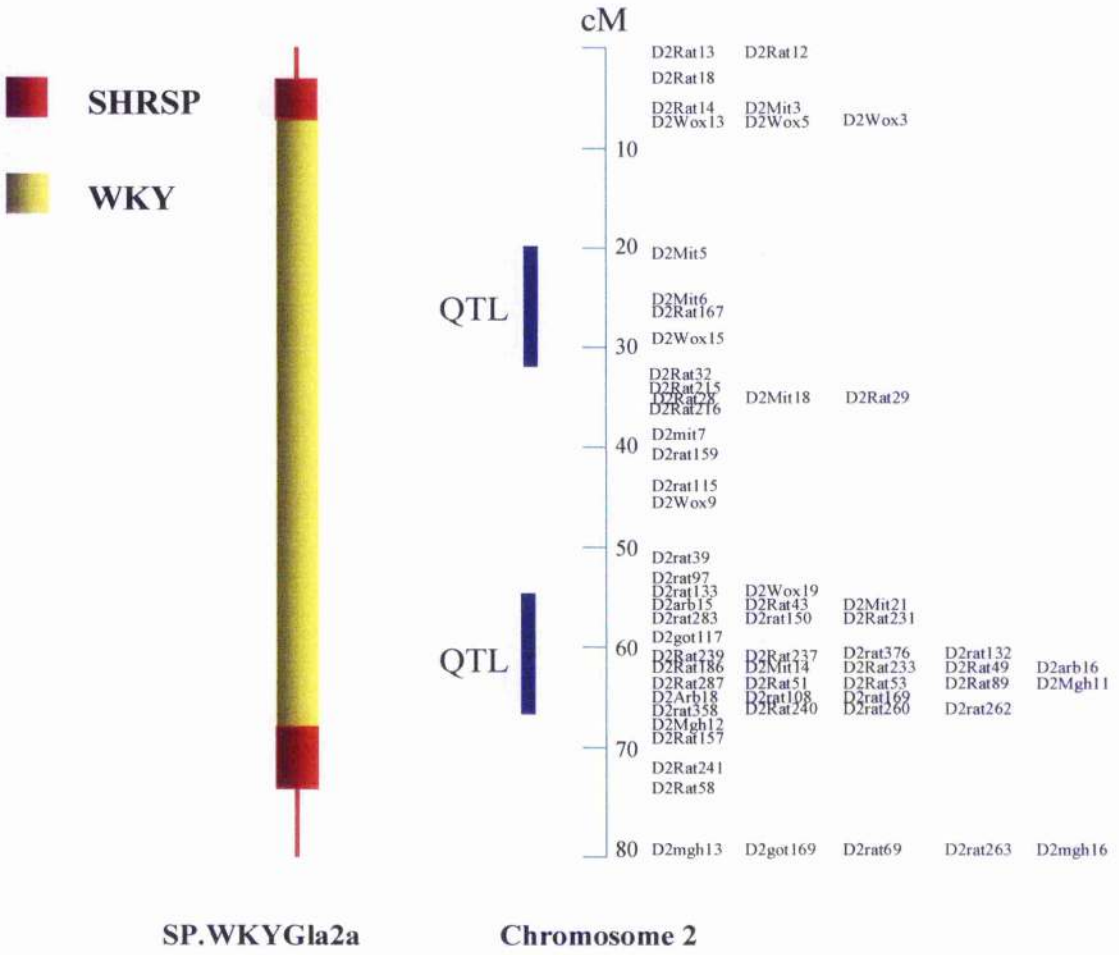

Figure 5.1 Graphic illustration of SP.WKYGla2a congenic strain. A genetic linkage map for rat chromosome 2 genetic is shown on the right. The approximate locations of 2 blood pressure QTL identified from a previous genome wide scan (Clark *et al.*, 1996) are highlighted in blue. The SP.WKYGla2a congenic strain is shown on the left – the yellow block represents a 65 cM WKY chromosome 2 segment introgressed onto a SHRSP (red) background (McBride *et al.* 2003).

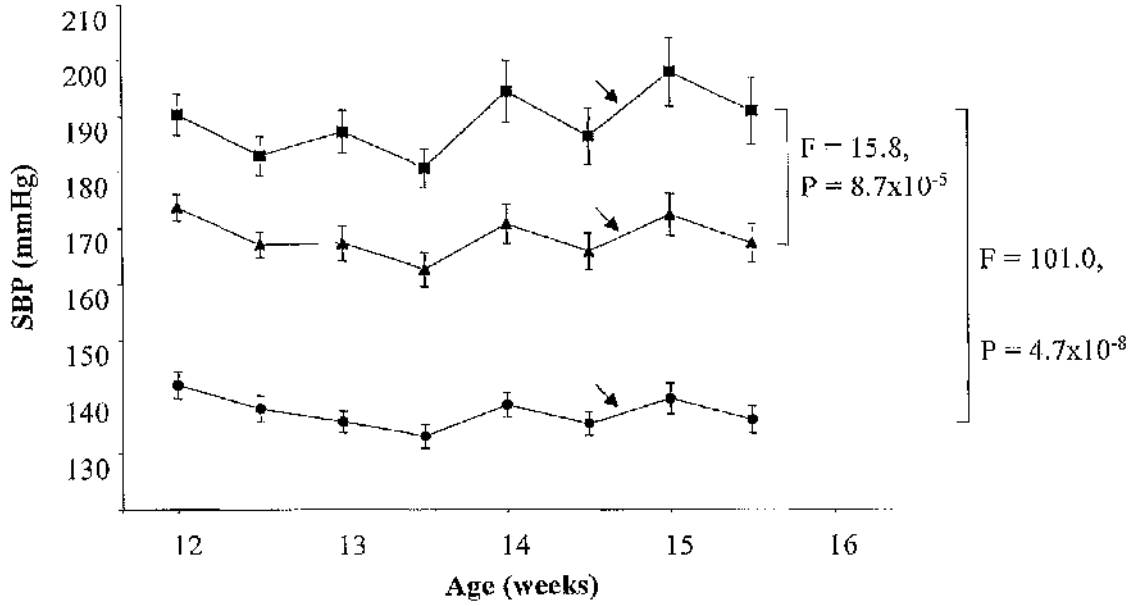

Figure 5.2 Representative radiotelemetry data for averaged daytime and night time SBP. F-statistics and P-values are for relevant main effects from repeated measures analysis of variance. The congenic SP.WKYGla2a strain has a reduced SBP in comparison to the parental SHRSP strain (F=15.8, P<0.0001) but is not normotensive (McBride *et al.* 2003).

measured according to the leading edge method of the American Society of Echocardiography (ASE) at end diastole, with all measurements performed by two observers (Sahn *et al.*, 1978); Figure 5.3. LVM was calculated first using three statistical methods for comparison:

1. ASE-cube formula (Sahn *et al.*, 1978)
   - LV mass (g) = 1.04 (IVSd + LVIDd + PWTd) 3 -. LVIDd3)
2. Troy formula (Troy, Pombo & Rackley, 1972)
   - LV mass (g) = 1.05 (4/3π[(EDD/2+PWT)2(EDD+PWT)]-[(EDD/2)2-EDD])
3. Devereux correction factor (Devereux *et al.*, 1984)
   - LV mass (g) = 0.8 (1.04 (IVSd + LVIDd + PWTd) 3 -. LVIDd3) + 0.6

Relative wall thickness (RWT) was estimated using the formula RWT = AWT + PWT / EDD.

5.2.3 Animal preparation for MRI imaging

Twelve 16-week-old male rats (WKY n=4; SHRSP n=4; SP.WKYGla2a n=4) examined by echocardiography approximately 24hrs previously, were anaesthetized with halothane in nitrous oxide: oxygen (70:30) prior to MRI scanning. An exchangeable radiofrequency (RF) birdcage was used as a transmitter and a 32mm diameter surface coil as the receiver (Bruker Biospin MRI, Germany). In addition, an animal cradle designed specifically to accommodate rodents, was optimized for use in the RF resonator (Bruker Biospin MRI, Germany) and facilitated monitoring of ECG, heart rate, respiration rate, and temperature. The animal's chest and leg was shaved to allow adhesion of 8-lead ECG pads. The animal was positioned horizontally in a Bruker animal thermal cradle and then placed in the magnet (Bruker Biospin MRI, Germany) and sagittal images of the thoracic cavity were obtained. A 70/30 USR 7 Tesla Biospec system (Bruker Biospin MRI, Germany) and Bruker software Paravision 3.0.2 was used for image acquisition with the following parameters: Single slice Flash cine, TE=108ms, TR=14ms, Averages=6, field of view=50X50mm, image matrix=256X192, flip angle=10°. The entire volume of the heart

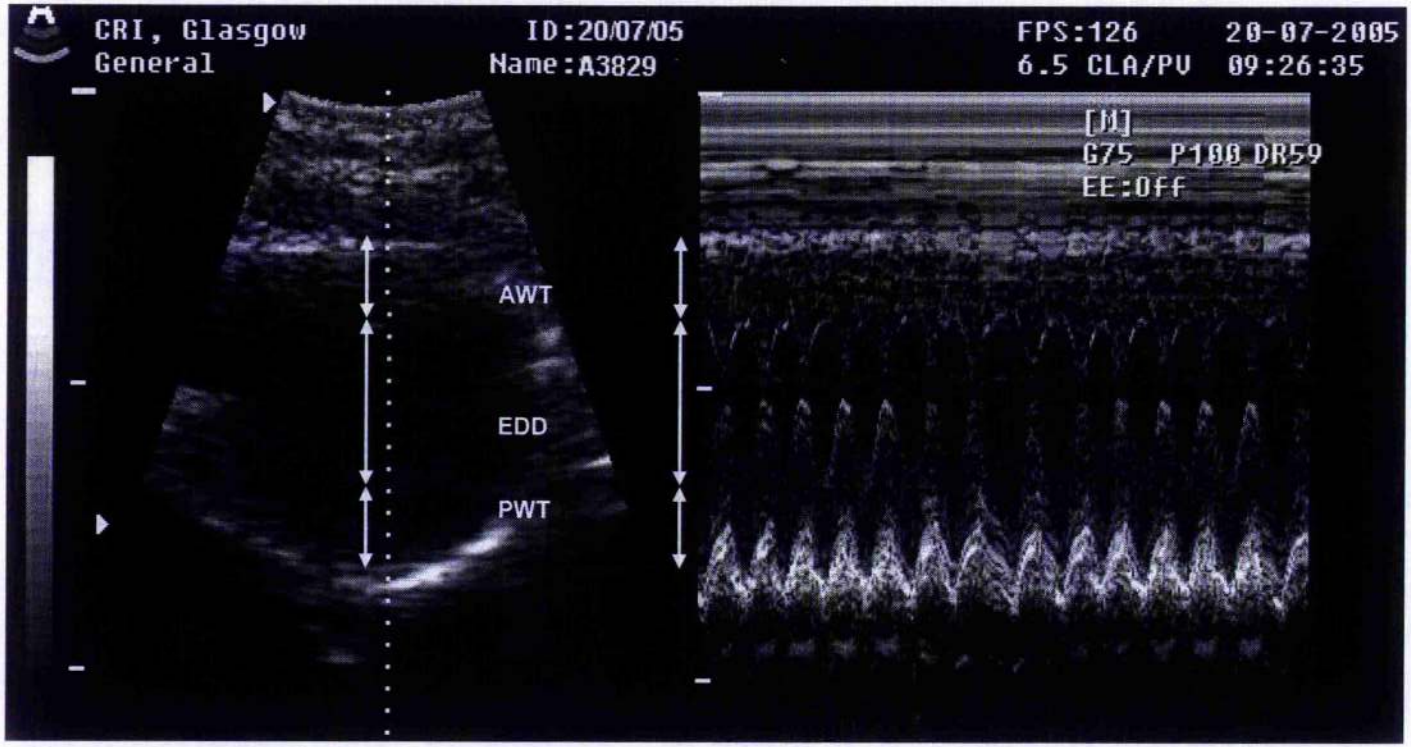

Figure 5.3 Echocardiograph image output. B-mode (left) and M-mode (right) images of left ventricle from a WKY. Measurements are taken for anterior wall thickness (AWT), end diastolic dimension (EDD) and posterior wall thickness (PWT).

was scanned by acquiring 1mm slices. ECG gating was carried out using the Biotrig monitoring system (SpinSystems LTD, Australia) with image sequences triggered in synchrony with the R signal of the QRS waveform. MR images were analysed using ImageJ (NIH).

5.2.4 MRI Assessed LV determination and calculations

Using a sagittal image with the clearest representation of the heart, short axis multi slice images were acquired. The images in Figure 5.3a-b demonstrate how the plane is angled between transverse and coronal orientations. The contours of the left ventricle were determined by delineation of the epicardial and endocardial boundaries. The endocardial value was subtracted from the epicardial value, multiplied by slice thickness and then multiplied by 1.05 (density of the myocardium). Multi-slice values were calculated, summed and divided by 1000 (1Kg). Measurements were taken separately at both systole (ESV) and diastole (EDV). Stroke volume (SV) was defined as EDV - ESV, and ejection fraction (LVEF) was defined as SV/EDV. Relative wall thickness (RWT) was calculated as RWT = AWT + PWT / EDD from a single MRI slice at the level of the papillary muscles. A compact disc (CD) of moving rat hearts (at mid-ventricle) is included inside the front cover. The images are in AVI format and represent a complete cardiac cycle for each strain.

5.2.5 *Post mortem* evaluation

After MRI examination, animals were euthanized under halothane anaesthesia. The hearts were removed; pericardium, fat and blood vessels were trimmed. The whole heart was blotted and weighed using an analytical balance. The atria and the right ventricular free wall were then carefully removed and the LV + septum was blotted and weighed to obtain LVM value; LVM index (LVMI) was calculated by indexing LVM to body weight.

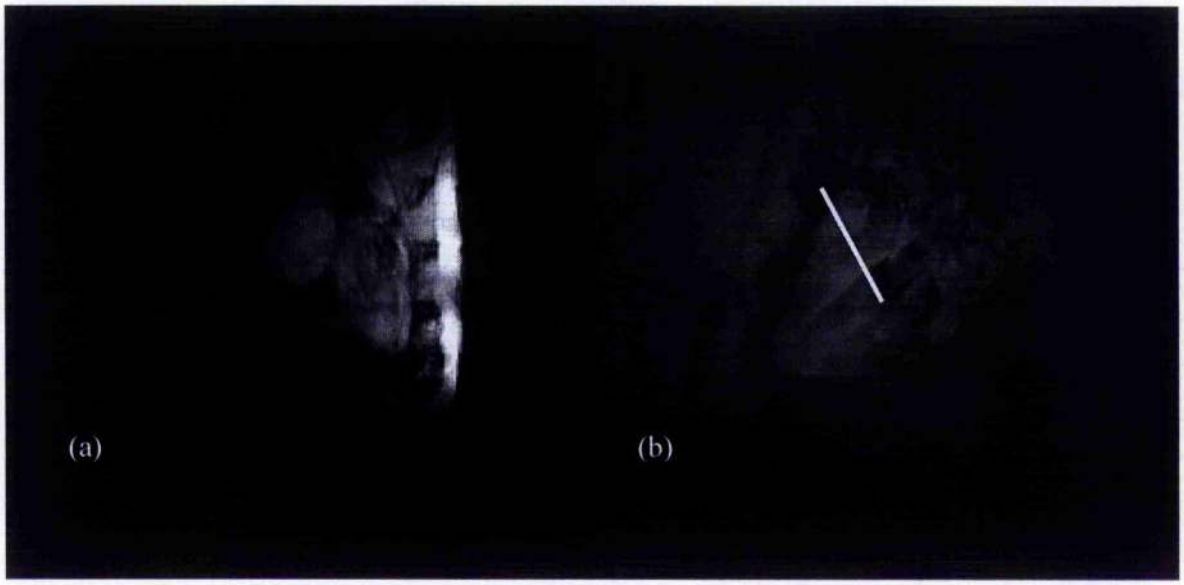

Figure 5.4 Pilot images. Sagittal **(a)** and transverse-coronal **(b)** pilot images were used to establish the cardiac axes and to position the transverse cardiac sections used in image acquisition.

5.3 RESULTS

The main parameter of the experimental protocol was to acquire MRI images of the entire heart at 1mm intervals through a complete cardiac cycle beginning with the heart at end diastole. Figure 5.5 displays a time series of MRI images at the level of the papillary muscles. All images show a clearly demarcated ventricular wall, ventricular lumen and the thoracic cavity. From Figure 5.5 (panel a) a fully dilated ventricle can be seen in the image, triggered by the R wave with a progressive decrease in luminal diameter in subsequent images (panel b-j). Both epicardial and endocardial surfaces of the left ventricle retained circular cross-sections throughout the cardiac cycle, in contrast to the crescent cross-section of the right ventricle (highlighted by white arrow).

From the MRI images, left ventricle quantitative analysis was carried out for each strain and compared directly with obtained gravimetric values. The mean values for this data show no significant difference between MRI derived LVM and LVM determined at autopsy (Figure 5.6a). Means and standard error of means (SEM) for haemodynamic measurements are shown in Table 5.1. Acquisition time was heavily dependent on both a steady heart rate synchronized with a stable ECG trace and was therefore affected by inter and intra-strain heart rate variability. From the analysis of MRI images, LVEF was not significantly different between all three strains. The results of linear regression analysis of MRI estimated LVM and echocardiographic analysis, compared to gravimetric values at *post mortem* (PM) and are shown in Figure 5.7. There is a good correlation between MRI derived LVM and *post mortem* weight (R^2= 0.56; P= 0.008) shown in Figure 5.7, however echocardiographic assessment of LVM in small animal number groups (n=12) showed a poor correlation with gravimetric values.

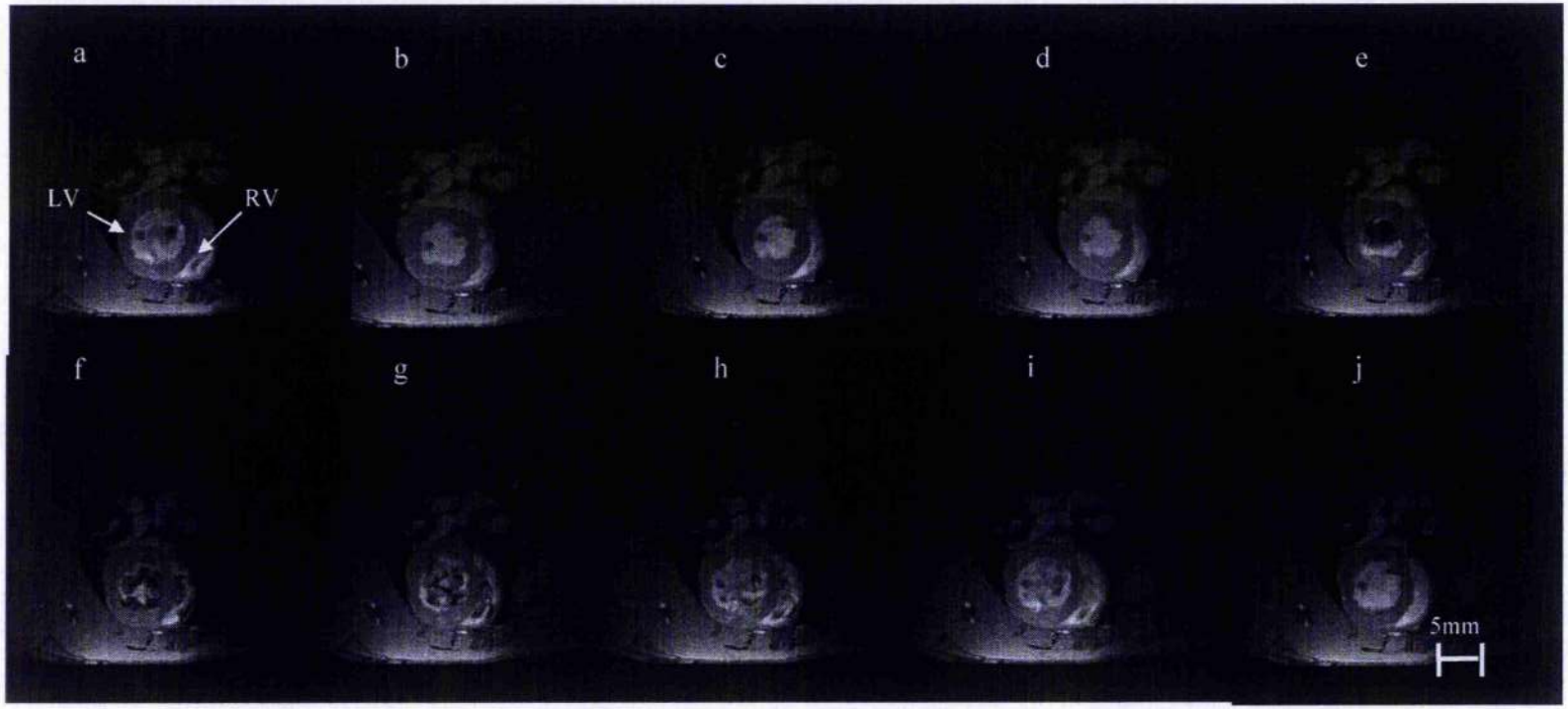

Figure 5.5 Series of short axis transverse sections from a 16 week old WKY male. Ten frames labelled a-j are of the same spatial slice at sequential time points in the cardiac cycle following the initial R wave (panel a) with approximately 12ms between each image. LV and right ventricle (RV) are highlighted in panel a. The weight of this animal was 372g with an intrinsic heart rate of 195±5 beats min^{-1}. From the images, a diminished contraction in systole can be seen from the moderate reduction in ventricle diameter prior to ventricular filling.

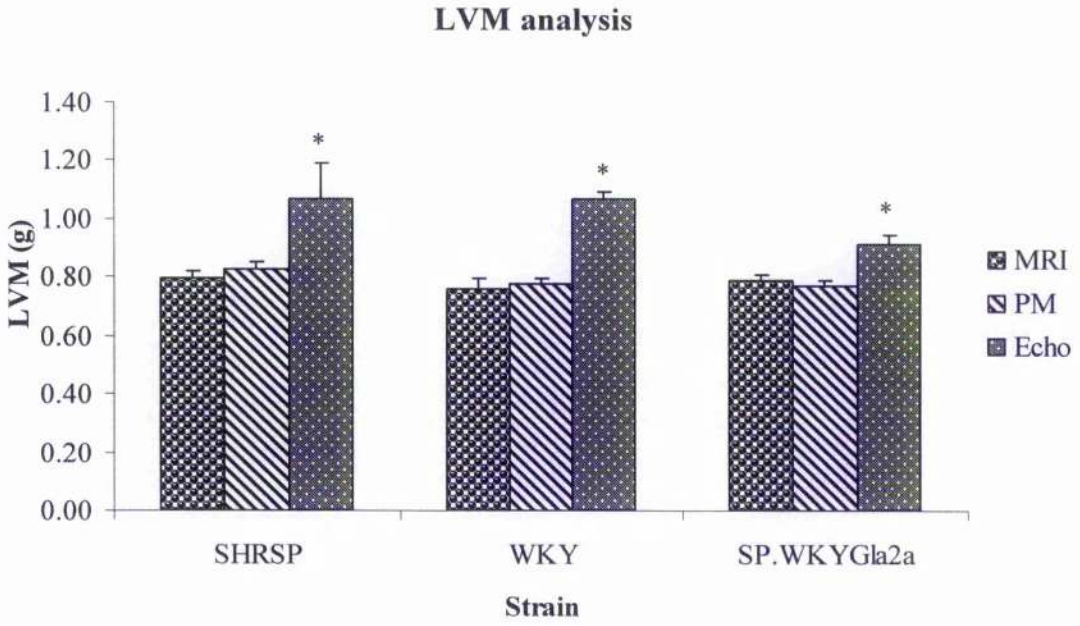

Figure 5.6 Comparison of MRI, echocardiography and *post mortem* (PM) for LVM in 16 week old males. In comparison to PM, echocardiographic estimated LVM was significantly increased in SHRSP, WKY and SP.WKYGla2a (*, P>0.05, CI -0.103 to 0.052; n=4 *, P>0.05, -0.148 to 0.071, n=4; *, P>0.05, CI -0.091 to 0.059, n=4, respectively).There was no statistical difference between the MRI estimated LVM and PM values, grouped according to strain. All data shown is mean ±SEM, single factor ANOVA and *post hoc* Bonferroni adjustment for multiple comparisons.

Table 5.1 MRI summary data for animals

Strain	LVEF (%)	HR (beats min^{-1})	Weight (g)
SHRSP (n=4)	45.1±1.0	249±10	289.9±29.0
SP.WKYGla2a (n=4)	51.1±6.0	190±7	281.5±3.4
WKY (n=4)	41.7±5.6	195±5	335.6±29.3

Data shown is mean ±SEM

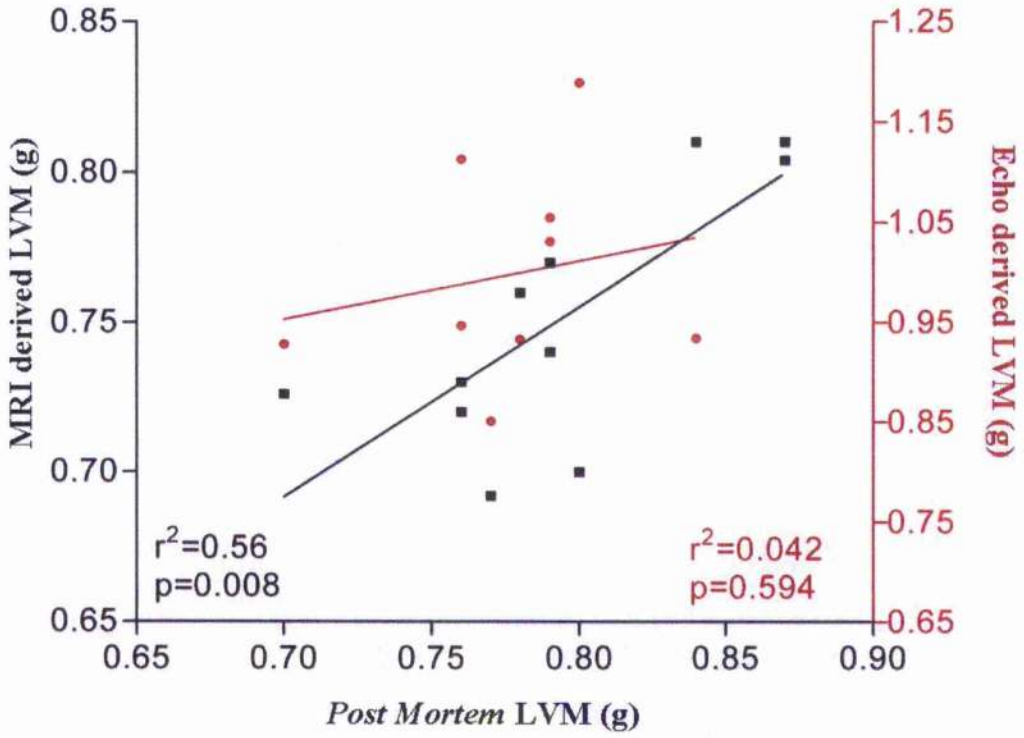

Figure 5.7 Linear regression analysis of LVM. Calculations from MRI (n=12) and echocardiographic (n=9) images compared with *post mortem* weight of the left ventricle. The results demonstrate a good correlation between MRI derived LVM and gravimetric values (black squares, line), with no statistical relationship observed between echocardiographic estimated LVM (calculated using Devereux modified ASE-cube formula) and *post mortem* LV weight (red circles, line).

In order to compare calculation estimates for LVM as determined by echocardiography, three different formulae were used and the results contrasted. Figure 5.8a illustrates the results of this statistical comparison in thirty animals. The Troy formula and ASE-cube formula overestimate LVM significantly with a more accurate estimation of LVM using the Devereux modified ASE-cube equation. When animal numbers are increased, estimated LVM is in higher concordance with gravimetric values; a correlation of R^2=0.84, P<0.001 (Figure 5.8b). In Figure 5.9a, MRI derived RWT mean values for the three strains are shown. From the data, RWT is significantly increased in SHRSP (P<0.001) versus WKY, SHRSP versus SP.WKYGla2a (P<0.05) and SP.WKYGla2a (P<0.05) versus WKY. RWT values obtained from echocardiographic images did not show any significant variation between the three strains (Figure 5.9b).

5.4 Discussion

The principal aims of this study were to develop MRI techniques to image a moving rat heart for accurate quantitative analysis of LVM and in addition compare the method directly with *post mortem* LV weight and echocardiography. In this study, MRI analysis was sufficiently sensitive to detect significant differences in RWT between the SP.WKYGla2a and the parental SHRSP strain, indicating concentric remodelling, undetected by simple LVM quantification. Previous assessment using echocardiography and simple post-mortem evaluation has shown no statistically significant difference in either LVM or LV dimensions between the SP.WKYGla2a congenic and the SHRSP parental strain, despite an approximate SBP difference of 20mmHg. This is the first instance LVM, relative wall thickness (RWT) and left ventricular ejection fraction (LVEF) have been measured using MRI in the SP.WKYGla2a congenic strain.

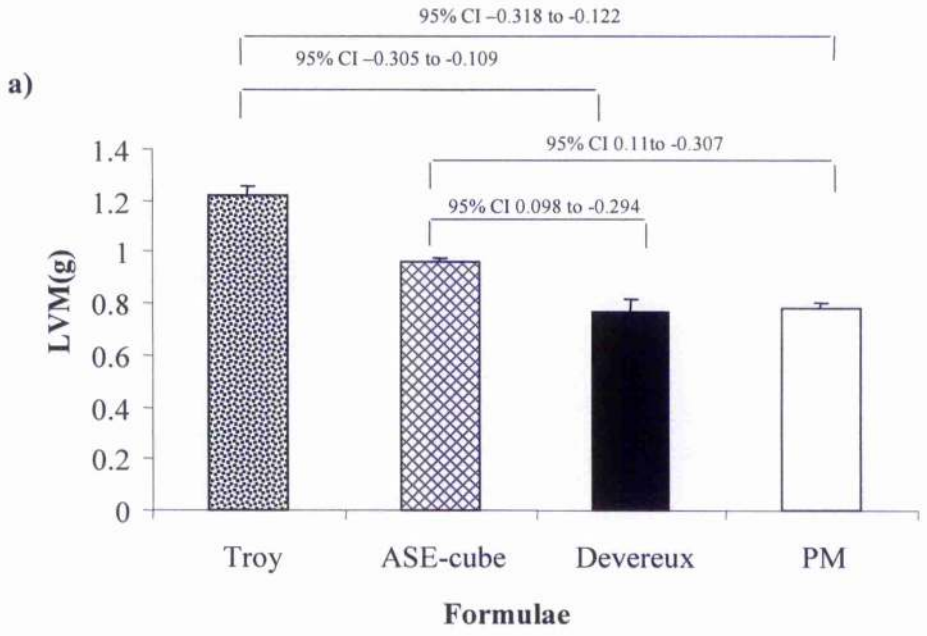

Figure 5.8a Comparison of echocardiographic statistical evaluation. *Post mortem* (PM) weight contrasted with three statistical formulae for calculation of LVM, derived from echocardiography in SHRSP (n=10), SP.WKYGla2a (n=10) and WKY (n=10). There is no significant difference between Devereux modified ASE-cube formula and *post mortem* LVM ($p>0.05$). Application of the Troy and ASE-cube formulae resulted in a respective 34% and 15% overestimation of LVM compared to gravimetric values ($p<0.001$). All data shown is mean ±SEM, single factor ANOVA and *post hoc* Bonferroni adjustment for multiple testing.

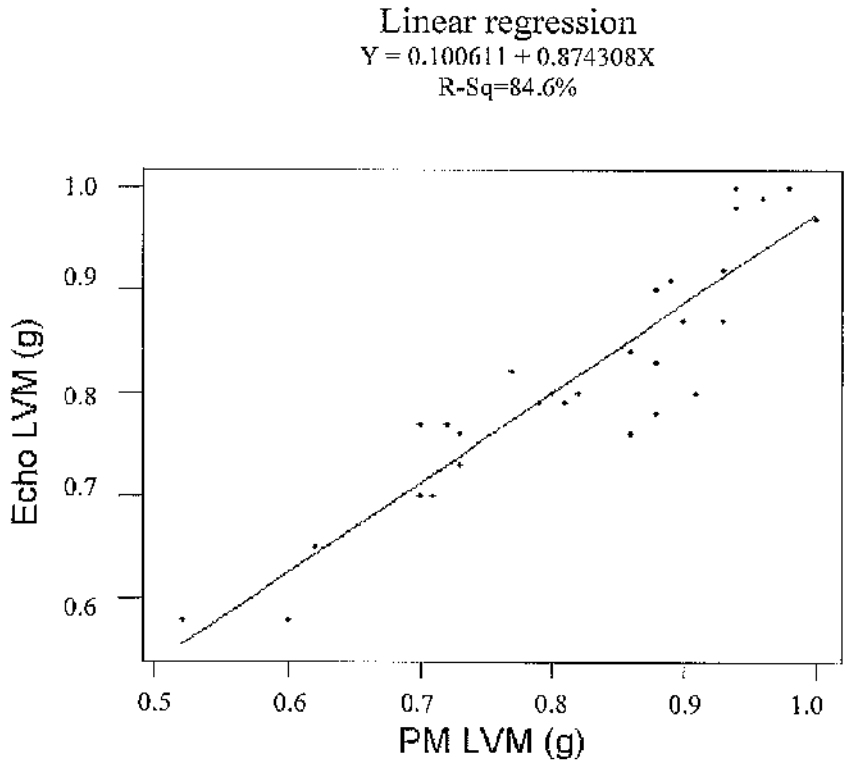

Figure 5.8b Linear regression analysis plot of echocardiographic derived LVM with *post mortem* (PM) values. LVM was assessed in thirty animals ranging in age and weight from 8-21 weeks and 115-340g respectively using echocardiography. Devereux modified ASE-cube formula was used to quantify LVM and directly compared to gravimetric values obtained at sacrifice. Correlation between both methods was achieved; $R^2 = 0.84$, $P < 0.001$, n=30).

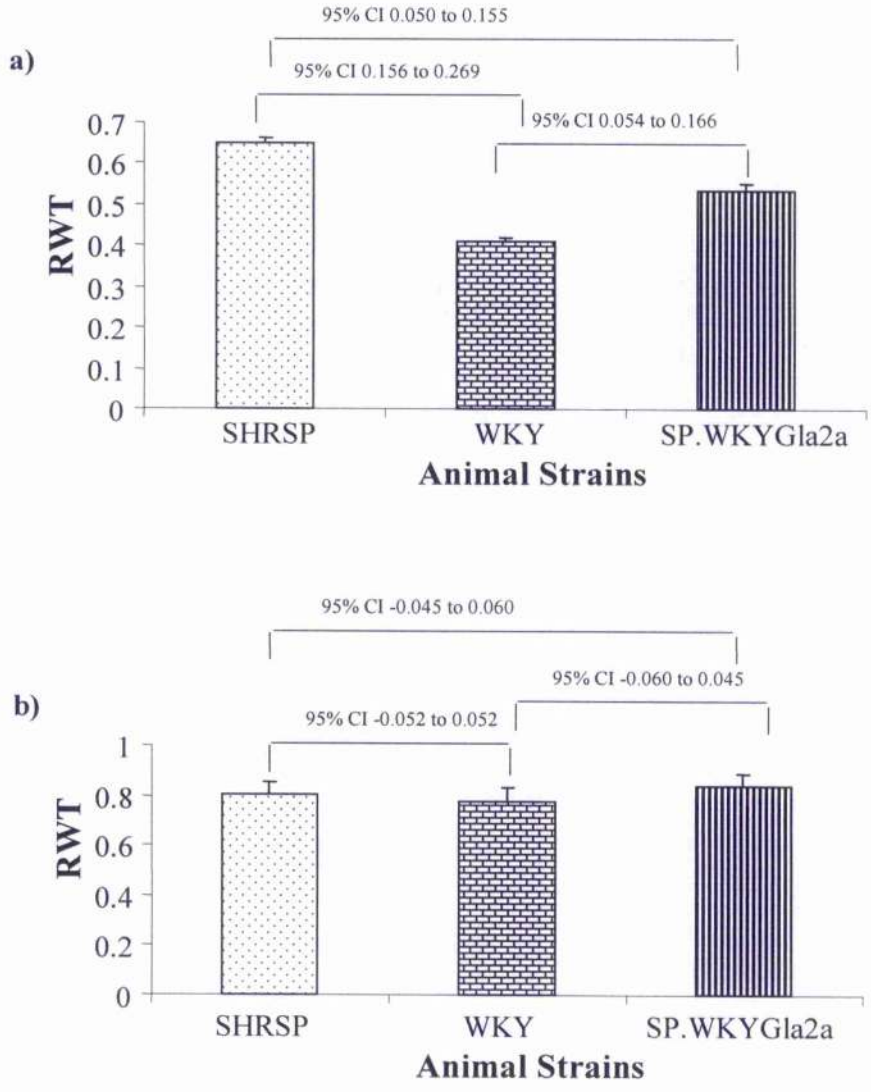

Figure 5.9 Relative wall thickness (RWT) calculated at end diastole from **(a)** MRI images n=12) and **(b)** echocardiographic images (n=9). From MRI analysis, there is a significant increased RWT observed in SHRSP versus WKY and SP.WKYGla2a ($P<0.001$, $P<0.05$, respectively) and SP.WKYGla2a versus WKY ($p<0.05$). There is no significant difference in RWT observed between strains by echocardiographic estimation ($p>0.05$). In addition, RWT is consistently overestimated by echocardiographic evaluation versus MRI derived values ($P>0.001$). All data shown is mean ±SEM, single factor ANOVA with *post hoc* Bonferroni adjustment for multiple testing.

MRI correlates well with gravimetric *post mortem* values, providing qualitative images which allow identification of differences in LV morphology, not apparent from echocardiographic imaging or simple *post mortem* evaluation. This study is novel, in that high fidelity phenotyping of the rat is taken to a further level of *in vivo* assessment, facilitating detection of subtle changes in left ventricle geometry and remodelling, demonstrating significant differences between parental and congenic strains, even in small number groups. Moreover, MRI imaging allowed for an improved characterization of the congenic rodent strain, which demonstrates concentric remodelling versus concentric hypertrophy as seen in the SHRSP parental, which was not possible with echocardiography or simple *post mortem* evaluation.

Whilst several groups have validated the use of echocardiography as a means of estimating LVM in the rat (Devereux *et al.*, 1994; Graham *et al.*, 2004), estimations are based on geometric assumptions (Jones *et al.* 1992). Previously, our group showed a good correlation between *post mortem* and echocardiographic estimated LVM (n=58), calculated using the ASE-cube formula (Graham *et al.*, 2004). In this study (n=30), use of the Devereux modified ASE-cube formula results in a higher correlation between echocardiographic estimated LVM and gravimetric values. Despite these improvements in LVM calculation, use of echocardiography for analysis in the small subset of animals used in the MRI study provided a poor correlation and did not allow for anatomical differences such as heart shape, which is assumed to be the same in every subject. Similarly, cardiac remodelling events such as wall thickening are over estimated with echocardiography in comparison to MRI, which provided a precision of analysis sufficient to detect discrete changes in LV geometry between the SP.WKYgla2a and SHRSP for the first time.

More precise and exact correction factors could of course be derived for individual strains to circumvent the issue or strain variation and LVM estimation, although this introduces a further element of guesswork, which detracts from the accuracy of results obtained and does not aid in identification of subtle inter strain LV geometric variations. MRI analysis of the rat heart provided a precise estimation of LVM in small animal groups (n=4), in accordance with data obtained from other groups investigating murine and rat heart mass

by means of MRI analysis (Siri *et al.* 1997; Crowley *et al.*, 1997; Wise *et al.*, 1999) and demonstrates the potential utility of MRI to assess LVM quantification and structure in small sample groups.

LVEF was also measured from MRI images using data from both systole and diastole. From the results it appears that the method of anaesthesia used in this study may have reduced cardiac output in these animals, as LVEF values for normotensive WKY hearts are somewhat lower in comparison to hypertensive SHRSP hearts and differ from MRI derived values obtained from other groups (Wise *et al.*, 1998). Although the effects of inhalant anaesthesia were not assessed in this study, other groups have reported cardiac depressant effects associated with use of halothane, in both humans and rodents (Merin, 1975; Friesen, Wurl & Charlton, 2000), which may indicate a requirement to change the anaesthetic used.

The actual time involved in optimisation of the MRI protocol was increased due to several factors, including heart rate variation between strains and signal interference associated with the ECG wires inside the magnet. In comparison to 2-dimensional techniques, such as echocardiography, MRI requires an initial set up period to optimise the stability of the animal and procedures such as motion gating. Standardising image acquisition is also fundamental in development of a MRI protocol in order to achieve precise and reproducible data, which ultimately leads to an overall increase in cost and time.

Crowley *et al.* (1997) devised a strategy to reduce the time of cardiac MRI image acquisition by application of an empirical formula to provide a more economical reconstruction of ventricular volumes at end diastole and end systole from a limited number of strategic images over a shortened image time. Following on from the work of Crowley *et al.*, Wise *et al.*, (1999) developed an ellipsoid of revolution predictor for accurate determination of epicardial and endocardial geometries across the cardiac cycle using a reduced set of imaging planes and imaging times. The application of a reduced imaging protocol such as described requires time to validate the method fully and the introduction of additional MRI related equipment and therefore was not attempted in this study. Although, the utility of analysis approximating the ellipsoidal model could demonstrate further inter

strain differences at different time points throughout the cardiac cycle and may be applicable to studies assessing cardiac function.

In conclusion, despite the fact that MRI imaging is costly in terms of time and technical input, the advantages gained in using 3-dimensional imaging over 2-dimensional imaging are numerous. MRI provides good soft tissue contrast and temporal image resolution with improved accuracy of LVM estimation. In addition, it was possible to identify cardiac structures and detect discrete changes not easily distinguished using 2-dimensional imaging or simple *post mortem* evaluation. MRI is an extremely powerful tool for cardiac imaging in relatively small animal groups, offering unrestricted multi-planar imaging and as such provides a more advanced and superior method of experimental animal model phenotyping; in particular when the detection of subtle changes and slight differences are important. In addition, the reproducibility of results from MRI analysis is more consistent than 2-dimensional echocardiography, allowing for repeated acquisition of identical imaging planes and a more concise method of serial imaging, which will be of particular benefit in longitudinal studies.

CHAPTER 6
CONSTRUCTION OF SPEED CONGENICS

6.1 INTRODUCTION

The identification of chromosomal regions harbouring quantitative trait loci (QTL) is only the initial step towards gene identification (Rapp & Deng, 1995), mainly due to the relatively broad QTL regions implicated from analyses which in general do not underpin a single gene relating to a phenotype of interest. In addition, there is a requirement to validate statistical QTL analyses, by physical confirmation or 'capture' of the QTL in a whole organism. Therefore in order to verify the existence of a QTL and narrow the chromosomal region of interest, thereby facilitating gene identification, a more definitive and stringent genetic test is required, in the form of congenic strain production.

Traditionally congenic strains are developed by serial backcrossing a donor strain (containing the genomic region of interest) with the recipient inbred strain, then selecting for progeny heterozygous for the desired region in each backcross generation (Wakeland *et al.*, 1997). Essentially, this leads to a successive dilution of the donor genome into the recipient genome, with continuous maintenance of introgressed region containing the QTL. According to Mendel's laws, it is expected that half of the unrelated genetic material will be transmitted to a subsequent backcross generation, 8-10 generations of backcross mating should result in a congenic strain in which more than 99% of the genome unlinked to the target gene(s) will be of recipient strain origin. The introgressed region is then 'fixed' homozygous by intercrossing and the resultant congenic strain theoretically contains a genetic background identical to that of the recipient inbred strain with the exception of the introgressed region.

Whilst this breeding protocol is theoretically straightforward, in practice several years are required to ensure the recipient background homozygosity of the new congenic strain. The completion of the rat genome sequence in the Brown Norway strain (Gibbs *et al.*, 2004) in addition to concerted efforts to revise and update microsatellite based rat maps, provides the opportunity to reduce time taken to produce congenic strains, via a DNA marker assisted or congenic 'speed' strategy. This approach involves the analysis of polymorphic marker loci distributed throughout the genome in order to specifically select male progeny

carrying the genetic region of interest, whilst also retaining the lowest background heterozygosity at each backcross generation. Breeding with these 'best' males accelerates elimination of the donor genetic segment thereby reducing the number of generations necessary to produce a congenic strain.

There are many examples of rat congenic strains successfully produced using both the traditional and speed congenic breeding approach (Deng *et al.*, 1997; Zhang *et al.*, 1997; Rapp *et al.*, 1998 Cicila *et al.*, 1999). In 2000, our group (Jeffs *et al.*, 2000) were the first to successfully produce reciprocal congenic strains, via a speed congenic protocol. This was achieved by introgressing segments of chromosome 2 containing 2 blood pressure QTL between WKY_{Gla} and $SHRSP_{Gla}$ rats, using 83 background genetic markers. Baseline and salt-loaded systolic blood pressure was reduced by approximately 20 and 40 mmHg respectively in male congenic rats with a SHRSP background compared with the SHRSP parental strain. This study not only confirmed QTL for blood pressure on chromosome 2, but supported the application and validity of this strategy.

Boutin-Ganache *et al.* (2002) produced a normotensive congenic strain from WKY and WKY hypertensive (WKHA) rats, which exhibited differences in LVMI in the absence of high blood pressure. Their data implicated a region on chromosome 5 showing linkage to both LVMI and atrial natriuretic protein (ANP), in males only. These results formed the basis of further investigative studies examining the association between chromosome 5 and heart weight. Souzeau *et al.* (2006) recently identified alleles at a specific locus (locus Cm24) on chromosome 5, which may be responsible for the observed differences in LVMI between WKY and WKHA rats. The group also suggest, that this genetic locus induces either mild or no concentric LV remodelling in male rats and is associated with LV dilatation and dysfunction when hearts are subjected to volume overload. These data provide evidence, which clearly demonstrates the involvement of a strong genetic element affecting cardiac weight and LV geometry, which although influenced to some extent by volume overload, is independent of a blood pressure effect.

The aim of this current study was to generate reciprocal congenic strains from SHRSP and WKY parental stock, in order to investigate genetic linkage (identified in chapter 3) between cardiac and LV weight and rat chromosome 14. It is expected that congenic strains produced will be hypertensive (SHRSP background) and normotensive (WKY background), as no blood pressure QTL was identified on rat chromosome 14 from the F_2 genome wide linkage analysis study. Production of these congenic strains will not only allow for investigation of genes underlying the QTL peaks, but will provide insights into heart weight and cardiac remodelling in the presence and absence of high blood pressure.

6.2 METHODS

6.2.1 Congenic Strain Production

Congenic strains were constructed by introgressing approximately a 64cM region of chromosome 14 (boundary flanking markers – D14Rat54, D14Rat110) from SHRSP into the genetic background of WKY and vice versa, using a previously tested DNA marker assisted protocol as outlined in Chapter 2.2.2. The actual number of backcrosses required was dependant on the rate at which heterozygosity was reduced in the genetic background, as well as litter size and male: female ratio. Once a suitable male and female were identified, in which all background heterozygosity was eliminated, they were intercross mated to obtain offspring homozygous for the donor alleles throughout the chromosome 14 region of interest. Congenic lines were then maintained via brother-sister mating. Care was taken to ensure the correct Y chromosome was paired with the relevant genetic background i.e. WKY background males retain the originating WKY Y chromosome and vice versa, as is illustrated in Figure 6.1.

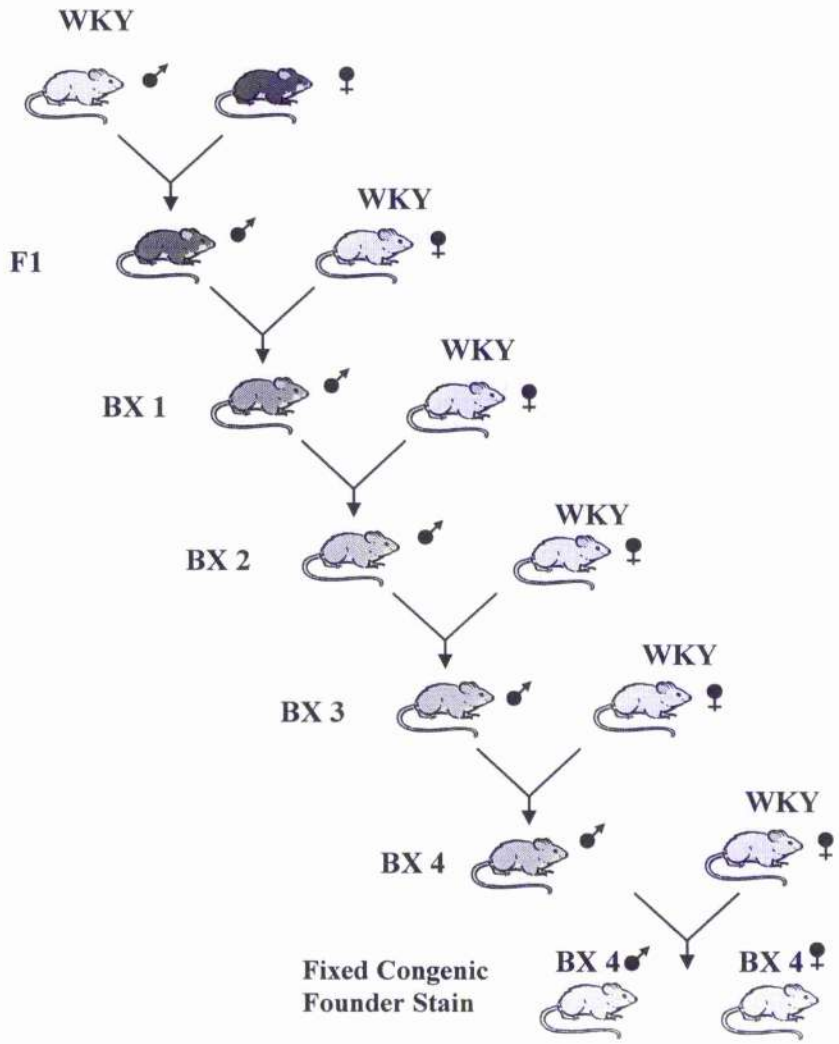

Figure 6.1 Cartoon of congenic breeding strategy and correct Y chromosome orientation in a WKY background congenic strain. To ensure the correct Y chromosome is paired with the appropriate genetic background, a parental male from the donor strain (WKY) is mated with a recipient parental female (SHRSP) to produce F_1 offspring. All F_1 males will have a correctly paired WKY Y chromosome. As the majority of the Y chromosome does not recombine, the origin of the male F_1 progenitor will determine the Y chromosome in all F_1 hybrid males and male offspring.

6.2.2 Tail-Tipping and DNA extraction

Animals were lightly anaesthetized at 6-weeks of age with halothane and less than 5mm tip was removed from the tail end and placed into a 1.5ml microfuge tube. The wound was immediately cauterized electronically (Engel Loter 100S) and the tail tips stored at 4°C. Genomic DNA was extracted from using a simplified mammalian DNA extraction kit (Nucleon), described in *Chapter 2.4.1*. All DNA samples were stored at -20°C prior to PCR analysis.

6.2.3 PCR and Genotyping

PCR was performed as previously described in *Chapter 2.4.2*, using fluorescent markers provided by MWG Biotech. Genotype analysis was carried out by two independent observers, using GeneMapper v.3.0 software (Applied Biosystems, USA). Genotype data was exported in text file format and imported to an in-house designed Microsoft Access database for further analysis. Animals were selected for breeding on the basis of a 'preferred' genotype – heterozygous (WS) for chromosome 14 polymorphic markers and mostly homozygous (WW or SS) for the recipient alleles (WKY and SHRSP respectively) on the remaining genetic background. Chromosome 14 polymorphic microsatellite markers used are detailed in Chapter 3, Table.3.1 with background microsatellite markers shown in Appendix V.

6.2.4 Design of Microsoft Access Database

A relational database system was designed using Microsoft Visual Basic Code 6.0 and structured query language (SQL). The database was designed to (i) retain breeding information for all animals held at the facility (ii) link to an in-house designed genotype database. The genotype database was optimised to facilitate upload of breeding data and indexing for quicker searching and data output. Consistency between both databases was achieved by including declared constraints (a logical schema) in the database design. This

involved 'normalization', with the desirable properties of both databases selected from a set of logically equivalent alternatives to prevent overlap and improve overall efficiency (E.F. Codd, 1979). A visual representation of logical schema relations is shown in Figure 6.2 and the GUI search facility is shown in Figure 6.3.

6.2.5 Phenotype Measurements

Tail-cuff plethysmography was used to obtain blood pressure measurements from animals at ages 10 and 18 weeks, as detailed in *Chapter 2.3.1*. Left ventricular mass and geometry were evaluated by echocardiography and gravimetric values recorded at *post mortem*. Echocardiographic measurements were carried out at 10 weeks of age for baseline measurements and repeated again at 18 weeks. For a detailed discussion of this method see *Chapter 2.3.3*. Immediately post exsanguination, the thorax was opened and the heart removed, blotted and weighed to within three decimal places. Both atria and right ventricle were removed free and the left ventricle and septum weighed. The indices of cardiac mass (heart weight to body weight ratio) and LVM (left ventricle weight to body weight ratio) were calculated and determined.

6.2 RESULTS

A breakdown of background heterozygosity, determined from genotype analysis of 168 background microsatellite markers, is shown in Table 6.1. The percentage of heterozygosity progressing from the initial backcross 1 stage to backcross 4, demonstrates the effective dilution of donor genetic background to that of a homozygous recipient origin. Three fixed congenic females were identified; one female matching to a WKY background and two females correspondent to a SHRSP background. There were no appropriate genotype males identified for interbreeding with females to achieve a founder congenic

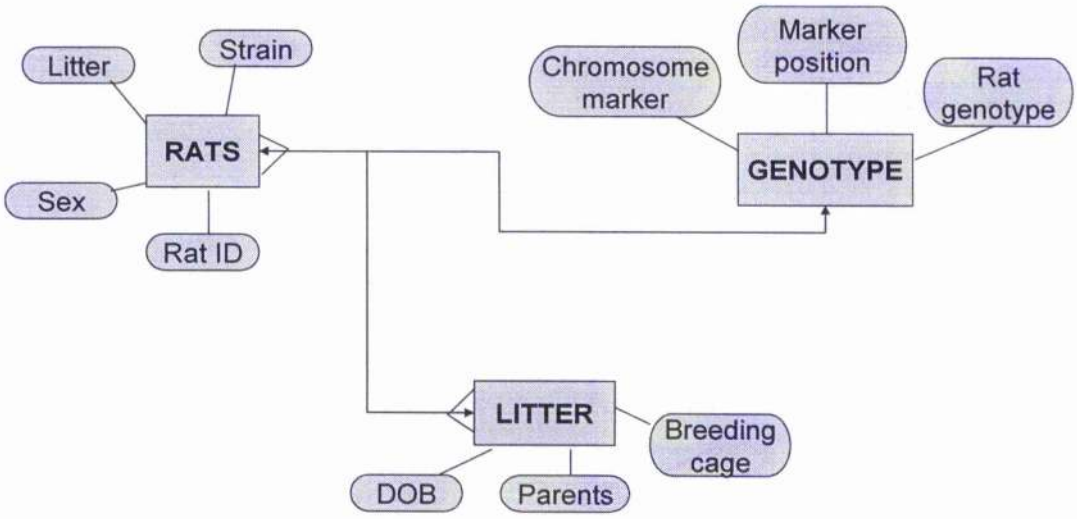

Figure 6.2. Conceptual relationship schema joining breeding and genotype database systems. Entities are shown in boxes with attributes shown in ovals. In this integrated schema, relationships are represented as one - many (genotype - rats) or many - many (rats - litter).

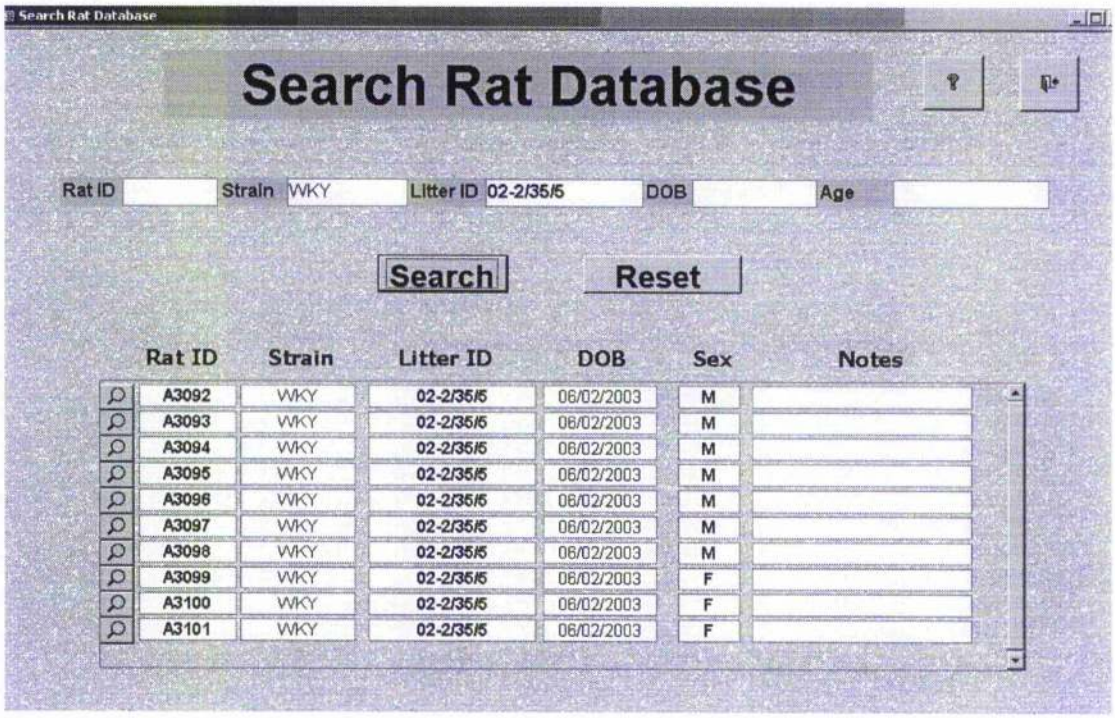

Figure 6.3 Search GUI for the breeding database. Search queries are based on Input of one or more identifiers. A quick indexed return of animals is output with options to link to individual animal data.

Table 6.1. Background heterogeneity in backcross strains generated

Background Strain	Bx1	Bx2	Bx3	Bx4
WKY	47%	25%	5%	0%
SHRSP	62%	37%	18%	0%

Bx = Backcross

line, in the available time frame. A graphical representation of the introgressed chromosome 14 segment and relative approximation of LVMI QTL is illustrated in Figure 6.4.

Analysis of LVMI in F_2 males at marker loci *D14Wox14* and *D14Got33* (*Chapter 3*) identified a WKY allele dominant effect, which is shown in Figures 6.5a-b. A significant reduction in LVMI was noted between homozygote SHRSP (SS) and heterozygote WKY/SHRSP (WS) animals, with no significant difference between homozygote WKY (WW) and WS heterozygotes. Based on this observation, backcross 4 males on a SHRSP background ($SHRSP_{GlaBX4}$) were expected to have a lower LVMI in comparison to the respective SHRSP parental strain. SBP measurements and LVMI calculated from echocardiographic B-mode and M-mode images are shown in Figures 6.6a-b. In Figure 6.6a, SBP measurements for both SHRSP and $SHRSP_{GlaBX4}$ are equivalent with no significant differences observed between the strains. Despite comparable haemodynamic profiles, Figure 6.6b illustrates a significantly reduced LVMI in $SHRSP_{GlaBX4}$ animals, compared to age matched SHRSP. A significant increased weight is observed in $SHRSP_{GlaBX4}$ at 10 weeks of age, however by 18 weeks there is no significant difference in body mass between the two strains (Figure 6.7). At the time of writing this thesis, reciprocal congenic strain production was at the stage of intercross breeding to fix the homozygous congenic segment, however due to time constraints phenotypic examination of these animals could not be completed and therefore is not included in this chapter.

6.4 DISCUSSION

Data relating to the production of congenic strains is presented in this study, providing initial evidence in support of LVMI QTL within a region of rat chromosome 14 identified in *Chapter 3*. Introgressing a segment approximating to a 56 Mb region of chromosome 14 from WKY into the genetic background of SHRSP resulted in a significantly reduced LVMI in comparison to age matched SHRSP, highlighting the importance of this region in the genetic control and development of LV hypertrophy. It is important to note the LVMI reduction observed in this study occurs in the absence of any

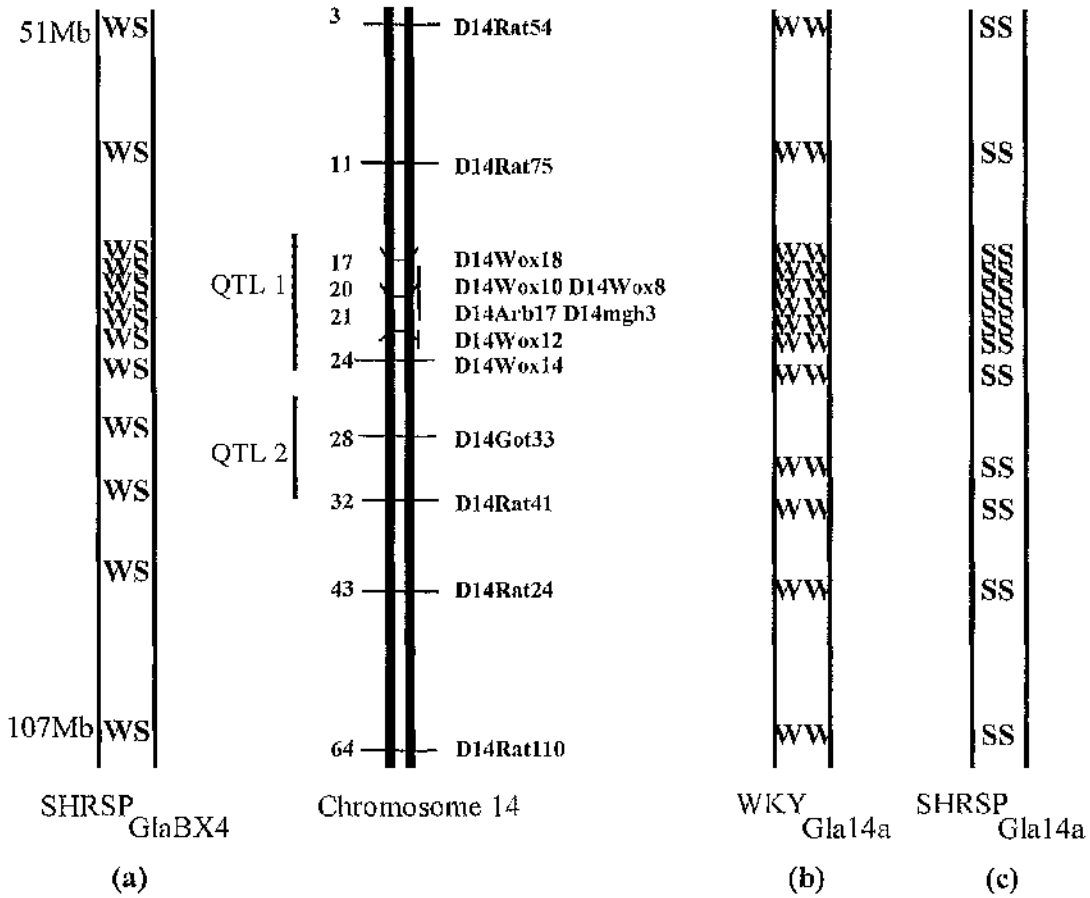

Figure 6.4 A diagram of chromosome 14 showing QTL1 and QTL2. The region of chromosome 14 encompassing both LVMI QTL spans approximately 56 million base pairs (Mb). This region is heterozygous WKY/SHRSP in backcross 4 animals ($SHRSP_{GlaBX4}$); the remaining genome is homozygous SHRSP **(a)**. A depiction of the anticipated fixed homozygous WKY **(b)** and SHRSP **(c)** chromosome 14 strains are also illustrated to highlight the difference between these fixed strains and the heterozygous $SHRSP_{GlaBX4}$.

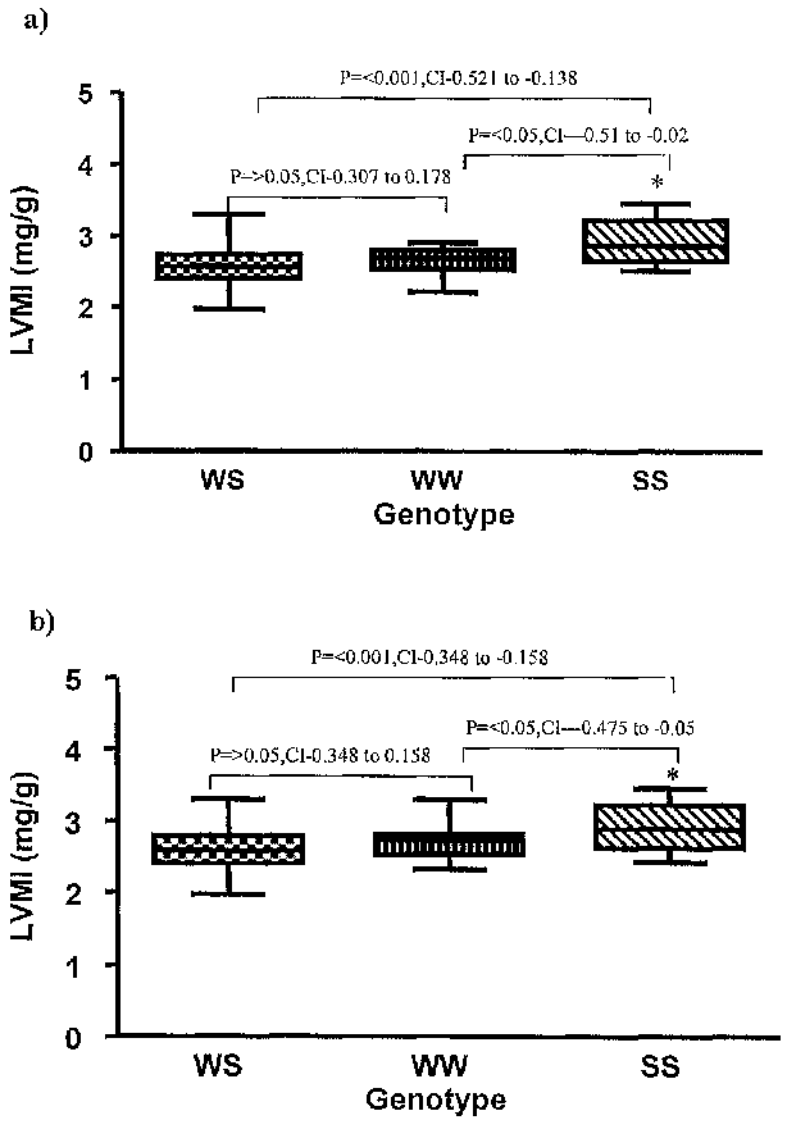

Figure 6.5 Single factor ANOVA analysis of LVMI at marker loci **(a)** *D14Wox14* for homozygous (WW, n=12), homozygous (SS, n=26) and heterozygous (WS, n=27) and **(b)** *D14Got33* (WW, n=16; SS, n=21; WS, n=27). At both marker loci, there is no statistical difference between WW and WS. Analysis of SS and WS at both marker loci shows a recessive SHRSP allele effect: *D14Wox14*; *, P<0.001, F=14.65; *D14Got33*; *, P<0.001, F=14.9. Data shown is mean ±SEM with *post hoc* Bonferroni adjustment for multiple comparisons.

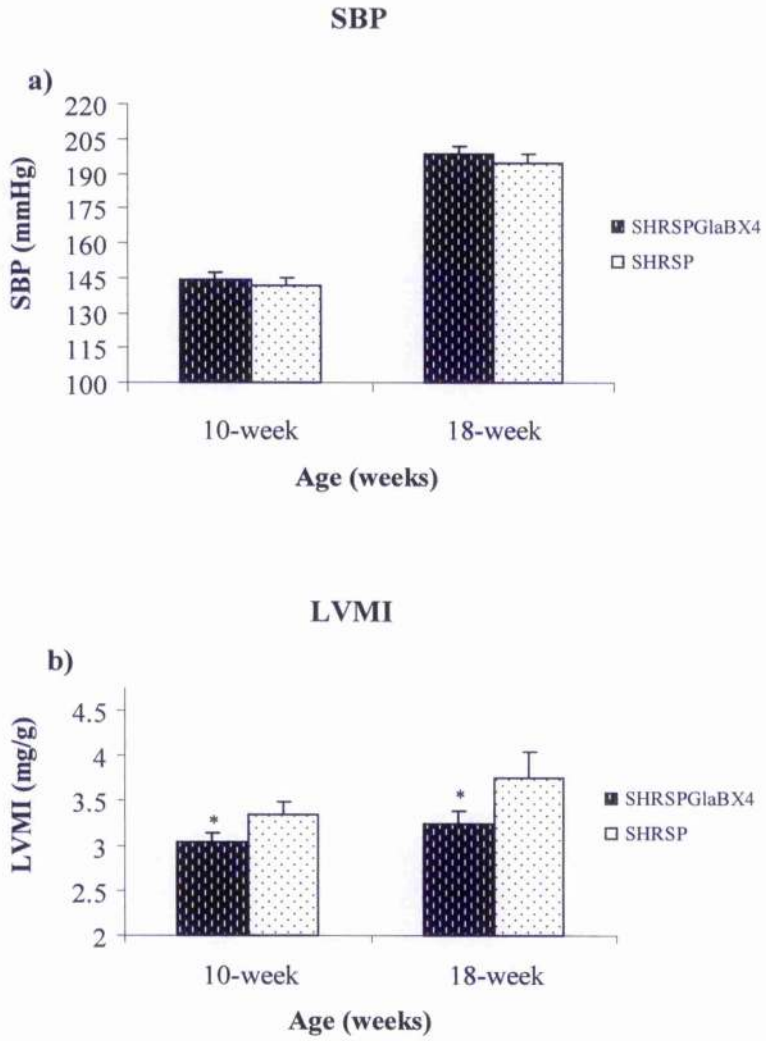

Figure 6.6 Analysis of **(a)** SBP and **(b)** LVMI in $SHRSP_{GlaBX4}$ and parental SHRSP strains. There is no significant difference in SBP between SHRSP aged 10 and 18-weeks (n=10, n=8 respectively) and $SHRSP_{GlaBX4}$ at 10 and 18-weeks of age (n=10, n=6 respectively). Gravimetric estimated LVMI is significantly reduced in $SHRSP_{GlaBX4}$ strain at both time points (P=0.018, P=0.0041 respectively), compared to age matched parental SHRSP. All data shown are mean ±SEM, analysis by unpaired student t-test.

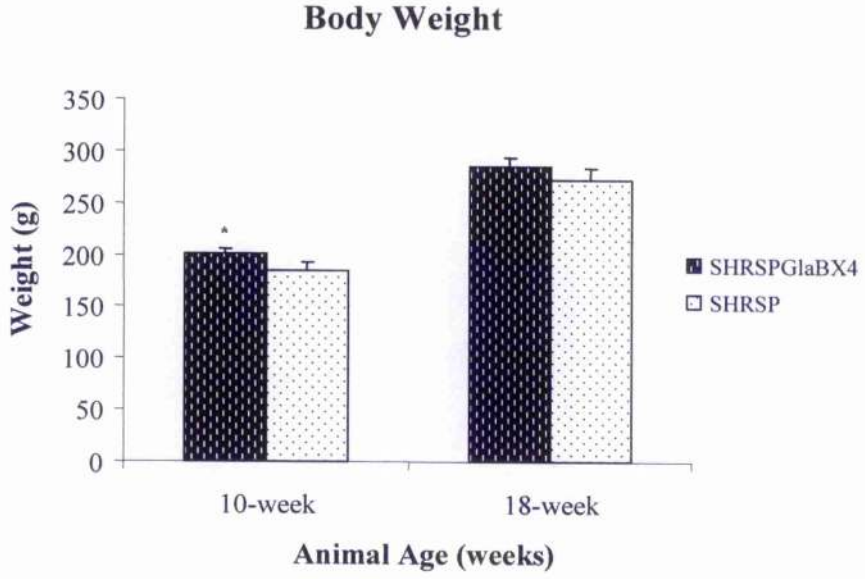

Figure 6.7 Analysis of $SHRSP_{GlaBX4}$ and parental SHRSP body weights. At 10 weeks of age, body weight in $SHRSP_{GlaBX4}$ (n=10) is statistically higher (P=0.012, n=10), compared to age matched parental SHRSP (n=10) with no statistical difference observed at 18 weeks of age between SHRSP (n=8) and $SHRSP_{GlaBX4}$ (n=6). All data shown are mean ±SEM, analysis by unpaired student t-test.

significant blood pressure difference between the strains. The $SHRSP_{GlaBX4}$ strain are unique in this respect, as findings from other groups (Cicila *et al.*, 1998; Garrett *et al.*, 2000) show differences in cardiac mass and LVM are consistently associated with a parallel reduction in blood pressure, in the other hypertensive congenic rat models.

Cardiovascular physiology alone does not explain sequent cardiac remodelling mechanisms in response to pressure overload, therefore a priori it is reasonable to assume loci influencing heart weight (independent of blood pressure regulation) exist within the genome. Innes *et al.* (1998) has previously shown that a QTL (Lvm-1) on chromosome 2 near D2Mgh15 influences LVMI, but not blood pressure in F_2 (SHR × Fischer 344 (F344)) animals. The association of this locus with the SHR genotype is recessive in relation to increased LVMI as F_2 animals homozygous for the SHR allele for Lvm-1 had significantly greater LVMI than rats homozygous or heterozygous for the F344 allele. This particular QTL lies is at the edge of a well-established blood pressure QTL, therefore from these results alone it is difficult to ascertain the actual effect blood pressure exerts on LVMI in the absence of further evidence (e.g. a congenic strain for heart weight independent of BP and body weight). Harrap *et al.* (2002) has gone some way to address this with the development of a genetic model of cardiac and cardiomyocyte hypertrophy, without hypertension (HHR strain) using selectively bred rats with large hearts and low blood pressure from a second-generation cross of SHR and F344 strains. Recently Harrap's laboratory confirmed the Lvm1 QTL with further QTL analyses and fine mapping of the region, identifying a number of putative candidate genes (Nicolantonio *et al.*, 2006). Nonetheless, this QTL is still to be validated by physiology and phenotypic evidence. The application of gene expression profiling and/or the generation of a fixed congenic and substrain congenic line may facilitate detection of biological in situ effects relating to candidate genes as well as identification of gene-gene and gene-environment interactions.

A seminal microarray experiment, combining the application of congenic strain production with genome wide expression analysis was the identification of the Cd36 gene on rat chromosome 4; a gene responsible for defective fatty acid and glucose metabolism (Aitman *et al.*, 1999). This study included investigation of over 10,000 cDNA probe sets in SHR,

BN and congenic strain SHR 4 (in which a 36cM region of rat chromosome 4 of BN was introgressed into a SHR background). A deficiency in Cd36 was identified in the SHR strain in addition to other differentially expressed genes. Moreover, they established multiple coding sequence variants in Cd36 cDNA and negligible protein product, in SHR adipocyte plasma membrane. The group continued study with the gene, to develop transgenic mice expressing Cd36, characterised by reduced plasma triglycerides and fatty acids (Aitman *et al.*, 1999). Further work included radiation hybrid mapping of 70 other genes, also differentially expressed between the SHR and BN strains (Wallace *et al.*, 2002)

McBride *et al.* (2003) and Garrett *et al.* (2005) also used congenic substitution mapping in conjunction with microarray technology to identify candidate genes of positional and functional interest. Our group identified a significant reduced expression of glutathione S-transferase mu-type 1 (a gene involved in oxidative stress defence) in a congenic strain (SP.WKYGla2c*; SHRSP background with a portion of chromosome 2 introgressed) compared to the parental SHRSP strain. Garrett *et al.* successfully localised a previously identified blood pressure QTL to within a 117 kb region on rat chromosome 9, by production of substrain congenic strains and high resolution mapping combined with gene expression profiling, thereby reducing the region of interest and excluding a previously identified candidate gene. In using the congenic substrain approach, there is a possibility that the phenotype of interest may be lost due to continued reduction of the congenic region. Nevertheless, with careful dissection of larger congenic segments, congenic substrain production allows closer inspection of the phenotype and underlying genetic components. Combining methods of both gene array systems with congenic substrains provides greater power to identify candidate genes and allows in depth analysis of background associated effects and interactions.

Therefore, production of congenic strains offers an extremely powerful resource for investigating the functional and physiological differences associated with QTL effects on a primary phenotype of interest, allowing facilitation of QTL isolation. In addition, genetic analysis of the phenotype can be further tested with the production of substrain congenic lines, which used in parallel with gene expression systems such as microarray may reduce

the number of candidate genes and biological pathways for investigation. Due to time constraints, data for the fixed congenic strain is not presented here, however it is anticipated that future assessment of the fixed congenic strains will support the echocardiographic estimations of LVM observed in the $SHRSP_{GlaBX4}$ strain. Generation of reciprocal strains will then allow for further study into the importance of genetic background in the context of LVMI.

CHAPTER 7

GENOME WIDE EXPRESSION ANALYSIS

7.1 INTRODUCTION

Recent complementary advances, in both knowledge and technology have greatly facilitated the study of gene expression resulting in the identification of genes and biological interactions within the context of disease progression. Microarray technology is a powerful means to examine thousands of RNA transcripts concurrently, allowing exploration of genome complexity at a fundamental level (The chipping forecast, 1999). The use of high throughput gene expression to investigate experimental animal models of human disease, affords the opportunity to establish links between genotype and phenotype of complex traits. Moreover, the versatility of design by experimental condition and various analysis methods, allow for a comprehensive approach to candidate gene identification, on a genome wide scale.

Over the last few years, advances in technology, online resources and data analysis has resulted in several successful cardiovascular directed microarray experiments. A seminal paper from Aitman *et al.* (1999) indicated the potential of genome wide expression analysis for candidate gene identification, using a combined approach of cDNA microarray and a congenic strain, identifying a gene involved in defective fatty acid and glucose metabolism - Cd36. Following on from the work of Aitman *et al.* (1999), other laboratories have since used microarray technology to detect genes that may contribute towards a disease phenotype of interest. In particular, our group identified glutathione S-transferase mu-type 1 (Gstm1) as a putative positional and physiological candidate gene involved in the defence against oxidative stress (McBride *et al.* 2003).

Heart specific microarray experiments to date have mainly focussed on cardiac hypertrophy in the context of heart failure or single gene disorders such as familial hypertrophic cardiomyopathy (FHC) (Rajan *et al.*, 2006; Schiekofer *et al.*, 2006; Kong *et al.*, 2005; Rysa *et al.* 2005). Rysa *et al.* (2005) analysed gene expression in 12-, 16-, and 20-month-old SHR and age-matched WKY using cDNA microarray and identified LVH in SHR was associated with increased expression of hypertrophy-associated genes, including contractile protein and natriuretic peptide genes. Recently, Schiekofer *et al.* (2006) conducted a

detailed comparative analysis of gene expression between 2.5-month-old control mice and two transgenic mouse models with familial hypertrophic cardiomyopathy (FHC) associated mutations in alpha-tropomyosin. Their results showed 754 genes (from a total of 22,600) were differentially expressed between the control and FHC hearts. The transgenic models used in this study exhibited a varying degree of observed hypertrophy - FHC alpha-TM175 mice have patchy areas of ventricular disorganization and mild hypertrophy, whereas FHC alpha-TM180 mice show severe hypertrophy and fibrosis, with a short lifespan of approximately 6 months. Between transgenic groups, 266 genes were differentially expressed, with the largest increased expression in the secreted/extracellular matrix class and the most significant decreased expression in the metabolic enzymes group (Rajan *et al.*, 2006). There has been no definitive study thus far, in which investigation of the shift from a healthy to pathogenic phenotype with respect to genotype and in the context of environmental stimuli.

Experimental design and sensitive statistical methods of data analysis are fundamentally important to the success of any study however microarray is particularly dependant on the quality of analysis, mainly due to the limited biological replicates per experiment, the large number of genes identified and the background noise of data (Breitling *et al.*, 2004). A quick and simple method to identify differentially expressed genes from microarray experiments, which is based on calculating rank products (RP), was developed by Breitling *et al.* (2004). In particular, RP can provide reliable analysis of results in small datasets providing a stringent method of analysing large numbers of genes more reliably than previously used statistical approaches, such as t-test and significance analysis of microarray (Tusher *et al.*, 2001). However the investigation of interactive effects, such as genotype and environmental factors, cannot be tested with the RP statistical method. An alternative statistical approach is two-way ANOVA, which offers both the identification of main effects between factors of investigation and the detection of genes based on an interaction between two (or more) specific conditions (Pavlidis, 2003).

The main objective of this study is to identify differentially expressed genes in cardiac tissue taken from hypertensive and normotensive 21 week old male rats in the presence and

absence of dietary salt manipulation, using a genome wide expression approach. The use of a two-way experimental design has also enabled the application of more than one statistical approach, which will allow the identification of differentially expressed genes by RP method and ANOVA.

7.2 METHODS

7.2.1 Experimental Animals, Dietary Manipulation and Phenotypic Measurement

12 male rats aged 18 weeks (SHRSP, n = 6; WKY, n=6) were given 1% salt water (SHRSP, n = 3; WKY, n=3) or plain drinking water (SHRSP, n = 3; WKY, n=3) ad libitum over a 3 week period. At 21 weeks of age, systolic blood pressure (SBP) was measured by tail-cuff plethysmography, as described in Chapter 2.3.1. Body weight of each rat was measured prior to sacrifice; cardiac and left ventricle (LV) + septum weight was measured after removal of the heart, as described in Chapter 2.3.3. Whole heart and LV + septum weight were indexed to body mass in order to obtain CMI and LVMI respectively.

7.2.2 RNA Extraction and Microarray Experiment

RNA was extracted using Qiagen RNeasy Maxi kit and quantified using a NanoDrop® ND-1000 Spectrophotometer as described in detail in *Chapter 2.6.1.* A TEST-3 Affymetrix chip was run for 2 samples to assess cRNA quality on a transcript level after biotin labeling of heart tissue, starting from 5.0 μg total RNA. Biotinylated amplified target cRNA was prepared and hybridised to the Affymetrix GeneChip® Rat Genome 230 2.0 Array set (which is comprised of 31,000 probe sets, analyzing over 30,000 transcripts and variants from over 28,000 rat genes). Following hybridisation, the microarray was washed, stained and scanned (see *Chapter 2.8.1* for detailed description).

7.2.3 Microarray Data Analysis

Data was normalized using Robust Multichip Average (RMA) (Irizarry *et al.*, 2003) as described in *Chapter 2.82*. Cluster analysis was used to partition samples on the basis of variance. The Rank Product (RP) method of analysis was used to determine the significance of each gene (Breitling *et al.*, 2004). An additional statistical analysis method was used to test for interactions between stain and environment; 2-way analysis of variance (ANOVA). Figure 7.1 illustrates the two-way factor design template used in this experiment. Data was imported to Ingenuity Pathways Analysis (https://analysis.ingenuity.com) and functional and network pathways of significance generated. A diagram key for data output from Ingenuity Pathway Analysis is given in Figure 7.2. Networks were graded as significant using hypergeometric distribution, calculated via the Fisher's Exact Test for 2 x 2 contingency tables. A numerical value was assigned as a score and used to rank networks according to how relevant they are to genes in the input dataset.

7.3 RESULTS

Daytime averaged haemodynamic and cardiac parameters for representative SHRSP and WKY strains are given in Figures 7.3a-c. SBP, CMI and LVMI are significantly increased in SHRSP compared to WKY at 21 weeks of age with and without dietary salt manipulation ($P<0.001$, $P<0.001$, $P<0.001$, respectively). After 1% salt loading, CMI and LVMI increase significantly in salt versus non-salt groups. SBP is unaltered in WKY salt versus no salt group, with an increase trend observed in SHRSP after salt loading that does not reach significance.

In order to consider data structure as a further quality control measure, cluster analysis of normalised data was carried out and charted using Sammon mapping and Manhattan distance metric plots, the results are shown in Figures 7.4 and 7.5a-b. Sammon maps provide a useful method of visualizing data as a measure of quality control; Figure 7.4 illustrates four distinct homogeneous data groups clustered by gene expression.

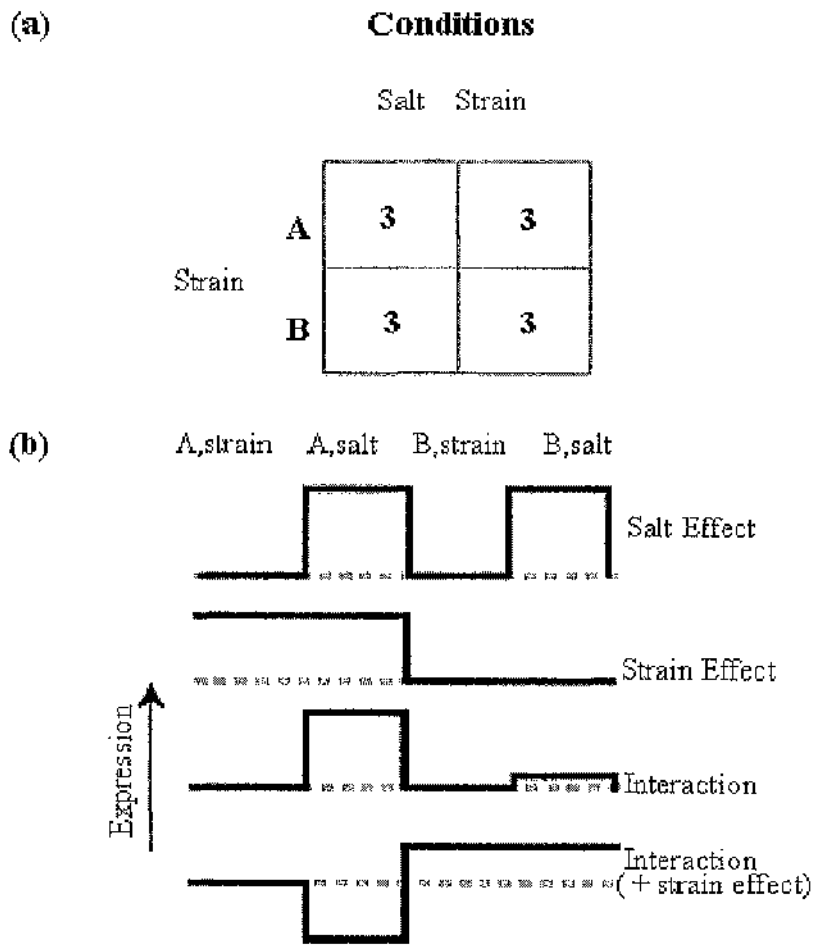

Figure 7.1 (a) A two-way factor design template. Combinations of experimental conditions are represented in boxes detailing the number of biological replicates [3]. **(b)** Examples of various effects that can be identified by ANOVA. Grey dotted lines indicate a 'baseline' level (adapted from Pavlidis, 2003).

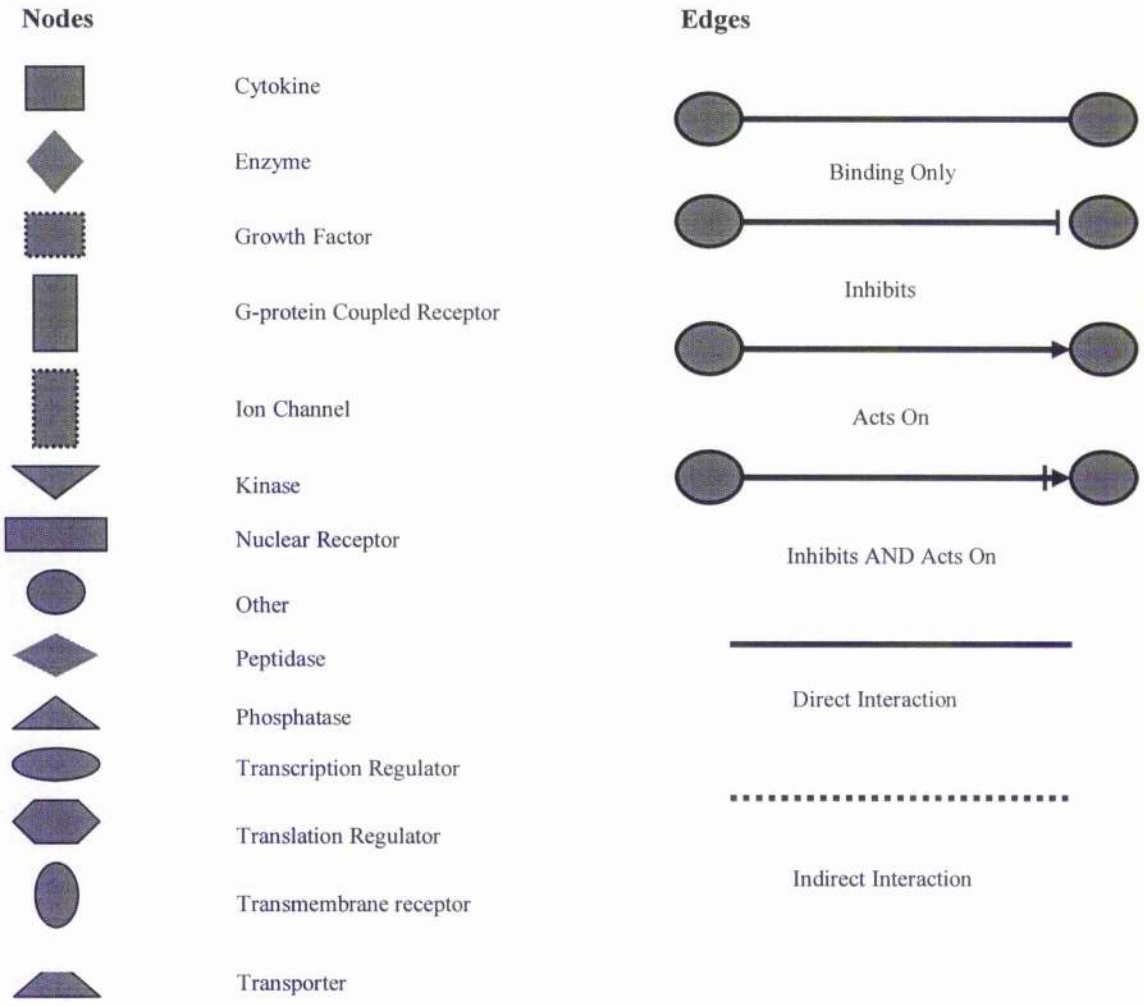

Figure 7.2 Diagram key for Ingenuity Pathway Analysis data output.

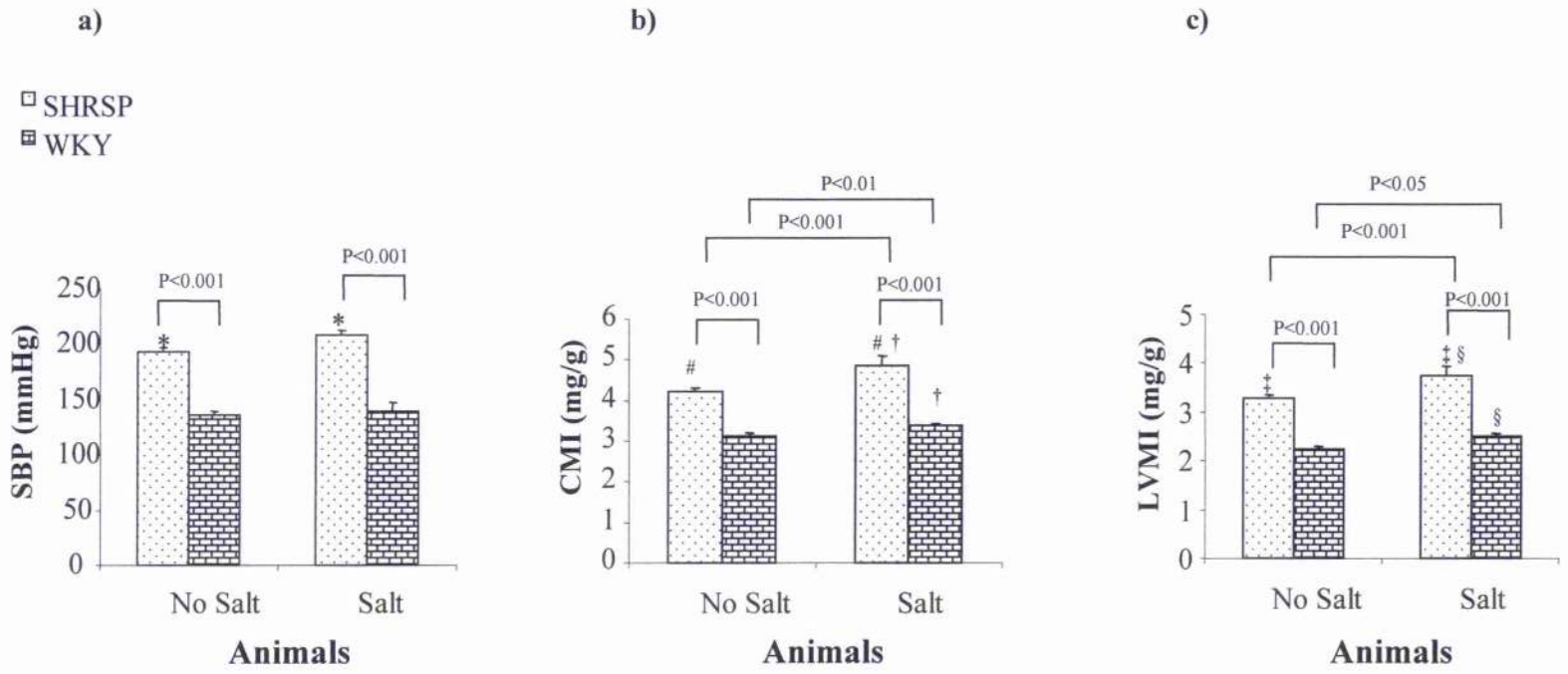

Figure 7.3 Daytime averaged haemodynamic and *post mortem* cardiac and LV parameters for SHRSP (salt, n=8; no-salt, n=9) and WKY (salt, n=8; no-salt, n=7). **a)** SBP is increased in SHRSP (⁎, P<0.001, CI 25.17 to 102.62; ⁎, P<0.001, CI 37.97 to 115.42) versus WKY before and after a 3 week 1% salt loading, respectively. SBP is not significantly increased in SHRSP (P>0.05, CI -34.32 to 43.12) and WKY (P>0.05, CI -47.12 to 30.32) salt versus non salt groups. **b)** CMI and **c)** LVMI are increased in SHRSP (#, P<0.001, CI 0.9413 to 1.346; ‡, P<0.001, CI 0.8319 to 1.123, respectively) versus WKY. A significant increase is observed for CMI and LVMI in SHRSP (†, P<0.001, CI 0.1251 to 0.5303; §, P<0.001, CI 0.1361 to 0.4275, respectively) and WKY (†, P<0.01, CI 0.05521 to 0.4604; §, P<0.05, CI 0.02442 to 0.3440, respectively) between salt and no-salt groups. Data shown are mean ±SEM, unpaired student t-test with *post hoc* Tukey adjustment for multiple comparisons.

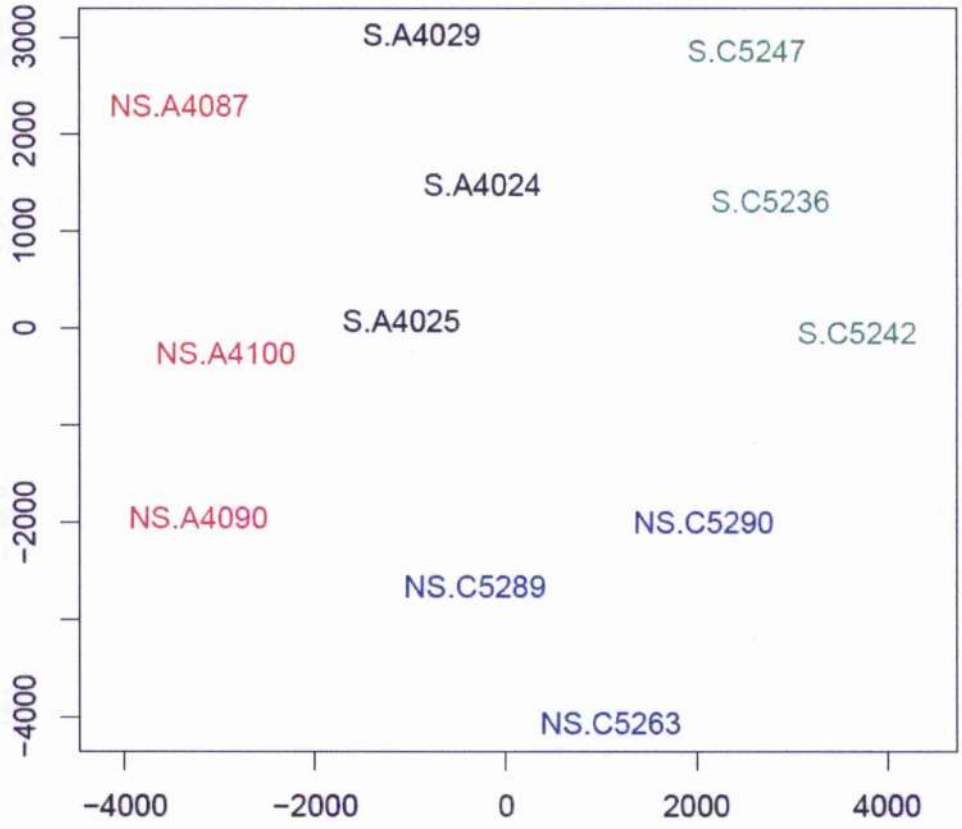

Figure 7.4 Sammon Plot. Groups are prefix annotated NS (non-salt), S (salt) and colour coded: WKY NS, red; WKY S, black; SHRSP NS, blue; SHRSP S, green. Relative distances shown are Euclidean, a mathematical distance used to represent a distance between two points in a straight line as measured with a ruler, which can be validated by Pythagoras theorem. In using this formula as a distance, Euclidean space becomes a metric space allowing visualisation of data from a high dimensional space (e.g. 3 dimensional) to a 2 dimensional or 1 dimensional graph. Data subsets of genes or sample datasets of gene expression values are grouped together (clustered) based on their similarities; the larger the Euclidean distance, the smaller the similarity. This plot shows similarities within datasets, grouping by colour in clusters, thus illustrating separate homogenous data groups.

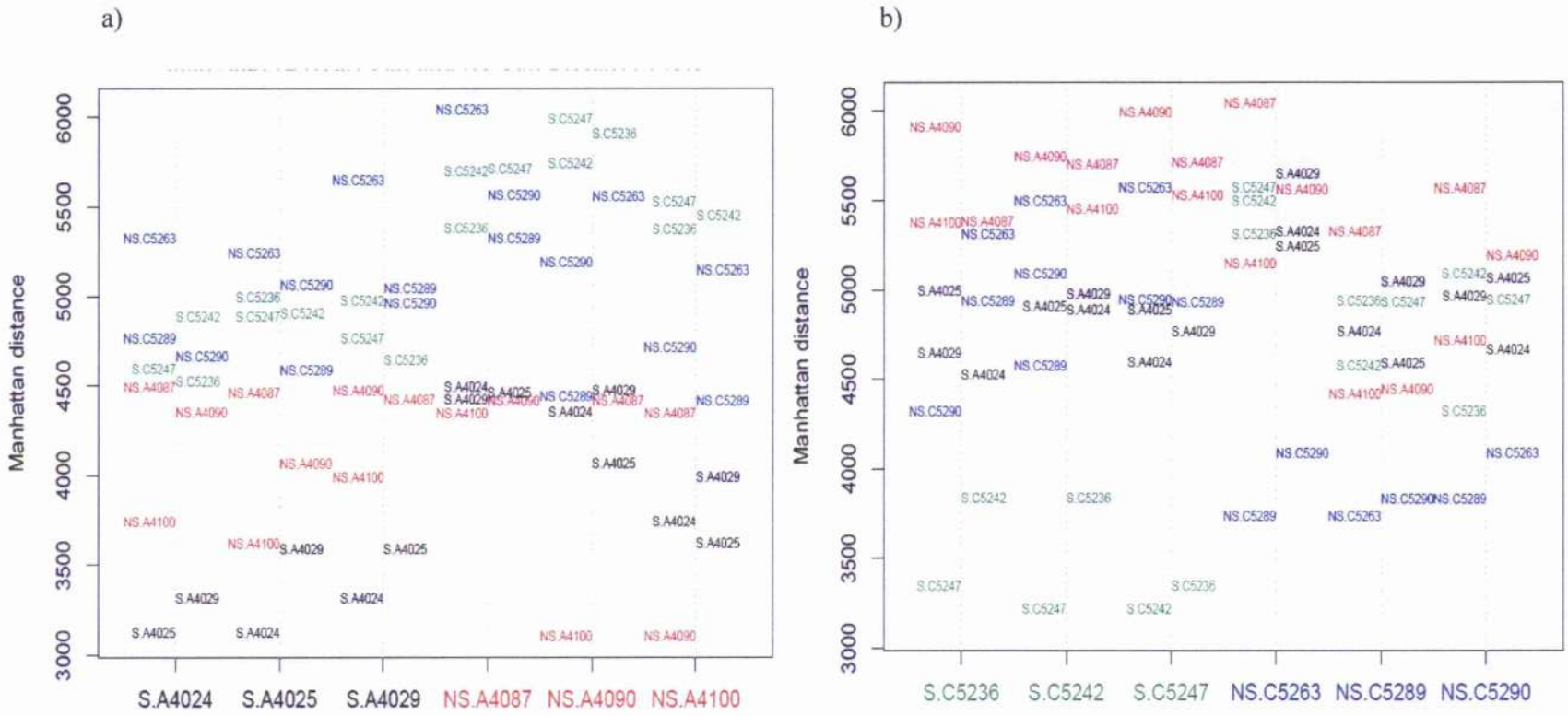

Figure 7.5 Manhattan distance metric plot. Groups are prefix annotated NS (non-salt), S (salt) and colour coded (WKY NS, red; WKY S, black; SHRSP NS, blue; SHRSP S, green. Individual animals are plotted against an x-axis of a) WKY and b) SHRSP datasets. Relative distances are shown as a Manhattan distance (the shortest path between two points in a city block) and is therefore a greater distance than Euclidean metric, as the distance is not measured in a straight line but in right angles. The data from this plot is consistent with the Sammon mapping chart showing clustering of datasets, but is particularly useful as an additional quality control measure to identify dissimilarities within datasets; outliers within each group can be observed as lying a further distance from respective x-axis data points, e.g. NS A4087, showing a larger distance from other samples in the grouping.

distributions for sample groups. Figures 7.5a-b, illustrates distance partition clustering by group. Samples cluster within a relatively short distance to biological replicates, in distinctive groups. The validity of these groupings was further confirmed by genetic profiling, compiled by separation on the basis of strain and dietary salt intake, for a total of 2,215 differentially expressed genes. These data are illustrated as Venn diagrams shown in Figures 7.6a-b. The majority of significant changes occurred in the SHRSP group after 3 weeks 1% salt stimuli (798 genes differentially expressed) and in the WKY salt (s) versus SHRSP (s) groups (566 genes differentially expressed) with 90 genes differentially expressed between WKY (s) and non-salt (ns) groups.

A list of differentially expressed genes on chromosome 14 identified from RP analysis, is given in Table 7.1. Ingenuity Pathway Analysis was used to generate networks from RP data for each sample group comparison, based on a level of scoring by means of right tailed Fisher's Exact Test; 80 networks were identified, outlined in Table 7.2. Data was filtered to illustrate the highest ranked network for a single group comparison and the number of common overlapping genes, shown in Figure 7.7. A list of genes, from these identified networks is given in Table 7.3; the highest ranking network pathway for each group comparison is illustrated in Figures 7.8a-d, 7.9a-d, 7.10a-d and 7.11a-d.

Two-way ANOVA analysis was used to specifically investigate interactions between strain and salt. A diagram of probe sets identified as significant for an interaction event is shown in Figure 7.12. From the total of genes analysed, 31 genes were significantly differentially expressed at <0.05 and positive for an interaction between strain and salt. Further filtering was achieved by removal of duplicate probe sets and those showing a flat line pattern of expression; a list of 17 differentially expressed genes is given in Table 7.5. Alignment of these genes with cited cardiac mass QTL data (http://rgd.mcw.edu) identified 7 genes corresponding to a LVMI or CMI QTL region, indicated in Table 7.5 by an asterisk. A full list of current cited heart weight and LVMI QTL are given in Appendix VI. The majority of genes identified from ANOVA analysis are transcriptional regulators, growth factors and transporter proteins.

a)

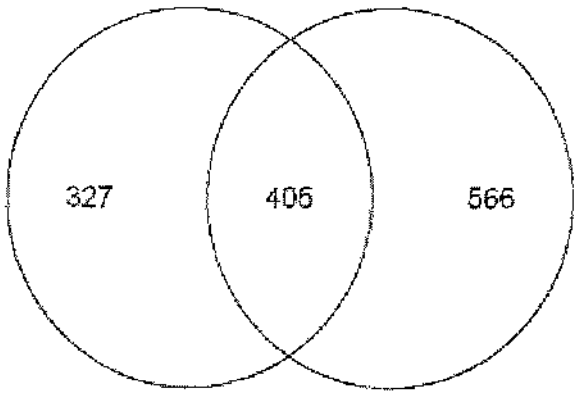

WKY (ns)
vs.
SHRSP (ns)

WKY (s)
vs.
SHRSP (s)

b)

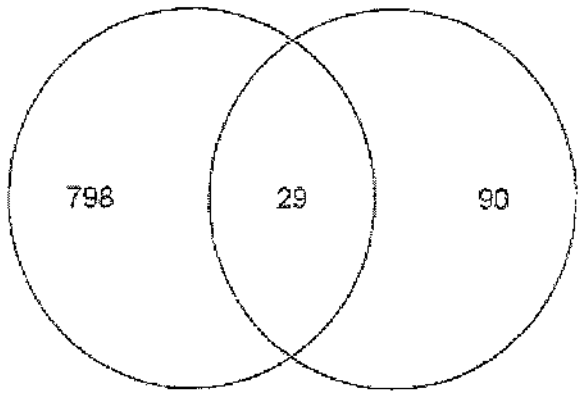

SHRSP (s)
vs.
SHRSP (ns)

WKY (s)
vs.
WKY (ns)

Figure 7.6 Venn diagrams of pairwise comparisons for 21 week salt (s) and no-salt (ns) groupings. Results shown are of 5% false discovery rate (FDR) probe sets. a) Strain comparisons - in no-salt groups, 327 genes are differentially expressed with 566 differentially expressed after salt exposure and 405 genes in common between both groupings. b) Salt comparisons - 798 genes are differentially expressed in SHRSP (s) and (ns) groups, with 90 genes differentially expressed between WKY (s) and (ns) sets and 29 genes in common between both groupings.

Table 7.1 Differentially expressed genes mapping to chromosome 14

Probe Set	Gene Symbol	†FDR	*Fold Change	Entrez Gene ID (Human)	Entrez Gene ID (Mouse)	Entrez Gene ID (Rat)
WKY (ns) vs. SHRSP (ns)						
1367555_at	ALB	0.00000	6.0005	213	11657	24186
1367816_at	HOP	0.00247	-2.4572	84525	74318	171160
1370962_at	CIPAR1	0.00569	-2.1053	25849	231440	286894
1398390_at	CXCL13	0.00588	2.3985	10563	55985	498335
1395327_at	SCARB2	0.05864	1.6057	950	12492	117106
WKY (s) vs. SHRSP (s)						
1367555_at	ALB	0.00043	6.4770	213	11657	24186
1370962_at	CIPAR1	0.00613	-2.1612	25849	231440	286894
1368379_at	SCARB2	0.03983	-1.6872	950	12492	117106
1398390_at	CXCL13	0.05188	2.3541	10563	55985	498335
SHRSP (s) vs. SHRSP (ns)						
1384985_at	CIPAR1	0.01933	2.5048	25849	231440	286894
1395327_at	SCARB2	0.03516	1.9145	950	12492	117106
WKY (s) vs. WKY (ns)						
1370830_at	EGFR	0.01899	-1.98322	1956	13649	24329

*A positive fold change indicates an increased expression and a negative fold change indicates a decreased expression, in the first sample group of the comparison shown

†A false discovery rate <0.05 is considered significant

Table 7.2 Networks identified from RP analysis for each sample group comparison

Analysis Comparison	Score	Focus Gene No.	*Highest Ranking Functions
WKY (ns) vs. SHRSP (ns)	55	34	Cardiovascular System Development and Function, Cancer, Cell Death
	55	35	Lipid Metabolism, Small Molecule Biochemistry, Carbohydrate Metabolism
	24	20	Cellular Development, Embryonic Development, Cardiovascular System Development and Function
	19	18	Cancer, Cellular Growth and Proliferation, Cell Cycle
	17	17	Tissue Morphology, Cellular Growth and Proliferation, Cellular Movement
	15	16	Lipid Metabolism, Small Molecule Biochemistry, Cardiovascular Disease
	15	16	Cell Cycle, Cell Death, Cancer
	15	16	Cell Death, Organismal Survival, Haematological Disease
	15	15	Endocrine System Disorders, Metabolic Disease, Gene Expression
	14	15	Lipid Metabolism, Molecular Transport, Small Molecule Biochemistry
	14	15	Metabolic Disease, Carbohydrate Metabolism, Lipid Metabolism
	13	13	Cell-To-Cell Signalling and Interaction, Immune Response, Immune and Lymphatic System Development and Function
	13	14	Cellular Growth and Proliferation, DNA Replication, Recombination, and Repair, Cellular Movement
	13	14	Gene Expression, Cellular Development, Behaviour
	11	13	Cell Morphology, Cell-To-Cell Signalling and Interaction, Tissue Development
	1	1	Nucleic Acid Metabolism, Small Molecule Biochemistry, Amino Acid Metabolism
	1	1	Viral Infection, Cell Death, Cell-To-Cell Signalling and Interaction
	1	1	Lipid Metabolism, Small Molecule Biochemistry, Connective Tissue Development and Function
	1	1	Cancer, Cell-To-Cell Signalling and Interaction, Cellular Assembly and Organization

Analysis Comparison	Score	Focus Gene No.	*Highest Ranking Functions
WKY (s) vs. SHRSP (s)	1	1	Cellular Assembly and Organization, Cancer, Cell Cycle
	1	1	Cancer, Neurological Disease, Tumour Morphology
	1	1	Cell Death, Cell Morphology, Cellular Development
	52	34	Cancer, Connective Tissue Disorders, Immunological Disease
	52	35	Cellular Movement, Cellular Growth and Proliferation, Cancer
	52	35	Cell Cycle, Cell Death, Cancer
	18	19	Lipid Metabolism, Small Molecule Biochemistry, Carbohydrate Metabolism
	17	17	Endocrine System Disorders, Gene Expression, Carbohydrate Metabolism
	17	17	Lipid Metabolism, Molecular Transport, Small Molecule Biochemistry
	15	17	Haematological System Development and Function, Tissue Morphology, Haematological Disease
	15	16	Cell Cycle, Cancer, Cell Death
	14	16	Cellular Growth and Proliferation, Tissue Development, Cellular Development
	14	16	Cellular Growth and Proliferation, Cellular Movement, Cell Cycle
	14	15	Cellular Growth and Proliferation, Cell Cycle, Cellular Development
	13	15	Metabolic Disease, Endocrine System Disorders, Lipid Metabolism
	13	15	Cell-To-Cell Signalling and Interaction, Haematological System Development and Function, Tissue Morphology
	13	15	Cell Morphology, Cell Death, Immune and Lymphatic System Development and Function
	13	15	Cellular Development, Connective Tissue Development and Function, Gene Expression
	13	15	Gene Expression, Cellular Growth and Proliferation, DNA Replication, Recombination, and Repair
	11	14	Immune Response, Haematological System Development and Function, Immune and Lymphatic System Development and Function

Analysis Comparison	Score	Focus Gene No.	*Highest Ranking Functions
WKY (s) vs. SHRSP (s) Cont.	11	14	Cellular Growth and Proliferation, Cellular Function and Maintenance, Cellular Movement
	1	1	Cancer, Cellular Movement, Lipid Metabolism
	1	1	RNA Post-Transcriptional Modification
	1	1	Lipid Metabolism, Small Molecule Biochemistry, Connective Tissue Development and Function
	1	1	Cellular Compromise, Renal and Urological Disease, Cell-To-Cell Signalling and Interaction
	1	1	Embryonic Development, Tissue Development
	1	0	Cell Morphology, Cellular Assembly and Organization, Genetic Disorder
SHRSP (s) vs. SHRSP (ns)	51	35	Cancer, Cell Death, Reproductive System Disease
	51	32	Cell-To-Cell Signalling and Interaction, Tissue Development, Cancer
	51	35	Cell Death, Behaviour, Nervous System Development and Function
	51	35	Cell Death, Cell-To-Cell Signalling and Interaction, Cancer
	23	22	Cellular Growth and Proliferation, Cancer, Cell Death
	19	20	Cell Cycle, Developmental Disorder, Cellular Growth and Proliferation
	15	17	Cellular Growth and Proliferation, Cancer, Haematological Disease
	14	16	Cell Death, Infectious Disease, Cell-To-Cell Signalling and Interaction
	14	16	Cellular Development, Lipid Metabolism, Molecular Transport
	12	15	Cell Cycle, Cancer, Cellular Growth and Proliferation
	12	14	Carbohydrate Metabolism, Lipid Metabolism, Small Molecule Biochemistry
	12	15	Cellular Movement, Skeletal and Muscular System Development and Function, Cancer
	12	15	Cellular Development, Cellular Growth and Proliferation, Developmental Disorder
	11	14	DNA Replication, Recombination and Repair, Cellular Growth and Proliferation
SHRSP (s) vs. SHRSP (ns)	10	13	Cancer, Cell Cycle, Cellular Development
	10	12	Cell Death, Cellular Development, Tissue Morphology

Analysis Comparison	Score	Focus Gene No.	*Highest Ranking Functions
SHRSP (s) vs. SHRSP (ns)	10	13	Cell-To-Cell Signalling and Interaction, Cancer, Cellular Growth and Proliferation
	9	12	Protein Synthesis, DNA Replication, Recombination, and Repair, Free Radical Scavenging
	1	1	Viral Infection, Cell Death, Cell-To-Cell Signalling and Interaction
	1	1	RNA Post-Transcriptional Modification
	1	1	No function assigned
	1	1	Carbohydrate Metabolism, Molecular Transport, Small Molecule Biochemistry
	1	1	Embryonic Development, Tissue Development
	1	0	Cell Morphology, Cellular Assembly and Organization, Genetic Disorder
	1	1	Cell Death, Cell Morphology, Cellular Development
WKY (s) vs. WKY (ns)	31	17	Developmental Disorder, Cellular Development, Cancer
	22	13	Cellular Movement, Haematological System Development and Function, Immune Response
	19	12	Gene Expression, Cancer, Cell Cycle
	2	1	Developmental Disorder, Genetic Disorder, Skeletal and Muscular Disorders
	2	1	Molecular Transport, Cardiovascular Disease, Genetic Disorder
	2	0	Molecular Transport, Small Molecule Biochemistry, Cardiovascular System Development and Function
	2	1	Cellular Assembly and Organization, RNA Post-Transcriptional Modification
	2	1	Gene Expression, Embryonic Development, Genetic Disorder
	2	1	Cancer, Cell-To-Cell Signalling and Interaction, Reproductive System Disease

*The three highest ranking functions for networks

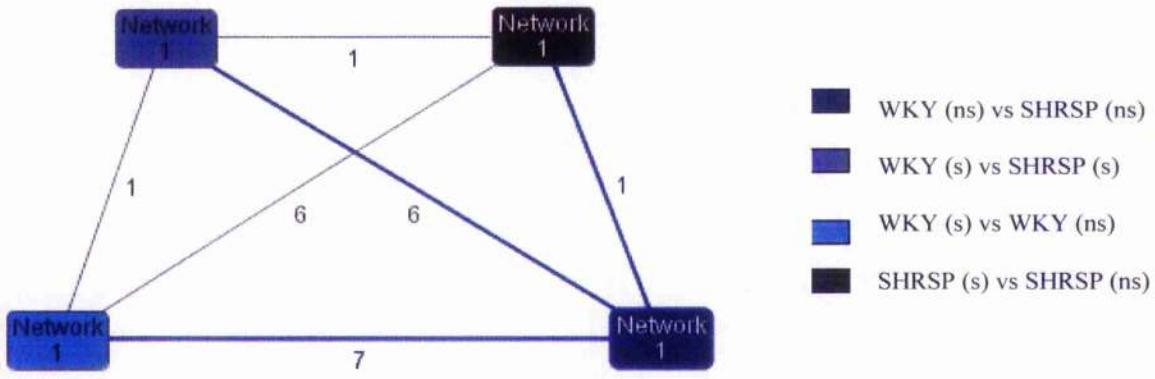

Figure 7.7 Overlapping network analyses from rank product data showing the highest ranked network for each group comparison. Each node represents one network with edges (lines) indicating a link between networks and the number of common genes shared.

Table 7.3 List of 119 genes identified from highest significant network

Name	Affymetrix	*FDR q-value	Entrez ID Human	Entrez ID Mouse	Entrez ID Rat
ACTA1	1369928_at	0	58	11459	29437
ACTA2	1370857_at	0.00127273	59	11475	81633
ACTB	AFFX_Rat_beta-actin_M_at	0.14163934	60	11461	81822
ACTC	1385797_at	0.69494658	70	11464	29275
ACTG1	1384581_at	0.92746177	71	11465	287876
ACTG2	1386869_at	0.20855856	72	11468	25365
ACTN1	1398294_at	0.25465753	87	109711	81634
ACTR2	1379687_at	0.66546157	10097	66713	289820
ACTR3	1395886_at	0.49142731	10096	74117	81732
ADAMTS1	1368223_at	0.25516418	9510	11504	79252
AK2	1386954_at	0.74862845	204	11637	24184
ALAS2	1367985_at	0.00942149	212	11656	25748
ANGPT1	1381487_at	0.54105848	284	11600	89807
ARPC1B	1386925_at	0.66031382	10095	11867	54227
ARPC2	1375137_at	0.89988413	10109	76709	301511
ATRX	1393798_at	0.01675325	546	22589	246284
BGN	1367594_at	0.19494318	633	12111	25181
CAMK2D	1371263_a_at	0.19648649	817	108058	24246
CAMK4	1375598_at	0.49061892	814	12326	25050
CAP1	1368808_at	0.73846179	10487	12331	64185
CAV1	1370131_at	0.33156109	857	12389	25404
CAV2	1370135_at	0.62566017	858	12390	363425
CDC25B	1370034_at	0.35063492	994	12531	171103
CDKN1A	1388674_at	0.38461539	1026	12575	114851
CDR2	1374139_at	0.39858543	1039	12585	308958
CEACAM1	1374620_at	0.46080819			
CHI3L1	1392171_at	0.4566302	1116	12654	89824
CLIC4	1377765_at	0.14193548	25932	29876	83718
COL18A1	1388143_at	0.32709677	80781	12822	85251
COL4A1	1372439_at	0.5695814	1282	12826	290905
COL5A1	1369955_at	0.40283862	1289	12831	85490
COL5A2	1373463_at	0.79124895	1290	12832	85250
COL5A3	1368347_at	0.9550375	50509	53867	60379
COL6A3	1396055_at	0.66516957	1293	12835	367313
COL8A2	1394748_at	0.92057272	1296	329941	313592
CSDA	1370376_a_at	1.07134191	8531	56449	83807
CSPG2	1388054_a_at	0.40215543	1462	13003	114122
CTSC	1374778_at	0.67668744	1075	13032	25423
CXADR	1374273_at	0.13636364	1525	13052	89843
CXCL12	1387655_at	0.03534091	6387	20315	24772
CYR61	1368290_at	0.25561047	3491	16007	83476
DDIT4	1368025_at	0.79391449	54541	74747	140942
DDR1	1370216_at	0.73873338	780	12305	25678

Name	Affymetrix	*FDR q-value	Entrez ID Human	Entrez ID Mouse	Entrez ID Rat
EGFR	1370830_at	0.01898701	1956	13649	24329
EGLN1	1392603_at	0.67870739	54583	112405	308913
EGR1	1368321_at	0.00474748	1958	13653	24330
EMP1	1369736_at	0.21987552	2012	13730	25314
ENO1	1367575_at	0.91049345	2023	13806	24333
ERBB3	1377821_at	0.35663778	2065	13867	29496
ERBB4	1369353_at	1.03590673	2066	13869	59323
F3	1369182_at	0.7380332	2152	14066	25584
FBLN2	1389533_at	0.75501725	2199	14115	282583
FBN1	1387351_at	0.77134371	2200	14118	83727
FGF1	1387301_at	0.1696	2246	14164	25317
FOS	1375043_at	0.00181818	2353	14281	314322
FZD2	1398304_at	0.55638298	2535	57265	64512
GART	1390787_at	1.02706078	2618	14450	288259
GATA4	1370293_at	0.54332842	2626	14463	54254
GCNT1	1368770_at	0.87343997	2650	14537	64043
GDF15	1370153_at	0.45682171	9518	23886	29455
GHR	1373803_a_at	0.54104755	2690	14600	25235
GJA1	1369640_at	0.02844697	2697	14609	24392
GSN	1371414_at	1.04079017	2934	227753	296654
HBP1	1368549_at	0.95428331	26959	73389	27080
HES1	1387036_at	1.02397237	3280	15205	29577
HES5	1375713_at	0.49213321	388585	15208	79225
HEY2	1384515_at	0.8891105	23493	15214	155430
HLA-DMB	1382788_at	0.96416454	3109	14999|15000	294273
HLA-DQA1	1370822_at	0.75113789	3117	14960	309621
HLA-DQB1	1371033_at	0.17670886	3119	14961	309622
HLA-DRB1	1370383_s_at	0.36174168	3123	14969	294270
HSPA1B	1368247_at	0.4926899	3304	15511	24472
IDI1	1368878_at	0.48716636	3422	319554	89784
IER3	1388587_at	0.443213	8870	15937	294235
IL13	1369618_at	1.02719088	3596	16163	116553
IL2RB	1387394_at	0.96190977	3560	16185	25746
JAG1	1368725_at	0.88236255	182	16449	29146
JUN	1369788_s_at	0.04929619	3725	16476	24516
KLF2	1386041_a_at	0.52783094	10365	16598	306330
KLF6	1387060_at	0.82655139	1316	23849	58954
LAMA5	1396159_at	0.66575298	3911	16776	140433
LAMC2	1379889_at	0.70679985	3918	16782	192362
LOXL1	1388902_at	0.66940386	4016	16949	315714
LOXL2	1391450_at	0.74439365	4017	94352	290350
MAF	1392566_at	0.02945076	4094	17132	54267
MMP14	1378225_at	0.80846134	4323	17387	81707
MT1A	1371237_a_at	0.50195251	4489	17748	24567
MYC	1368308_at	1.01916269	4609	17869	24577
MYCN	1376648_at	0.62007361	4613	18109	298894
MYH6	1393540_at	0.04861601	4624	17888	29556

Name	Affymetrix	*FDR q-value	Entrez ID Human	Entrez ID Mouse	Entrez ID Rat
MYH7	1392401_s_at	0.00490909	4625	140781	29557
MYH9	1387402_at	0.24830389	4627	17886	25745
NOV	1376734_at	0	4856	18133	81526
P4HA1	1370954_at	0.73718992	5033	18451	64475
PDLIM7	1370347_at	0.62469722	9260	67399	286908
PLS3	1371139_at	0.95615059	5358	102866	81748
RBM3	1371583_at	0.81596344	5935	19652	114488
RBP1	1367939_at	1.06364791	5947	19659	25056
RTN4	1388027_a_at	0.05511831	57142	68585	83765
S100A6	1367661_at	1.03470305	6277	20200	85247
S100B	1386903_at	0.17585635	6285	20203	25742
SCD2	1367668_a_at	0.90184156		20250	83792
SERPINE1	1392264_s_at	0.59016255	5054	18787	24617
SERPINE2	1372440_at	0.38010638	5270	20720	29366
SLC16A6	1376267_at	0.00488636	9120	104681	303772
SRF			6722	20807	445445
STAT3	1370224_at	0.04814229	6774	20848	25125
SYCP3	1376785_at	0.84487931	50511	20962	25561
TFRC	1371113_a_at	0.26249169	7037	22042	64678
TGFB1	1370082_at	0.103	7040	21803	59086
TGM2	1387776_at	0.17464052	7052	21817	56083
TIMP1	1367712_at	0.44976109	7076	21857	116510
TNFRSF12A	1371785_at	0.45662597	51330	27279	302965
TPM1	1379936_at	0.01916667	7168	22003	24851
TPM3	1398303_s_at	0.40008955	7170	59069	117557
TPM4	1368838_at	1.04469602	7171	326618	24852
UBE2V2	1372143_at	0.91174146	7336	70620	287927
WBSCR1	1397675_at	0.2138326	7458	22384	288599
YY1	1398564_at	0.01796791	7528	22632	24919

*FDR signifies false discovery rate. Genes highlighted in grey, indicate shared between networks and empty cells represent no equivalent data.

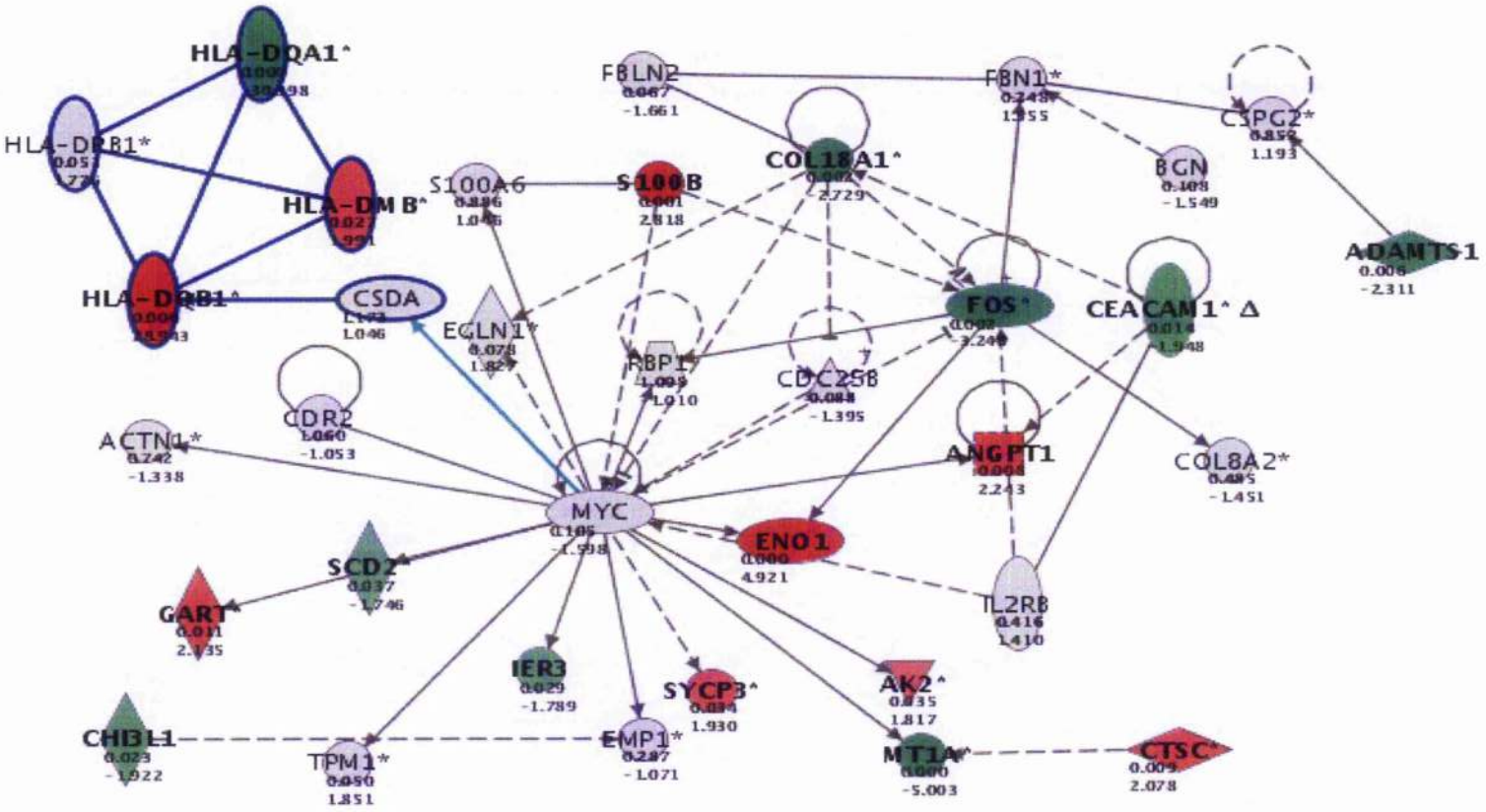

Figure 7.8a V-myc myelocytomatosis viral oncogene homolog (MYC) network pathway. Overlay sample group is WKY (ns) vs. SHRSP (ns). The FDR value is given as the top number, with the fold change indicated below based on the first sample group versus the second sample group. Red colour denotes increased gene expression, green decreased gene expression and grey no change. An asterisk signifies more than one probe set for this gene was included in analysis. For a full diagram key refer to section 7.2.4, Figure 7.2).

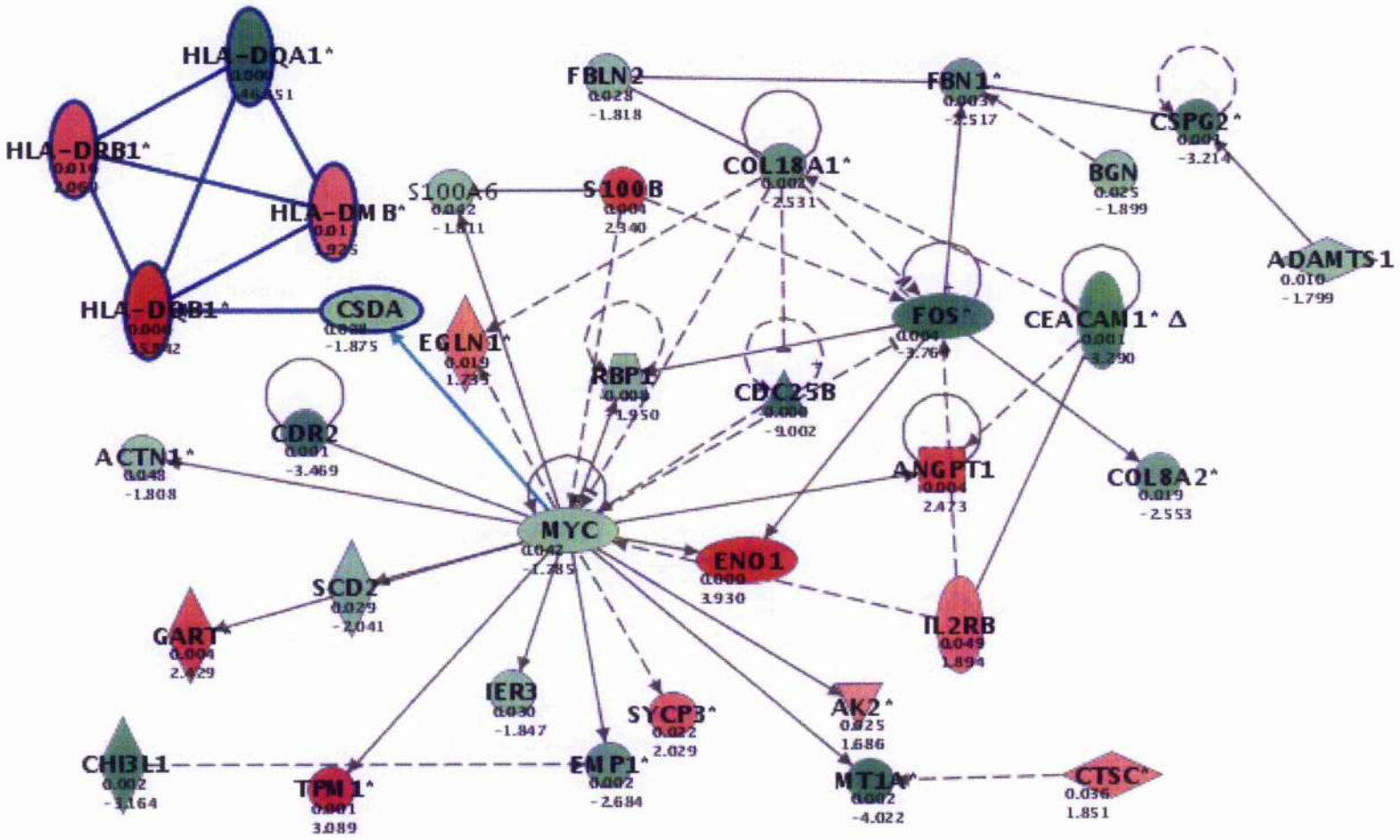

Figure 7.8 b V-myc myelocytomatosis viral oncogene homolog (MYC) network pathway. Overlay sample group comparison is WKY (s) vs. SHRSP (s), highest scoring network =52, focus genes = 34

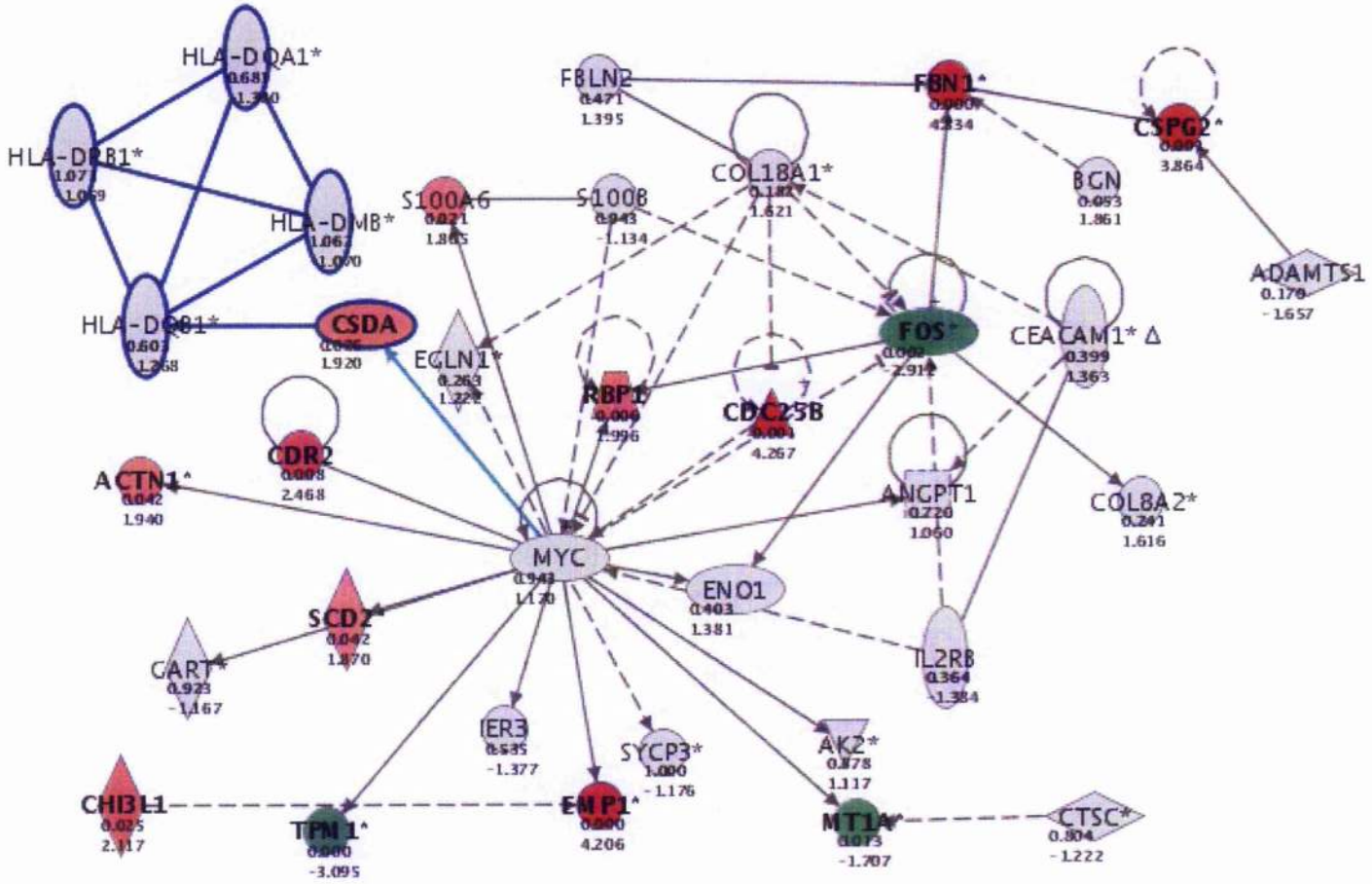

Figure 7.8c V-myc myelocytomatosis viral oncogene homolog (MYC) network pathway. Overlay sample group comparison is SHRSP (s) vs. SHRSP ns).

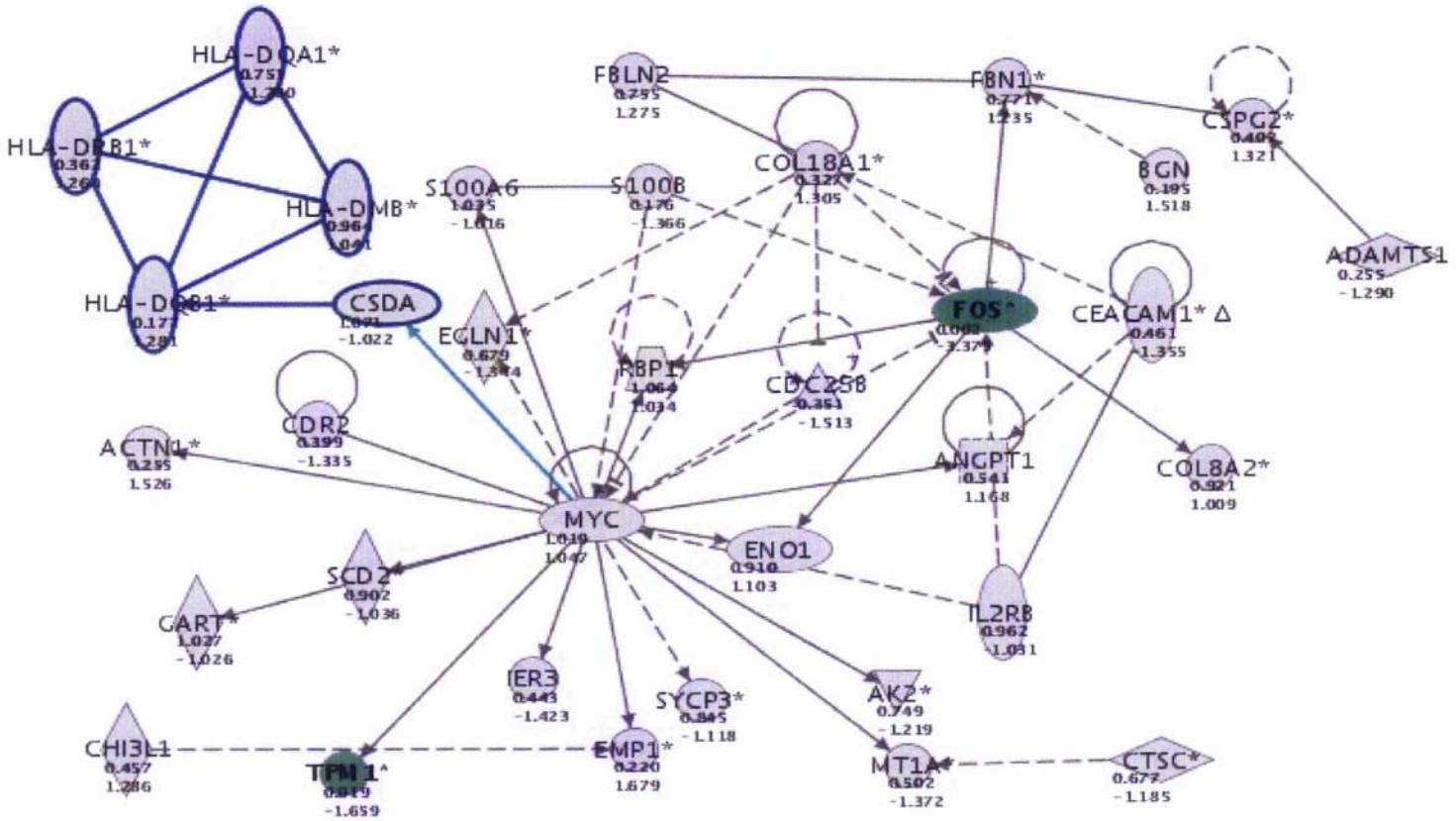

Figure 7.8d V-myc myelocytomatosis viral oncogene homolog (MYC) network pathway. Overlay sample group comparison is WKY (s) vs. WKY (ns).

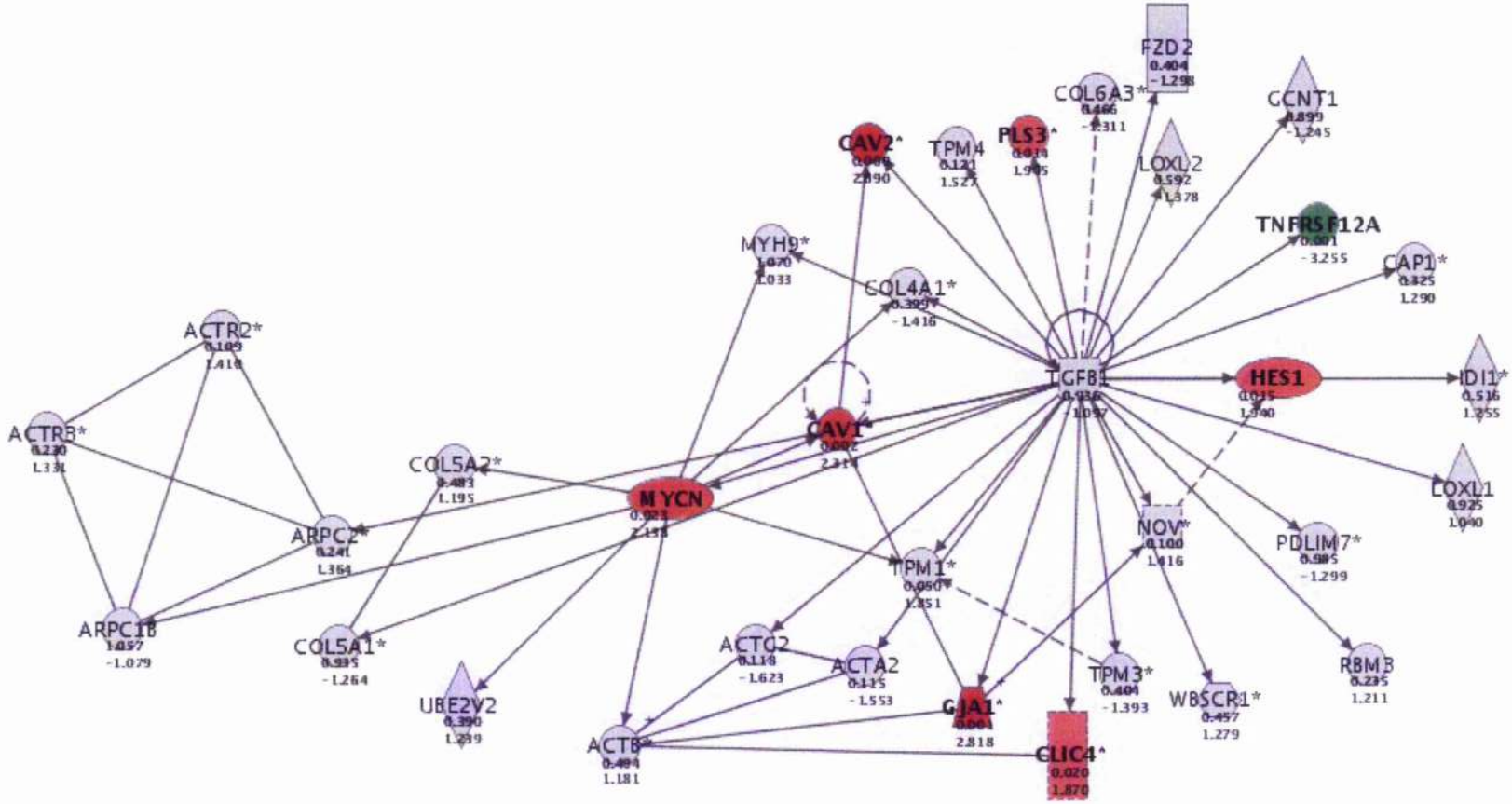

Figure 7.9a Transforming growth factor β1 network pathway. Overlay sample group comparison is WKY (ns) vs. SHRSP (ns).

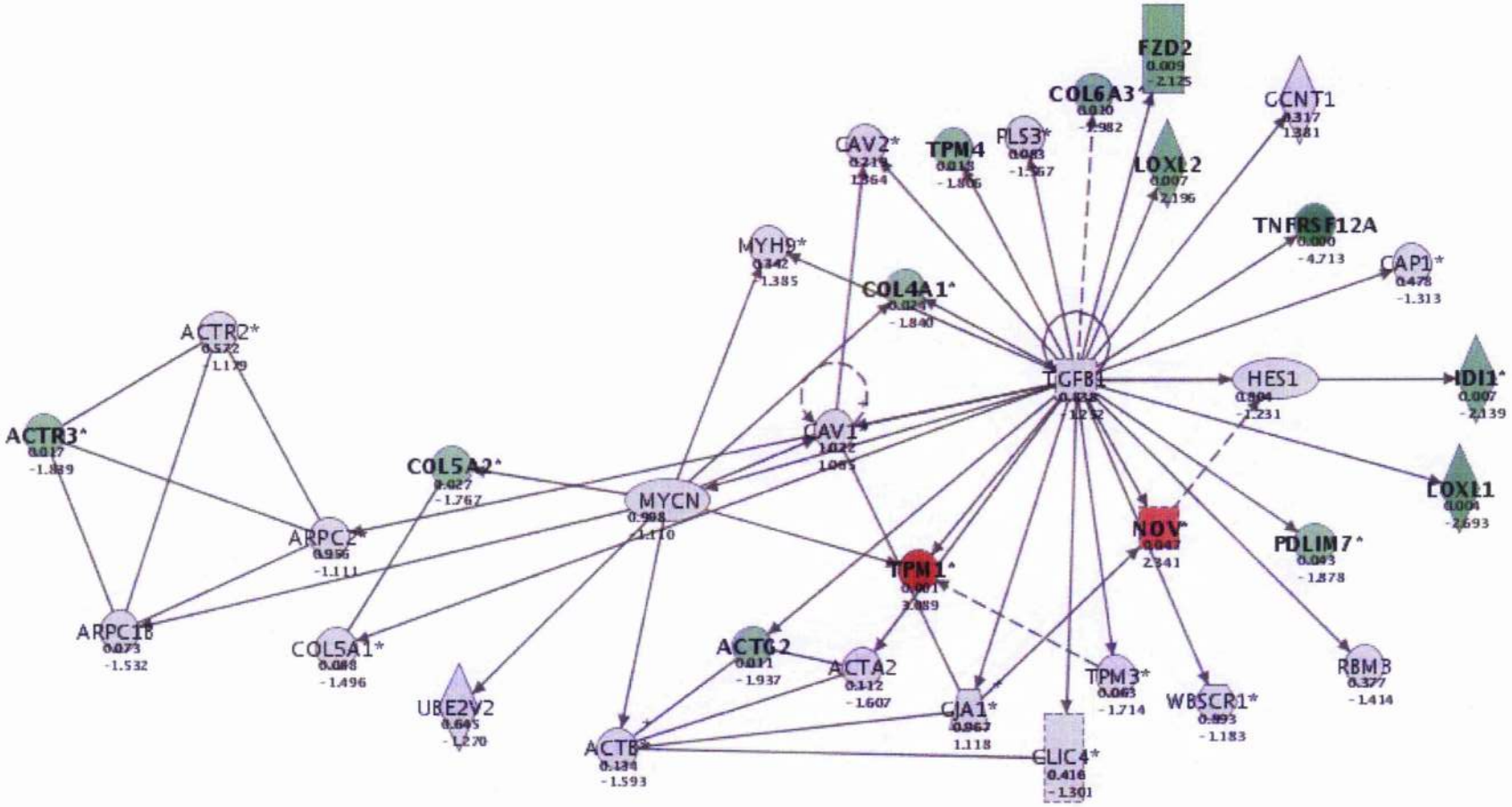

Figure 7.9b Transforming growth factor β1 network pathway. Overlay sample group comparison is WKY (s) vs. SHRSP (s).

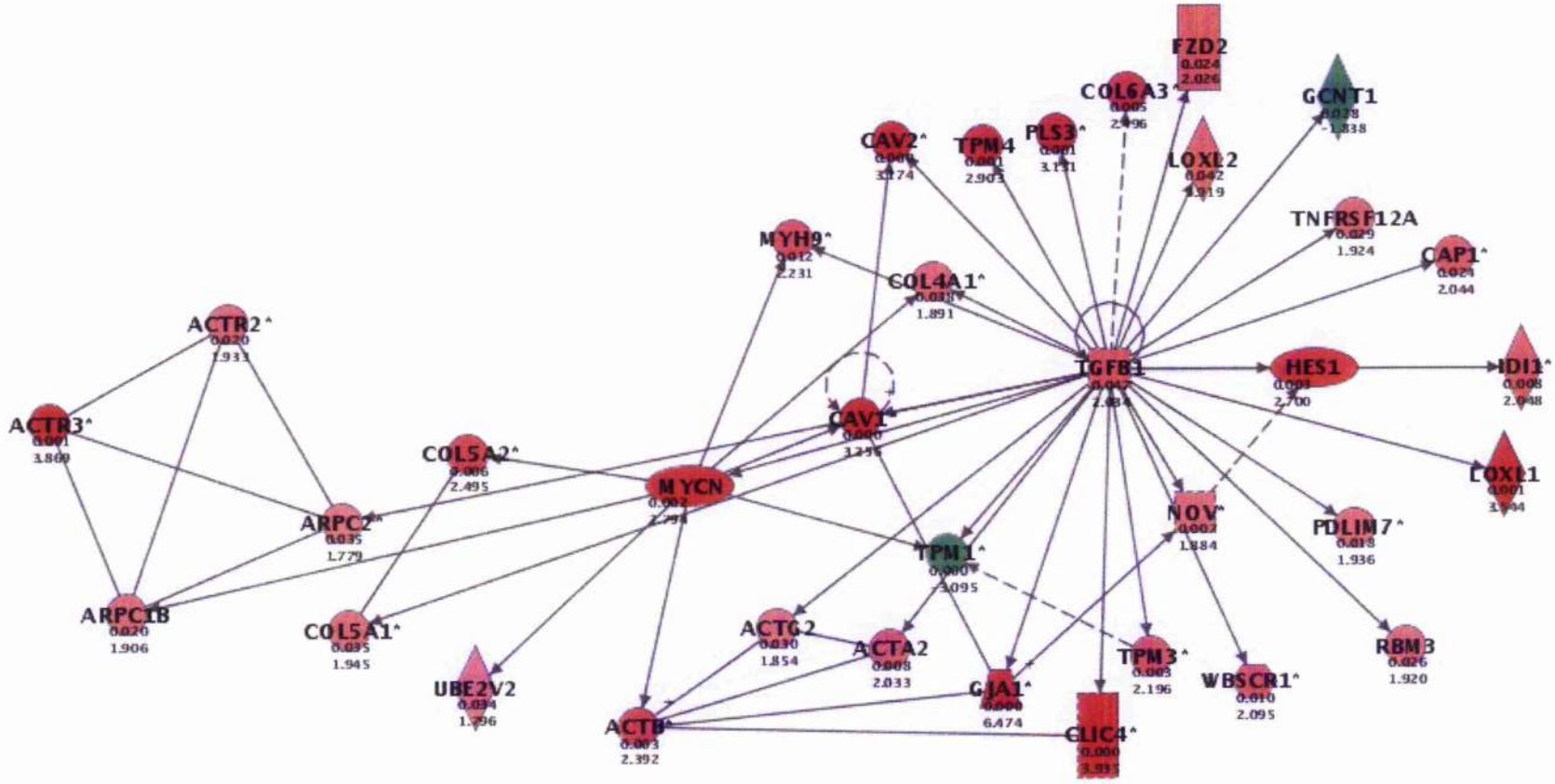

Figure 7.9c Transforming growth factor β 1 network pathway. Overlay sample group comparison is SHRSP (s) vs. SHRSP (ns), highest scoring network = 51, focus genes = 35.

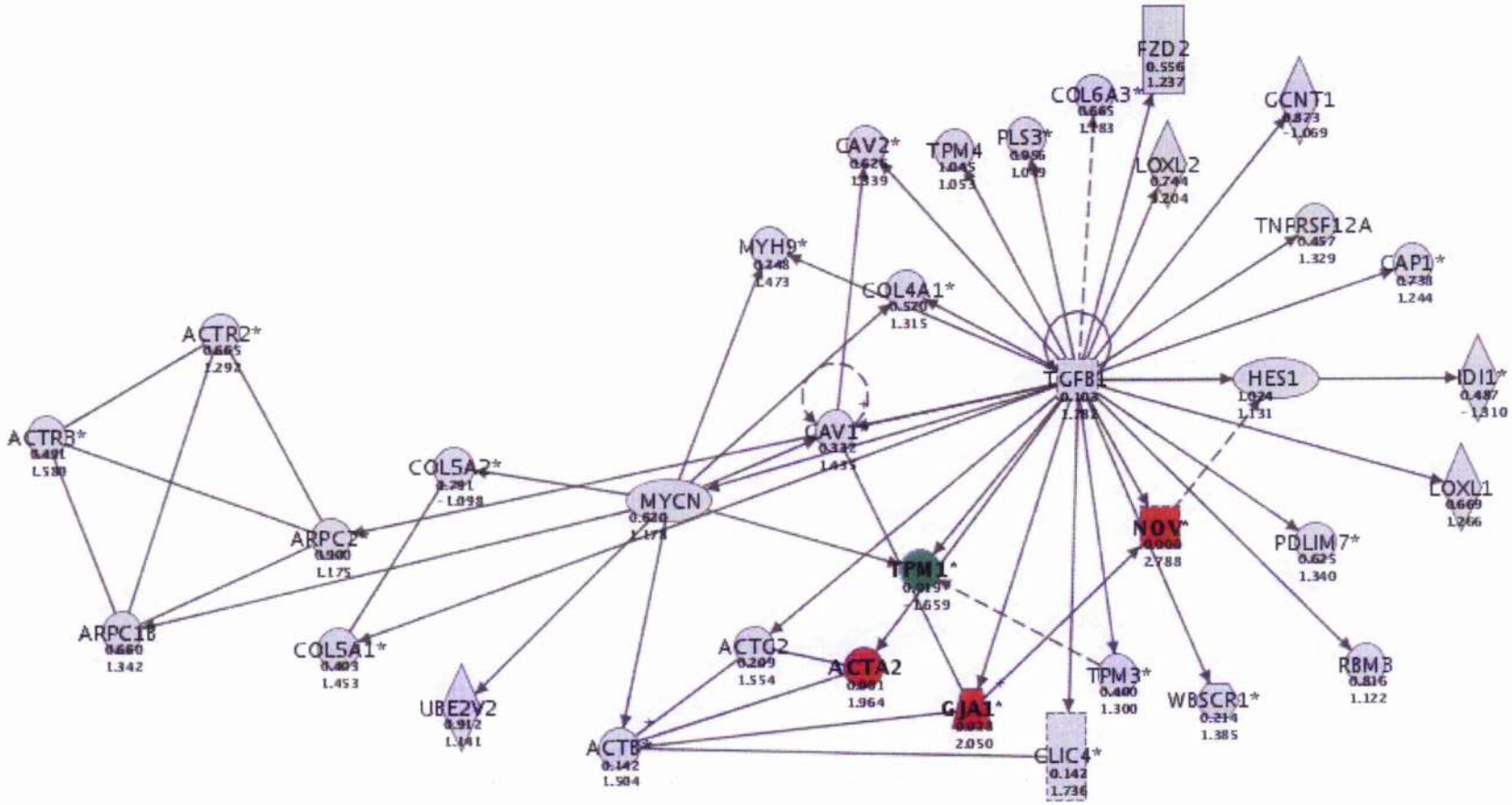

Figure 7.9d Transforming growth factor β 1 network pathway. Overlay sample group comparison is WKY (s) vs. WKY (ns).

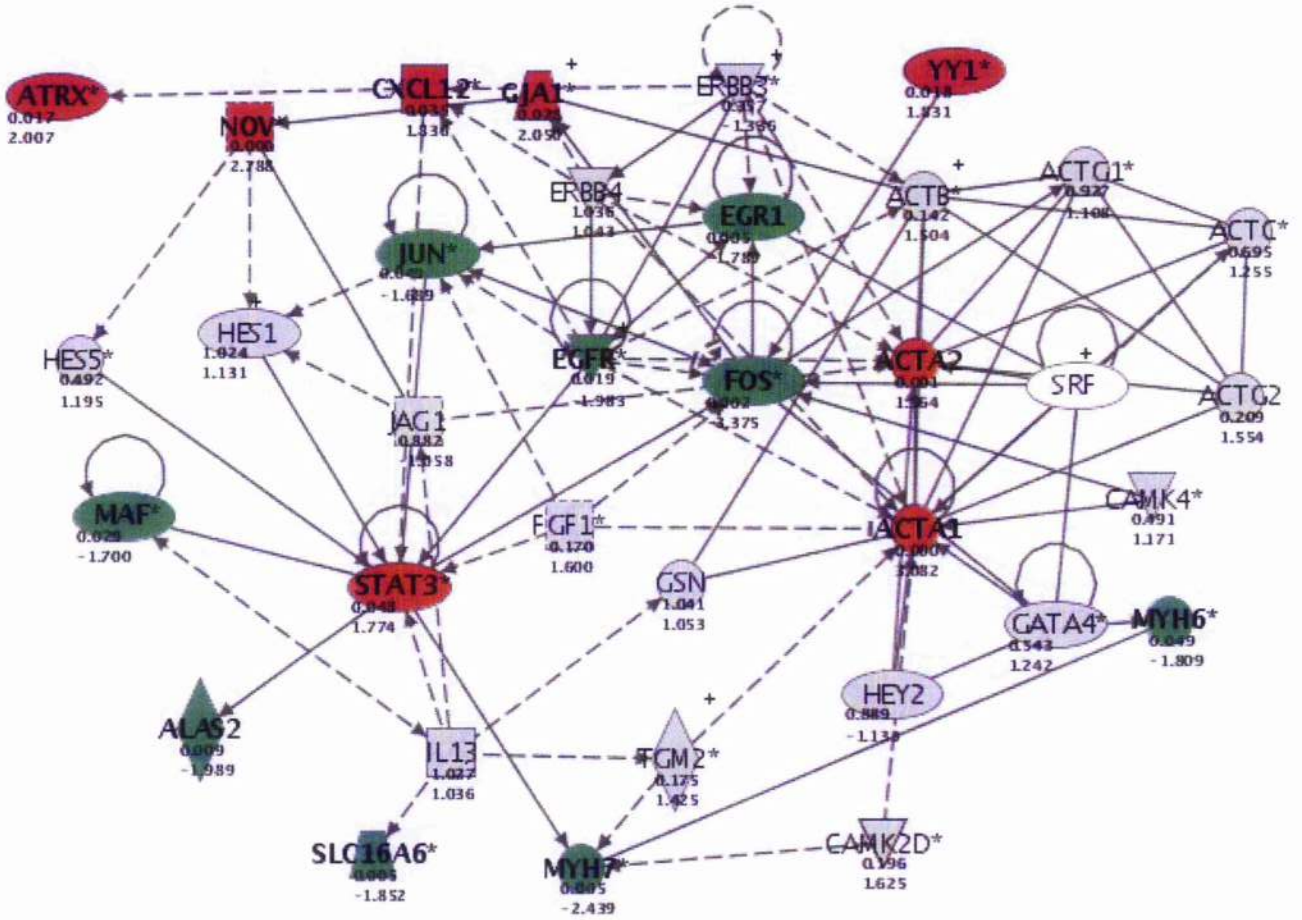

Figure 7.10a V-fos murine osteosarcoma viral oncogene homolog (FOS). Overlay sample group is WKY (ns) vs. SHRSP (ns).

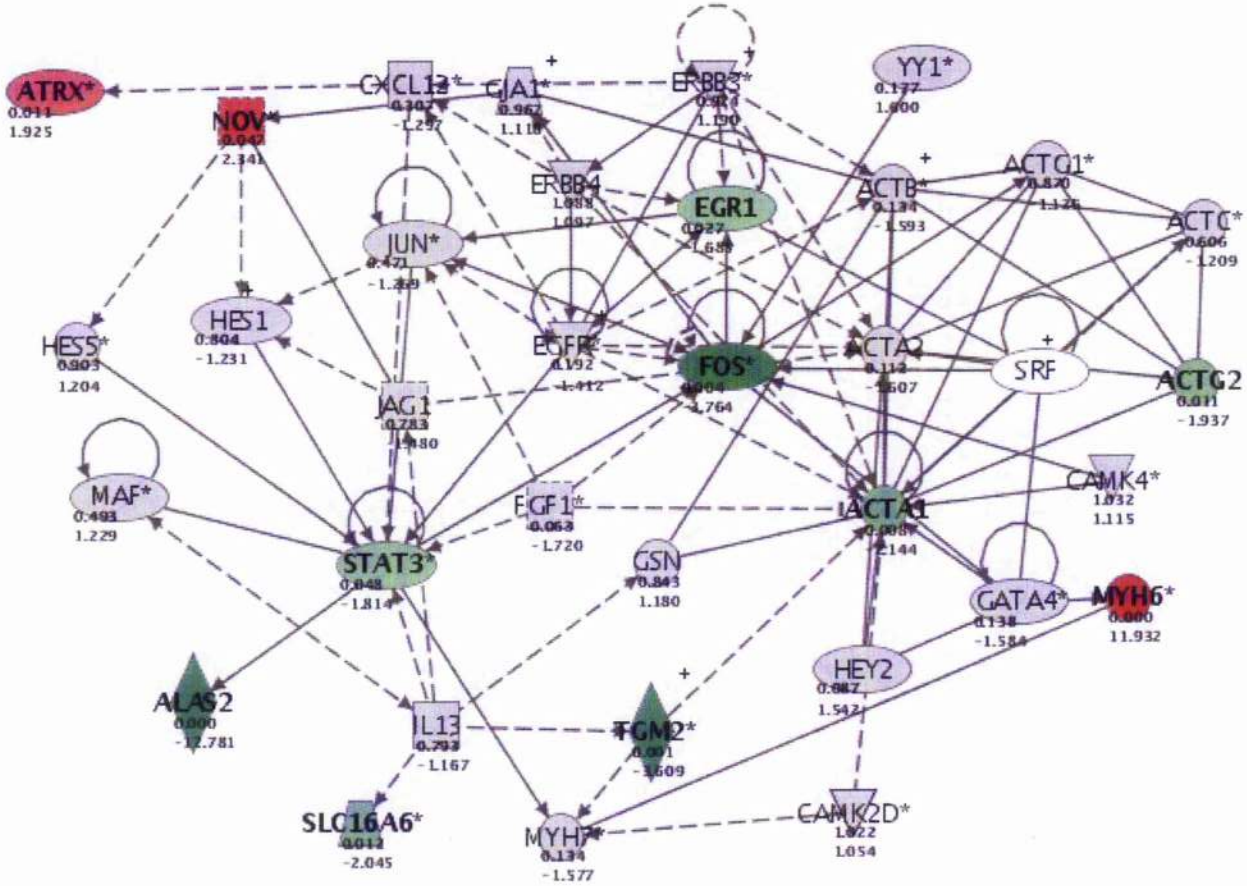

Figure 7.10b V-fos murine osteosarcoma viral oncogene homolog (FOS). Overlay sample group comparison is WKY (s) vs. SHRSP (s).

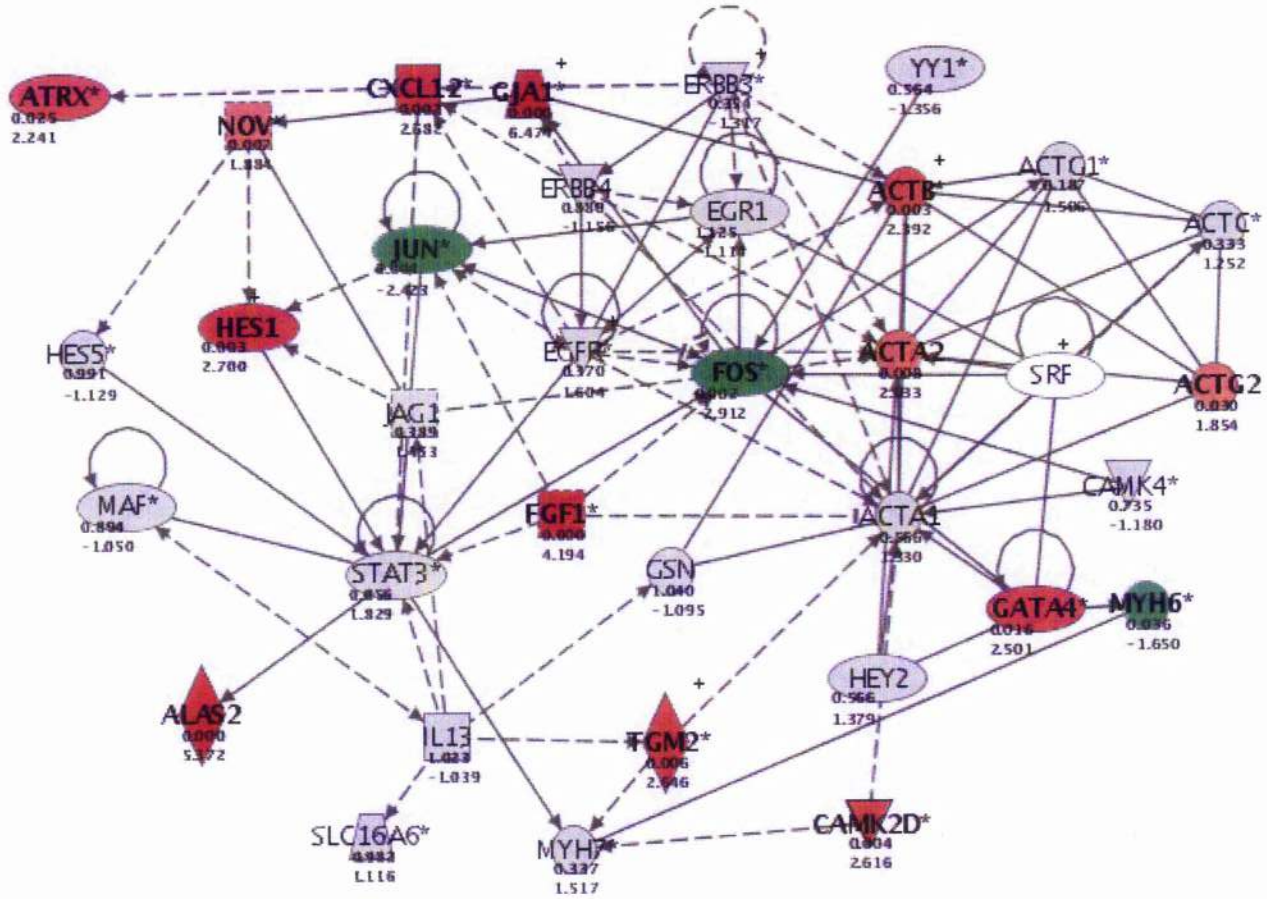

Figure 7.10c V-fos murine osteosarcoma viral oncogene homolog (FOS). Overlay sample group comparison is SHRSP (s) vs. SHRSP (ns).

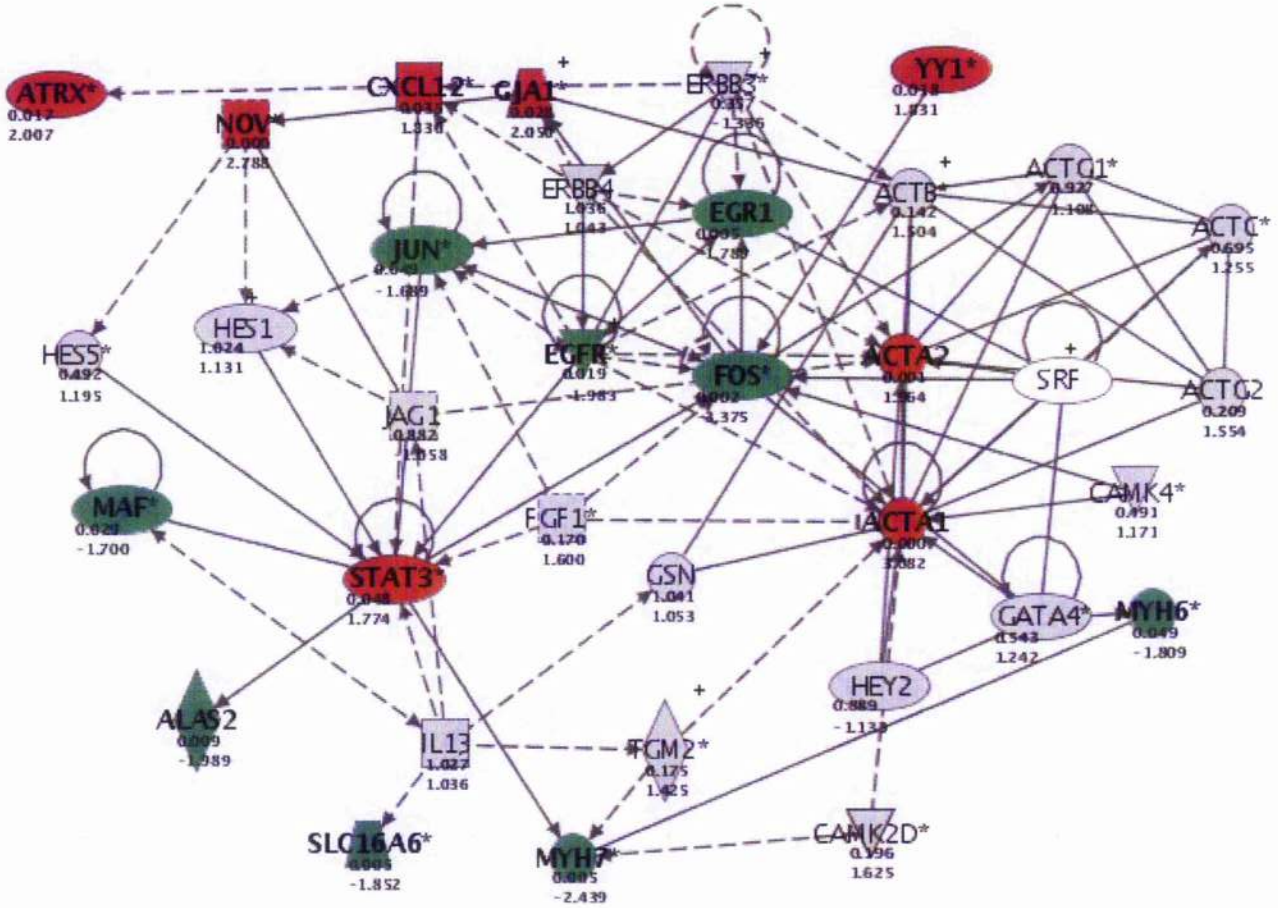

Figure 7.10d V-fos murine osteosarcoma viral oncogene homolog (FOS). Overlay sample group comparison is WKY (s) vs. WKY (ns), highest scoring network = 31, focus genes = 17.

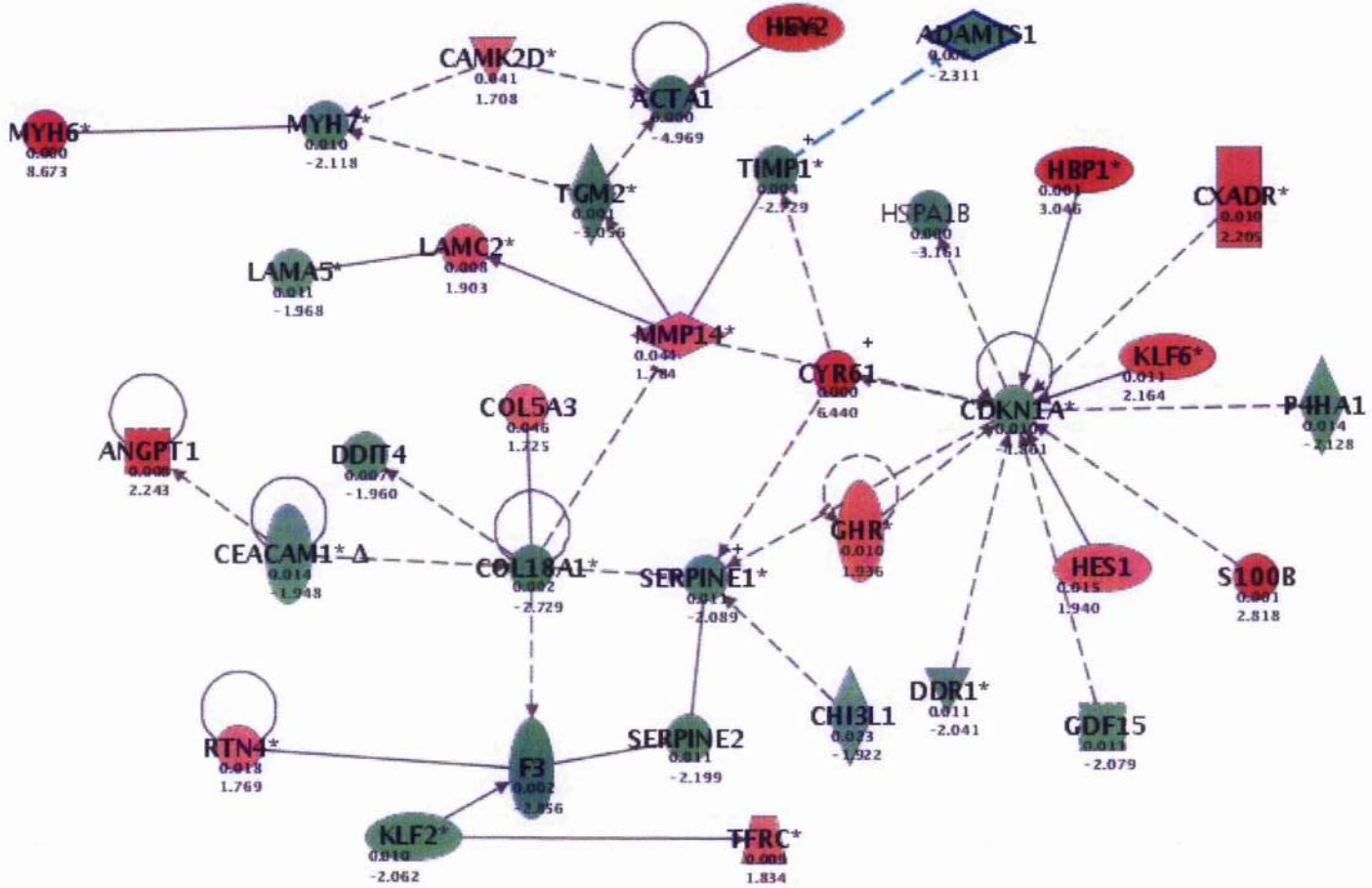

Figure 7.11a Cyclin dependant kinase inhibitor 1A (CDKN1A). Overlay sample group comparison is WKY (ns) vs. SHRSP (ns), highest scoring network = 55, focus genes = 34.

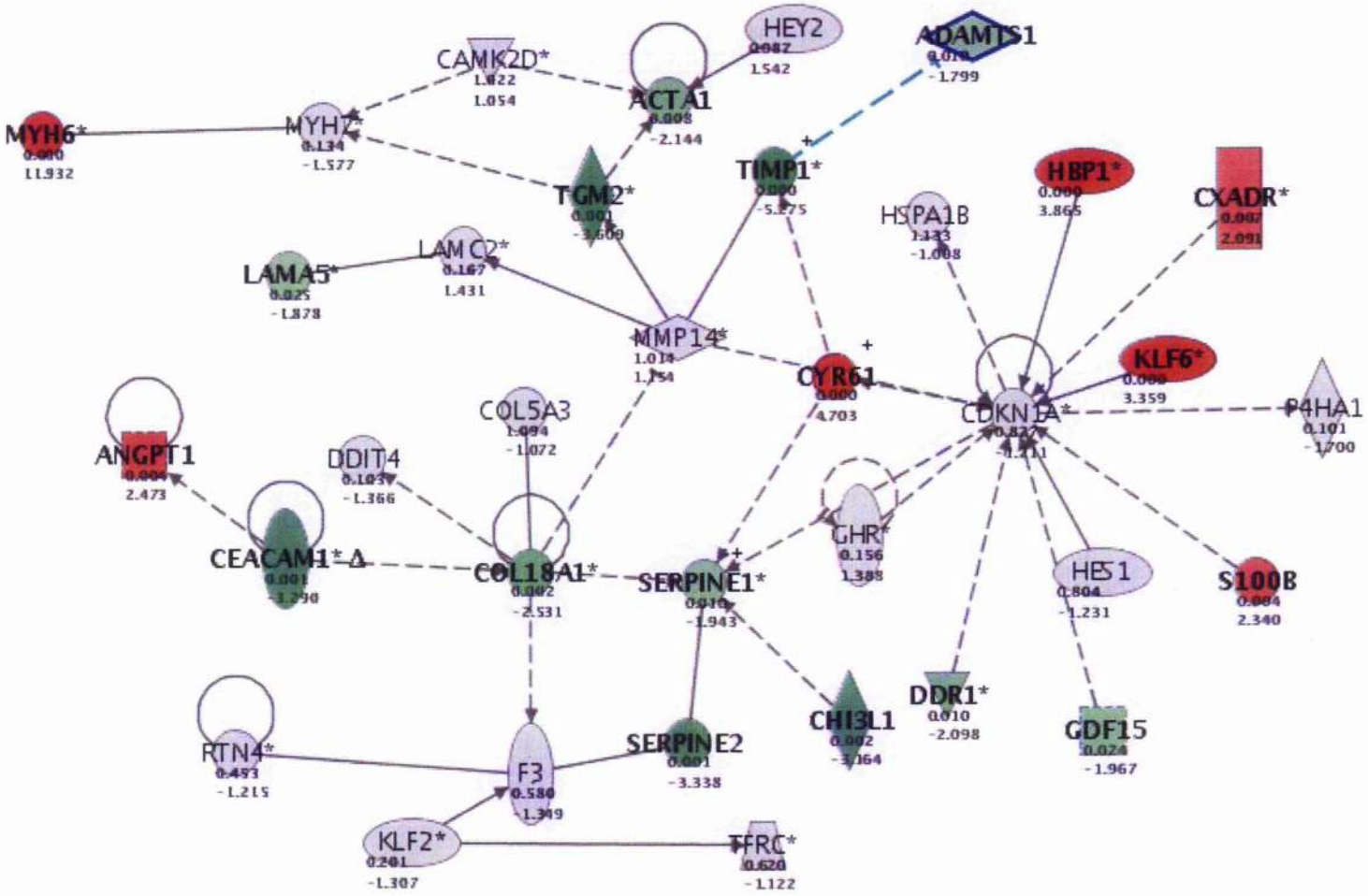

Figure 7.11b Cyclin dependant kinase inhibitor 1° (CDKN1A). Overlay sample group comparison is WKY (s) vs. SHRSP (s).

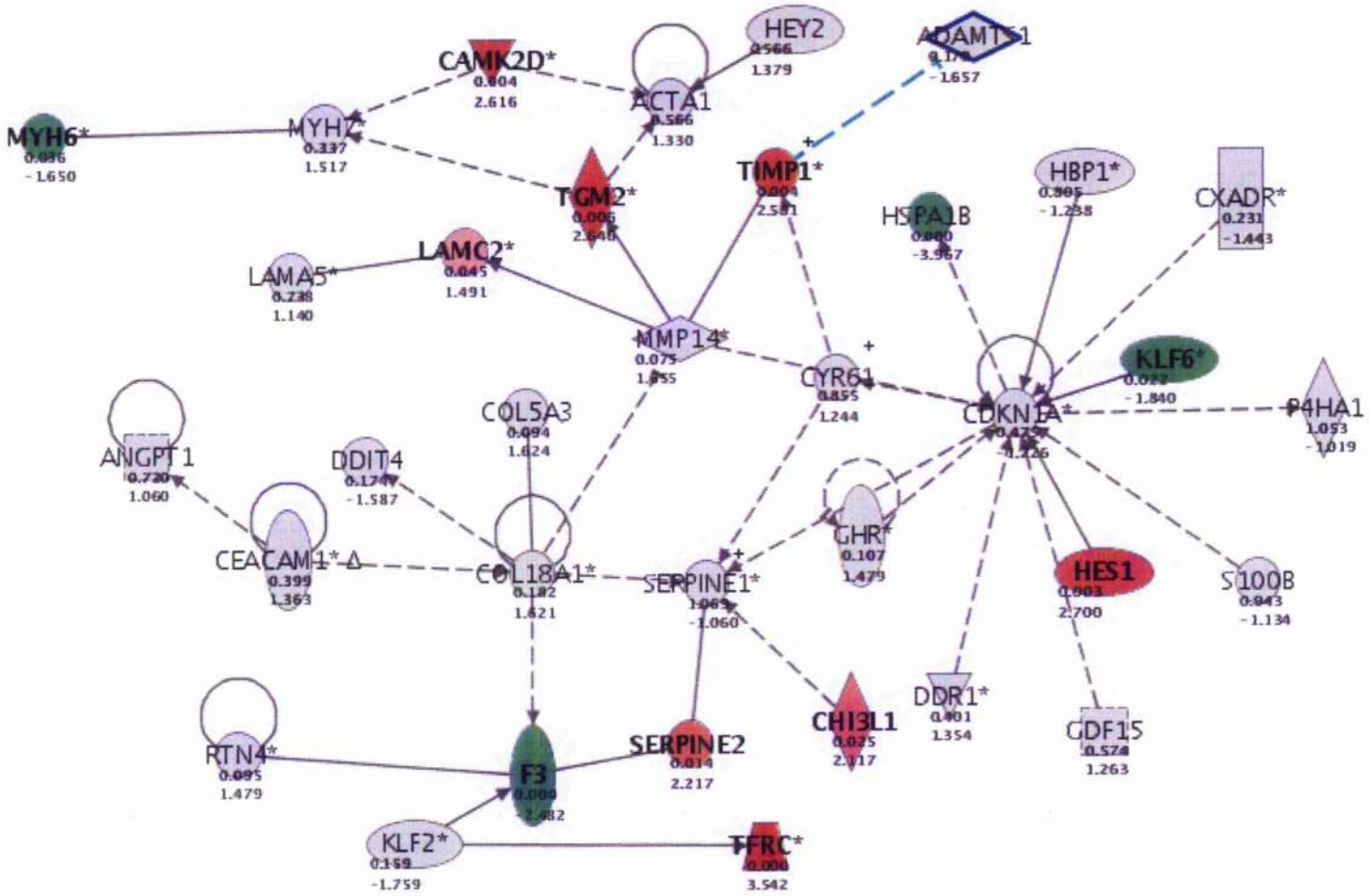

Figure 7.11c Cyclin dependant kinase inhibitor 1° (CDKN1A). Overlay sample group comparison is SHRSP (s) vs. SHRSP (ns).

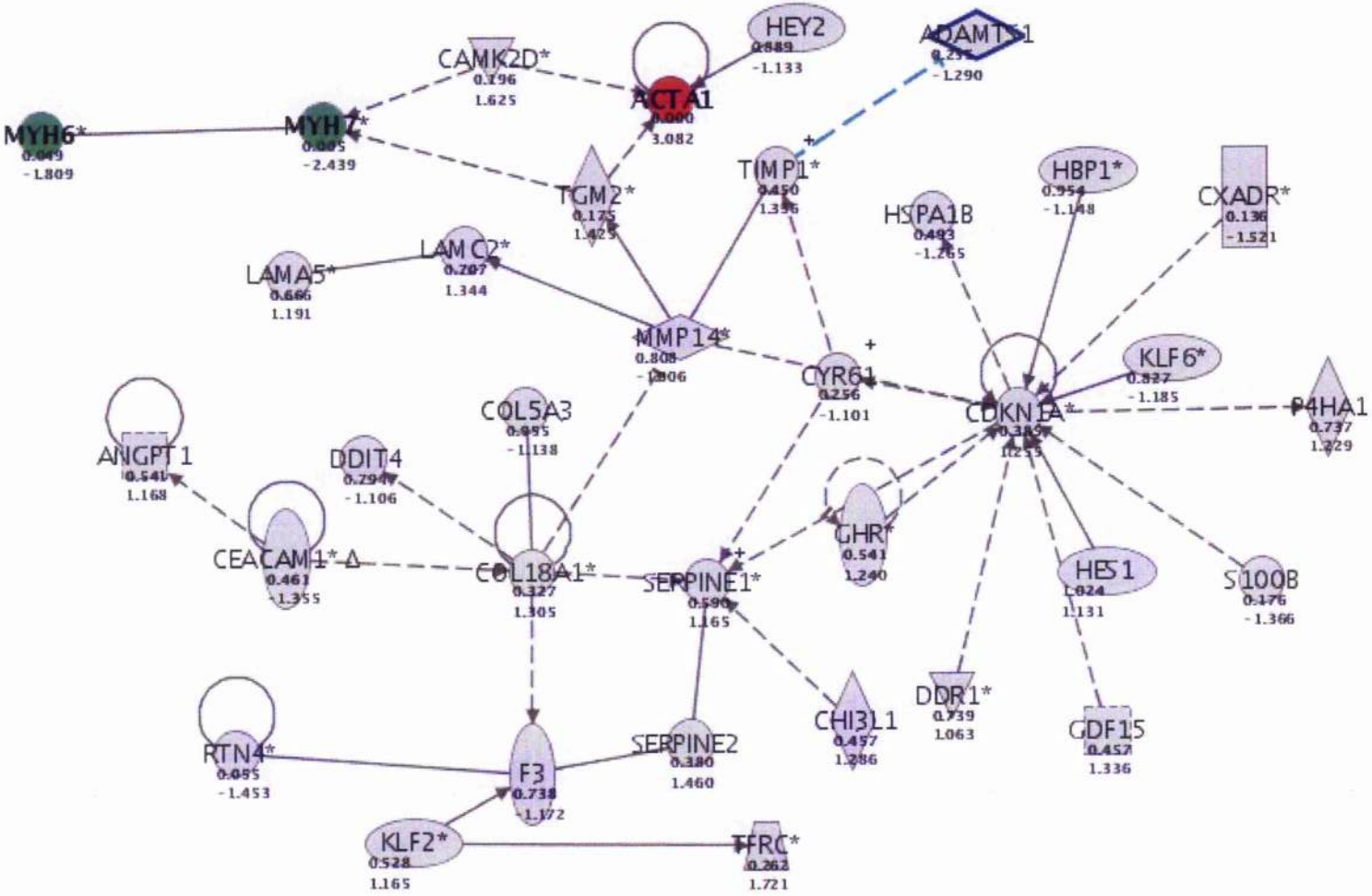

Figure 7.11d Cyclin dependant kinase inhibitor 1A (CDKN1A). Overlay sample group comparison is WKY (s) vs. WKY (ns).

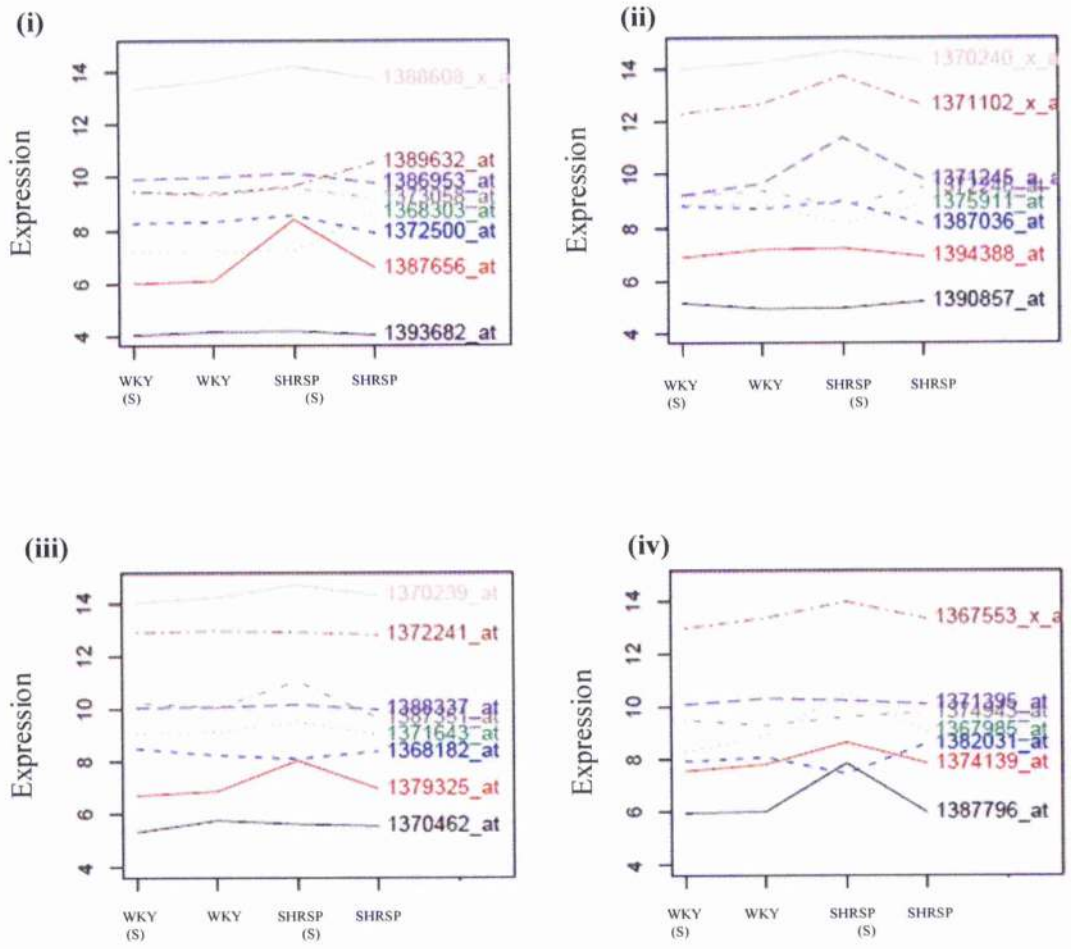

Figure 7.12 Representation of two-way ANOVA results for strain-salt interaction. Thirty one probe sets were initially identified as significantly for an interaction event and plotted to illustrate fold changes between groups. Multiple represented probe sets were removed from the list. A probe set plot displaying a straight line i.e. the overall fold change was close to ±1, was removed. An example of this can be seen in panel (iii) probe set 1372241_at and probe set 1388337_at, with a fold change across all groups of 1.09 and -1.002 respectively, reflecting very little differential expression between the groups. In panel (iv) probe set 1387796_at shows no change in WKY expression after salt manipulation, but shows a large increase after salt exposure in SHRSP, indicated by the upturned incline for SHRSP (s).

Table 7.4 Two-way ANOVA strain-salt interaction

Probe Set ID	Gene Symbol	Chromosome Location	UniGene ID	Entrez Gene ID	P - value
1367553_x_at	Hbb*	1q22	36966	24440	0.007
1367985_at	Alas2*	Xq21	32517	25748	0.03
1368182_at	Acsl6	10q22	33697	117243	0.01
1368303_at	Per2*	9q36	25935	63840	0.01
1370462_at	Hmmr	10q12	92304	25460	0.01
1371643_at	Ccnd1*	1q42	22279	58919	0.01
1372248_at	Sesn1	20q13	22395	294518	0.01
1372500_at	Tmod3*	8q24	146101	300838	0.03
1373058_at	Tmem30a	8q31	161918	300857	0.01
1374139_at	Cdr2*	1q35-q36	3537	308958	0.02
1375911_at	RGD735140	3q36	11612	362219	0.01
1386953_at	Hsd11b1	13q27	888	25116	0.03
1387036_at	Hes1	11q22	19727	29577	0.01
1387351_at	Fbn1*	3q36	12759	83727	0.02
1387656_at	Slc4a1	10q32	32202	24779	0.02
1387796_at	Alox15	10q24	11318	81639	0.01
1388608_x_at	Hba-a1	10q12	107334	25632	0.02

*Genes mapping to cited heart weight QTL regions

7.4 DISCUSSION

The use of microarray gene expression profiling in whole heart tissue of age matched animals with and without dietary salt manipulation, was used successfully to gain some insight into the identity and expression levels of cardiac genes associated with an adaptive response to hypertension (in the absence of environmental stimuli) and salt intake (in the presence and absence of hypertension). In addition, two contrasting analytical methods were used to assess normalised data and produce gene pathways of potential interest for individual strains and interactions between genotype-environmental stimuli.

An interesting result from the phenotype data of SHRSP and WKY before and after 1% salt intake is increased CMI and LVMI in both strains after salt, despite no parallel increase in SBP. This finding lends credence to the hypothesis that blood pressure independent gene(s) may interact with environmental factors to influence cardiac weight. However, it's also important to note that SBP was measured by tail cuff plethysmography, which although a validated method is not as accurate or consistent for data acquisition of blood pressure as radiotelemetry.

From the list of positional genes of interest identified on chromosome 14, *Egfr* forms part of the most significant network pathway for group WKY (s) vs. WKY (ns). Growth factor regulation and signaling affects tissue remodelling through autocrine/paracrine mechanisms (Lauffenburger *et al.*, 1998) and is central to myocardial extracellular matrix homeostasis (Mauviel, 1993). Several groups have shown that *Egfr* receptor transactivation by heparin-binding EGF (HB-EGF) is a primary factor in hypertrophic cardiomyocyte signaling and cell co-ordinated remodelling within the myocardium (Yoshioka *et al.*, 2005).

Tgfβ1 was identified as the most significant network pathway in group SHRSP (s) vs. SHRSP (ns). *Tgfβ1* is induced by injury and is normally involved in repair however excessive or prolonged signaling of this pathway has been shown as a factor in pathologic fibrosis, scarring and matrix deposition in a variety of diseases, including cardiac hypertrophy (Ju & Dixon, 1996, Lim *et al.*, 2005). In this network pathway, gene

expression is increased in SHRSP (s) compared to SHRSP (ns) in all genes with the exception of germ cell nuclear antigen (*Gcna1*; a marker of steroidogenic cells) and *Tpm1α*.

From RP network analysis, *Tpm1α* was identified as interacting between salt and strain. There are currently eight reported missense mutations in *Tpm1α*, associated with varying degrees of FHC (Thierfelder *et al.*, 1994; Jongbloed *et al.*, 2003). In this study, *Tpm1α* is upregulated in WKY (s) vs. SHRSP (s) and down regulated in SHRSP (s) vs. SHRSP (ns), indicating salt is an important regulatory control factor. Prabhakar *et al.* (2001) developed transgenic mouse lines encoding a FHC mutation in *Tpm1α*, in a troponin T binding region. They showed expression of mutant tropomyosin leads to a parallel decrease in endogenous *Tpm1α*, without altering expression of other contractile proteins. Observed disease-associated changes, in particular functional differences in diastolic performance and increased sensitivity to calcium, were detected within 1 month, resulting in death within 5 months. This report demonstrates the importance of *Tpm1α* gene expression and sarcomeric function, consequently resulting in a hypertrophic response.

Genes identified from both RP and two-way ANOVA analyses as interacting between strain and salt, were *Fbn1, Alas2 and Hes1*. Known mutations in *Alas2* isoforms involved in catalysing the first and rate-limiting step in the haeme synthesis pathway, lead to ineffective erythropoiesis and typify X-linked sideroblastic anemia (Fontenay *et al.*, 2006). *Fbn1* mutations are associated with Marfan syndrome, an autosomal dominant connective tissue disorder characterized by pleiotropic characteristics involving the skeletal, ocular, and cardiovascular systems (Coucke *et al.*, 2006). More recently, mutations in *Tgfβ1* (which acts directly to control transcription factor *Hes1*) has been described as an important factor relating to Marfan syndrome in *Fbn1* negative patients (Disabella *et al.*, 2006), adding further weight that overlapping network analysis of RP, although Fnot designed to identify interacting genes, is an important tool for studying large datasets.

There are numerous factors to consider prior to a genome wide expression study - probe selection (including high hybridization stringency and low susceptibility to gene

polymorphisms), study design and data analysis (Watson A., Mazumder, Stewart & Balasubramanian, 1998; Privalis, 2003). Ambiguity regarding probe sets from both types of microarray platforms, united with their respective and well documented experimental noise, such as compression of gene expression ratios (Yuen *et al.*, 2002) requires a cautious approach to data analysis and interpretation, therefore the application of more than one statistical approach may be useful. This microarray experiment was carried out in animals with an established pathology, making it difficult to distinguish between primary target and secondary target effects from direct and/or indirect association of pathways, using RP analysis only. The processes governing any observed changes in gene expression may be a cardiac hypertrophic adaptive response to pressure overload in the SHRSP or alternatively a protective reaction to salt stimuli in the normotensive WKY. For this reason the addition of a more complex analytical approach was desirable.

Increasing the level of stringency in any study introduces a potential for failure to spot genes of interest, due to variation observed within groups. An example of this is the number of interactions identified from manual breakdown of RP data using Ingenuity Pathway Analysis but missed by two-way ANOVA for example Tpm1α. A further complication of using a more complex analytical method in small sample groups is the number of false positive results identified as significant. An illustration of this, are probe sets identified as interacting yet showing little differential expression between groups (a flat line when plotted relative to other data groups). In conclusion, a genome wide expression stratagem is a powerful tool for investigating genotype in conjunction with a phenotype of interest and provides a basis for identification of genes and pathways which may be stimulated and/or suppressed by environmental stimuli. This work can be systematically followed up by confirmation of genes identified, functional analysis of significant genes/pathways identified and the inclusion of a congenic strain to localise region/genes of interest to current study.

CHAPTER 8
GENERAL DISCUSSION

Cardiovascular diseases in man are determined by a network array of genes and environmental factors, interacting at various stages in development and throughout the lifetime of the individual. Previously used strategies such as linkage analysis in families segregating for rare Mendelian disorders or investigation of putative candidate genes have had a limited success in identifying the major genetic determinants of multifactorial diseases. Practical difficulties add to the complexity in direct study of the genetic determinants of such complex traits and have been a driving force behind the development of similar but fundamentally simpler paradigms, such as experimental animal models. In particular, crosses between hypertensive and normotensive inbred rat strains have led to the identification of chromosomal regions containing QTL for several cardiovascular related phenotypes.

The research described in this thesis included re-evaluation of data from a previously reported genome wide in F_2 crosses derived from Glasgow colonies of SHRSP and WKY rat strains. In addition, stringent QTL analysis and high fidelity phenotyping was carried out, to identify QTL containing genetic determinants for cardiac and left ventricular hypertrophy. There are several features of the QTL mapping strategies used in this thesis, which make them particularly appropriate for congenic production, fine mapping and ultimately identification of primary genes. Firstly, in contrast to previous studies, which used only a single analysis, the use of more than one QTL analysis package offered a more robust localisation of, and confidence in QTL identified. Secondly, the use of MRI was demonstrated as an additional means of reproducible high fidelity phenotyping of animals and subsequent congenic strains, which provides a more accurate assessment of the heart, in particular in small animal groups and characterisation of rat strains. Thirdly, preliminary data from congenic strains give confidence in QTL regions identified that may harbour gene(s) influencing the development of left ventricular hypertrophy in SHRSP. Finally, the current study also combined a genome wide expression approach to candidate gene identification in the absence of a fixed congenic strain, using 2 different analytical strategies, which identified several gene pathways of interest for follow up study in conjunction with the continued production and phenotyping of congenic strains.

The results from this thesis confirm the congenic SP.WKYGla2a strain has an equivalent LVMI to the parental SHRSP, despite an approx. 20mmHg reduction in SBP, consistent with previous unpublished results from our group. Relative wall thickness differences identified indicate a different pattern of remodelling in the congenic strain previously not reported; concentric remodelling in the SP.WKYGla2a, as opposed to concentric hypertrophy observed in the SHRSP. Preliminary data from phenotype analysis of male $SHRSP_{BX4}$ congenic animals indicates a reduced LVMI despite equivalent SBP to the parental SHRSP. In order to identify the significance of this finding, a more precise and in depth cardiac phenotyping of parental rat strains and fixed congenic strains on both genetic backgrounds is necessary. The validation of MRI as an improved tool for measuring left ventricle mass and LV geometry will provide a more superior and robust method for rodent cardiac phenotyping, and offers the potential for assessment of cardiac function including structure, contractility and perfusion. In human studies, the quality of information collected for patients has been shown to impact on the power of results achieved (Kuznetsova *et al.*, 2002; Wingfield *et al.*, 2002), therefore any improvement in this area will add to the knowledge of physiological characteristics and promote a more exact and uniform quantification of disease.

Given the results of the current study, the demonstrated propensity for high fidelity phenotyping coupled with the rapidly increasing availability of appropriate genetic resources for the rat, including dense genetic and physical maps and access to microarray data there can be little doubt that identified QTL will be completely dissected over time. In particular, phenotype and gene expression comparison of age matched animals differing only by genotype and/or diet can be tested using statistical approaches such as rank product (RP) and two-way ANOVA. High fidelity phenotyping of blood pressure and the production of congenic strains, was successfully used by our group previously to confirm two identified BP QTL on rat chromosome 2 (Clark *et al.*, 1996) and verify the application of a speed congenic strategy to dissect QTL in the rat (Jeffs *et al.*, 2000). Furthermore, the combined use of microarray technology and substrain congenic animals resulted in the identification of a positional and functional candidate gene, glutathione-s-transferase-mu-type-1.

In the post genomic era, there is a greater understanding of the human genome as well as a wide assortment of pharmacological and mechanical therapies available for the treatment of cardiovascular diseases (Murray *et al.*, 2003, Wald *et al.*, 2003). The use of comparative mapping to identify regions of shared synteny between species is one route of investigation together with the analysis of differences in response or outcome by "candidate gene", in both animals and humans. These areas of therapeutics and genomics can benefit from an inter-relationship between human and experimental pharmacogenetics. As with many association studies, preliminary data does not always translate well to larger groups, nevertheless strong evidence has been presented by Chasman *et al.* (2004) by way of haplotype analysis used to generate a pharmacogenetic profile for patients receiving cholesterol reducing, statin therapy. A poorer cholesterol-lowering response to Pravastatin was reported in 7% of patients carrying a particular haplotype of the HMG CoA reductase gene (14% fall versus 19%). Another example is determination of genotype at the CYP2C9 locus with respect to warfarin treatment, since carriers for functional variants (>20% of the population) require lower doses for optimal anticoagulation, and homozygotes (although rare), may be have a greater risk of bleeding when given a typical dose. The full potential of this field will only be realised with further work and although it is unlikely this will ultimately lead to an individually tailored prognosis and therapy for patients, it may allow for a less generic treatment, by specific targeting of the genetic aspect or involved pathway.

In this thesis, several candidate genes were identified by both comparative mapping and genome wide expression profiling. Further investigation is required to confirm or refute functional relevance of these genes to CMI and LVMI in the SHRSP. The effect of dietary salt intake on *Dbp* gene expression in WKY is of interest, in particular as microarray phenotype data from 21 week old animals, indicates no SBP increase in the WKY after 1% salt challenge, but a significant increase in CMI and LVMI. Gene networks and pathways of interest generated from microarray analysis can be taken forward and explored in more depth using a combination of congenic strains (currently in production), congenic substrain lines and functional genomics, to localise QTL and dissect the underlying genetic elements influencing heart and LV weight. Quantitative RT-PCR investigation of the most

significant genes identified from both RP and two-way ANOVA statistics will allow for validation of microarray results and sequencing will allow a full characterisation of these genes in the SHRSP and WKY strains. Further, the production of congenic substrain animals may enable filtering of data and the study of epistatic interactions and localised regions of gene activity, in comparison to parental and congenic strains. Additionally, functional studies such as RNA interference (RNAi) and/or gene transfer will facilitate investigation of candidate genes *in vivo* prior to the production of knockout or phenotype rescue transgenic animal models.

In conclusion, the production of congenic strains to confirm, both a previously identified and second newly identified QTL involved in the development of concentric left ventricular hypertrophy in the SHRSP in this study, should enable the translation from experimental model to human cardiovascular disease. This information will also lead to an improved understanding of the genes and biochemical pathways involved in pathogenesis of cardiac hypertrophy and in turn may lead to the continued development of preventative medicine and/or therapies directed against complex traits, which are major causes of morbidity and mortality worldwide.

REFERENCES

Aiello, E. A., Villa-Abrille, M. C., Escudero, E. M., Portiansky, E. L., Perez, N. G., de Hurtado, M. C., & Cingolani, H. E. 2004, "Myocardial hypertrophy of normotensive Wistar-Kyoto rats", *AJP - Heart and Circulatory Physiology*, vol. **286**, no. 4, p. H1229-H1235.

Ahmad, F., Seidman, J. G., & Seidman, C. E. 2005, "The genetic basis for cardiac remodeling", *Annu.Rev.Genomics Hum Genet*, vol. **6**, pp. 185-216.

Akkad, A. A., Halligan, A. W., Abrams, K., & Al Azzawi, F. 1997, "Differing responses in blood pressure over 24 hours in normotensive women receiving oral or transdermal estrogen replacement therapy", *Obstet.Gynecol.*, vol. **89**, no. 1, pp. 97-103.

Al Shafei, A. I., Wise, R. G., Gresham, G. A., Carpenter, T. A., Hall, L. D., & Huang, C. L. 2002, "Magnetic resonance imaging analysis of cardiac cycle events in diabetic rats: the effect of angiotensin-converting enzyme inhibition", *J Physiol*, vol. **538**, no. Pt 2, pp. 555-572.

Anan, R., Greve, G., Thierfelder, L., Watkins, H., McKenna, W. J., Solomon, S., Vecchio, C., Shono, H., Nakao, S., Tanaka, H., & . 1994, "Prognostic implications of novel beta cardiac myosin heavy chain gene mutations that cause familial hypertrophic cardiomyopathy", *J Clin Invest*, vol. **93**, no. 1, pp. 280-285.

Andress, D. L. 2005, "Vitamin D treatment in chronic kidney disease", *Semin.Dial.*, vol. 18, no. **4**, pp. 315-321.

Annest, J. L., Sing, C. F., Biron, P., & Mongeau, J. G. 1979, "Familial aggregation of blood pressure and weight in adoptive families. II. Estimation of the relative contributions of genetic and common environmental factors to blood pressure correlations between family members", *Am J Epidemiol*, vol. **110**, no. 4, pp. 492-503.

Annest, J. L., Sing, C. F., Biron, P., & Mongeau, J. G. 1983, "Familial aggregation of blood pressure and weight in adoptive families. III. Analysis of the role of shared genes and shared household environment in explaining family resemblance for height, weight and selected weight/height indices", *Am J Epidemiol*, vol. **117**, no. 4, pp. 492-506.

Arnett, D. K., Strogatz, D. S., Ephross, S. A., Hames, C. G., & Tyroler, H. A. 1992, "Greater incidence of electrocardiographic left ventricular hypertrophy in black men than in white men in Evans County, Georgia", *Ethn.Dis*, vol. **2**, no. 1, pp. 10-17.

Arnett, D. K., Tyroler, H. A., Burke, G., Hutchinson, R., Howard, G., & Heiss, G. 1996, "Hypertension and subclinical carotid artery atherosclerosis in blacks and whites. The Atherosclerosis Risk in Communities Study. ARIC Investigators", *Arch.Intern Med*, vol. **156**, no. 17, pp. 1983-1989.

Ashton, N. & Balment, R. J. 1991, "Sexual dimorphism in renal function and hormonal status of New Zealand genetically hypertensive rats", *Acta Endocrinol (Copenh)*, vol. **124**, no. 1, pp. 91-97.

August, P. & Oparil, S. 1999, "Hypertension in women", *Journal of Clinical Endocrinology Metabolism*, vol. **84**, no. 6, pp. 1862-1866.

Bachmann, H., Horacek, U., Leowsky, M., & Hirche, H. 1987, "[Blood pressure in children and adolescents aged 4 to 18. Correlation of blood pressure values with age, sex, body height, body weight and skinfold thickness (Essen Blood Pressure Study)]", *Monatsschr.Kinderheilkd.*, vol. **135**, no. 3, pp. 128-134.

Baima, J., Nicolaou, M., Schwartz, F., DeStefano, A. L., Manolis, A., Gavras, I., Laffer, C., Elijovich, F., Farrer, L., Baldwin, C. T., & Gavras, H. 1999, "Evidence for linkage between essential hypertension and a putative locus on human chromosome 17", *Hypertension*, vol. **34**, no. 1, pp. 4-7.

Barlassina, C., Lanzani, C., Manunta, P., & Bianchi, G. 2002, "Genetics of Essential Hypertension: From Families to Genes", *Journal of the American Society of Nephrology*, vol. **13**, no. 90003, p. S155-S164.

Bastarrika, G., Sprengel, U., Saenz, d. B., Romero, C., Alegria, E., Benito, A., & Barba, J. 2005, "[Cardiac magnetic resonance: clinical applications]", *An.Sist.Sanit.Navar.*, vol. **28**, no. 1, pp. 49-58.

Bauwens, F. R., Duprez, D. A., De Buyzere, M. L., De Backer, T. L., Kaufman, J. M., Van Hoecke, J., Vermeulen, A., & Clement, D. L. 1991, "Influence of the arterial blood pressure and nonhemodynamic factors on left ventricular hypertrophy in moderate essential hypertension", *Am J Cardiol.*, vol. **68**, no. 9, pp. 925-929.

Beaglehole, R., Salmond, C. E., Hooper, A., Huntsman, J., Stanhope, J. M., Cassel, J. C., & Prior, I. A. M. 1977, "Blood pressure and social interaction and Tokelau and migrants in New Zealand", *J Chron Dis*, vol. **30**, pp. 803-812.

Benarroch, E. E. 1993, "The central autonomic network: functional organization, dysfunction, and perspective", *Mayo Clin Proc.*, vol. **68**, no. 10, pp. 988-1001.

Berne, R. & Levy, M. 1997, *in"Cardiovascular Physiology"*, ed. St. Louis, MO: Mosby, ch. 10, p. 225.

Bhatnagar, D., Anand, I. S., Durrington, P. N., Patel, D. J., Wander, G. S., Mackness, M. I., Creed, F., Tomenson, B., Chandrashekhar, Y., & Winterbotham, M. "Coronary risk factors in people from the Indian subcontinent living in west London and their siblings in India", *Lancet*, vol. **345**, no. 8947, pp. 405-409.

Bhopal, R., Unwin, N., White, M., Yallop, J., Walker, L., & Alberti, K. G. 1999, "Heterogeneity of coronary heart disease risk factors in Indian, Pakistani, Bangladeshi, and European origin populations: cross sectional study", *BMJ*, vol. **319**, no. 7204, pp. 215-220.

Bie, P., Wamberg, S., & Kjolby, M. 2004, "Volume natriuresis vs. pressure natriuresis", *Acta Physiologica Scandinavica*, vol. **181**, no. 4, pp. 495-503.

Bihoreau, M. T., Gauguier, D., Kato, N., Hyne, G., Lindpaintner, K., Rapp, J. P., James, M. R., & Lathrop, G. M. 1997, "A linkage map of the rat genome derived from three F2 crosses", *Genome Res*, vol. **7**, no. 5, pp. 434-440.

Bogin, E., Massry, S. G., & Harary, I. 1981, "Effect of parathyroid hormone on rat heart cells", *J Clin Invest*, vol. **67**, no. 4, pp. 1215-1227.

Bonne, G., Carrier, L., Richard, P., Hainque, B., & Schwartz, K. 1998, "Familial hypertrophic cardiomyopathy: from mutations to functional defects", *Circulation Research*, vol. **83**, no. 6, pp. 580-593.

Booz, G. W. & Baker, K. M. 1996, "Role of type 1 and type 2 angiotensin receptors in angiotensin II-induced cardiomyocyte hypertrophy", *Hypertension*, vol. **28**, no. 4, pp. 635-640.

Boutin-Ganache, I., Picard, S., & Deschepper, C. F. 2002, "Distinct gene-sex interactions regulate adult rat cardiomyocyte width and length independently", *Physiol Genomics*, vol. **12**, no. 1, pp. 61-67.

Brand, E., Chatelain, N., Keavney, B., Caulfield, M., Citterio, L., Connell, J., Grobbee, D., Schmidt, S., Schunkert, H., Schuster, H., Sharma, A. M., & Soubrier, F. 1998, "Evaluation of the angiotensinogen locus in human essential hypertension: a European study", *Hypertension*, vol. **31**, no. 3, pp. 725-729.

Brede, M., Hadamek, K., Meinel, L., Wiesmann, F., Peters, J., Engelhardt, S., Simm, A., Haase, A., Lohse, M. J., & Hein, L. 2001, "Vascular hypertrophy and increased P70S6 kinase in mice lacking the angiotensin II AT(2) receptor", *Circulation*, vol. **104**, no. 21, pp. 2602-2607.

Breitling, R., Armengaud, P., Amtmann, A., & Herzyk, P. 2004, "Rank products: a simple, yet powerful, new method to detect differentially regulated genes in replicated microarray experiments", *FEBS Letters*, vol. **573**, no. 1-3, pp. 83-92.

Brockway, B. P., Mills, P. A., & Azar, S. H. 1991, "A new method for continuous chronic measurement and recording of blood pressure, heart rate and activity in the rat via radio-telemetry", *Clin Exp Hypertens A*, vol. **13**, no. 5, pp. 885-895.

Brooks, V. L. & Osborn, J. W. 1995, "Hormonal-sympathetic interactions in long-term regulation of arterial pressure: an hypothesis", *AJP - Regulatory, Integrative and Comparative Physiology*, vol. **268**, no. 6, p. R1343-R1358.

Brown, D. M., Matise, T. C., Koike, G., Simon, J. S., Winer, E. S., Zangen, S., McLaughlin, M. G., Shiozawa, M., Atkinson, O. S., Hudson, J. R., Jr., Chakravarti, A., Lander, E. S., & Jacob, H. J. 1998, "An integrated genetic linkage map of the laboratory rat", *Mamm.Genome*, vol. **9**, no. 7, pp. 521-530.

Bukoski, R. D., Ishibashi, K., & Bian, K. 1995, "Vascular actions of the calcium-regulating hormones", *Semin.Nephrol*, vol. **15**, no. 6, pp. 536-549.

Bunag, R. D. 1983, "Facts and fallacies about measuring blood pressure in rats", *Clin Exp Hypertens A*, vol. **5**, no. 10, pp. 1659-1681.

Bunag, R. D. & Teravainen, T. L. 1991, "Tail-cuff detection of systolic hypertension in different strains of ageing rats", *Mech.Ageing Dev.*, vol. **59**, no. 1-2, pp. 197-213.

Burnstock, G. 1986, "The changing face of autonomic neurotransmission", *Acta Physiol Scand*, vol. **126**, no. 1, pp. 67-91.

Cameron, V. A. & Ellmers, L. J. 2003, "Minireview: Natriuretic Peptides during Development of the Fetal Heart and Circulation", *Endocrinology*, vol. **144**, no. 6, pp. 2191-2194.

Carretero, O. A. & Oparil, S. 2000, "Essential Hypertension : Part I: Definition and Etiology", *Circulation*, vol. **101**, no. 3, pp. 329-335.

Chan, J. C., Knudson, O., Wu, F., Morser, J., Dole, W. P., & Wu, Q. 2005, "Hypertension in mice lacking the proatrial natriuretic peptide convertase corin", *Proc.Natl.Acad.Sci.U.S.A*, vol. **102**, no. 3, pp. 785-790.

Chen, J., Song, S. K., Liu, W., McLean, M., Allen, J. S., Tan, J., Wickline, S. A., & Yu, X. 2003, "Remodeling of cardiac fiber structure after infarction in rats quantified with diffusion tensor MRI", *AJP - Heart and Circulatory Physiology*, vol. **285**, no. 3, p. H946-H954.

Chen, Y. F. & Meng, Q. C. 1991, "Sexual dimorphism of blood pressure in spontaneously hypertensive rats is androgen dependent", *Life Sci.*, vol. **48**, no. 1, pp. 85-96.

Chitayat, D., Grix, A., Balfe, J. W., Abramowicz, J. S., Garza, J., Fong, C. T., Silver, M. M., Saller, D. N., Jr., Bresnick, G. H., Giedion, A., Lachman, R. S., & Rimoin, D. L. 1997, "Brachydactyly-short stature-hypertension (Bilginturan) syndrome: report on two families", *Am J Med Genet*, vol. **73**, no. 3, pp. 279-285.

Churchill, G. A. & Doerge, R. W. 1994, "Empirical threshold values for quantitative trait mapping", *Genetics*, vol. **138**, no. 3, pp. 963-971.

Cicila, G. T. & Lee, S. J. 1998, "Identifying candidate genes for blood pressure quantitative trait loci using differential gene expression and a panel of congenic strains", *Hypertens Res*, vol. **21**, no. 4, pp. 289-296.

Cicila, G. T., Choi, C., Dene, H., Lee, S. J., & Rapp, J. P. 1999, "Two blood pressure/cardiac mass quantitative trait loci on chromosome 3 in Dahl rats", *Mamm.Genome*, vol. **10**, no. 2, pp. 112-116.

Clark, J. S., Jeffs, B., Davidson, A. O., Lee, W. K., Anderson, N. H., Bihoreau, M. T., Brosnan, M. J., Devlin, A. M., Kelman, A. W., Lindpaintner, K., & Dominiczak, A. F. 1996, "Quantitative Trait Loci in Genetically Hypertensive Rats: Possible Sex Specificity", *Hypertension*, vol. **28**, no. 5, pp. 898-906.

Colditz, G. A., Willett, W. C., Stampfer, M. J., Rosner, B., Speizer, F. E., & Hennekens, C. H. 1987, "Menopause and the risk of coronary heart disease in women", *N.Engl.J Med*, vol. **316**, no. 18, pp. 1105-1110.

Cooper, R. & Rotimi, C. 1997, "Hypertension in blacks", *Am J Hypertens*, vol. **10**, pp. 804-812.

Cooper, R. S., Wolf-Maier, K., Luke, A., Adeyemo, A., Banegas, J. R., Forrester, T., Giampaoli, S., Joffres, M., Kastarinen, M., Primatesta, P., Stegmayr, B., & Thamm, M. "An International Comparative Study of Blood Pressure in Populations of European vs. African Descent", *BMC Med*, vol. **3**, p. 2.

Cordell, H. J. 2002, "Epistasis: what it means, what it doesn't mean, and statistical methods to detect it in humans", *Human Molecular Genetics*, vol. **11**, no. 20, pp. 2463-2468.

Coucke, P., Van Acker, P., & De Paepe, A. 2006, "Mutation analysis of the FBN1 gene in patients with Marfan syndrome", *Methods Mol Med*, vol. **126**, pp. 81-95.

Crowley, J. J., Huang, C. L., Gates, A. R., Basu, A., Shapiro, L. M., Carpenter, T. A., & Hall, L. D. 1997, "A quantitative description of dynamic left ventricular geometry in anaesthetized rats using magnetic resonance imaging", *Exp Physiol*, vol. **82**, no. 5, pp. 887-904.

Cruickshank, J. K., Jackson, S. H. D., Beevers, D. G., Bannan, L. T., Beevers, M., & Stewart, V. L. 1985, "Similarity of blood pressure in blacks, whites and Asians in England: The Birmingham Factory study", *J Hypertension*, vol. **3**, pp. 365-371.

Davidson, A. O., Schork, N., Jaques, B. C., Kelman, A. W., Sutcliffe, R. G., Reid, J. L., & Dominiczak, A. F. 1995, "Blood pressure in genetically hypertensive rats. Influence of the Y chromosome", *Hypertension*, vol. **26**, no. 3, pp. 452-459.

de Simone, G., Wallerson, D. C., Volpe, M., & Devereux, R. B. 1990, "Echocardiographic measurement of left ventricular mass and volume in normotensive and hypertensive rats. Necropsy validation", *Am J Hypertens*, vol. **3**, no. 9, pp. 688-696.

de Simone, G., Devereux, R. B., Roman, M. J., Ganau, A., Saba, P. S., Alderman, M. H., & Laragh, J. H. 1994, "Assessment of left ventricular function by the midwall fractional shortening/end-systolic stress relation in human hypertension", *J Am Coll.Cardiol.*, vol. **23**, no. 6, pp. 1444-1451.

De Wardener, H. E. 2001, "The Hypothalamus and Hypertension", *Physiological Reviews*, vol. **81**, no. 4, pp. 1599-1658.

Deng, A. Y. & Rapp, J. P. 1995, "Locus for the inducible, but not a constitutive, nitric oxide synthase cosegregates with blood pressure in the Dahl salt-sensitive rat", *J Clin Invest*, vol. **95**, no. 5, pp. 2170-2177.

Deng, A. Y., Dene, H., & Rapp, J. P. 1997, "Congenic strains for the blood pressure quantitative trait locus on rat chromosome 2", *Hypertension*, vol. **30**, no. 2 Pt 1, pp. 199-202.

Deschepper, C. F., Masciotra, S., Zahabi, A., Boutin-Ganache, I., Picard, S., & Reudelhuber, T. L. 2001, "Functional alterations of the Nppa promoter are linked to cardiac ventricular hypertrophy in WKY/WKHA rat crosses", *Circulation Research*, vol. **88**, no. 2, pp. 223-228.

Devereux, R. B., Lutas, E. M., Casale, P. N., Kligfield, P., Eisenberg, R. R., Hammond, I. W., Miller, D. H., Reis, G., Alderman, M. H., & Laragh, J. H. 1984, "Standardization of M-mode echocardiographic left ventricular anatomic measurements", *J Am Coll.Cardiol.*, vol. **4**, no. 6, pp. 1222-1230.

Devereux, R. B. 1987, "Cardiac involvement in essential hypertension. Prevalence, pathophysiology, and prognostic implications", *Med Clin North Am*, vol. **71**, no. 5, pp. 813-826.

Devereux, R. B., de Simone, G., Koren, M. J., Roman, M. J., & Laragh, J. H. 1991, "Left ventricular mass as a predictor of development of hypertension", *Am J Hypertens*, vol. **4**, no. 11, pp. 603S-607S.

Devereux, R. B., de Simone, G., Ganau, A., Koren, M. J., & Roman, M. J. 1993, "Left ventricular hypertrophy associated with hypertension and its relevance as a risk factor for complications", *J Cardiovasc Pharmacol*, vol. **21** Suppl 2, p. S38-S44.

Devereux, R. B., de Simone, G., Ganau, A., & Roman, M. J. 1994, "Left ventricular hypertrophy and geometric remodeling in hypertension: stimuli, functional consequences and prognostic implications", *J Hypertens Suppl*, vol. **12**, no. 10, p. S117-S127.

Devereux, R. B., Wallerson, D. C., de Simone, G., Ganau, A., & Roman, M. J. 1994, "Evaluation of left ventricular hypertrophy by M-mode echocardiography in patients and experimental animals", *Am J Card Imaging*, vol. **8**, no. 4, pp. 291-304.

Devereux, R. B. & Roman, M. J. 1995, "Evaluation of the heart and arterial tree in hypertension", *J Cardiovasc Risk*, vol. 2, no. 1, pp. 4-15.

Devereux, R. B., Roman, M. J., Liu, J. E., Lee, E. T., Wang, W., Fabsitz, R. R., Welty, T. K., & Howard, B. V. 2003, "An appraisal of echocardiography as an epidemiological tool. The Strong Heart Study", *Ann Epidemiol*, vol. **13**, no. 4, pp. 238-244.

Di Nicolantonio, R., Kostka, V., Kwitek, A., Jacob, H., Thomas, W. G., & Harrap, S. B. 2006, "Fine mapping of Lvm1: a quantitative trait locus controlling heart size independently of blood pressure", *Pulm.Pharmacol Ther.*, vol. **19**, no. 1, pp. 70-73.

Dickhuth, H. H., Reindell, H., Lehmann, M., & Keul, J. 1985, "Capacity for regression of the athletic heart", *Z.Kardiol.*, vol. **74** Suppl 7, pp. 135-143.

Diez-Roux, A. V., Nieto, F. J., & Muntaner, C. 1997, "Neighbourhood environments and coronary heart disease: A multilevel analysis", *Am J Epidemiol*, vol. **146**, pp. 48-63.

Disabella, E., Grasso, M., Marziliano, N., Ansaldi, S., Lucchelli, C., Porcu, E., Tagliani, M., Pilotto, A., Diegoli, M., Lanzarini, L., Malattia, C., Pelliccia, A., Ficcadenti, A., Gabrielli, O., & Arbustini, E. 2006, "Two novel and one known mutation of the TGFBR2 gene in Marfan syndrome not associated with FBN1 gene defects", *Eur J Hum Genet*, vol. **14**, no. 1, pp. 34-38.

Doerge, R. W. & Churchill, G. A. 1996, "Permutation tests for multiple loci affecting a quantitative character", *Genetics*, vol. **142**, no. 1, pp. 285-294.

Doerge, R. W. 2002, "Mapping and analysis of quantitative trait loci in experimental populations", *Nat.Rev.Genet*, vol. **3**, no. 1, pp. 43-52.

Dominiczak, A.F. & Lindpaintner, K. 1994, "Genetics of hypertension: a current appraisal", *News in Physiological Sciences*, vol. **9**, pp. 246-251.

Dominiczak, A. F., Devlin, A. M., Lee, W. K., Anderson, N. H., Bohr, D. F., & Reid, J. L. 1996, "Vascular Smooth Muscle Polyploidy and Cardiac Hypertrophy in Genetic Hypertension", *Hypertension*, vol. **27**, no. 3, pp. 752-759.

Dominiczak, A. F., Devlin, A. M., Brosnan, M. J., Anderson, N. H., Graham, D., Clark, J. S., McPhaden, A., Hamilton, C. A., & Reid, J. L. 1997, "Left ventricular hypertrophy and arterial blood pressure in experimental models of hypertension", *Adv.Exp Med Biol*, vol. **432**, pp. 23-33.

Dominiczak, A. F. & McBride, M. W. 2003, "Genetics of common polygenic stroke", *Nat.Genet*, vol. **35**, no. 2, pp. 116-117.

Dominiczak, A. F., Brain, N., Charchar, F., McBride, M., Hanlon, N., & Lee, W. K. 2004, "Genetics of hypertension: lessons learnt from mendelian and polygenic syndromes", *Clin Exp Hypertens*, vol. **26**, no. 7-8, pp. 611-620.

Dominiczak, A. F., Graham, D., McBride, M. W., Brain, N. J., Lee, W. K., Charchar, F. J., Tomaszewski, M., Delles, C., & Hamilton, C. A. 2005, "Corcoran Lecture. Cardiovascular genomics and oxidative stress", *Hypertension*, vol. **45**, no. 4, pp. 636-642.

Dueland, S., Bouillon, R., Van Baelen, H., Pedersen, J. I., Helgerud, P., & Drevon, C. A. 1985, "Binding protein for vitamin D and its metabolites in rat mesenteric lymph", *AJP - Legacy*, vol. **249**, no. 1 Pt 1, p. E1-E5.

Durand, J. B. 1999, "Genetic basis of cardiomyopathy", *Curr Opin.Cardiol.*, vol. **14**, no. 3, pp. 225-229.

Dzau, V. J. 1988, "Vascular renin-angiotensin system in hypertension. New insights into the mechanism of action of angiotensin converting enzyme inhibitors", *Am J Med*, vol. **84**, no. 4A, pp. 4-8.

Edler, I. & Hertz, C. H. 2004, "The use of ultrasonic reflectoscope for the continuous recording of the movements of heart walls. 1954", *Clin Physiol Funct.Imaging*, vol. **24**, no. 3, pp. 118-136.

Ekins, R., Chu, F., & Micallef, J. 1989, "High specific activity chemiluminescent and fluorescent markers: their potential application to high sensitivity and 'multi-analyte' immunoassays", *J Biolumin.Chemilumin.*, vol. **4**, no. 1, pp. 59-78.

Ely, D. L. & Turner, M. E. 1990, "Hypertension in the spontaneously hypertensive rat is linked to the Y chromosome", *Hypertension*, vol. **16**, no. 3, pp. 277-281.

Espiner, E. A., Richards, A. M., Yandle, T. G., & Nicholls, M. G. 1995, "Natriuretic hormones", *Endocrinol Metab Clin North Am*, vol. **24**, no. 3, pp. 481-509.

Shen, R., Fan, J. B., Campbell, D., Chang, W., Chen, J., Doucet, D., Yeakley, J., Bibikova, M., Wickham, G. E., McBride, C., Steemers, F., Garcia, F., Kermani, B. G., Gunderson, K., & Oliphant, A. 2005, "High-throughput SNP genotyping on universal bead arrays", *Mutat.Res*, vol. **573**, no. 1-2, pp. 70-82.

Farrall, M. 2004, "Quantitative genetic variation: a post-modern view", *Hum.Mol.Genet*, vol. **13** Spec No 1, p. R1-R7.

Feigenbaum, H. 1996, "Echocardiographic tissue diagnosis", *European Heart Journal*, vol. **17**, no. 1, pp. 6-7.

Feinleib, M., Garrison, R. J., Fabsitz, R., Christian, J. C., Hrubec, Z., Borhani, N. O., Kannel, W. B., Rosenman, R., Schwartz, J. T., & Wagner, J. O. 1977, "The NHLBI twin study of cardiovascular disease risk factors: methodology and summary of results", *Am J Epidemiol*, vol. **106**, no. 4, pp. 284-285.

Feng, J. A., Perry, G., Mori, T., Hayashi, T., Oparil, S., & Chen, Y. F. 2003, "Pressure-independent enhancement of cardiac hypertrophy in atrial natriuretic peptide-deficient mice", *Clinical and Experimental Pharmacology and Physiology*, vol. **30**, no. 5-6, pp. 343-349.

Fischer, M., Baessler, A., Hense, H. W., Hengstenberg, C., Muscholl, M., Holmer, S., Doring, A., Broeckel, U., Riegger, G., & Schunkert, H. 2003, "Prevalence of left ventricular diastolic dysfunction in the community: Results from a Doppler echocardiographic-based survey of a population sample", *European Heart Journal*, vol. **24**, no. 4, pp. 320-328.

Foley, R. N., Parfrey, P. S., Harnett, J. D., Kent, G. M., O'Dea, R., Murray, D. C., & Barre, P. E. 1998, "Mode of dialysis therapy and mortality in end-stage renal disease", *Journal of the American Society of Nephrology*, vol. **9**, no. 2, pp. 267-276.

Franco, F., Thomas, G. D., Giroir, B., Bryant, D., Bullock, M. C., Chwialkowski, M. C., Victor, R. G., & Peshock, R. M. 1999, "Magnetic resonance imaging and invasive evaluation of development of heart failure in transgenic mice with myocardial expression of tumor necrosis factor-alpha", *Circulation*, vol. **99**, no. 3, pp. 448-454.

Friesen, R. H., Wurl, J. L., & Charlton, G. A. 2000, "Haemodynamic depression by halothane is age-related in paediatric patients", *Paediatr.Anaesth.*, vol. **10**, no. 3, pp. 267-272.

Frohlich, E. D., Dunn, F. G., & Messerli, F. H. 1983, "Pharmacologic and physiologic considerations of adrenoceptor blockade", *Am J Med*, vol. **75**, no. 4A, pp. 9-14.

Frohlich, E. D. 2001, "Local hemodynamic changes in hypertension: insights for therapeutic preservation of target organs", *Hypertension*, vol. **38**, no. 6, pp. 1388-1394.

Gaasch, W. H., Levine, H. J., Quinones, M. A., & Alexander, J. K. 1976, "Left ventricular compliance: mechanisms and clinical implications", *Am J Cardiol.*, vol. **38**, no. 5, pp. 645-653.

Gabe, I. T. 1965, "Arterial Blood Flow by Analogue Solution of the Navier-Stokes Equation", *Physics in Medicine and Biology* no. 2, pp. 271-280.

Gairard, A., Pernot, F., Bergmann, C., & van Overloop, B. 1994, "Ions, parathyroids, and genetic hypertension", *Am J Med Sci.*, vol. **307** Suppl 1, p. S126-S129.

Gamba, G. 2005, "Role of WNK kinases in regulating tubular salt and potassium transport and in the development of hypertension", *AJP - Renal Physiology*, vol. **288**, no. 2, p. F245-F252.

Ganau, A., Devereux, R. B., Pickering, T. G., Roman, M. J., Schnall, P. L., Santucci, S., Spitzer, M. C., & Laragh, J. H. 1990, "Relation of left ventricular hemodynamic load and contractile performance to left ventricular mass in hypertension", *Circulation*, vol. **81**, no. 1, pp. 25-36.

Ganau, A., Devereux, R. B., Roman, M. J., de Simone, G., Pickering, T. G., Saba, P. S., Vargiu, P., Simongini, I., & Laragh, J. H. 1992, "Patterns of left ventricular hypertrophy and geometric remodeling in essential hypertension", *J Am Coll.Cardiol.*, vol. **19**, no. 7, pp. 1550-1558.

Ganten, D., Unger, T., & Lang, R. E. 1987, "Brain peptides and blood pressure control", *Verh.Dtsch.Ges.Inn.Med*, vol. **93**, pp. 418-421.

Ganten, U., Schroder, G., Witt, M., Zimmermann, F., Ganten, D., & Stock, G. 1989, "Sexual dimorphism of blood pressure in spontaneously hypertensive rats: effects of anti-androgen treatment", *J Hypertens*, vol. 7, no. 9, pp. 721-726.

Garcia, E. A., Newhouse, S., Caulfield, M. J., & Munroe, P. B. 2003, "Genes and hypertension", *Curr Pharm Des*, vol. **9**, no. 21, pp. 1679-1689.

Garner, C., Lecomte, E., Visvikis, S., Abergel, E., Lathrop, M., & Soubrier, F. 2000, "Genetic and Environmental Influences on Left Ventricular Mass : A Family Study", *Hypertension*, vol. **36**, no. 5, pp. 740-746.

Garrett, M. R., Saad, Y., Dene, H., & Rapp, J. P. 2000, "Blood pressure QTL that differentiate Dahl salt-sensitive and spontaneously hypertensive rats", *Physiol Genomics*, vol. **3**, no. 1, pp. 33-38.

Garrett, M. R., Zhang, X., Dukhanina, O. I., Deng, A. Y., & Rapp, J. P. 2001, "Two linked blood pressure quantitative trait loci on chromosome 10 defined by dahl rat congenic strains", *Hypertension*, vol. **38**, no. 4, pp. 779-785.

Garrett, M. R., Meng, H., Rapp, J. P., & Joe, B. 2005, "Locating a blood pressure quantitative trait locus within 117 kb on the rat genome: substitution mapping and renal expression analysis", *Hypertension*, vol. **45**, no. 3, pp. 451-459.

Geller, D. S., Farhi, A., Pinkerton, N., Fradley, M., Moritz, M., Spitzer, A., Meinke, G., Tsai, F. T., Sigler, P. B., & Lifton, R. P. 2000, "Activating mineralocorticoid receptor mutation in hypertension exacerbated by pregnancy", *Science*, vol. **289**, no. 5476, pp. 119-123.

George, T. C., Carl, C., Howard, D., Soon, J. L., & John, P. R. 1999, "Two blood pressure/cardiac mass quantitative trait loci on Chromosome 3 in Dahl rats", *Mammalian Genome*, vol. **10**, no. 2, pp. 112-116.

Gibbons, R. J. & Araoz, P. A. 2005, "The year in cardiac imaging", *J Am Coll.Cardiol.*, vol. **46**, no. 3, pp. 542-551.

Gibbs, R. A., Weinstock, G. M., Metzker, M. L., Muzny, D. M., Sodergren, E. J., Scherer, *et al.* 2004, "Genome sequence of the Brown Norway rat yields insights into mammalian evolution", *Nature*, vol. **428**, no. 6982, pp. 493-521.

Goetz, R. M., Morano, I., Calovini, T., Studer, R., & Holtz, J. 1994, "Increased expression of endothelial constitutive nitric oxide synthase in rat aorta during pregnancy", *Biochem.Biophys.Res Commun.*, vol. **205**, no. 1, pp. 905-910.

Gong, M., Zhang, H., Schulz, H., Lee, Y. A., Sun, K., Bahring, S., Luft, F. C., Nurnberg, P., Reis, A., Rohde, K., Ganten, D., Hui, R., & Hubner, N. 2003, "Genome-wide linkage reveals a locus for human essential (primary) hypertension on chromosome 12p", *Human Molecular Genetics*, vol. **12**, no. 11, pp. 1273-1277.

Gordon, T., Kannel, W. B., Hjortland, M. C., & McNamara, P. M. 1978, "Menopause and coronary heart disease. The Framingham Study", *Annals of Internal Medicine*, vol. **89**, no. 2, pp. 157-161.

Graham, D., McBride, M. W., Brain, N. J., & Dominiczak, A. F. 2004, "Congenic/Consomic models of hypertension", *Methods Mol Med*, vol. **108**, pp. 3-16.

Grim, C. E., Wilson, T. W., Nicholson, G. D., Hassel, T. A., Fraser, H. S., Grim, C. M., & Wilson, D. M. 1990, "Blood pressure in blacks. Twin studies in Barbados", *Hypertension*, vol. **15**, pp. 803-809.

Gross, V., Tank, J., Obst, M., Plehm, R., Blumer, K. J., Diedrich, A., Jordan, J., & Luft, F. C. 2005, "Autonomic Nervous System and Blood Pressure Regulation in RGS2-deficient Mice", *AJP - Regulatory, Integrative and Comparative Physiology* p. 00246.

Gustavsen, P. H., Hoegholm, A., Bang, L. E., & Kristensen, K. S. 2003, "White coat hypertension is a cardiovascular risk factor: a 10-year follow-up study", *J Hum Hypertens*, vol. **17**, no. 12, pp. 811-817.

Hacia, J. G., Fan, J. B., Ryder, O., Jin, L., Edgemon, K., Ghandour, G., Mayer, R. A., Sun, B., Hsie, L., Robbins, C. M., Brody, L. C., Wang, D., Lander, E. S., Lipshutz, R., Fodor, S. P., & Collins, F. S. 1999, "Determination of ancestral alleles for human single-nucleotide polymorphisms using high-density oligonucleotide arrays", *Nat.Genet*, vol. **22**, no. 2, pp. 164-167.

Haley, C. S. & Knott, S. A. 1992, "A simple regression method for mapping quantitative trait loci in line crosses using flanking markers", *Heredity*, vol. **69**, no. 4, pp. 315-324.

Hansson, J. H., Schild, L., Lu, Y., Wilson, T. A., Gautschi, I., Shimkets, R., Nelson-Williams, C., Rossier, B. C., & Lifton, R. P. 1995, "A de novo missense mutation of the beta subunit of the epithelial sodium channel causes hypertension and Liddle syndrome, identifying a proline-rich segment critical for regulation of channel activity", *Proc.Natl.Acad.Sci.U.S.A*, vol. **92**, no. 25, pp. 11495-11499.

Hara, Y., Tagawa, M., Ejima, H., Orima, H., Yamagami, T., Umeda, M., Komori, S., & Washizu, M. 1995, "Regression of hypertrophic osteopathy following removal of intrathoracic neoplasia derived from vagus nerve in a dog", *J Vet.Med Sci.*, vol. **57**, no. 1, pp. 133-135.

Harburg, E., Erfurt, J. C., & Chape, C. 1973, "Socioecological stressor areas and African-white blood pressure: Detroit", *J Chronic Dis*, vol. **26**, pp. 595-611.

Harrap, S. B., Louis, W. J., & Doyle, A. E. 1984, "Failure of psychosocial stress to induce chronic hypertension in the rat", *J Hypertens*, vol. **2**, no. 6, pp. 653-662.

Harrap, S. B., Danes, V. R., Ellis, J. A., Griffiths, C. D., Jones, E. F., & Delbridge, L. M. 2002, "The hypertrophic heart rat: a new normotensive model of genetic cardiac and cardiomyocyte hypertrophy", *Physiol Genomics*, vol. **9**, no. 1, pp. 43-48.

Harris, E. L., Phelan, E. L., Thompson, C. M., Millar, J. A., & Grigor, M. R. 1995, "Heart mass and blood pressure have separate genetic determinants in the New Zealand genetically hypertensive (GH) rat", *J Hypertens*, vol. **13**, no. 4, pp. 397-404.

Harshfield, G. A., Alpert, B. S., Pulliam, D. A., Somes, G. W., & Wilson, D. K. 1994, "Ambulatory blood pressure recordings in children and adolescents", *Pediatrics*, vol. **94**, no. 2 Pt 1, pp. 180-184.

He, F. J. & MacGregor, G. A. 2003, "Cost of poor pressure control in the UK: 62000 unnecessary deaths per year", *J Human Hypertens*, vol. **17**, pp. 455-457.

Helmer, O. M. 1965, "The renin-angiotensin system and its relation to hypertension", *Prog.Cardiovasc Dis*, vol. 8, no. 2, pp. 117-128.

Hess, P., Clozel, M., & Clozel, J. P. 1996, "Telemetry monitoring of pulmonary arterial pressure in freely moving rats", *J Appl.Physiol*, vol. **81**, no. 2, pp. 1027-1032.

Higgins, C. B., Holt, W., Pflugfelder, P., & Sechtem, U. 1988, "Functional evaluation of the heart with magnetic resonance imaging", *Magn Reson.Med*, vol. **6**, no. 2, pp. 121-139.

Hilbert, P., Lindpaintner, K., Beckmann, J. S., Serikawa, T., Soubrier, F., Dubay, C., Cartwright, P., De Gouyon, B., Julier, C., Takahasi, S., & . 1991, "Chromosomal mapping of two genetic loci associated with blood-pressure regulation in hereditary hypertensive rats", *Nature*, vol. **353**, no. 6344, pp. 521-529.

Hinderliter, A. L., Sherwood, A., Blumenthal, J. A., Light, K. C., Girdler, S. S., McFetridge, J., Johnson, K., & Waugh, R. 2002, "Changes in hemodynamics and left ventricular structure after menopause", *Am J Cardiol.*, vol. **89**, no. 7, pp. 830-833.

Hinojosa-Laborde, C., Chapa, I., Lange, D., & Haywood, J. R. 1999, "Gender differences in sympathetic nervous system regulation", *Clinical and Experimental Pharmacology and Physiology*, vol. **26**, no. 2, pp. 122-126.

Hinojosa-Laborde, C., Craig, T., Zheng, W., Ji, H., Haywood, J. R., & Sandberg, K. 2004, "Ovariectomy Augments Hypertension in Aging Female Dahl Salt-Sensitive Rats", *Hypertension*, vol. **44**, no. 4, pp. 405-409.

Hoehe, M. R., Kopke, K., Wendel, B., Rohde, K., Flachmeier, C., Kidd, K. K., Berrettini, W. H., & Church, G. M. 2000, "Sequence variability and candidate gene analysis in complex disease: association of {micro} opioid receptor gene variation with substance dependence", *Human Molecular Genetics*, vol. **9**, no. 19, pp. 2895-2908.

Horan, M. J. & Lenfant, C. 1990, "Epidemiology of blood pressure and predictors of hypertension", *Hypertension*, vol. **15**, no. 2 Suppl, p. I20-I24.

Hughes, T. A. 2006, "Regulation of gene expression by alternative untranslated regions", *Trends Genet*, vol. **22**, no. 3, pp. 119-122.

Ibsen, K. K. 1984, "Blood-pressures in offspring of hypertensive parents", *Acta Paediatr.Scand*, vol. **73**, no. 6, pp. 842-847.

Ichihara, S., Senbonmatsu, T., Price E Jr, Ichiki, T., Gaffney, F. A., & Inagami, T. 2001, "Angiotensin II type 2 receptor is essential for left ventricular hypertrophy and cardiac fibrosis in chronic angiotensin II-induced hypertension", *Circulation*, vol. **104**, no. 3, pp. 346-351.

Iemitsu, M., Miyauchi, T., Maeda, S., Sakai, S., Fujii, N., Miyazaki, H., Kakinuma, Y., Matsuda, M., & Yamaguchi, I. 2003, "Cardiac hypertrophy by hypertension and exercise training exhibits different gene expression of enzymes in energy metabolism", *Hypertens Res*, vol. **26**, no. 10, pp. 829-837.

Ikeuchi, M., Tsutsui, H., Shiomi, T., Matsusaka, H., Matsushima, S., Wen, J., Kubota, T., & Takeshita, A. 2004, "Inhibition of TGF-beta signaling exacerbates early cardiac dysfunction but prevents late remodeling after infarction", *Cardiovasc Res*, vol. **64**, no. 3, pp. 526-535.

Innes, B. A., McLaughlin, M. G., Kapuscinski, M. K., Jacob, H. J., & Harrap, S. B. 1998, "Independent genetic susceptibility to cardiac hypertrophy in inherited hypertension", *Hypertension*, vol. **31**, no. 3, pp. 741-746.

Inomata, H., Watanabe, T., Iizuka, Y., Liang, Y. Q., Mashimo, T., Nabika, T., Ikeda, K., Yanai, K., Gotoda, T., Yamori, Y., Isobe, M., & Kato, N. 2005, "Identification of quantitative trait loci for cardiac hypertrophy in two different strains of the spontaneously hypertensive rat", *Hypertens Res*, vol. **28**, no. 3, pp. 273-281.

Irizarry, R. A., Ooi, S. L., Wu, Z., & Boeke, J. D. 2003, "Use of mixture models in a microarray-based screening procedure for detecting differentially represented yeast mutants", *Stat.Appl.Genet Mol Biol* , vol. **2**, no. 1, p. Article1.

Iwamoto, R., Yamazaki, S., Asakura, M., Takashima, S., Hasuwa, H., Miyado, K., Adachi, S., Kitakaze, M., Hashimoto, K., Raab, G., Nanba, D., Higashiyama, S., Hori, M., Klagsbrun, M., & Mekada, E. 2003, "Heparin-binding EGF-like growth factor and ErbB signaling is essential for heart function", *Proc.Natl.Acad.Sci.U.S.A*, vol. **100**, no. 6, pp. 3221-3226.

Jacob, H. J., Lindpaintner, K., Lincoln, S. E., Kusumi, K., Bunker, R. K., Mao, Y. P., Ganten, D., Dzau, V. J., & Lander, E. S. 1991, "Genetic mapping of a gene causing hypertension in the stroke-prone spontaneously hypertensive rat", *Cell*, vol. **67**, no. 1, pp. 213-224.

Jacob, H. J., Brown, D. M., Bunker, R. K., Daly, M. J., Dzau, V. J., Goodman, A., Koike, G., Kren, V., Kurtz, T., Lernmark, A., & . 1995, "A genetic linkage map of the laboratory rat, Rattus norvegicus", *Nat.Genet*, vol. **9**, no. 1, pp. 63-69.

Jansen, R. C. 1993, "Interval mapping of multiple quantitative trait loci", *Genetics*, vol. **135**, no. 1, pp. 205-211.

Jeffs, B., Negrin, C. D., Graham, D., Clark, J. S., Anderson, N. H., Gauguier, D., & Dominiczak, A. F. 2000, "Applicability of a "Speed" Congenic Strategy to Dissect Blood

Pressure Quantitative Trait Loci on Rat Chromosome 2", *Hypertension*, vol. **35**, no. 1, pp. 179-187.

Jiang, C. & Zeng, Z. B. 1995, "Multiple trait analysis of genetic mapping for quantitative trait loci", *Genetics*, vol. **140**, no. 3, pp. 1111-1127.

John, S. W., Krege, J. H., Oliver, P. M., Hagaman, J. R., Hodgin, J. B., Pang, S. C., Flynn, T. G., & Smithies, O. 1995, "Genetic decreases in atrial natriuretic peptide and salt-sensitive hypertension", *Science*, vol. 267, no. 5198, pp. 679-681.

Jongbloed, R. J., Marcelis, C. L., Doevendans, P. A., Schmeitz-Mulkens, J. M., Van Dockum, W. G., Geraedts, J. P., & Smeets, H. J. 2003, "Variable clinical manifestation of a novel missense mutation in the alpha-tropomyosin (TPM1) gene in familial hypertrophic cardiomyopathy", *J Am Coll.Cardiol.*, vol. **41**, no. 6, pp. 981-986.

Jones, E. F., Harrap, S. B., Calafiore, P., & Tonkin, A. M. 1992, "Development and validation of echocardiographic methods for estimating left ventricular mass in rats", *Clin Exp Pharmacol Physiol*, vol. **19**, no. 5, pp. 361-364.

Ju, H. & Dixon, I. M. 1996, "Extracellular matrix and cardiovascular diseases", *Can.J Cardiol.*, vol. **12**, no. 12, pp. 1259-1267.

Julier, C., Delepine, M., Keavney, B., Terwilliger, J., Davis, S., Weeks, D. E., Bui, T., Jeunemaitre, X., Velho, G., Froguel, P., Ratcliffe, P., Corvol, P., Soubrier, F., & Lathrop, G. M. 1997, "Genetic susceptibility for human familial essential hypertension in a region of homology with blood pressure linkage on rat chromosome 10", *Hum Mol Genet*, vol. **6**, no. 12, pp. 2077-2085.

Kaganovsky, E., Belkin, V., Barhum, Y., Schaper, J., Schaper, W., & Kessler-Icekson, G. 2001, "Occurrence and distribution of atrial natriuretic peptide-containing cells in the left ventricle of hypertensive rats. Effect of antihypertensive treatment", *Cell Tissue Res*, vol. **303**, no. 1, pp. 57-67.

Kannel, W. B., Gordon, T., Castelli, W. P., & Margolis, J. R. 1970, "Electrocardiographic left ventricular hypertrophy and risk of coronary heart disease. The Framingham study", *Annals of Internal Medicine*, vol. **72**, no. 6, pp. 813-822.

Kannel, W. B. 1983, "Prevalence and natural history of electrocardiographic left ventricular hypertrophy", *Am J Med*, vol. **75**, no. 3A, pp. 4-11.

Kannel, W. B. & Wilson, P. W. 1995, "Risk factors that attenuate the female coronary disease advantage", *Arch.Intern Med*, vol. **155**, no. 1, pp. 57-61.

Karet, F. E. & Lifton, R. P. 1997, "Mutations contributing to human blood pressure variation", *Recent Prog.Horm.Res*, vol. **52**, pp. 263-276.

Katoh, Y., Klein, K. L., Kaplan, R. A., Sanborn, W. G., & Kurokawa, K. 1981, "Parathyroid hormone has a positive inotropic action in the rat", *Endocrinology*, vol. **109**, no. 6, pp. 2252-2254.

Kim, S. D. & Piano, M. R. 2000, "The Natriuretic Peptides: Physiology and Role in Left-Ventricular Dysfunction", *Biological Research For Nursing*, vol. **2**, no. 1, pp. 15-29.

Kishimoto, I., Rossi, K., & Garbers, D. L. 2001, "A genetic model provides evidence that the receptor for atrial natriuretic peptide (guanylyl cyclase-A) inhibits cardiac ventricular myocyte hypertrophy", *Proc.Natl.Acad.Sci.U.S.A*, vol. **98**, no. 5, pp. 2703-2706.

Kloss, S., Rodenbach, D., Bordel, R., & Mulsch, A. 2005, "Human-antigen R (HuR) expression in hypertension: downregulation of the mRNA stabilizing protein HuR in genetic hypertension", *Hypertension*, vol. **45**, no. 6, pp. 1200-1206.

Knapp, S. J. & Bridges, W. C. 1990, "Using molecular markers to estimate quantitative trait locus parameters: power and genetic variances for unreplicated and replicated progeny", *Genetics*, vol. **126**, no. 3, pp. 769-777.

Knowles, J. W., Esposito, G., Mao, L., Hagaman, J. R., Fox, J. E., Smithies, O., Rockman, H. A., & Maeda, N. 2001, "Pressure-independent enhancement of cardiac hypertrophy in natriuretic peptide receptor A-deficient mice", *J Clin Invest*, vol. **107**, no. 8, pp. 975-984.

Kong, S. W., Bodyak, N., Yue, P., Liu, Z., Brown, J., Izumo, S., & Kang, P. M. 2005, "Genetic expression profiles during physiological and pathological cardiac hypertrophy and heart failure in rats", *Physiol Genomics*, vol. **21**, no. 1, pp. 34-42.

Kong, S. W., Bodyak, N., Yue, P., Liu, Z., Brown, J., Izumo, S., & Kang, P. M. 2005, "Genetic expression profiles during physiological and pathological cardiac hypertrophy and heart failure in rats", *Physiological Genomics*, vol. **21**, no. 1, pp. 34-42.

Koren, M. J., Devereux, R. B., Casale, P. N., Savage, D. D., & Laragh, J. H. 1991, "Relation of left ventricular mass and geometry to morbidity and mortality in uncomplicated essential hypertension", *Annals of Internal Medicine*, vol. **114**, no. 5, pp. 345-352.

Kurisu, S., Ozono, R., Oshima, T., Kambe, M., Ishida, T., Sugino, H., Matsuura, H., Chayama, K., Teranishi, Y., Iba, O., Amano, K., & Matsubara, H. 2003, "Cardiac angiotensin II type 2 receptor activates the kinin/NO system and inhibits fibrosis", *Hypertension*, vol. **41**, no. 1, pp. 99-107.

Kurtz T.W., St Letzin, E.M . & Pravenet M. 1994,"Development of hypertension strains", in *Textbook of Hypertension*, ed. Swales, J.D. Ch.22A, pp441-447. Oxford: Blackwell.

Lander, E. S. & Botstein, D. 1989, "Mapping mendelian factors underlying quantitative traits using RFLP linkage maps", *Genetics*, vol. **121**, no. 1, pp. 185-199.

Lander, E. S. & Schork, N. J. 1994, "Genetic dissection of complex traits", *Science*, vol. **265**, no. 5181, pp. 2037-2048.

Landry, D. W., Levin, H. R., Gallant, E. M., Ashton, R. C., Jr., Seo, S., D'Alessandro, D., Oz, M. C., & Oliver, J. A. 1997, "Vasopressin deficiency contributes to the vasodilation of septic shock", *Circulation*, vol. 95, no. 5, pp. 1122-1125.

Lane, D. A. & Lip, G. Y. H. 2001, "Ethnic differences in hypertension and blood pressure control in the UK", *QJM*, vol. **94**, no. 7, pp. 391-396.

Langenickel, T. H., Pagel, I., Buttgereit, J., Tenner, K., Lindner, M., Dietz, R., Willenbrock, R., & Bader, M. 2004, "Rat corin gene: molecular cloning and reduced expression in experimental heart failure", *AJP - Heart and Circulatory Physiology*, vol. **287**, no. 4, p. H1516-H1521.

Lauffenburger, D. A., Oehrtman, G. T., Walker, L., & Wiley, H. S. 1998, "Real-time quantitative measurement of autocrine ligand binding indicates that autocrine loops are spatially localized", *Proc.Natl.Acad.Sci.U.S.A*, vol. **95**, no. 26, pp. 15368-15373.

Laurent, D., Allergrini, P. R., & Zierhut, W. 1995, "Different left ventricular remodelling and function in two models of pressure overload as assessed in vivo by magnetic resonance imaging", *J Hypertens*, vol. **13**, no. 6, pp. 693-700.

Lavoie, J. L. & Sigmund, C. D. 2003, "Minireview: Overview of the Renin-Angiotensin System--An Endocrine and Paracrine System", *Endocrinology*, vol. **144**, no. 6, pp. 2179-2183.

Lee, L. G., Connell, C. R., & Bloch, W. 1993, "Allelic discrimination by nick-translation PCR with fluorogenic probes", *Nucleic Acids Res*, vol. **21**, no. 16, pp. 3761-3766.

Levin, A. & Li, Y. C. 2005, "Vitamin D and its analogues: do they protect against cardiovascular disease in patients with kidney disease?", *Kidney Int.*, vol. **68**, no. 5, pp. 1973-1981.

Levy, D., Garrison, R. J., Savage, D. D., Kannel, W. B., & Castelli, W. P. 1990, "Prognostic implications of echocardiographically determined left ventricular mass in the Framingham Heart Study", *N.Engl.J Med*, vol. **322**, no. 22, pp. 1561-1566.

Levy, D., Wilson, P. W., Anderson, K. M., & Castelli, W. P. 1990, "Stratifying the patient at risk from coronary disease: new insights from the Framingham Heart Study", *Am Heart J*, vol. **119**, no. 3 Pt 2, pp. 712-717.

Lewontin, R. C. 1972, "The apportionment of human diversity", *Evol Biol*, vol. **6**, pp. 381-398.

Li, M., Ma, J., Cheng, R., Dupont, R., Williams, N., Crews, K., Payne, T., & Elston, R. 2003, "A genome-wide scan to identify loci for smoking rate in the Framingham Heart Study population", *BMC Genetics*, vol. **4**, no. Suppl 1, p. S103.

Lifton, R. P., Dluhy, R. G., Powers, M., Rich, G. M., Cook, S., Ulick, S., & Lalouel, J. M. 1992, "A chimaeric 11 beta-hydroxylase/aldosterone synthase gene causes glucocorticoid-remediable aldosteronism and human hypertension", *Nature*, vol. **355**, no. 6357, pp. 262-265.

Lifton, R. P., Dluhy, R. G., Powers, M., Ulick, S., & Lalouel, J. M. 1992, "The molecular basis of glucocorticoid-remediable aldosteronism, a Mendelian cause of human hypertension", *Trans.Assoc.Am Physicians*, vol. **105**, pp. 64-71.

Lifton, R. P. 1995, "Genetic determinants of human hypertension", *Proc.Natl.Acad.Sci.U.S.A*, vol. **92**, no. 19, pp. 8545-8551.

Lifton, R. P. 1996, "Molecular genetics of human blood pressure variation", *Science*, vol. **272**, no. 5262, pp. 676-680.

Lim, J. Y., Park, S. J., Hwang, H. Y., Park, E. J., Nam, J. H., Kim, J., & Park, S. I. 2005, "TGF-beta1 induces cardiac hypertrophic responses via PKC-dependent ATF-2 activation", *J Mol Cell Cardiol.*, vol. **39**, no. 4, pp. 627-636.

Lindpaintner, K. 1992, "Genetic linkage analysis in hypertension: principles and practice", *J Hypertens*, vol. **10**, no. 2, pp. 121-124.

Linzbach, A. J. 1960, "Heart failure from the point of view of quantitative anatomy", *Am J Cardiol.*, vol. **5**, pp. 370-382.

Lip, G. Y. & Beevers, D. G. 1995, "Alcohol, hypertension, coronary disease and stroke", *Clin Exp Pharmacol Physiol*, vol. **22**, no. 3, pp. 189-194.

Lipshutz, R. J., Fodor, S. P., Gingeras, T. R., & Lockhart, D. J. 1999, "High density synthetic oligonucleotide arrays", *Nat.Genet*, vol. **21**, no. 1 Suppl, pp. 20-24.

Livak, K. J., Flood, S. J., Marmaro, J., Giusti, W., & Deetz, K. 1995, "Oligonucleotides with fluorescent dyes at opposite ends provide a quenched probe system useful for detecting PCR product and nucleic acid hybridization", *PCR Methods Appl.*, vol. **4**, no. 6, pp. 357-362.

Llamas, B., Jiang, Z., Rainville, M. L., Picard, S., & Deschepper, C. F. 2005, "Distinct QTLs are linked to cardiac left ventricular mass in a sex-specific manner in a normotensive inbred rat inter-cross", *Mamm.Genome*, vol. **16**, no. 9, pp. 700-711.

Loganathan, R., Bilgen, M., Al Hafez, B., & Smirnova, I. V. 2006, "Characterization of alterations in diabetic myocardial tissue using high resolution MRI", *Int.J Cardiovasc Imaging*, vol. **22**, no. 1, pp. 81-90.

London, G. M., Fabiani, F., Marchais, S. J., de Vernejoul, M. C., Guerin, A. P., Safar, M. E., Metivier, F., & Llach, F. 1987, "Uremic cardiomyopathy: an inadequate left ventricular hypertrophy", *Kidney Int.*, vol. **31**, no. 4, pp. 973-980.

Lovenberg, W. 1987, "Animal models for hypertension research", *Prog.Clin Biol Res*, vol. **229**, pp. 225-240.

Luft, F. C. 1999, "Bad genes, good people, association, linkage, longevity and the prevention of cardiovascular disease", *Clinical and Experimental Pharmacology and Physiology*, vol. 26, no. 7, pp. 576-579.

Lyons, L. A., Laughlin, T. F., Copeland, N. G., Jenkins, N. A., Womack, J. E., & O'Brien, S. J. 1997, "Comparative anchor tagged sequences (CATS) for integrative mapping of mammalian genomes", *Nat.Genet*, vol. **15**, no. 1, pp. 47-56.

Maducll, F., Navarro, V., Torregrosa, E., Rius, A., Dicenta, F., Cruz, M. C., & Ferrero, J. A. 2003, "Change from three times a week on-line hemodiafiltration to short daily on-line hemodiafiltration", *Kidney International*, vol. **64**, no. 1, pp. 305-313.

Mann, G. V., Roels, A. A., Price, D. L., & Merrill, J. M. 1962, "Cardiovascular disease in African pygmies", *J Chron Dis*, vol. **15**, pp. 341-371.

Mann, G. V., Shafer, R., Anderson, R. S., & Stanstead, H. H. 1964, "Cardiovascular disease in the Masai", *J Atherosclerosis Res*, vol. **4**, pp. 289-312.

Manning, W. J., Wei, J. Y., Fossel, E. T., & Burstein, D. 1990, "Measurement of left ventricular mass in rats using electrocardiogram-gated magnetic resonance imaging", *Am J Physiol*, vol. **258**, no. 4 Pt 2, p. H1181-H1186.

Mansfield, T. A., Simon, D. B., Farfel, Z., Bia, M., Tucci, J. R., Lebel, M., Gutkin, M., Vialettes, B., Christofilis, M. A., Kauppinen-Makelin, R., Mayan, H., Risch, N., & Lifton, R. P. 1997, "Multilocus linkage of familial hyperkalaemia and hypertension, pseudohypoaldosteronism type II, to chromosomes 1q31-42 and 17p11-q21", *Nat.Genet*, vol. **16**, no. 2, pp. 202-205.

Marcus, R., Krause, L., Weder, A. B., Dominguez-Meja, A., Schork, N. J., & Julius, S. 1994, "Sex-specific determinants of increased left ventricular mass in the Tecumseh Blood Pressure Study", *Circulation* , vol. **90**, no. 2, pp. 928-936.

Markel, P. D., Fulker, D. W., Bennett, B., Corley, R. P., DeFries, J. C., Erwin, V. G., & Johnson, T. E. 1996, "Quantitative trait loci for ethanol sensitivity in the LS x SS recombinant inbred strains: interval mapping", *Behav.Genet*, vol. **26**, no. 4, pp. 447-458.

Maron, B. J., Gardin, J. M., Flack, J. M., Gidding, S. S., Kurosaki, T. T., & Bild, D. E. 1995, "Prevalence of Hypertrophic Cardiomyopathy in a General Population of Young Adults : Echocardiographic Analysis of 4111 Subjects in the CARDIA Study", *Circulation*, vol. **92**, no. 4, pp. 785-789.

Masaki, H., Kurihara, T., Yamaki, A., Inomata, N., Nozawa, Y., Mori, Y., Murasawa, S., Kizima, K., Maruyama, K., Horiuchi, M., Dzau, V. J., Takahashi, H., Iwasaka, T., Inada, M., & Matsubara, H. 1998, "Cardiac-specific overexpression of angiotensin II AT2

receptor causes attenuated response to AT1 receptor-mediated pressor and chronotropic effects", *J Clin Invest*, vol. **101**, no. 3, pp. 527-535.

Masciotra, S., Picard, S., & Deschepper, C. F. 1999, "Cosegregation Analysis in Genetic Crosses Suggests a Protective Role for Atrial Natriuretic Factor Against Ventricular Hypertrophy", *Circulation Research*, vol. **84**, no. 12, pp. 1453-1458.

Masubuchi, Y., Kumai, T., Uematsu, A., Komoriyama, K., & Hirai, M. 1982, "Gonadectomy-induced reduction of blood pressure in adult spontaneously hypertensive rats", *Acta Endocrinol (Copenh)*, vol. 101, no. 1, pp. 154-160.

Matsumoto, K., Yamada, T., Natori, T., Ikeda, K., Yamada, J., & Yamori, Y. 1991, "Genetic variability in SHR (SHRSR), SHRSP and WKY strains", *Clin Exp Hypertens A*, vol. **13**, no. 5, pp. 925-938.

Mauviel, A., Qiu, C. Y., Dong, W., Evans, C. H., & Uitto, J. 1993, "Transcriptional interactions of transforming growth-factor-beta with pro-inflammatory cytokines", *Curr Biol*, vol. **3**, no. 12, pp. 822-831.

McBride, M. W., Carr, F. J., Graham, D., Anderson, N. H., Clark, J. S., Lee, W. K., Charchar, F. J., Brosnan, M. J., & Dominiczak, A. F. 2003, "Microarray analysis of rat chromosome 2 congenic strains", *Hypertension*, vol. **41**, no. 3 Pt 2, pp. 847-853.

McIntyre, M., Hamilton, C. A., Rees, D. D., Reid, J. L., & Dominiczak, A. F. 1997, "Sex Differences in the Abundance of Endothelial Nitric Oxide in a Model of Genetic Hypertension", *Hypertension*, vol. **30**, no. 6, pp. 1517-1524.

Medina, A., Bodick, N., Goldberger, A. L., Mahon, M. M., & Lipsitz, L. A. 1997, "Effects of Central Muscarinic-1 Receptor Stimulation on Blood Pressure Regulation", *Hypertension*, vol. **29**, no. 3, pp. 828-834.

Mein, C. A., Caulfield, M. J., Dobson, R. J., & Munroe, P. B. 2004, "Genetics of essential hypertension", *Hum.Mol.Genet*, vol. **13** Spec No 1, p. R169-R175.

Merin, R. G. 1975, "Effect of anesthetics on the heart", *Surg.Clin North Am*, vol. **55**, no. 4, pp. 759-774.

Merlo, J., Asplund, K., Lynch, J., Rastam, L., & Dobson, A. 2004, "Population Effects on Individual Systolic Blood Pressure: A Multilevel Analysis of the World Health Organization MONICA Project", *American Journal of Epidemiology*, vol. **159**, no. 12, pp. 1168-1179.

Messerli, F. H. 1983, "Clinical determinants and consequences of left ventricular hypertrophy", *Am J Med*, vol. **75**, no. 3A, pp. 51-56.

Meyer, P. 1965, "[The renin-angiotensin system]", *Pathol.Biol*, vol. **13**, no. 19, pp. 934-939.

Miall, W. E., Kass, E. H., Ling, J., & Stuart, E. L. 1962, "Factors influencing arterial blood pressures in the general population in Jamaica", *BMJ*, vol. **2**, pp. 497-506.

Mikhail, N. & Cope, D. 2004, "The JNC-7 guidelines and the optimal target for systolic blood pressure", *Hypertension*, vol. **43**, no. 5, p. e31.

Mongeau, J. G., Biron, P., & Sing, C. F. 1986, "The influence of genetics and household environment upon the variability of normal blood pressure: the Montreal Adoption Survey", *Clin Exp Hypertens A*, vol. **8**, no. 4-5, pp. 653-660.

Mongeau, J. G. 1989, "Heredity and blood pressure", *Semin.Nephrol*, vol. **9**, no. 3, pp. 208-216.

Mori, T., Chen, Y. F., Feng, J. A., Hayashi, T., Oparil, S., & Perry, G. J. 2004, "Volume overload results in exaggerated cardiac hypertrophy in the atrial natriuretic peptide knockout mouse", *Cardiovasc Res*, vol. **61**, no. 4, pp. 771-779.

Morrison, A. C., Cooper, R., Hunt, S., Lewis, C. E., Luke, A., Mosley, T. H., & Boerwinkle, E. 2004, "Genome scan for hypertension in nonobese African Americans: The national heart, lung, and blood institute family blood pressure program", *American Journal of Hypertension*, vol. **17**, no. 9, pp. 834-838.

Mulatero, P., Veglio, F., Pilon, C., Rabbia, F., Zocchi, C., Limone, P., Boscaro, M., Sonino, N., & Fallo, F. 1998, "Diagnosis of Glucocorticoid-Remediable Aldosteronism in Primary Aldosteronism: Aldosterone Response to Dexamethasone and Long Polymerase Chain Reaction for Chimeric Gene", *Journal of Clinical Endocrinology Metabolism*, vol. **83**, no. 7, pp. 2573-2575.

Mune, T., Rogerson, F. M., Nikkila, H., Agarwal, A. K., & White, P. C. 1995, "Human hypertension caused by mutations in the kidney isozyme of 11 beta-hydroxysteroid dehydrogenase", *Nat.Genet*, vol. **10**, no. 4, pp. 394-399.

Nabika, T., Nara, Y., Ikeda, K., Endo, J., & Yamori, Y. 1991, "Genetic heterogeneity of the spontaneously hypertensive rat", *Hypertension*, vol. **18**, no. 1, pp. 12-16.

Nabika, T., Ito, T., Kitada, K., Serikawa, T., Mashimo, T., Soubrier, F., Julier, C., Ohno, Y., Saruta, T., Tanase, H., Masuda, J., Yamori, Y., & Nara, Y. 1997, "Comparative mapping of novel simple sequence repeat markers in a hypertension-related region on rat chromosome 1", *Mamm.Genome*, vol. **8**, no. 3, pp. 215-217.

Nabika, T., Kobayashi, Y., & Yamori, Y. 2000, "Congenic Rats For Hypertension: How Useful Are They For The Hunting Of Hypertension Genes?", *Clinical and Experimental Pharmacology and Physiology*, vol. **27**, no. 4, pp. 251-256.

Nadeau, J. H. 1989, "Maps of linkage and synteny homologies between mouse and man", *Trends Genet*, vol. **5**, no. 3, pp. 82-86.

Nagaoka, A., Iwatsuka, H., Suzuoki, Z., & Okamoto, K. 1976, "Genetic predisposition to stroke in spontaneously hypertensive rats", *AJP - Legacy*, vol. **230**, no. 5, pp. 1354-1359.

Nahrendorf, M., Hiller, K.-H., Hu, K., Ertl, G., Haase, A., & Bauer, W. R. 2003, "Cardiac magnetic resonance imaging in small animal models of human heart failure", *Medical Image Analysis*, vol. **7**, no. 3, pp. 369-375.

Nara, Y., Nabika, T., Ikeda, K., Sawamura, M., Endo, J., & Yamori, Y. 1991, "Blood pressure cosegregates with a microsatellite of angiotensin I converting enzyme (ACE) in F2 generation from a cross between original normotensive Wistar-Kyoto rat (WKY) and stroke-prone spontaneously hypertensive rat (SHRSP)", *Biochem.Biophys.Res Commun.*, vol. **181**, no. 3, pp. 941-946.

Nash, W. G. & O'Brien, S. J. 1982, "Conserved regions of homologous G-banded chromosomes between orders in mammalian evolution: carnivores and primates", *Proc.Natl.Acad.Sci.U.S.A*, vol. **79**, no. 21, pp. 6631-6635.

Naveh-Many, T., Bell, O., Silver, J., & Kilav, R. 2002, "Cis and trans acting factors in the regulation of parathyroid hormone (PTH) mRNA stability by calcium and phosphate", *FEBS Lett.*, vol. **529**, no. 1, pp. 60-64.

Nunez, D. J., Clifford, C. P., al Mahdawi, S., & Dutka, D. 1996, "Hypertensive cardiac hypertrophy--is genetic variance the missing link?", *Br.J Clin Pharmacol*, vol. **42**, no. 1, pp. 107-117.

Oakey, R. J., Watson, M. L., & Seldin, M. F. 1992, "Construction of a physical map on mouse and human chromosome 1: comparison of 13 Mb of mouse and 11 Mb of human DNA", *Hum Mol Genet*, vol. 1, no. **8**, pp. 613-620.

Ogawa, Y., Nakao, K., Mukoyama, M., Hosoda, K., Shirakami, G., Arai, H., Saito, Y., Suga, S., Jougasaki, M., & Imura, H. 1991, "Natriuretic peptides as cardiac hormones in normotensive and spontaneously hypertensive rats. The ventricle is a major site of synthesis and secretion of brain natriuretic peptide", *Circulation Research*, vol. **69**, no. 2, pp. 491-500.

Okamoto, K. & Aoki, K. 1963, "Development of a strain of spontaneously hypertensive rats", *Jpn.Circ J*, vol. **27**, pp. 282-293.

Oldham, P. D., Pickering, G., Roberts, J. A., & Sowry, G. S. 1960, "The nature of essential hypertension", *Lancet*, vol. **1**, pp. 1085-1093.

Oostlander, A. E., Meijer, G. A., & Ylstra, B. 2004, "Microarray-based comparative genomic hybridization and its applications in human genetics", *Clinical Genetics*, vol. **66**, no. 6, pp. 488-495.

Ordunez-Garcia, P. O., Espinosa-Brito, A. D., & Cooper, R. S. 1998, "Hypertension in Cuba: Evidence of a narrow African-white difference", *J Hum Hypertens*, vol. **12**, pp. 111-116.

Park, C. W., Oh, Y. S., Shin, Y. S., Kim, C. M., Kim, Y. S., Kim, S. Y., Choi, E. J., Chang, Y. S., & Bang, B. K. 1999, "Intravenous calcitriol regresses myocardial hypertrophy in hemodialysis patients with secondary hyperparathyroidism", *Am J Kidney Dis*, vol. **33**, no. 1, pp. 73-81.

Parzy, E., Fromes, Y., Wary, C., Vignaux, O., Giacomini, E., Leroy-Willig, A., & Carlier, P. G. 2003, "Ultrafast multiplanar determination of left ventricular hypertrophy in spontaneously hypertensive rats with single-shot spin-echo nuclear magnetic resonance imaging", *J Hypertens*, vol. **21**, no. 2, pp. 429-436.

Pease, A. C., Solas, D., Sullivan, E. J., Cronin, M. T., Holmes, C. P., & Fodor, S. P. 1994, "Light-generated oligonucleotide arrays for rapid DNA sequence analysis", *Proc.Natl.Acad.Sci.U.S.A*, vol. **91**, no. 11, pp. 5022-5026.

Perera, G. A., Gearing, F. R., & Schweitzer, M. D. 1972, "A family study of primary hypertension--final report", *J Chronic Dis*, vol. **25**, no. 3, pp. 127-132.

Pfeffer, J. M., Pfeffer, M. A., Mirsky, I., & Braunwald, E. 1982, "Regression of left ventricular hypertrophy and prevention of left ventricular dysfunction by captopril in the spontaneously hypertensive rat", *Proc.Natl.Acad.Sci.U.S.A*, vol. **79**, no. 10, pp. 3310-3314.

Pfeufer, A., Busjahn, A., Vergopoulos, A., Knoblauch, H., Urata, H., Osterziel, K. J., Menz, M., Wienker, T. F., Faulhaber, H. D., & Steinmetz, A. 1998, "Chymase gene locus is not associated with myocardial infarction and is not linked to heart size or blood pressure", *The American Journal of Cardiology*, vol. **82**, no. 8, pp. 979-981.

Pickering, G. 1965, "Hypertension: natural history, diagnosis, prognosis and management", *Med Times*, vol. **93**, pp. 939-955.

Piepho, H. P. 2001, "A quick method for computing approximate thresholds for quantitative trait loci detection", *Genetics*, vol. **157**, no. 1, pp. 425-432.

Pines, A., Fisman, E. Z., Shapira, I., Drory, Y., Weiss, A., Eckstein, N., Levo, Y., Averbuch, M., Motro, M., Rotmensch, H. H., & Ayalon, D. 1996, "Exercise echocardiography in postmenopausal hormone users with mild systemic hypertension", *Am J Cardiol.*, vol. **78**, no. 12, pp. 1385-1389.

Poetz, O., Schwenk, J. M., Kramer, S., Stoll, D., Templin, M. F., & Joos, T. O. 2005, "Protein microarrays: catching the proteome", *Mechanisms of Ageing and Development*, vol. **126**, no. 1, pp. 161-170.

Porter, K.R., Bonneville, M. A. 1973, in "An Introduction to the Fine Structure of Cells and Tissues", 4th edition, Philadelphia, PA: Lea & Febiger.

Poulter, N., Khaw, K. T., Hopwood, B. E. C., Mugambi, M., Peart, W. S., & Sever, P. S. 1984, "Salt and blood pressure in various populations", *J Cardiovasc Pharmacol*, vol. **6**, p. S197-S203.

Poulter, N. R., Khaw, K. T., & Hopwood, B. E. 1990, "The Kenyan Luo migration study: Observations on the initiation of a rise in blood pressure", *BMJ*, vol. **300**, pp. 967-972.

Prabhakar, R., Boivin, G. P., Grupp, I. L., Hoit, B., Arteaga, G., Solaro, J. R., & Wieczorek, D. F. 2001, "A familial hypertrophic cardiomyopathy alpha-tropomyosin mutation causes severe cardiac hypertrophy and death in mice", *J Mol Cell Cardiol.*, vol. **33**, no. 10, pp. 1815-1828.

Prakash, E. S., Madanmohan, & Pal, G. K. 2004, "What is the ultimate goal in neural regulation of cardiovascular function?", *Advances in Physiology Education*, vol. 28, no. 3, pp. 100-101.

Pravenec, M., Gauguier, D., Schott, J. J., Buard, J., Kren, V., Bila, V., Szpirer, C., Szpirer, J., Wang, J. M., Huang, H., & . 1995, "Mapping of quantitative trait loci for blood pressure and cardiac mass in the rat by genome scanning of recombinant inbred strains", *J Clin Invest*, vol. **96**, no. 4, pp. 1973-1978.

Pravenec, M., Gauguier, D., Schott, J. J., Buard, J., Kren, V., Bila, V., Szpirer, C., Szpirer, J., Wang, J. M., Huang, H., St Lezin, E., Spence, M. A., Flodman, P., Printz, M., Lathrop, G. M., Vergnaud, G., & Kurtz, T. W. 1996, "A genetic linkage map of the rat derived from recombinant inbred strains", *Mamm.Genome*, vol. 7, no. 2, pp. 117-127.

Pravenec, M., Zidek, V., Simakova, M., Kren, V., Krenova, D., Horky, K., Jachymova, M., Mikova, B., Kazdova, L., Aitman, T. J., Churchill, P. C., Webb, R. C., Hingarh, N. H., Yang, Y., Wang, J. M., Lezin, E. M., & Kurtz, T. W. 1999, "Genetics of Cd36 and the clustering of multiple cardiovascular risk factors in spontaneous hypertension", *J Clin Invest*, vol. **103**, no. 12, pp. 1651-1657.

Pripp, U., Hall, G., Csemiczky, G., Eksborg, S., Landgren, B. M., & Schenck-Gustafsson, K. 1999, "A randomized trial on effects of hormone therapy on ambulatory blood pressure and lipoprotein levels in women with coronary artery disease", *J Hypertens*, vol. **17**, no. 10, pp. 1379-1386.

Rajan, S., Williams, S. S., Jagatheesan, G., Ahmed, R. P., Fuller-Bicer, G., Schwartz, A., Aronow, B. J., & Wieczorek, D. F. 2006, "Micrarray analysis of gene expression during early stages of mild and severe cardiac hypertrophy", *Physiological Genomics*, vol. 26, no.3, pp. 72-102.

Rapp, J. P. 1983, "A paradigm for identification of primary genetic causes of hypertension in rats", *Hypertension*, vol. **5**, no. 2 Pt 2, p. I198-I203.

Rapp, J. P. 1991, "Dissecting the primary causes of genetic hypertension in rats", *Hypertension*, vol. **18**, no. 3 Suppl, p. I18-I28.

Rapp, J. P., Garrett, M. R., & Deng, A. Y. 1998, "Construction of a double congenic strain to prove an epistatic interaction on blood pressure between rat chromosomes 2 and 10", *J Clin Invest*, vol. **101**, no. 8, pp. 1591-1595.

Rapp, J. P. 2000, "Genetic Analysis of Inherited Hypertension in the Rat", *Physiological Reviews*, vol. **80**, no. 1, pp. 135-172.

Ray, K., Wang, X. K., Zhao, M., & Cooke, N. E. 1991, "The rat vitamin D binding protein (Gc-globulin) gene. Structural analysis, functional and evolutionary correlations", *J Biol Chem.*, vol. **266**, no. 10, pp. 6221-6229.

Reckelhoff, J. F., Zhang, H., & Granger, J. P. 1998, "Testosterone exacerbates hypertension and reduces pressure-natriuresis in male spontaneously hypertensive rats", *Hypertension*, vol. **31**, no. 1 Pt 2, pp. 435-439.

Reckelhoff, J. F., Zhang, H., Srivastava, K., & Granger, J. P. 1999, "Gender differences in hypertension in spontaneously hypertensive rats: role of androgens and androgen receptor", *Hypertension*, vol. **34**, no. 4 Pt 2, pp. 920-923.

Reckelhoff, J. F., Zhang, H., & Srivastava, K. 2000, "Gender differences in development of hypertension in spontaneously hypertensive rats: role of the renin-angiotensin system", *Hypertension*, vol. **35**, no. 1 Pt 2, pp. 480-483.

Reckelhoff, J. F. 2001, "Gender Differences in the Regulation of Blood Pressure", *Hypertension*, vol. **37**, no. 5, pp. 1199-1208.

Reddy, K. S. 2004, "Cardiovascular disease in non-Western countries", *N.Engl.J Med*, vol. **350**, no. 24, pp. 2438-2440.

Rodriguez, C. J., Sciacca, R. R., Diez-Roux, A. V., Boden-Albala, B., Sacco, R. L., Homma, S., & DiTullio, M. R. 2004, "Relation between socioeconomic status, race-ethnicity, and left ventricular mass: the Northern Manhattan study", *Hypertension*, vol. **43**, no. 4, pp. 775-779.

Rosengren, A., Hawken, S., Ounpuu, S., Sliwa, K., Zubaid, M., Almahmeed, W. A., Blackett, K. N., Sitthi-amorn, C., Sato, H., Yusuf, S., & INTERHEART, i. 2004, "Association of psychosocial risk factors with risk of acute myocardial infarction in 11119 cases and 13648 controls from 52 countries (the INTERHEART study): case-control study", *Lancet*, vol. **364**, no. 9438, pp. 953-962.

Rubattu, S. & Volpe, M. 2001, "The atrial natriuretic peptide: a changing view", *J Hypertens*, vol. **19**, no. 11, pp. 1923-1931.

Rushmer, R. F. 1955, "Initial Phase of Ventricular Systole: Asynchronous Contraction", *AJP - Legacy*, vol. **184**, no. 1, pp. 188-194.

Rysa, J., Leskinen, H., Ilves, M., & Ruskoaho, H. 2005, "Distinct upregulation of extracellular matrix genes in transition from hypertrophy to hypertensive heart failure", *Hypertension*, vol. **45**, no. 5, pp. 927-933.

Saeed, M., Watzinger, N., Krombach, G. A., Lund, G. K., Wendland, M. F., Chujo, M., & Higgins, C. B. 2002, "Left Ventricular Remodeling after Infarction: Sequential MR

Imaging with Oral Nicorandil Therapy in Rat Model", *Radiology*, vol. **224**, no. 3, pp. 830-837.

Sagnella, G. A. 1998, "Measurement and significance of circulating natriuretic peptides in cardiovascular disease", *Clin Sci.(Lond)*, vol. **95**, no. 5, pp. 519-529.

Sahn, D. J., DeMaria, A., Kisslo, J., & Weyman, A. 1978, "Recommendations regarding quantitation in M-mode echocardiography: results of a survey of echocardiographic measurements", *Circulation*, vol. **58**, no. 6, pp. 1072-1083

Samani, N. J., Swales, J. D., Jeffreys, A. J., Morton, D. B., Naftilan, A. J., Lindpaintner, K., Ganten, D., & Brammar, W. J. 1989, "DNA fingerprinting of spontaneously hypertensive and Wistar-Kyoto rats: implications for hypertension research", *J Hypertens*, vol. **7**, no. 10, pp. 809-816.

Samani, N. J. 2003, "Genome scans for hypertension and blood pressure regulation", *American Journal of Hypertension*, vol. **16**, no. 2, pp. 167-171.

Sawyer, J. R. & Hozier, J. C. 1986, "High resolution of mouse chromosomes: banding conservation between man and mouse", *Science*, vol. **232**, no. 4758, pp. 1632-1635.

Schalla, S., Higgins, C. B., Chujo, M., & Saeed, M. 2004, "Effect of potassium-channel opener therapy on reperfused infarction in hypertrophied hearts: demonstration of preconditioning by using functional and contrast-enhanced magnetic resonance imaging", *J Cardiovasc Pharmacol Ther.* , vol. **9**, no. 3, pp. 193-202

Schena, M., Shalon, D., Davis, R. W., & Brown, P. O. 1995, "Quantitative monitoring of gene expression patterns with a complementary DNA microarray", *Science*, vol. **270**, no. 5235, pp. 467-470.

Schena, M. 1996, "Genome analysis with gene expression microarrays", *Bioessays*, vol. **18**, no. 5, pp. 427-431.

Scherthan, H., Seisenberger, C., Greulich, K., & Winnacker, E. L. 1994, "Mapping of the murine nuclear factor I/X gene (Nfix) to mouse chromosome 8 C1-2 by FISH", *Genomics*, vol. **22**, no. 1, pp. 247-249.

Schiekofer, S., Shiojima, I., Sato, K., Galasso, G., Oshima, Y., & Walsh, K. 2006, "Microarray analysis of Akt1 activation in transgenic mouse hearts reveal transcript expression profiles associated with compensatory hypertrophy and failure", *Physiological Genomics*, vol. **26**, no.3, pp. 234-297.

Schillaci, G., Verdecchia, P., Borgioni, C., Ciucci, A., & Porcellati, C. 1998, "Early cardiac changes after menopause", *Hypertension*, vol. **32**, no. 4, pp. 764-769.

Schillaci, G., Verdecchia, P., Porcellati, C., Cuccurullo, O., Cosco, C., & Perticone, F. 2000, "Continuous relation between left ventricular mass and cardiovascular risk in essential hypertension", *Hypertension*, vol. **35**, no. 2, pp. 580-586.

Schlieper, G., Kim, J. H., Molojavyi, A., Jacoby, C., Laussmann, T., Flogel, U., Godecke, A., & Schrader, J. 2004, "Adaptation of the myoglobin knockout mouse to hypoxic stress", *AJP - Regulatory, Integrative and Comparative Physiology*, vol. **286**, no. 4, p. R786-R792.

Schluter, K. D., Weber, M., & Piper, H. M. 1995, "Parathyroid hormone induces protein kinase C but not adenylate cyclase in adult cardiomyocytes and regulates cyclic AMP levels via protein kinase C-dependent phosphodiesterase activity", *Biochem.J*, vol. **310** (Pt 2), pp. 439-444.

Schork, N. J. 1997, "Genetics of complex disease: approaches, problems, and solutions", *Am J Respir.Crit Care Med*, vol. **156**, no. 4 Pt 2, p. S103-S109.

Schwartzkopff, B. & Strauer, B. E. 2000, "Coronary reserve and arteriolosclerosis in hypertensive heart disease", *Z.Kardiol.* , vol. 89 Suppl 9, p. IX/132-IX/135.

Sebkhi, A., Zhao, L., Lu, L., Haley, C. S., Nunez, D. J., & Wilkins, M. R. 1999, "Genetic determination of cardiac mass in normotensive rats: results from an F344xWKY cross", *Hypertension*, vol. **33**, no. 4, pp. 949-953.

Senbonmatsu, T., Ichihara, S., Price E Jr, Gaffney, F. A., & Inagami, T. 2000, "Evidence for angiotensin II type 2 receptor-mediated cardiac myocyte enlargement during in vivo pressure overload", *J Clin Invest*, vol. **106**, no. 3, p. R25-R29.

Sharma, P., Middelberg, R. P., Andrew, T., Johnson, M. R., Christley, H., & Brown, M. J. 2006, "Heritability of left ventricular mass in a large cohort of twins", *J Hypertens*, vol. 24, no. 2, pp. 321-324.

Sharma, U. C., Pokharel, S., Evelo, C. T. A., & Maessen, J. G. 2005, "A systematic review of large scale and heterogeneous gene array data in heart failure", *Journal of Molecular and Cellular Cardiology*, vol. **38**, no. 3, pp. 425-432.

Shen, R., Fan, J. B., Campbell, D., Chang, W., Chen, J., Doucet, D., Yeakley, J., Bibikova, M., Wickham, G. E., McBride, C., Steemers, F., Garcia, F., Kermani, B. G., Gunderson, K., & Oliphant, A. 2005, "High-throughput SNP genotyping on universal bead arrays", *Mutat.Res*, vol. 573, no. 1-2, pp. 70-82.

Shimkets, R. A., Warnock, D. G., Bositis, C. M., Nelson-Williams, C., Hansson, J. H., Schambelan, M., Gill, J. R., Jr., Ulick, S., Milora, R. V., Findling, J. W., & . 1994, "Liddle's syndrome: heritable human hypertension caused by mutations in the beta subunit of the epithelial sodium channel", *Cell*, vol. **79**, no. 3, pp. 407-414.

Shoji, T., Shinohara, K., Kimoto, E., Emoto, M., Tahara, H., Koyama, H., Inaba, M., Fukumoto, S., Ishimura, E., Miki, T., Tabata, T., & Nishizawa, Y. 2004, "Lower risk for cardiovascular mortality in oral 1alpha-hydroxy vitamin D3 users in a haemodialysis population", *Nephrol Dial.Transplant.*, vol. **19**, no. 1, pp. 179-184.

Silva, J. A., Jr., Araujo, R. C., Baltatu, O., Oliveira, S. M., Tschope, C., Fink, E., Hoffmann, S., Plehm, R., Chai, K. X., Chao, L., Chao, J., Ganten, D., Pesquero, J. B., &

Bader, M. 2000, "Reduced cardiac hypertrophy and altered blood pressure control in transgenic rats with the human tissue kallikrein gene", *FASEB J*, vol. **14**, no. 13, pp. 1858-1860.

Siri, F. M., Jelicks, L. A., Leinwand, L. A., & Gardin, J. M. 1997, "Gated magnetic resonance imaging of normal and hypertrophied murine hearts", *Am J Physiol*, vol. **272**, no. 5 Pt 2, p. H2394-H2402.

Slama, M., Ahn, J., Peltier, M., Maizel, J., Chemla, D., Varagic, J., Susic, D., Tribouilloy, C., & Frohlich, E. D. 2005, "Validation of echocardiographic and Doppler indexes of left ventricular relaxation in adult hypertensive and normotensive rats", *AJP - Heart and Circulatory Physiology*, vol. **289**, no. 3, p. H1131-H1136.

Snieder, H., Hayward, C. S., Perks, U., Kelly, R. P., Kelly, P. J., & Spector, T. D. 2000, "Heritability of Central Systolic Pressure Augmentation : A Twin Study", *Hypertension*, vol. **35**, no. 2, pp. 574-579.

Sola, S., White, R. D., & Desai, M. 2006, "MRI of the heart: promises fulfilled?", *Cleve.Clin J Med*, vol. **73**, no. 7, pp. 663-670.

Somsen, R. J. M., Jennings, J. R., & Van der Molen, M. W. 2004, "The cardiac cycle time effect revisited: Temporal dynamics of the central-vagal modulation of heart rate in human reaction time tasks", *Psychophysiology*, vol. **41**, no. 6, pp. 941-953.

Souzeau, E., Llamas, B., Belanger, S., Picard, S., & Deschepper, C. F. 2006, "A genetic locus accentuates the effect of volume overload on adverse left ventricular remodeling in male and female rats", *Hypertension*, vol. **47**, no. 1, pp. 128-133.

Staessen, J., Bulpitt, C. J., Fagard, R., Lijnen, P., & Amery, A. 1989, "The influence of menopause on blood pressure", *J Hum Hypertens*, vol. **3**, no. 6, pp. 427-433.

Stewart, P. M., Krozowski, Z. S., Gupta, A., Milford, D. V., Howie, A. J., Sheppard, M. C., & Whorwood, C. B. 1996, "Hypertension in the syndrome of apparent mineralocorticoid excess due to mutation of the 11 beta-hydroxysteroid dehydrogenase type 2 gene", *Lancet*, vol. **347**, no. 8994, pp. 88-91.

Stober, T., Sen, S., Anstatt, T., Freier, G., & Schimrigk, K. 1985, "Direct evidence of hypertension and the possible role of post-menopause oestrogen deficiency in the pathogenesis of berry aneurysms", *J Neurol.*, vol. **232**, no. 2, pp. 67-72.

Stoll, M., Kwitek-Black, A. E., Cowley, A. W., Jr., Harris, E. L., Harrap, S. B., Krieger, J. E., Printz, M. P., Provoost, A. P., Sassard, J., & Jacob, H. J. 2000, "New target regions for human hypertension via comparative genomics", *Genome Res*, vol. **10**, no. 4, pp. 473-482.

Stubbs, L., Rinchik, E. M., Goldberg, E., Rudy, B., Handel, M. A., & Johnson, D. 1994, "Clustering of six human 11p15 gene homologs within a 500-kb interval of proximal mouse chromosome 7", *Genomics*, vol. **24**, no. 2, pp. 324-332.

Sugino, H., Ozono, R., Kurisu, S., Matsuura, H., Ishida, M., Oshima, T., Kambe, M., Teranishi, Y., Masaki, H., & Matsubara, H. 2001, "Apoptosis is not increased in myocardium overexpressing type 2 angiotensin II receptor in transgenic mice", *Hypertension*, vol. **37**, no. 6, pp. 1394-1398.

Sutherland, D. J., Ruse, J. L., & Laidlaw, J. C. 1966, "Hypertension, increased aldosterone secretion and low plasma renin activity relieved by dexamethasone", *Can.Med Assoc.J*, vol. **95**, no. 22, pp. 1109-1119.

Sutton, A. L. M. & MacDonald, P. N. 2003, "Vitamin D: More Than a "Bone-a-Fide" Hormone", *Molecular Endocrinology*, vol. **17**, no. 5, pp. 777-791.

Swales, J. D. 1994, "Guidelines for treating hypertension: improved care or retarded progress?", *Am J Hypertens*, vol. **7**, no. 10 Pt 1, pp. 873-876.

Swan, G. E. & Carmelli, D. 2002, "Evidence for genetic mediation of executive control: a study of aging male twins", *J Gerontol.B Psychol.Sci.Soc Sci.*, vol. **57**, no. 2, pp. 133-143.

Swan, L., Birnie, D. H., Padmanabhan, S., Inglis, G., Connell, J. M. C., & Hillis, W. S. 2003, "The genetic determination of left ventricular mass in healthy adults", *European Heart Journal*, vol. **24**, no. 6, pp. 577-582.

Takahashi, N. O. B. U. & Smithies, O. L. I. V. 1999, "Gene Targeting Approaches to Analyzing Hypertension", *Journal of the American Society of Nephrology*, vol. **10**, no. 7, pp. 1598-1605.

Takahashi, N., Hagaman, J. R., Kim, H. S., & Smithies, O. 2003, "Minireview: Computer Simulations of Blood Pressure Regulation by the Renin-Angiotensin System", *Endocrinology*, vol. **144**, no. 6, pp. 2184-2190.

Tanase, H., Yamori, Y., Hansen, C. T., & Lovenberg, W. 1982, "Heart size in inbred strains of rats. Part 2. Cardiovascular DNA and RNA contents during the development of cardiac enlargement in rats", *Hypertension*, vol. **4**, no. 6, pp. 872-880.

Teng, M., Wolf, M., Ofsthun, M. N., Lazarus, J. M., Hernan, M. A., Camargo, C. A., Jr., & Thadhani, R. 2005, "Activated injectable vitamin D and hemodialysis survival: a historical cohort study", *Journal of the American Society of Nephrology*, vol. **16**, no. 4, pp. 1115-1125.

The chipping forecast. 1999, *Nat Genet*, vol. **21**, no. **1**, pp 1-60.

Thierfelder, L., Watkins, H., MacRae, C., Lamas, R., McKenna, W., Vosberg, H. P., Seidman, J. G., & Seidman, C. E. 1994, "Alpha-tropomyosin and cardiac troponin T mutations cause familial hypertrophic cardiomyopathy: a disease of the sarcomere", *Cell*, vol. **77**, no. 5, pp. 701-712.

Thierry-Palmer, M., Doherty, A., Bayorh, M. A., & Griffin, K. 2003, "Dahl salt-sensitive rats excrete 25-hydroxyvitamin D into urine", *J Nutr.*, vol. **133**, no. 1, pp. 187-190.

Tingleff, J., Munch, M., Jakobsen, T. J., Torp-Pedersen, C., Olsen, M. E., Jensen, K. H., Jorgensen, T., & Kirchoff, M. 1996, "Prevalence of left ventricular hypertrophy in a hypertensive population", *European Heart Journal*, vol. **17**, no. 1, pp. 143-149.

Toka, H. R., Bahring, S., Chitayat, D., Melby, J. C., Whitehead, R., Jeschke, E., Wienker, T. F., Toka, O., Schuster, H., & Luft, F. C. 1998, "Families with Autosomal Dominant Brachydactyly Type E, Short Stature, and Severe Hypertension", *Annals of Internal Medicine*, vol. **129**, no. 3, pp. 204-208.

Tomson, J. & Lip, G. 2005, "Blood pressure demographics: nature or nurture ... ... genes or environment?", *BMC Medicine*, vol. **3**, no. 1, p. 3.

Tran, K. L., Lu, X., Lei, M., Feng, Q., & Wu, Q. 2004, "Upregulation of corin gene expression in hypertrophic cardiomyocytes and failing myocardium", *AJP - Heart and Circulatory Physiology*, vol. **287**, no. 4, p. H1625-H1631.

Troy, B. L., Pombo, J., & Rackley, C. E. 1972, "Measurement of left ventricular wall thickness and mass by echocardiography", *Circulation*, vol. **45**, no. 3, pp. 602-611.

Tsujita, Y., Iwai, N., Tamaki, S., Nakamura, Y., Nishimura, M., & Kinoshita, M. 2000, "Genetic mapping of quantitative trait loci influencing left ventricular mass in rats", *AJP - Heart and Circulatory Physiology*, vol. **279**, no. 5, p. H2062-H2067.

Tusher, V. G., Tibshirani, R., & Chu, G. 2001, "Significance analysis of microarrays applied to the ionizing radiation response", *Proc.Natl.Acad.Sci.U.S.A*, vol. **98**, no. 9, pp. 5116-5121.

Ulick, S., Tedde, R., & Mantero, F. 1990, "Pathogenesis of the type 2 variant of the syndrome of apparent mineralocorticoid excess", *Journal of Clinical Endocrinology Metabolism*, vol. **70**, no. 1, pp. 200-206.

Urbina, E. M., Gidding, S. S., Bao, W., Pickoff, A. S., Berdusis, K., & Berenson, G. S. 1995, "Effect of Body Size, Ponderosity, and Blood Pressure on Left Ventricular Growth in Children and Young Adults in the Bogalusa Heart Study", *Circulation*, vol. **91**, no. 9, pp. 2400-2406.

Van Vliet, B. N., Chafe, L. L., Antic, V., Schnyder-Candrian, S., & Montani, J. P. 2000, "Direct and indirect methods used to study arterial blood pressure", *Journal of Pharmacological and Toxicological Methods*, vol. **44**, no. 2, pp. 361-373.

Verhaaren, H. A., Schieken, R. M., Mosteller, M., Hewitt, J. K., Eaves, L. J., & Nance, W. E. 1991, "Bivariate genetic analysis of left ventricular mass and weight in pubertal twins (the Medical College of Virginia twin study)", *Am J Cardiol.*, vol. **68**, no. 6, pp. 661-668.

Vincent, M., Kaiser, M. A., Orea, V., Lodwick, D., & Samani, N. J. 1994, "Hypertension in the spontaneously hypertensive rat and the sex chromosomes", *Hypertension*, vol. **23**, no. 2, pp. 161-166.

Visscher, P. M., Thompson, R., & Haley, C. S. 1996, "Confidence intervals in QTL mapping by bootstrapping", *Genetics*, vol. **143**, no. 2, pp. 1013-1020.

Wakeland, E., Morel, L., Achey, K., Yui, M., & Longmate, J. 1997, "Speed congenics: a classic technique in the fast lane (relatively speaking)", *Immunol.Today*, vol. **18**, no. 10, pp. 472-477.

Walker, R., Kessar, P., Blanchard, R., Dimasi, M., Harper, K., DeCarvalho, V., Yucel, E. K., Patriquin, L., & Eustace, S. 2000, "Turbo STIR magnetic resonance imaging as a whole-body screening tool for metastases in patients with breast carcinoma: preliminary clinical experience", *J Magn Reson.Imaging*, vol. **11**, no. 4, pp. 343-350.

Wallace, C. A., Ali, S., Glazier, A. M., Norsworthy, P. J., Carlos, D. C., Scott, J., Freeman, T. C., Stanton, L. W., Kwitek, A. E., & Aitman, T. J. 2002, "Radiation hybrid mapping of 70 rat genes from a data set of differentially expressed genes", *Mamm.Genome*, vol. **13**, no. 4, pp. 194-197.

Wang, D. G., Fan, J. B., Siao, C. J., Berno, A., Young, P., Sapolsky, R., Ghandour, G., Perkins, N., Winchester, E., Spencer, J., Kruglyak, L., Stein, L., Hsie, L., Topaloglou, T., Hubbell, E., Robinson, E., Mittmann, M., Morris, M. S., Shen, N., Kilburn, D., Rioux, J., Nusbaum, C., Rozen, S., Hudson, T. J., Lipshutz, R., Chee, M., & Lander, E. S. 1998, "Large-scale identification, mapping, and genotyping of single-nucleotide polymorphisms in the human genome", *Science*, vol. **280**, no. 5366, pp. 1077-1082.

Ward, R. H. 1983, "Genetic and sociocultural components of high blood pressure", *Am J Phys.Anthropol.*, vol. **62**, no. 1, pp. 91-105.

Warden, C. H., Yi, N., & Fisler, J. 2004, "Epistasis among genes is a universal phenomenon in obesity:: evidence from rodent models", *Nutrition*, vol. **20**, no. 1, pp. 74-77.

Watkins, H., Thierfelder, L., Anan, R., Jarcho, J., Matsumori, A., McKenna, W., Seidman, J. G., & Seidman, C. E. 1993, "Independent origin of identical beta cardiac myosin heavy-chain mutations in hypertrophic cardiomyopathy", *Am J Hum Genet*, vol. **53**, no. 6, pp. 1180-1185.

Watkins, H., Conner, D., Thierfelder, L., Jarcho, J. A., MacRae, C., McKenna, W. J., Maron, B. J., Seidman, J. G., & Seidman, C. E. 1995, "Mutations in the cardiac myosin binding protein-C gene on chromosome 11 cause familial hypertrophic cardiomyopathy", *Nat.Genet*, vol. **11**, no. 4, pp. 434-437.

Watson, A., Mazumder, A., Stewart, M., & Balasubramanian, S. 1998, "Technology for microarray analysis of gene expression", *Curr Opin.Biotechnol.*, vol. **9**, no. 6, pp. 609-614.

Watzinger, N., Maier, R., Reiter, U., Reiter, G., Fuernau, G., Wonisch, M., Fruhwald, F. M., Schumacher, M., Zweiker, R., Rienmueller, R., & Klein, W. 2005, "Clinical applications of cardiovascular magnetic resonance", *Curr Pharm Des*, vol. **11**, no. 4, pp. 457-475.

Weinberger, M. H. 1996, "Salt sensitivity of blood pressure in humans", *Hypertension*, vol. **27**, no. 3 Pt 2, pp. 481-490.

Weiner, C. P., Knowles, R. G., Nelson, S. E., & Stegink, L. D. 1994, "Pregnancy increases guanosine 3',5'-monophosphate in the myometrium independent of nitric oxide synthesis", *Endocrinology*, vol. **135**, no. 6, pp. 2473-2478.

White, P. C. 1994, "Disorders of aldosterone biosynthesis and action", *N.Engl.J Med*, vol. 331, no. 4, pp. 250-258.

Wienberg, J. & Stanyon, R. 1995, "Chromosome painting in mammals as an approach to comparative genomics", *Curr Opin.Genet Dev.*, vol. **5**, no. 6, pp. 792-797.

Willaims, B., Poulter, N. R., Brown, M. J., Davis, M., McInnes, G. T., Potter, J. F., Sever, P. S., McG Thom, S., & British Hypertension Society 2004, "Guidelines for management of hypertension: report of the fourth working party of the British Hypertension Society, 2004-BHS IV", *J Hum Hypertens*, vol. **18**, no. 3, pp. 139-185.

Wilson, T. W. & Grim, C. E. 1991, "Biohistory of slavery and blood pressure differences in blacks today. A hypothesis", *Hypertension*, vol. **17**, no. suppl I, p. I.

Wise, R. G., Huang, C. L., Gresham, G. A., Al Shafei, A. I., Carpenter, T. A., & Hall, L. D. 1998, "Magnetic resonance imaging analysis of left ventricular function in normal and spontaneously hypertensive rats", *J Physiol*, vol. **513** (Pt 3), pp. 873-887.

Wise, R. G., Huang, C. L., Al Shafei, A. I., Carpenter, T. A., & Hall, L. D. 1999, "Geometrical models of left ventricular contraction from MRI of the normal and spontaneously hypertensive rat heart", *Phys.Med Biol*, vol. **44**, no. 10, pp. 2657-2676.

Woodman, S. E., Park, D. S., Cohen, A. W., Cheung, M. W., Chandra, M., Shirani, J., Tang, B., Jelicks, L. A., Kitsis, R. N., Christ, G. J., Factor, S. M., Tanowitz, H. B., & Lisanti, M. P. 2002, "Caveolin-3 knock-out mice develop a progressive cardiomyopathy and show hyperactivation of the p42/44 MAPK cascade", *J Biol Chem.*, vol. **277**, no. 41, pp. 38988-38997.

Wu, F. & Wu, Q. 2003, "Corin-mediated processing of pro-atrial natriuretic peptide in human small cell lung cancer cells", *Cancer Res*, vol. **63**, no. 23, pp. 8318-8322.

Xiang, W., Kong, J., Chen, S., Cao, L. P., Qiao, G., Zheng, W., Liu, W., Li, X., Gardner, D. G., & Li, Y. C. 2005, "Cardiac hypertrophy in vitamin D receptor knockout mice: role of the systemic and cardiac renin-angiotensin systems", *Am J Physiol Endocrinol Metab*, vol. 288, no. 1, p. E125-E132.

Yamori, Y., Tomimoto, K., Ooshima, A., Hazama, F., & Okamoto, K. 1974, "Proceedings: Developmental course of hypertension in the SHR-substrains susceptible to hypertensive cerebrovascular lesions", *Jpn.Heart J*, vol. **15**, no. 2, pp. 209-210.

Yamori, Y., Horie, R., Sato, M., & Ohta, K. 1976, "Proceedings: Prophylactic trials for stroke in stroke-prone SHR: effect of sex hormones", *Jpn.Heart J*, vol. **17**, no. 3, pp. 404-406.

Yamori, Y., Nara, Y., Kihara, M. Horie, R. & Ooshima, A. 1981, "Sodium and other dietary factors in exerimental and human hypertension: the Japanese experience", *in Frontiers in Hypertension Research*, eds. Laragh, J.H., Buhler, F.R. & Seldin, D.W. pp46-48. New York: Springer-Verlag.

Yamori, Y. & Lovenberg, W. 1987, "Spontaneously hypertensive rats", *Hypertension*, vol **9** (Suppl I), I-13-I-14.

Yamori, Y., Fukuda, S., Tsuchikura, S., Ikeda, K., Nara, Y., & Horie, R. 1991, "Stroke-prone SHR (SHRSP) as a model for osteoporosis", *Clin Exp Hypertens A*, vol. **13**, no. 5, pp. 755-762.

Yamori, Y & Swales, J.D. 1994, "The spontaneously hypertensive rat", in *Textbook of Hypertension*, ed. Swales, J.D. Ch.1.pp447-455. Oxford: Blackwell.

Yamori, Y. 1999, "Implication of hypertensive rat models for primordial nutritional prevention of cardiovascular diseases", *Clinical and Experimental Pharmacology and Physiology*, vol. **26**, no. 7, pp. 568-572.

Yan, W., Wu, F., Morser, J., & Wu, Q. 2000, "Corin, a transmembrane cardiac serine protease, acts as a pro-atrial natriuretic peptide-converting enzyme", *Proc.Natl.Acad.Sci.U.S.A*, vol. **97**, no. 15, pp. 8525-8529.

Ye, P. & West, M. J. 2003, "Cosegregation analysis of natriuretic peptide genes and blood pressure in the spontaneously hypertensive rat", *Clinical and Experimental Pharmacology and Physiology*, vol. **30**, no. 12, pp. 930-936.

Yoshioka, J., Prince, R. N., Huang, H., Perkins, S. B., Cruz, F. U., MacGillivray, C., Lauffenburger, D. A., & Lee, R. T. 2005, "Cardiomyocyte hypertrophy and degradation of connexin43 through spatially restricted autocrine/paracrine heparin-binding EGF", *Proc.Natl.Acad.Sci.U.S.A*, vol. **102**, no. 30, pp. 10622-10627.

Young, J. H., Parler, P., Bristol, B., & Klag, M. J. "The coming epidemic: hypertension in rural Kyrgyzstan, Central Asia", *J Hum Hypertens*.

Yu, H., Harrap, S. B., & Di Nicolantonio, R. 1998, "Cosegregation of spontaneously hypertensive rat renin gene with elevated blood pressure in an F2 generation", *J Hypertens*, vol. **16**, no. 8, pp. 1141-1147.

Yuen, P. K., Li, G., Bao, Y., & Muller, U. R. 2003, "Microfluidic devices for fluidic circulation and mixing improve hybridization signal intensity on DNA arrays", *Lab Chip.*, vol. **3**, no. 1, pp. 46-50.

Zaman, M. A., Oparil, S., & Calhoun, D. A. 2002, "Drugs targeting the renin-angiotensin-aldosterone system", *Nat.Rev.Drug Discov.*, vol. **1**, no. 8, pp. 621-636.

Zeng, Z. B. 1994, "Precision mapping of quantitative trait loci", *Genetics*, vol. **136**, no. 4, pp. 1457-1468.

Zhang, L., Summers, K. M., & West, M. J. 1996, "Cosegregation of genes on chromosome 5 with heart weight and blood pressure in genetic hypertension", *Clin Exp Hypertens*, vol. **18**, no. 8, pp. 1073-1087.

Zhang, Q. Y., Dene, H., Deng, A. Y., Garrett, M. R., Jacob, H. J., & Rapp, J. P. 1997, "Interval mapping and congenic strains for a blood pressure QTL on rat chromosome 13", *Mamm.Genome*, vol. **8**, no. 9, pp. 636-641.

Zittermann, A., Schleithoff, S. S., & Koerfer, R. 2007, "Vitamin D and vascular calcification", *Curr Opin.Lipidol.*, vol. 18, no. 1, pp. 41-46.

Zhou, R., Pickup, S., Glickson, J. D., Scott, C. H., & Ferrari, V. A. 2003, "Assessment of global and regional myocardial function in the mouse using cine and tagged MRI", *Magn Reson.Med*, vol. **49**, no. 4, pp. 760-764.

Zhou, C., Ziegler, C., Birder, L. A., Stewart, A. F., & Levitan, E. S. 2006, "Angiotensin II and stretch activate NADPH oxidase to destabilize cardiac Kv4.3 channel mRNA", *Circulation Research*, vol. **98**, no. 8, pp. 1040-1047.

APPENDIX I

Suppliers of all the chemicals and reagents used

Chemical Reagents	Suppliers
Absolute Ethanol	Sigma
Advantage RT for PCR kit	Clontech Laboratories Inc.
Agarose	Gibco BRL
Antibody (goat), Anti-streptavidin, biotinylated	Vector Laboratories
Antibody, IgG, Goat, reagent grade	Sigma
Ammonium Acetate, 7.5M	Sigma
Ammonium persulphate	BDH
Blue dextran	Perkin-Elmer
Bovine Serum Albumin (BSA)	Gibco BRL
Bromophenol blue	Sigma
Buffer tablets	BDH
Cellulose patches	Data Sciences Int.
Chloroform	Fisher Scientific
Concentrated hydrochloric acid	BDH
Cresol Red	Sigma
Decon 75	Decon Laboratories Ltd.
dNTPs/deoxynucleoside triphosphates	Promega
ddNTPs/dideoxynucleoside triphosphates	Perkin-Elmer
DNA, Herring Sperm	Promega
Dimethyl sulfoxide	Sigma
EDTA	Bio-Rad
Ethanol	Sigma
Ethidium bromide	Sigma
Formamide	BDH
GENESCAN-350 Tamra	Perkin-Elmer

Chemical Reagents	Suppliers
Glycogen	Ambion
Goat IgG, Reagent Grade	Sigma
Halothane	Zeneca Ltd.
HotStartTaq DNA polymerase	Qiagen
Hybond-N+ membrane	Amersham
Hypnorm©	Vetapharma
Isoamylalcohol	BDH
10X kinase buffer	Promega
Long Ranger 5% stock gel solution	BioWhittaker
Magnesium chloride/MgCl2	Promega
Magnesium acetate	Sigma
Megascript T7 Kit	Ambion
MES free acid monohydrate SigmaUltra	Sigma
MES sodium salt	Sigma
Metaphor agarose	FMC
NaCl	Ambion
Nucleotides, labeled, Biotin-11-CTP/UTP	Sigma
[α-^{32}P]dCTP	Amersham
[α-^{32}P]dATP	Amersham
10X PCR buffer	Qiagen
Oligo B2, control oligo for antisense probe array, HPLC purified	MWG Biotech
PBS, pH 7.2	Gibco BRL
Phenol/chloroform/isoamyl alcohol	Ambion
Phenol, water-saturated in Tris buffer	Life Sciences
Phycoerythrin-streptavidin	Molecular Probes
Powered milk	Premier Beverages
Polyoxyethylene	Life Technologies
Primers (including T7-(dT)24)	MWG Biotech
Ready Reaction mix	Perkin-Elmer

Chemical Reagents	Suppliers
Resin AG 501-X8	Bio-Rad
RNase solution	Promega
RNeasy Maxi kit	Qiagen
0.9% Saline	Baxter Scientific
20X SSC	National Diagnostics
SDS (sodium dodecyl sulphate) powder	Bio-Rad
Sigmacote	Sigma
Sodium acetate	Sigma
Sodium chloride	Fisher Scientific
Sodium hydroxide pellets	Fisher Scientific
Sodium hypochlorite	Sigma
SSPE (20X)	BioWhittaker
Sucrose	Fisher Scientific
Superscript choice system	Gibco BRL
Tartrazine	Sigma
10X TBE	National Diagnostics
TEMED	Sigma
TEMED	Amresco
Terminal deoxynucleotidyl transferase/TdT	Promega
TdT buffer	Promega
10X Thermophilic buffer	Promega
Tris base	Bio-Rad
Tween-20, 10%	Pierce Chemical
Ultra-pure formamide	Amresco
Universal Taqman mastermix	Applied Biosystems
Urea	Sigma
VetBond	3M Animal Care Products
Water, DEPC-treated	Ambion
Water, nuclease-free (not DEPC-treated)	Ambion

Chemical Reagents	Suppliers
Xylene cyanol	Sigma

List of all reagents used in preparation of solutions

10% Ammonium Persulphate (10 ml)

1 g APS dissolved in 10 ml sterile distilled water. Store at 4°C.

Chloroform Isoamylalcohol mixture (250 ml)

240 ml chloroform added to 10 ml isoamylalcohol. Store at 4°C wrapped in light resistant bottle.

dNTPs (200 µl, 25 mm)

5 µl of each dGTP, dATP, dTTP, and dCTP (provided in 100 mm stock solutions) added to 180 µl sterile distilled water. Store frozen.

dNTPs (1, 000µl, 1 mm)

10 µl of each dGTP, dATP, dTTP, and dCTP (provided in 100 mm stock solutions) added to 960 µl of sterile distilled water. Store frozen.

0.5M EDTA, pH 8.0 (1 L)

186.1 g EDTA dissolved in 1 L sterile distilled water, pH adjusted with sodium hydroxide pellets. Sterilised by autoclave. Store at room temperature.

70% Ethanol (100 ml)

70 ml of 100% ethanol mixed with 30 ml sterile distilled water.

90% Ethanol (100 ml)

90 ml of 100% ethanol added to 10 ml of water.

80% Ethanol (100ml)

80ml of 100% ethanol added to 20ml of water

2X Formamide Loading Buffer (10 ml)

9 ml formamide, 160 µl bromophenol blue, 160 µl xylene cyanol, 680 µl sterile distilled water. Store at 4°C.

10 mg/mm Goat IgG stock

Resuspend 50 mg in 5 ml PBS. Store at 4°C.

2X Hybridisation Buffer (50ml)

8.3ml of 12X MES stock, 17.7ml of 5M NaCl, 4.0ml of 0.5M EDTA, 0.1ml of 10% Tween 20, 19.9ml of water.

Non-Stringent Wash Buffer (Buffer A)

300 ml of 20X SSPE, 1.0 ml of 10% Tween-20, and 698 ml of water. Filter through a 0.2 µm filter. After filtering, add 1.0 ml 5% Antifoam.

PCR Master Mix (15 µl, n=1) fluorescent

Contains 2 µl of 10X buffer (Qiagen), 1 µl of polioxyethylene, 4 µL of dNTPs (1 mm), 6.96 µl of sterile distilled water, 0.04 µl of HotStartTaq polymerase (Qiagen), and 0.5 µl of each primer (20 µm), preparation is ready for PCR in a thermal cycler.

PCR Master Mix (10 µl, n=1) non-fluorescent

Contains 4 µl 5X Red, 2 µl 10X Promega thermophilic buffer, 1.2 µl 25 mm $MgCl_2$, 1.1 µl 2.5 mm dNTPs, 1.6 µl sterile distilled water and 0.08 µl *Taq* polymerase. The *Taq* was added immediately prior to the PCR reaction to avoid denaturation. Can be stored frozen until required without the polymerase enzyme.

Phenol choroform isoamylalcohol (200 ml)

100 ml water saturated phenol mixed with 100 ml chloroform isoamylalcohol mixture. Store at 4°C, in light resistant bottle.

8% Polyacrylamide Gel Mix (100 ml)

32 ml SequaGel concentrate, 58 ml SequaGel diluent, and 10 ml SequaGel buffer mixed together.

Post-Hybridisation Wash Solution (1 L)

10 ml 20% SDS, 20 X SSC and 890 ml sterile distilled water mixed together.

Primer Solution (500 µL, 20 µm) for fluorescent PCR

100 µl of each primer (forward and reverse) mixed with 300 µl of sterile distilled water. Store frozen.

Primer Solution (5 µl, n=1) for non-fluorescent PCR

0.8 µl of each 6 µm primer (forward and reverse) mixed with 3.4 µl sterile distilled water. Final addition of a few particles of tartrazine to aid identification. Can be stored frozen until required.

Proteinase K Solution

5 ml Proteinase K (Qiagen) added to 10 ml DNAse free water.

5X Red (10 ml)

6.5 g sucrose dissolved in 10 ml sterile distilled water. Addition of 1 µl cresol red for colour. Store at 4°C.

5X RNA Fragmentation Buffer

4.0 ml 1M Tris acetate pH 8.1(Trizma base, Ph adjusted with glacial acetic acid), 0.64 g MgOAc, 0.98 g KOAc, DEPC-treated water to a total volume of 20 ml.

Single Stranded cDNA Synthesis (Clontech RT for PCR kit)

5X reaction buffer 4.0 µl, dNTP mix (10 mM each) 1.0 µl , Recombinant RNase inhibitor 0.5 µl and MMLV reverse transcriptase 1.0 µl

0.4% SDS (500 ml)

2 g SDS powder dissolved in 500 ml sterile distilled water by heating to 68°C in microwave.

10% SDS (1 L)

500 ml 20% SDS mixed with 500 ml sterile distilled water.

3M Sodium Acetate, pH 6.0 (1 L)

408.1 g sodium acetate dissolved in 1 L of sterile distilled water. pH adjusted with glacial acetic acid. Sterilised by autoclave.

1% Sodium Chloride (1 L)

10 g sodium chloride dissolved in 1 L sterile distilled water.

4M Sodium Chloride.

117 g sodium chloride dissolved in 500 ml sterile distilled water. Sterilised by autoclave.

0.4M Sodium Hydroxide (1 L)

16 g sodium hydroxide pellets dissolved with stirring in 1 L sterile distilled water.

2 X SSC (1 L)

100 ml 20 X SSC mixed with 900 ml sterile distilled water.

2X Stain Buffer (250 ml)

41.7 ml 12X MES stock buffer, 92.5 ml 5M NaCl, 2.5 ml 10% Tween-20, 112.8 ml water. Filter through a 0.2 µm filter. After filtering, add 0.5 ml of 5% Anti-foam.

Stringent Wash Buffer (Buffer B)

For 1000ml. 83.3 ml of MES stock buffer, 5.2 ml of 5M NaCl, 1.0 ml of 10% Tween 20, 910.5 ml of water. Filter through a 0.2 µm filter.

Suspension Buffer (500 ml)

25 ml 1M Tris (pH 8.0), 100 ml 0.5M EDTA (pH 8.0), and 375 ml sterile distilled water mixed together.

1X TBE (1 L)

100 ml 10X TBE mixed with 900 ml sterile distilled water.

TE (20 ml).

200 µl 1M Tris (pH 8.0), 40 µL 0.5M EDTA (pH 8.0), and 19.76 ml sterile distilled water mixed together.

1M Tris, pH 8.0 (1 L).

121.1 g Tris base dissolved in 1 L sterile distilled water. pH adjusted with concentrated hydrochloric acid. Sterilised by autoclave.

Solution for extraction of DNA from rat tails (20 ml).

1 ml 1M Tris (pH 8.0), 100 ml 0.5M EDTA (pH 8.0), 1 ml 10% SDS and 14 ml sterile distilled water mixed together.

Taqman PCR reaction Mastermix

2 µl housekeeping gene probe, 2 µl target gene probe, 8 µl Taqman Universal mastermix and 2 µl sterile distilled water.

APPENDIX II

Raw Phenotype Data

Codes as follows: Cross G refers to F2 hyrbids (n=134) with a SHRSP grandfather, Cross H a WKY grandfather. CMI is cardiac mass indexed to body weight; LVMI is left ventricular mass indexed to body weight; PRA is plasma renin activity; SBP and DBP values are means after salt loading period (Clark *et al.*, 1996).

Cross	CMI mg/g	LVMI mg/g	PRA	SBP(s) mmHg	DBP(s) mmHg	Sex
G1	5.91	4.8	1.3	147.93	100.07	F
G2	3.35	2.66	6.8	173.3	120	F
G3	3.34	2.79	3.7	168.56	115.73	F
G4	3.53	2.81	1.8	163.95	112.8	F
G5	3.4	2.71	5.2	171.57	117.94	F
G6	3.26	2.72	1.8	181.96	126.13	M
G7	3.92	3.12	0.35	211.33	146.46	F
G8	3.63	2.82	0.25	173.61	119.66	F
G9	3.32	2.73	0.23	154.98	105.26	F
G10	3.16	2.37	2.1	168.69	116.4	M
G11	3.37	2.61	1.2	182.11	125.52	M
G12	3.86	3.33	0.82	194.9	132.74	M
G13	3.87	3.16	0.1	209.57	146.95	M
G14	3.77	3.3	3.1	193.91	130.44	M
G15	3.74	3.22	0.37	196.82	132.08	M
G16	3.2	2.79	0.22	204.7	141.06	M
G17	3.96	3.3	0.1	181.66	126	F
G18	4.1	3.5	0.65	203	147.03	F
G21	3.78	3.22	1.6	182.6	128.11	M
G22	3.25	2.76	0.34	183.01	126.24	M
G43	4.28	3.68	0.1	159.54	104.61	F
G44	3.76	3.07	0.33	235.43	166.98	F
G26	4.15	3.69	2.4	178.47	134.1	F
G27	3.43	2.8	0.26	153.41	105.07	F
G28	4.71	4.05	1.7	229.25	162.76	F
G30	3.47	2.74	0.6	165.65	112.18	F

Cross	CMI mg/g	LVMI mg/g	PRA	SBP(s) mmHg	DBP(s) mmHg	Sex
G32	3.55	2.92	0.58	167.62	112.33	F
G33	4.64	3.51	0.61	175.99	115.19	F
G34	3.3	2.7	0.2	193.36	134.83	M
G35	3.16	2.69	0.49	177.07	120.62	M
G36	3.78	3.22	0.52	223.34	155.43	M
G37	3.74	3	0.19	199.14	132.27	M
G39	3.56	2.77	0.69	177.33	119.71	M
G40	3.19	2.6	0.16	173.83	117.53	M
G41	3.29	2.65	0.1	206.23	143.5	M
G46	4.19	3.33	0.5	181.56	122.72	F
G48	4.34	3.14	0.1	199.53	134.46	M
G49	4.14	3.08	0.36	218.61	147.9	M
G50	3.8	2.58	0.92	170.99	115.65	M
G52	4.47	3.43	0.1	194.44	131.1	F
G53	3.95	2.73	0.28	159.68	110.63	F
G54	4.39	3.27	0.21	244.01	170.6	M
G55	3.82	2.79	0.1	189.85	127.71	M
G57	4.26	3.06	0.38	166.2	114.01	F
G58	4.42	2.91	0.72	162.63	108.55	F
H1	3.19	2.4	2.2	182.448	121.36	M
H2	3.82	2.66	0.52	173.9	116.38	M
H3	4.19	3.1	0.5	170.983	114.61	F
H4	3.41	2.42	1.3	167.894	116.83	M
H5	3.64	2.64	0.7	171.023	118.01	M
H6	4.07	2.99	0.7	174.969	118.2	M
H7	3.73	2.7	1.5	180.502	125.24	M
H8	3.39	2.52	0.3	177.21	123.59	M
H9	4.14	3	1.3	166.44	115	F
H10	3.72	2.62	1.9	-	-	M
H11	3.89	2.83	1.1	197.24	131.1	M
H12	4.49	3.28	1.5	180.05	118.27	M
H13	3.99	2.83	1.2	154.6	99.64	F
H14	3.98	2.82	1.8	170.43	115.4	F
H41	3.41	2.57	2	171.41	115.38	M
H42	3.43	2.57	1.4	184.29	126.14	M
H17	3.68	2.79	2.5	171.58	116.29	F
H18	3.86	2.77	0.9	171.92	116.88	F
H19	3.37	2.4	1.9	151.35	105.22	F

Cross	CMI mg/g	LVMI mg/g	PRA	SBP(s) mmHg	DBP(s) mmHg	Sex
H20	3.18	2.31	2.3	167	116.39	M
H21	3.68	2.68	1.6	199.74	135.84	M
H22	3.61	2.58	0.21	160.85	109.01	F
H23	3.3	2.33	2.3	142.83	99.82	F
H24	3.39	2.46	3.3	161.88	111.93	F
H25	3.68	2.59	1.3	158.58	106.15	F
H28	3.49	2.68	0.57	189.71	129.97	M
H29	2.8	1.97	0.61	183.31	124.1	M
H30	3.74	2.7	-	196.18	132.32	M
H31	3.26	2.31	0.5	181.19	125.53	M
H32	3.09	2.29	-	169.3	112.14	F
H33	3.74	2.43	0.1	163.61	112.33	F
H34	3.29	2.34	2.9	170.37	117.78	M
H35	3.76	2.7	2.4	164.09	114.46	F
H36	4.13	2.83	1.2	180.34	124.34	F
H38	3.61	2.57	2.1	159.35	108.25	F
H39	3.88	2.76	0.1	163.24	109.41	F
H40	3.93	2.81	4.1	187.25	126.51	F
H43	3.19	2.22	2.7	171.48	116.49	M
H44	4.16	3.04	4.1	170.51	115.89	F
H46	2.94	2.32	1.4	157.02	107.12	F
H47	3.31	2.48	0.4	168.8	120.5	F
H48	3.83	2.79	0.41	148.13	103.54	M
H49	3.58	2.73	0.1	189.18	113.11	M
H50	3.35	2.36	3.1	147.89	99.01	F
H51	3.66	2.42	0.7	157.84	107.68	F
G59	-	-	-	279.44	208.54	F
G60	4.71	3.1	0.1	165.24	113.75	F
G62	3.733	2.866	0.23	169.88	113.32	F
G64	3.761	2.906	0.1	176.35	121.12	M
G65	4.356	3.208	0.81	234.68	169.95	M
G66	4.245	2.775	0.16	187.52	130.55	M
G67	4.188	2.938	0.1	205.54	143.4	M
G68	3.9	2.927	0.9	192.62	135.62	M
G71	4.921	3.448	0.27	209.08	143.05	M
H52	3.09	2.25	0.3	170.12	115.17	M
H53	3.35	2.48	0.37	183.13	123.7	M
H55	3.55	2.39	0.44	157.99	106.39	F

Cross	CMI mg/g	LVMI mg/g	PRA	SBP(s) mmHg	DBP(s) mmHg	Sex
H56	3.9	2.95	0.31	160.72	105.85	F
H57	3.52	2.66	0.26	161.68	109.37	F
H58	3.74	2.74	0.58	149.04	98.2	F
H59	3.5	2.77	0.87	170.84	115.6	F
H60	3.36	2.42	1.3	172.21	118.8	M
H61	3.45	2.61	3.5	174.57	119.1	M
H62	3.32	2.48	1.9	185.04	130.09	M
H63	3.38	2.62	0.72	195.45	136.94	F
H64	3.84	2.93	0.57	180.21	123.68	F
H65	3.19	2.4	2.4	172.51	119.77	M
H66	3.29	2.33	1.5	154.33	106.87	F
H67	3.76	2.71	1.2	162.85	111.92	F
H68	3.6	2.73	1.6	187.56	130.49	M
H69	4.38	3.15	0.54	174.53	123.98	M
H70	3.6	2.52	1.2	163.64	113.47	M
H71	3.88	2.85	1.4	159.64	108.61	M
H72	3.58	2.43	0.4	160.68	114.12	M
H73	3.55	2.51	0.81	160.14	108.87	M
H81	4.01	3.04	0.61	208.65	140.74	F
II82	4.14	2.82	0.23	185.9	120.91	F
H88	3.68	2.62	0.7	194.02	134.96	F
H74	3.97	2.79	3.5	197.82	136.73	M
H75	4.04	2.86	3.8	165.66	113.89	F
H76	3.67	2.52	2.6	148.57	99.68	F
H77	3.82	2.59	1.6	150.9	101.94	F
H78	4.11	2.9	3.9	166.16	111.04	F
H79	3.99	2.8	0.65	183.02	124.58	F
II84	3.8	2.66	14.5	141.48	96.49	F
II86	3.68	2.52	0.51	156.51	106.03	F
H91	2.71	1.94873	-	156.05	106.43	F
H89	3.71244	2.60888	-	172.27	118.99	M
H90	3.56483	2.59057	-	172.92	118.58	M

Raw Chromosome 14 Genotype Data

Microsatellite marker and genotype codes for data is given below. The symbol "-" indicates missing data. Heterozygote – 0; homozygote WKY – 1; homozygote SHRSP 2.

Cross	D14Rat54	D14Rat75	D14Wox18	D14Wox8	D14Wox10	D14mg3	DbpExon4	D14Arb17	D14Wox12	D14Wox14	D14Got33	D14Got41	D14Wox24	D14Rat110
G1	2	2	2	2	2	2	2	2	2	2	2	2	2	-
G2	2	2	1	1	1	1	1	1	1	1	1	1	0	0
G3	2	2	1	2	2	2	2	1	2	-	-	1	-	-
G4	2	2	1	1	1	1	1	1	1	1	-	1	1	0
G5	1	0	0	0	-	0	0	0	0	0	0	0	1	1
G6	1	1	2	1	1	1	1	1	1	1	-	2	2	1
G7	1	1	2	1	1	1	1	1	1	1	1	2	2	1
G8	1	-	-	1	1	1	1	1	1	1	-	0	0	1
G9	1	0	0	0	0	0	0	0	0	2	0	1	1	1
G10	1	1	1	1	-	1	1	1	1	1	1	1	1	1
G11	-	1	1	1	1	1	1	1	1	1	-	1	1	1
G12	-	2	2	2	2	2	2	2	2	2	2	1	1	1
G13	1	2	2	2	2	2	2	2	2	2	2	1	1	0
G14	-	1	1	1	1	1	1	1	1	1	1	1	1	2
G15	-	2	-	2	2	2	2	2	2	2	2	2	2	1
G16	0	0	1	1	1	1	1	1	1	1	1	1	1	1
G17	-	0	0	0	0	0	0	0	0	0	2	2	2	2
G18	-	1	1	1	1	1	1	1	1	1	1	1	1	1
G21	-	2	2	2	2	2	2	2	2	2	2	2	2	0
G22	-	1	1	1	1	1	1	1	1	1	1	1	1	1
G43	-	0	0	0	0	0	2	0	0	0	0	1	1	1
G44	-	0	0	0	0	0	2	0	0	1	1	1	2	2
G26	-	0	0	0	0	0	2	0	0	0	0	0	0	1
G27	-	1	1	1	1	1	1	1	1	1	1	1	1	1
G28	-	1	0	1	1	1	1	1	1	1	-	1	1	0
G30	-	2	2	2	2	2	2	2	2	2	2	2	2	1
G32	-	-	0	0	-	0	0	0	0	0	0	0	0	1
G33	-	1	1	2	2	2	2	2	2	2	-	2	2	2

Cross	D14Rat54	D14Rat75	D14Wox18	D14Wox8	D14Wox10	D14mg3	DbpExon4	D14Arb17	D14Wox12	D14Wox14	D14Got33	D14Got41	D14Wox24	D14Rat110
G34	-	2	-	2	2	2	2	2	2	2	2	2	2	2
G35	-	0	0	0	0	0	0	0	0	0	0	0	0	0
G36	-	2	2	2	-	2	2	2	2	2	2	2	1	1
G37	1	1	-	1	1	1	1	1	1	1	1	1	1	2
G39	0	0	0	0	0	0	0	0	0	0	0	0	0	0
G40	2	2	2	2	2	2	2	2	2	2	2	2	1	1
G41	2	2	-	2	2	2	2	2	2	2	2	2	2	1
G46	2	2	2	2	2	2	2	2	2	2	2	2	1	1
G48	1	1	1	1	1	1	1	1	1	1	-	2	2	1
G49	2	2	-	2	2	2	2	2	2	2	2	2	0	1
G50	1	1	-	1	1	1	1	1	1	1	1	1	1	0
G52	1	1	-	1	1	1	1	1	1	1	1	1	1	1
G53	2	2	2	2	2	2	2	2	2	2	2	2	2	2
G54	1	1	1	1	1	1	1	1	1	1	1	1	0	1
G55	1	-	1	1	1	-	1	1	1	2	2	2	2	2
G57	-	0	-	-	0	0	0	0	0	0	0	0	0	1
G58	1	0	0	0	0	0	-	0	0	0	-	0	0	1
H1	1	1	1	1	-	1	1	1	1	1	1	1	1	1
H2	2	2	2	2	2	2	2	2	2	2	-	2	1	1
H3	2	2	2	2	2	2	2	2	2	2	2	2	1	2
H4	-	2	-	1	1	-	-	1	-	1	-	-	0	1
H5	1	1	2	2	2	2	2	2	2	2	2	2	2	1
H6	2	-	2	2	2	2	2	2	2	2	2	2	2	0
H7	0	0	0	0	0	0	0	0	0	0	0	0	0	1
H8	2	2	2	2	2	2	2	2	2	2	1	-	2	1
H9	1	1	1	1	1	1	1	1	1	1	1	0	0	1
H10	1	1	1	1	1	1	1	1	1	1	1	1	1	2
H11	0	0	0	0	0	0	0	0	0	0	0	0	0	0
H12	-	2	2	-	2	2	2	2	2	2	2	2	2	0
H13	1	1	1	1	1	1	1	1	1	1	1	1	1	1
H14	1	-	1	1	1	1	1	1	1	1	1	1	1	0
H41	1	-	2	2	2	2	2	2	2	2	1	2	2	1
H42	1	-	1	1	1	1	1	1	1	1	1	0	0	1
H17	-	1	0	0	0	0	0	0	0	0	1	0	0	1
H18	2	2	2	2	2	2	2	2	2	2	2	2	2	2

Cross	D14Rat54	D14Rat75	D14Wox18	D14Wox8	D14Wox10	D14mg3	DbpExon4	D14Arb17	D14Wox12	D14Wox14	D14Got33	D14Got41	D14Wox24	D14Rat110
H19	2	1	1	1	1	1	1	1	1	1	-	1	1	1
H20	1	1	1	1	-	1	1	1	1	1	1	1	1	1
H21	1	1	0	0	0	0	0	0	0	0	1	0	0	0
H22	2	2	2	2	2	2	2	2	2	2	2	-	2	2
H23	2	-	2	2	2	2	-	2	2	2	1	2	1	0
H24	1	1	1	1	1	1	1	1	1	1	1	1	1	2
H25	0	0	0	0	0	0	0	0	0	0	0	0	0	
H28	1	0	0	0	0	0	0	0	0	0	0	1	1	2
H29	1	1	1	1	1	1	1	1	1	1	1	1	0	0
H30	2	2	2	2	2	2	2	2	2	2	2	2	2	2
H31	1	1	-	1	1	1	1	1	1	1	1	0	0	2
H32	1	1	1	1	1	1	1	1	1	1	1	1	0	2
H33	1	1	1	1	1	1	1	1	1	1	0	0	0	1
H34	-	0	0	0	0	0	0	0	0	1	0	0	0	2
H35	0	2	2	2	2	1	1	1	1	1	1	1	1	1
H36	2	1	1	1	1	1	1	1	1	1	2	2	2	0
H38	2	1	0	1	1	1	1	1	1	1	1	-	0	1
H39	1	0	0	0	0	0	0	0	0	0	0	0	0	0
H40	1	2	2	2	2	2	2	2	2	2	2	2	2	1
H43	1	2	2	2	2	2	2	2	2	0	1	1	1	1
H44	2	1	-	1	1	1	1	1	1	1	1	1	0	2
H46	1	1	1	1	1	1	1	1	1	-	-	1	2	1
H47	0	2	1	1	-	1	1	1	1	1	1	1	1	2
H48	2	2	2	2	2	2	2	2	2	2	-	2	2	0
H49	2	0	0	0	0	0	0	0	0	1	-	1	2	1
H50	0	2	1	1	1	1	-	1	1	1	1	1	1	2
H51	2	1	2	2	2	2	2	2	2	2	2	2	2	1
G59	-	0	0	0	0	0	0	0	0	0	-	0	1	1
G60	-	2	2	2	2	2	2	2	2	2	2	2	2	2
G62	1	-	0	0	0	0	0	0	0	0	0	0	0	2
G64	0	-	0	0	0	0	0	0	0	0	0	-	0	0
G65	2	-	2	2	2	2	2	2	2	2	2	2	2	0
G66	1	1	1	1	1	1	1	1	1	2	2	2	2	-
G67	2	2	2	2	2	2	2	2	2	2	1	2	1	2
G68	2	2	2	2	2	2	2	2	2	2	1	2	1	2

Cross	D14Rat54	D14Rat75	D14Wox18	D14Wox8	D14Wox10	D14mg3	DbpExon4	D14Arb17	D14Wox12	D14Wox14	D14Got33	D14Got41	D14Wox24	D14Rat110
G71	-	2	2	2	2	2	2	2	2	2	2	-	1	0
H52	1	1	1	1	1	1	1	1	1	1	1	1	1	1
H53	-	1	1	1	1	1	1	1	1	1	1	1	1	1
H55	0	0	-	0	0	0	0	0	0	0	0	-	0	1
H56	2	2	1	1	1	1	1	1	1	1	1	1	1	1
H57	0	1	1	1	1	1	1	1	1	1	1	1	1	1
H58	-	1	1	1	1	1	1	1	1	1	1	1	1	0
H59	-	-	0	0	0	0	0	0	0	1	1	0	1	1
H60	1	1	1	1	1	1	1	1	1	1	1	1	1	1
H61	1	1	1	1	1	1	1	1	1	1	1	1	1	1
H62	1	1	1	1	1	1	1	1	1	1	1	1	0	1
H63	1	1	1	1	1	1	1	1	1	1	1	1	1	1
H64	2	2	2	2	2	2	2	2	2	2	2	2	2	1
H65	2	1	1	1	1	1	1	1	1	1	1	1	1	0
H66	1	1	1	1	1	1	1	1	1	1	1	1	1	1
H67	0	0	0	0	0	0	0	0	0	0	0	0	0	1
H68	2	2	1	1	1	1	1	1	1	1	1	1	1	2
H69	2	2	2	2	2	2	2	2	2	2	2	2	2	2
H70	-	2	2	2	2	2	2	2	2	2	2	2	2	1
H71	-	0	0	0	0	0	0	0	0	0	1	0	0	2
H72	0	-	1	1	1	1	1	1	1	1	2	1	2	1
H73	0	2	2	2	2	-	2	2	2	2	2	0	2	2
H81	-	2	-	2	2	2	2	2	2	2	2	0	2	1
H82	-	1	1	1	1	1	1	1	1	1	1	1	2	1
H88	0	1	2	2	2	2	1	2	2	2	2	0	2	0
H74	-	1	1	1	1	1	1	1	1	1	1	1	1	2
H75	0	2	0	0	0	0	0	0	0	0	0	0	0	1
H76	2	1	2	2	2	2	2	2	2	2	2	2	2	0
H77	0	0	0	0	0	0	0	0	0	0	0	0	0	1
H78	-	-	-	-	-	-	-	-	-	-	-	-	-	-
H79	-	2	2	2	2	2	2	2	1	2	2	2	2	1
H84	1	-	1	1	1	1	1	1	2	1	1	1	0	2
H86	2	2	-	2	2	2	2	2	2	2	2	2	2	0
H91	1	1	0	0	0	0	0	0	0	0	0	0	0	1
H89	0	0	0	0	0	0	0	0	0	0	1	0	1	0

Cross	D14Rat54	D14Rat75	D14Wox18	D14Wox8	D14Wox10	D14mg3	DbpExon4	D14Arb17	D14Wox12	D14Wox14	D14Got33	D14Got41	D14Wox24	D14Rat110
H90	1	-	1	1	1	1	1	1	1	1	1	1	1	2

APPENDIX III

Genes located in regions of synteny between rat chromosome 14, mouse chromosome 5 and human chromosome 4.

Gene Description
similar to vomeronasal 2, receptor, 2
hypothetical protein LOC689413
similar to putative pheromone receptor
similar to vomeronasal 2, receptor, 1
similar to putative pheromone receptor Go-VN13C (predicted)
similar to vomeronasal 2, receptor, 1
similar to putative pheromone receptor
similar to vomeronasal 2, receptor, 1
similar to putative pheromone receptor (predicted)
similar to vomeronasal 2, receptor, 16
similar to putative pheromone receptor (predicted)
similar to ribosomal protein L13A
similar to putative pheromone receptor (predicted)
similar to Ankyrin repeat domain 13 (predicted)
hypothetical protein LOC689585
similar to putative pheromone receptor (predicted)
similar to vomeronasal 2, receptor, 1
similar to vomeronasal 2, receptor, 1
similar to vomeronasal 2, receptor, 1
similar to karyopherin (importin) alpha 2
similar to putative pheromone receptor (Go-VN2)
similar to putative pheromone receptor (Go-VN2)
similar to putative pheromone receptor
similar to putative pheromone receptor
similar to vomeronasal 2, receptor, 1
similar to vomeronasal 2, receptor, 2
similar to vomeronasal 2, receptor, 1
similar to vomeronasal 2, receptor, 11
similar to Glycoprotein 25L precursor (GP25L)
similar to D1081.9
fibroblast growth factor receptor-like 1
solute carrier family 26 (sulfate transporter), member 1

Gene Description
similar to RIKEN cDNA 3010001K23 gene
cyclin G associated kinase
complexin 1
ring finger protein 3 (predicted)
similar to RIKEN cDNA 4732482E20 (predicted)
ATP synthase, H+ transporting, mitochondrial F0 complex, subunit e
phosphodiesterase 6B, cGMP, rod receptor, beta polypeptide (predicted)
similar to glyceraldehyde-3-phosphate dehydrogenase (predicted)
similar to GPI7 (predicted)
down-regulator of transcription 1
similar to Sarcoma antigen NY-SAR-41 (predicted)
transmembrane emp24 protein transport domain containing 5
metal response element binding transcription factor 2
hypothetical protein LOC689871
similar to RIKEN cDNA 2900024C23 (predicted)
ribosomal protein L5
similar to RuvB-like 2
similar to DNA helicase
similar to RuvB-like 2
similar to 40S ribosomal protein S26
ubiquitin-conjugating enzyme E2D 2
hypothetical protein LOC689944
growth factor independent 1
similar to Expressed sequence AW060207
FKBP-associated protein
hypothetical protein LOC689986
similar to H43E16.1
similar to BTB (POZ) domain containing 8
similar to hypothetical protein A330042H22
abhydrolase domain containing 7 (predicted)
bromodomain, testis-specific
transforming growth factor, beta receptor III
hypothetical protein LOC690086
similar to ribosomal protein S11 (predicted)
cell division cycle 7 (S. cerevisiae) (predicted)
similar to UPF0197 protein C11orf10 homolog

Gene Description
similar to HFM1, ATP-dependent DNA helicase homolog
similar to H02F09.3
hypothetical protein LOC690213
zinc finger protein 644 (predicted)
hypothetical protein LOC690240
hypothetical protein LOC690245
BarH-class homeodomain transcription factor
hypothetical protein LOC690395
LOC501317
similar to spermatogenesis associated glutamate (E)-rich protein 4d
similar to spermatogenesis associated glutamate (E)-rich protein 4d
similar to RIKEN cDNA 5031410I06
similar to glutamate receptor, ionotropic, N-methyl D-aspartate-like 1A (predicted)
hypothetical protein LOC689797
similar to zinc finger CCCH type, antiviral 1
hypothetical protein LOC690525
similar to spermatogenesis associated glutamate (E)-rich protein 4d
hypothetical gene supported by BC082068 (predicted)
similar to spermatogenesis associated glutamate (E)-rich protein 4d
similar to glutamate receptor, ionotropic, N-methyl D-aspartate-like 1A
similar to spermatogenesis associated glutamate (E)-rich protein 4d (predicted)
similar to glutamate receptor, ionotropic, N-methyl D-aspartate-like 1A (predicted)
similar to RIKEN cDNA 5031410I06
leucine rich repeat containing 8 family, member D
leucine rich repeat containing 8 family, member C
similar to T-cell activation leucine repeat-rich protein (predicted)
similar to ATP-binding cassette, sub-family G (WHITE), member 3
similar to ATP-binding cassette transporter ABCG3
similar to ubiquitin-conjugating enzyme E2 variant 1
similar to Hypothetical protein E430029F06 (predicted)
similar to ATP-binding cassette, subfamily G, member 3 (predicted)

Gene Description
similar to ATP-binding cassette, sub-family G (WHITE), member 3 (predicted)
similar to 60S ribosomal protein L38
ATP-binding cassette, sub-family G (WHITE), member 3
similar to THO complex subunit 2 (Tho2)
similar to polycystic kidney disease 2 (predicted)
secreted phosphoprotein 1
matrix extracellular phosphoglycoprotein with ASARM motif (bone)
integrin binding sialoprotein
dentin matrix protein 1
dentin sialophosphoprotein
SPARC-like 1 (mast9, hevin)
nudix (nucleoside diphosphate linked moiety X)-type motif 9
dehydrogenase/reductase (SDR family) member 8
hydroxysteroid (17-beta) dehydrogenase 13
similar to NADH-ubiquinone oxidoreductase B9 subunit (Complex I-B9) (CI-B9)
kelch-like 8 (Drosophila) (predicted)
AF4/FMR2 family, member 1 (predicted)
hypothetical protein LOC680289
similar to hypothetical protein MGC26744
sodium-dependent organic anion transporter
similar to protein Tyr phosphatase
similar to NADH:ubiquinone oxidoreductase B15 subunit (predicted)
mitogen activated protein kinase 10
similar to 40S ribosomal protein S25
similar to RIKEN cDNA 2310005N03
Rho GTPase activating protein 24
similar to proliferating cell nuclear antigen (predicted)
similar to mKIAA1108 protein
WD repeat and FYVE domain containing 3 (predicted)
CDP-diacylglycerol synthase 1
NK6 transcription factor related, locus 1 (Drosophila)
similar to ribosomal protein L36
similar to SET protein (Phosphatase 2A inhibitor I2PP2A) (I-2PP2A) (Template-activating factor I) (TAF-I) (Liver regeneration-related protein LRRGR00002)
similar to hypothetical protein 4933408F15

Gene Description
similar to RIKEN cDNA 3830405G04
mitochondrial ribosomal protein S18C (predicted)
similar to DNA helicase HEL308
similar to 60S ribosomal protein L7a (Surfeit locus protein 3)
similar to peptidylprolyl isomerase D
heparanase
similar to 2310002F18Rik protein
placenta-specific 8 (predicted)
COP9 (constitutive photomorphogenic) homolog, subunit 4 (Arabidopsis thaliana)
similar to hypothetical protein
SEC31-like 1 (S. cerevisiae)
similar to RIKEN cDNA 2610318G18 (predicted)
hypothetical protein LOC681153
similar to RIKEN cDNA 2310057D15
heterogeneous nuclear ribonucleoprotein D-like
heterogeneous nuclear ribonucleoprotein D
similar to ASF1 anti-silencing function 1 homolog A
similar to ribosomal protein S17 (predicted)
similar to ribosomal protein L21
similar to 40S ribosomal protein SA (p40) (34/67 kDa laminin receptor) (predicted)
similar to Elongation factor 2 (EF-2)
hypothetical protein LOC685087
hypothetical protein LOC685100
protein kinase, cGMP-dependent, type II
bone morphogenetic protein 3
similar to CG8138-PA
similar to glyceraldehyde-3-phosphate dehydrogenase
fibroblast growth factor 5
PR domain containing 8 (predicted)
similar to Antxr2 protein
glucokinase activity, related sequence 2
similar to MGC10646 protein
similar to 40S ribosomal protein S19 (predicted)
similar to SPANX-N2 protein
progestin and adipoQ receptor family member III
BMP-2 inducible kinase
annexin A3

Gene Description
Fraser syndrome 1 homolog (human) (predicted)
mitochondrial ribosomal protein L1 (predicted)
CCR4-NOT transcription complex, subunit 6-like (predicted)
similar to Small inducible cytokine B13 precursor (CXCL13) (B lymphocyte chemoattractant) (CXC chemokine BLC)
similar to DNA segment, Chr 5, ERATO Doi 577, expressed (predicted)
similar to DNA segment, Chr 5, ERATO Doi 577, expressed (predicted)
similar to PRAME family member 8
similar to CDNA sequence BC061212 (predicted)
similar to NEDD4-binding protein 1 (N4BP1)
similar to PRAME family member DJ1198H6.2
similar to PRAME family member DJ1198H6.2
similar to PRAME family member 1
similar to PRAME family member 3
similar to DNA segment, Chr 5, ERATO Doi 577, expressed (predicted)
similar to DNA segment, Chr 5, ERATO Doi 577, expressed (predicted)
similar to CDNA sequence BC061212 (predicted)
similar to DNA segment, Chr 5, ERATO Doi 577, expressed (predicted)
similar to preferentially expressed antigen in melanoma
similar to PRAME family member 9
similar to DNA segment, Chr 5, ERATO Doi 577, expressed (predicted)
similar to homolog of yeast ribosome biogenesis regulatory protein RRS1 (predicted)
similar to PRAME family member DJ1198H6.2
similar to DNA segment, Chr 5, ERATO Doi 577, expressed (predicted)
similar to DNA segment, Chr 5, ERATO Doi 577, expressed (predicted)
similar to CDNA sequence BC061212
similar to DNA segment, Chr 5, ERATO Doi 577, expressed (predicted)
similar to PRAME family member 8
similar to DNA segment, Chr 5, ERATO Doi 577, expressed (predicted)
similar to CDNA sequence BC061212 (predicted)
cyclin G2 (predicted)

Gene Description
cyclin I (predicted)
septin 6 (predicted)
hypothetical LOC289501 (predicted)
similar to PDZ domain actin binding protein Shroom
similar to 60S ribosomal protein L12
similar to RIKEN cDNA 4932413O14 gene (predicted)
similar to genethonin 1
hypothetical protein LOC686140
similar to TSH receptor suppressor element-binding protein-1; TSEP-1 (predicted)
scavenger receptor class B, member 2
nucleoporin 54
ADP-ribosyltransferase 3
chemokine (C-X-C motif) ligand 11
chemokine (C-X-C motif) ligand 10
chemokine (C-X-C motif) ligand 9
SDA1 domain containing 1
N-acylsphingosine amidohydrolase (acid ceramidase)-like (predicted)
protein phosphatase, EF hand calcium-binding domain 2 (predicted)
vesicle docking protein
similar to Late endosomal/lysosomal Mp1-interacting protein (p14)
similar to RNA-binding protein isoform G3BP-2a
cyclin-dependent kinase-like 2 (CDC2-related kinase)
THAP domain containing 6 (predicted)
ring finger and CHY zinc finger domain containing 1
similar to ribosomal protein L21
similar to PRAME family member DJ1198H6.2
castration induced prostatic apoptosis-related protein 1
betacellulin
amphiregulin
epiregulin
hypothetical protein LOC688741
similar to Epigen protein (predicted)
similar to methylenetetrahydrofolate dehydrogenase (NAD) (EC 1.5.1.15) / methenyltetrahydrofolate cyclohydrolase (EC 3.5.4.9) precursor - mouse (predicted)
chemokine (C-X-C motif) ligand 2

Gene Description
chemokine (C-X-C motif) ligand 1
similar to Eno1 protein
gene model 1960, (NCBI)
hypothetical protein LOC688833
chemokine (C-X-C motif) ligand 4
chemokine (C-X-C motif) ligand 7
chemokine (C-X-C motif) ligand 5
similar to Ras association (RalGDS/AF-6) domain family 6
similar to alpha-fetoprotein
afamin
alpha-fetoprotein
albumin
similar to 60S ribosomal protein L8
similar to ankyrin repeat domain protein 17 isoform b (predicted)
similar to hypothetical protein FLJ38991 (predicted)
hypothetical protein LOC689097
a disintegrin-like and metalloprotease (reprolysin type) with thrombospondin type 1 motif, 3 (predicted)
neuropeptide FF receptor 2
group specific component
LRRGT00190
solute carrier family 4, member 4
deoxycytidine kinase
MOB1, Mps One Binder kinase activator-like 1A (yeast) (predicted)
G-rich RNA sequence binding factor 1
rap2 interacting protein x
charged amino acid rich leucine zipper 1
similar to microsomal glutathione S-transferase 3 (predicted)
immunoglobulin joining chain
enamelin (predicted)
ameloblastin
similar to Protein UNQ689/PRO1329 homolog precursor
mucin 10, submandibular gland salivary mucin
variable coding sequence A1
variable coding sequence A2
PR-Vbeta1
similar to peptidylprolyl isomerase D

Gene Description
RSD-6
casein kappa
follicular dendritic cell secreted
APIN precursor
similar to zinc finger DAZ interacting protein 1
hypothetical LOC289530 (predicted)
casein delta
casein gamma
hypothetical protein LOC689604
casein beta
casein alpha s1
similar to ribosomal protein L30 (predicted)
hypothetical protein LOC689650
sulfotransferase, estrogen preferring
estrogen sulfotransferase
sulfotransferase family 1D, member 1
sulfotransferase family 1B, member 1
UDP glucuronosyltransferase 2 family, polypeptide A1
UDP glucuronosyltransferase 2 family, polypeptide A3 (predicted)
UDP glycosyltransferase 2 family, polypeptide B
similar to UDP glucuronosyltransferase 2 family, polypeptide A3
similar to T-cell activation kelch repeat protein
similar to UDP-glucuronosyltransferase 2B2 precursor (UDPGT) (3-hydroxyandrogen specific) (UDPGTr-4) (RLUG23)
similar to UDP-glucuronosyltransferase 2B3 precursor (UDPGT) (Testosterone, dihydrotestosterone, and beta-estradiol specific) (17-beta-hydroxysteroid specific) (UDPGTr-3) (RLUG38)
UDP glycosyltransferase 2 family, member 3
UDP-glucuronosyltransferase 2 family, member 5
UDP glycosyltransferase 2 family, polypeptide B4
UDP-glucuronosyltransferase
similar to UDP-glucuronosyltransferase
similar to heterogeneous nuclear ribonucleoprotein A3 (predicted)
liver UDP-glucuronosyltransferase, phenobarbital-inducible form
similar to UDP-glucuronosyltransferase 2B1 precursor,

Gene Description
microsomal (UDPGTR-2) (predicted)
similar to Rho GTPase activating protein 11A
similar to heat shock protein 1, alpha
UDP glycosyltransferase 2 family, polypeptide B10 (predicted)
similar to Expressed sequence AI788959 (predicted)
splicing factor Y1521-B
transmembrane protease, serine 11e (predicted)
similar to 60S ribosomal protein L23a
airway trypsin-like 5
similar to RIKEN cDNA 4732406D01 gene (predicted)
similar to RIKEN cDNA 9930032O22 gene
transmembrane protease, serine 11d
airway trypsin-like 3
gonadotropin releasing hormone receptor
similar to RIKEN cDNA 5730469D23 (predicted)
similar to stem cell adaptor protein STAP-1
centromere protein C 1
similar to bactin2
similar to Phosphoglycerate kinase 1
similar to 60S ribosomal protein L9 (predicted)
EphA5
steroid 5 alpha-reductase 2-like 2 (predicted)
hypothetical protein LOC690095
similar to Ferritin light chain 1 (Ferritin L subunit 1)
latrophilin 3
similar to Importin 7 (Imp7) (Ran-binding protein 7) (RanBP7)
similar to RIKEN cDNA 5730434I03 gene (predicted)
insulin-like growth factor binding protein 7
similar to RAN guanine nucleotide release factor
polymerase (RNA) II (DNA directed) polypeptide B (predicted)
MMR_HSR1 domain containing protein RGD1359460
RE1-silencing transcription factor
similar to D1Ertd622e protein (predicted)
serine protease inhibitor, Kazal type 2
similar to 40S ribosomal protein S2
homeobox only domain
similar to testicular haploid expressed gene product isoform 2
ADP-ribosylation factor-like 9

Gene Description
similar to signal recognition particle,72 kDa subunit
phosphoribosylaminoimidazole carboxylase, phosphoribosylaminoribosylaminoimidazole succinocarboxamide synthetase
phosphoribosyl pyrophosphate amidotransferase
similar to 2-aminoadipic 6-semialdehyde dehydrogenase (predicted)
hypothetical LOC289568 (predicted)
similar to KIAA0635 gene product (predicted)
SEC3-like 1 (S. cerevisiae)
hypothetical protein LOC679526
neuromedin U
similar to phosducin-like 2 (predicted)
clock homolog (mouse)
TPA regulated locus
similar to SRD5A2L
hypothetical gene supported by NM_053330 (predicted)
v-kit Hardy-Zuckerman 4 feline sarcoma viral oncogene homolog
similar to CG1249-PA
platelet derived growth factor receptor, alpha polypeptide
genomic screened homeo box 2 (predicted)
cysteine-rich hydrophobic domain 2 (predicted)
similar to keratin associated protein 10-7
ligand of numb-protein X 1 (predicted)
FIP1 like 1 (S. cerevisiae)
similar to Sec1 family domain containing protein 2 (Syntaxin binding protein 1-like 1) (Neuronal Sec1)
RAS-like family 11 member B
similar to ubiquitin specific protease 46 (predicted)
similar to WW domain binding protein 11
hypothetical protein LOC680197
spermatogenesis associated 18
similar to Beta-sarcoglycan (Beta-SG) (43 kDa dystrophin-associated glycoprotein) (43DAG)
similar to hypothetical protein MGC38937
DCN1, defective in cullin neddylation 1, domain containing 4 (S. cerevisiae) (predicted)
similar to RIKEN cDNA C130090K23 (predicted)
OCIA domain containing 1

Gene Description
similar to 2510002A14Rik protein (predicted)
zygote arrest 1
solute carrier family 10 (sodium/bile acid cotransporter family), member 4
similar to RIKEN cDNA 5033405K12 (predicted)
similar to Phospholipid hydroperoxide glutathione peroxidase, mitochondrial precursor (PHGPx) (GPX-4)
tec protein tyrosine kinase
TXK tyrosine kinase
NIPA-like domain containing 1 (predicted)
cyclic nucleotide gated channel alpha 1
similar to nuclear transcription factor, X-box binding-like 1
corin
similar to Acidic leucine-rich nuclear phosphoprotein 32 family member A (Leucine-rich acidic nuclear protein)
similar to synaptonemal complex central element protein 2
similar to type IV putative aminophospholipid transporting ATPase
similar to 40S ribosomal protein S2
similar to myosin, light polypeptide 6, alkali, smooth muscle and non-muscle
COMM domain containing 8 (predicted)
gamma-aminobutyric acid (GABA-A) receptor, subunit beta 1
olfactory receptor pseudogene 1604
gamma-aminobutyric acid (GABA-A) receptor, subunit alpha 4
similar to Gamma-aminobutyric-acid receptor alpha-2 subunit precursor (GABA(A) receptor)
similar to 60S ribosomal protein L7a
gamma-aminobutyric acid A receptor, gamma 1
hypothetical protein LOC680769
glucosamine-6-phosphate deaminase 2 (predicted)
similar to expressed sequence AA407526 isoform a (predicted)
similar to YIP1B (predicted)
potassium channel tetramerisation domain containing 8 (predicted)
similar to 60 kDa heat shock protein, mitochondrial precursor (Hsp60) (60 kDa chaperonin) (CPN60) (Heat shock protein 60) (HSP-60) (Mitochondrial matrix protein P1) (HSP-65)
similar to Ab2-076 (predicted)
similar to acetyl-Coenzyme A acetyltransferase 2

Gene Description
similar to Ac1591
similar to 60 kDa heat shock protein, mitochondrial precursor (Hsp60) (60 kDa chaperonin) (CPN60) (Heat shock protein 60) (HSP-60) (Mitochondrial matrix protein P1) (HSP-65)
similar to CG12206-PA, isoform A (predicted)
ATPase, aminophospholipid transporter (APLT), class I, type 8A, member 1 (predicted)
similar to MGC68837 protein (predicted)
hypothetical protein LOC680948
similar to Glyceraldehyde-3-phosphate dehydrogenase (GAPDH)
hypothetical protein LOC680994
hypothetical protein LOC681008
similar to glyceraldehyde-3-phosphate dehydrogenase
similar to solute carrier family 30 (zinc transporter), member 9
transmembrane protein 33
paired-like homeobox 2b (predicted)
similar to hypothetical protein (predicted)
ubiquitin carboxy-terminal hydrolase L1
hypothetical protein LOC681146
similar to amyloid beta (A4) precursor protein-binding, family B, member 2 (predicted)
similar to NOL1R protein; Williams-Beuren syndrome critical region protein 20
hypothetical protein LOC681183
similar to ribosomal protein S23 (predicted)
hypothetical RNA binding protein RGD1359713
cholinergic receptor, nicotinic, alpha polypeptide 9
similar to RIKEN cDNA 2410004L22
ras homolog gene family, member H
similar to mKIAA1413 protein (predicted)
similar to KIAA0648 protein (predicted)
similar to ribosomal protein L14
huntingtin interacting protein 2 (predicted)
similar to RIKEN cDNA 1110003E01
UDP-glucose dehydrogenase
lipoic acid synthetase
ribosomal protein L9
klotho beta (predicted)
replication factor C 1

Gene Description
WD repeat domain 19 (predicted)
similar to Heterogeneous nuclear ribonucleoprotein A1 (Helix-destabilizing protein) (Single-strand RNA-binding protein) (hnRNP core protein A1) (HDP)
similar to Mitochondrial carrier triple repeat 1 (predicted)
kelch-like 5 (Drosophila)
hypothetical protein LOC498365
similar to RIKEN cDNA 9130005N14 (predicted)
toll-like receptor 6
toll-like receptor 10 (predicted)
Kruppel-like factor 3 (basic) (mapped)
hypothetical protein LOC685077
similar to 60S ribosomal protein L29 (P23) (predicted)
hypothetical protein LOC685112
TBC1 domain family, member 1 (predicted)
similar to H3 histone, family 3B
hypothetical protein LOC685134
phosphoglucomutase 1 (predicted)
similar to serine/threonine/tyrosine interacting protein
similar to 3110047P20Rik protein (predicted)
similar to RIKEN cDNA 0610040J01
similar to expressed sequence AA536743 (predicted)
similar to nidogen-2
similar to membrane protein NBR1
similar to glyceraldehyde-3-phosphate dehydrogenase (phosphorylating) (EC 1.2.1.12) - mouse
mitochondrial carrier triple repeat 2 (predicted)
similar to CG17293-PA
similar to CG17293-PA
similar to type I interferon receptor beta chain-associated
similar to lin-9 homolog
similar to Reticulocalbin-1 precursor
similar to reticulocalbin
similar to similar to RIKEN cDNA 4930555G01
similar to cDNA sequence AY358078 (predicted)
similar to reticulocalbin
similar to RIKEN cDNA 4930555G01
similar to Discs large homolog 5 (Placenta and prostate DLG) (Discs large protein P-dlg)
hypothetical protein LOC685573

Gene Description
hypothetical protein LOC685598
hypothetical protein LOC685615

APPENDIX IV

Body weights (g) as genotyped

	WW	WS	SS
D14Wox14	362.9±6.7g	360.48±5.58g	356.48±13.4g
D14Got33	363.9±6.32g	359.76±10.06g	344.25±6.79g

Taqman output – β-actin gene and GAPDH gene

Strain	β-actin (CT)	GAPDH (CT)
WKY	21.2593	17.3142
WKY	20.6447	17.2603
WKY	21.6301	17.2321
WKY	22.0733	17.7561
WKY	20.5314	17.1643
WKY	21.5487	17.8546
SHRSP	22.0050	17.1953
SHRSP	23.0103	17.1898
SHRSP	20.6415	17.2227
SHRSP	23.3812	17.2333
SHRSP	22.4896	17.1989
SHRSP	23.7895	17.3246

WKY CT Values for *Dbp* in Aorta

Dbp (CT)	GAPDH (CT)	*Dbp* (CT)	GAPDH (CT)
16 weeks		21 weeks	
38.5539	16.5392	37.1875	16.8403
34.2732	16.7670	36.9845	16.8254
37.7171	16.9213	37.2898	16.8351
33.7612	16.5486	35.0097	16.417
38.1302	16.8108	36.2345	16.6781
34.3274	16.5915	35.9987	16.5354

APPENDIX V

Background Markers for Genotyping and Sequencing

Tm °C	Marker	Size (bp)	Left	Right
50	D1Mit3	120	ACTTGGTGAAGAAGAG TCAGGG	GATTTACTGTGCCTGTGG TTTT
50	D8Mgh1	153	TTGTCTGTAAGTATGCA CATGTGG	GATGAGCAGGGGCATGTC
50	D8Wox16	208	GAAGGGTACAGTCTGG GAAAG	AAGGCTCCTACTCCAGGT CTA
50	D8Wox3	150	AAGGCAGCTTGTAAGC CTGGG	GCTCATTCTGGTGCAAAA CGC
50	D9Wox13	278	CCTTTGCGGGGTGTTGT A	ACCAACAATGCGACAGA GAAT
50	D12Wox1	401	GACATTAAGGGGTCTTC CTAAG	TATCTTTGCAACGCTGAG G
52	D1Mgh18	111	ATTTACAAACAGGGAA GAAAGTGT	CCAATTCTTCCCAAGAAT AGTCC
52	D1Wox37	146	TAGTGGGGACAATGCT ATCTC	ACTCAGATGTATAATTGA CTGACTG
52	D1Wox4	160	TTCGGACTCAGTCTTGA TTTGG	GCCTTCCTAGAATACTTG GT
52	D5Rat4	152	TCTGAGCATTGAGGGTT ATTGTT	AACACAAGACCTCAGGA GCG
52	D7Mit11	92	TCAAACAATACATGTA CGTGCC	ACAATGGAGTCTCCTTTT ATGC
52	D7Rat141	117	TCCACCCTTAGAAAGC ACAGA	CTGCTTTTCTGGGAGACT GG
52	D7Wox27	189	TGTAGGTATACATGCTA TACACCG	CATACTCCTCATCACCTA AGATAG
52	D9Wox15	194	TTATACCTCCAAGAGAT GAAGG	ACCAGTAGTATCTGTGCA GTTG
54	D18Wox3	226	GTATCTGATGCCCTCTT CTGG	CAAGTTTCTCTGGATGTT CTTC
55	D1Mgh19	166	TGTGCTGTTCATAACCC CAA	TGGTGGAGACAGAGATGC TG
55	D1Mit11	275	ATAAGCCAGCCCCCATT C	CCTACTGAAAGTGAAATG TCTGG

Tm °C	Marker	Size (bp)	Left	Right
55	D1Rat97	157	TTCTCCCCTTTTCAGTCCCT	AGGGGATTAGAAGCCTCTGC
55	D1Wox14	206	TGAGCCTGGGCACTATGTAG	GGACAGGGACTGGAATCATC
55	D1Wox21	104	GACATGGTGAGTGAAGACCC	TGAGGCTATCCTGAGCTAACTC
55	D4Mgh15	145	CCCTTCCTCAAGATTGTTTCC	CTCCTACAAGTGGTTCTTTGACC
55	D4Mit2	215	TTCTGTATTAACCACAGAAAGAAGC	AAGCCAGCCCAAAGTAAATG
55	D4Mit9	97	CAGGAATGGGACCCAAAAAT	GAGCAAGTGACTAGCTCTGG
55	D4Wox1	105	GATAGGTGGATATATGACAGACAG	GCTGTGCTCATTTATCTGCC
55	D4Wox16	189	TCACGTGTGTTCTCAAGATCC	TCATCGCCATGTTCAACTATTG
55	D4Wox17	149	CCCTCTAAGGTCAGCAAGGT	TCAGGAAACCTGTTCTTGAGATA
55	D4Wox21	138	AGGGAGTGGCAGCATTTAG	GAGATAGTTCAGAAGAAACCCATG
55	D5Got43	150	CCCTTCTACAGTGACTCATATTTGC	GGGCGCAATTAGTACTCTGATTT
55	D5Got73		CGATCTAAGACACACATGTGCAT	TTCAGTGTTTGCTCACAAGGA
55	D5Got79	175	GGAAGGAGACAGAAACTCCGA	CTCGCTTGTAGTGTCAGAACTGG
55	D5Got86	215	TGAGCCTTTCTCAGGGTCAT	AAAATTCAGCATGGGGACAG
55	D5Mgh15	159	CACCTCGACCAACACCAAC	TTAATCCCAACTGTGACATTCG
55	D5Mgh16	133	GCATACAGCTTTACAGTGCTGC	AGACAAGGGACATGCTCGAG
55	D5Mgh6	155	CTCACAAAACTTGACTGAAATTGC	TCAAGATGCTATGGAAAAGCC
55	D5Mit2	201	TCTGCATTGAAACTAATCTAAATCC	TTGCACACATTGGAATGTCA
55	D5Mit9	127	CTACTGGCCGTAGTGTTTGC	CCACTGTGGTTGCTGTTCAG
55	D5Rat229		TGTGCACACGTACCTGAACA	CCATGATTACCTTTCACCCG
55	D5Uia4	250	TTCCCTAAGAGCAGGTGATATG	AGCTACATGGTAAGGCTCTGTC
55	D5Uia6	246	TTCCCTAAGAGCAGGTGATATG	CATGGTAAAGGCTCTGTCTGA

Tm °C	Marker	Size (bp)	Left	Right
55	D5Wox14	227	TGGGTAGGTCGTGTCTTCTC	CCTGGTTAGAGGAGGGAGTC
55	D5Wox15		GGTAGAGGTGAGTGGAATGAA	CCTCCTCAGCTCTGCTAGTC
55	D5Wox16	154-160	CAGCCTTCATTCTCACAC	TGACTTCTGTGAGCTCCTAC
55	D5Wox4	157	CCTGCTGTTTCTGACTCCC	AGCATCCAAGACTGGGTGC
55	D5Wox7	169	TTGGTGGTGCTGCATCTATTG	CTTAAGGCAATATAGGAAACTAC
55	D7Mit7	260	ACAGCTGGAATCCTCTGGG	GAGCTAGCCATGCAGGAAAC
55	D8Mgh4	152	GAGTTAACCCAACAACTCTAAGCC	CCCAAATGCAGCAGTCTACA
55	D8Mgh6	150	CAACTCCTGCAGGTTGTCCT	CCAGCAGCTACCTCTTCCAG
55	D8Wox22	181	GCAGTGTGAGAGGAAAGTGTC	GAAGTCCTCACCTGTGTTCAG
55	D8Wox5	252	GAGATGGAGAAACAGGGACC	TCTTCCTGGAATCAATGTGG
55	D9Mit4	204	GCATAATGGAAGAAGACAACTACC	TCCATGCATGTGTATCTGCA
55	D11Rat31	153	ACTCACTCAACTCTACCATCAAAA	AGAAAGGAGGGGGTTGTTGT
55	D12Mit3	154	GTGTGCCATATATACATGCATGC	CTGAGACATAATATTTTCCCCCC
55	D12Wox2	194	TAACCTCCAAAGGACCTCTC	CTAGATAAGGTGTATGTGGCTC
55	D17Mit5	290	TCCCTTGGTTTATTTTGCCA	CCTCCTCGTGCTGGAAGTAG
55	D17Wox5	104	TCATCCAGTTGAGCAGGAAGC	AGAGTCTGGTAAAGTGGTGTG
55	D17Wox7		CAAGGGAGTAGGTGTGCCTA	TGCATCAGTGCTTACTGTGG
55	D18Mit8	146	AAAGCCAAGGTCTTAACTGAAGC	TCGACCACACACCTCCCT
55	D19Wox1	127	CCTTTCTTTGGGGAAAAAGC	CTGACATGCATCTGCTATATGG
55	D19Wox12	127	GCAAGAGGCTTACATAATAGCA	AGCCAGCTAATGTGTCAAGTG
55	D20Wox6	144	ACGCAAATCAAACCAGCC	CATCCCCATCTTCGTCCAG
56	D5Rat95	160	GGAACCTGCACAATCATGTG	CCATCTACTCCAGTCCTTGGTT

Tm °C	Marker	Size (bp)	Left	Right
58	D1Wox17	81	AGGAAAAGCATATAGAACACGC	TTTACTTACTAGGGCATGGGAT
58	D1Wox2	123	ATTGTATATTCCAGACTAGC	AATTGATGTGACATTATTTTCATTG
58	D1Wox34	140	GCGATTATATTGTCACCTTCC	GGTAATCAGGCGCTCTCC
58	D6Mgh5	106	ATAGGAATAAAGAGTGCACGTTTG	CAGTTAGCATAGAAAGCAAAGGG
58	D6Wox13	271	TTCTGATGGCTAAGCTGTTG	GCTCCACCCTGCAAGTAC
58	D7Mit10	171	TGCCCCAAAAAGGAAAAAC	TCAGCTTCATACGGAAGCAA
58	D8Got151	263	ACAAAAAGATGAAAGGTTGGC	GAAGGCCACTGGTCTCTGTTAC
58	D9Wox21	136	CGGAAAGGGAATAACAATCG	CACGAGCATGGTGCATACAC
58	D19Mit2	200	AAGGTTGGCAGTTTCCCAG	ACCATTTATGTGCCCAGATG
60	D1Wox20	118	CAAGGACTGAGTGCATGCTC	TTCTCTCTTGCTAGCTGCCA
60	D4Mgh17	132	CTCAAGCCTCAGGCATCTG	AAGGACGTTATCCATTTTGGG
60	D4Mit14	150	AGGACAGGTTTTTGGGCTTT	TCTGCCGCCACCTTAGAG
60	D6Mit3	111	TCATCCCAGGCCATAAAGAG	ACGGTCACACAGTGGCCT
60	D7Mgh9	126	AGCAAAGCAAGTTAGCAGATCC	AATTTTAAGGAAAGAGGCCTGG
60	D7Mit1	182	ACCTCAGGTCCCAGGAGTG	AGGTAAGCCAGTGGATGCTT
60	D7Wox1	80	GTAGAAGGTTCTGCAAAACATGC	GGGTCCCAACTGCATCAGCC
60	D8Mgh10	142	CTTTGATACTGTACCAACAGCACC	AATGTCAGGATGGCAGAGAC
60	D8Wox2	158	GCACACACACCCCCTTCAC	CATGGATTTGATTCCTGGAC
60	D9Wox2	162	CTCCTGCCTGGGTAACCTG	CCTCTTCTGGGCTTCTTAGG
60	D10Wox26	170	CTTGTATTGACACCCATGTGC	GGATGCAAAGCATATCCTGAG
60	D13Mgh1	147	CACTTCCCAAATGCTAGCGT	AGAGAAAATATGTGGACAGAAGCC
60	D13Mgh6	112	CACACTGGTTCATCCACAGG	GAAGCAGGTGATCCTAGAGTGA

Tm °C	Marker	Size (bp)	Left	Right
60	D15Mgh6	216	AGCAGCGGTATCTCCA GTGT	GGGTGACGGAGACAGAG AAA
60	D16Mgh1	237	GACCTCCAGGATTGGT GAGA	ACAACCCATGAGGCAGAC AG
60	D16Mgh2	151	TCATTTCTGCTTCTTTCC TATGG	CTGCAGGAAGGAAAGCA AAC
60	D16Wox15	171	CGGCTCAGAGTTACTA AATAGGT	TTACCAATACAAGTGCGA GTTT
60	D16Wox4	100	GCCAAGGCTACATAAT GATACCC	CACACTCCCATTCAGCCC CTC
60	D17Mit3	186	TAAGGTCCCTCCAGACT CCA	TGGGCAGAGAACAGCAG TC
60	D17Wox10	147	ATCTGTGTGCGAGTGCG T	CTGGCGAAGTGACGTGAG
60	D17Wox21	153	TAAGGACCCCTGATACT CTGG	AGATCTTTGTCAAATTCA TGGC
60	D18Mgh4	120-210	CCTAGGCAGTAGTTACC ATGTGC	TGTTTCTGTTGCCCTCGAG
60	D18Wox1	101	CAAACAATTCTAAAAC AAAAAGTG	CACCTACTACTGACGGCA GG
60	D20Mgh1	136	CTCTCCCTTCAGTCCCA TTG	TCCTAGAGCCCCTTTTCA CA
60	D20Wox8	132	GATGAGTCTCTCCCCAG CC	GTCTAGCCTGGGCAACCT TC
60	DXMit4	188	ACTCCAACACCCAGTC AACC	GCCAAAGCATCTCCCTAT CA
61	D6Got131	220	TGGTGGCTCACAACAG ACAG	CCAGTCATACTGCATCTG CAATA
62	D19Rat4	360	GATTCCAGGTTGTGGCA AGT	ATGCATGCATGGAGTTTG TG
64	D13Mgh4	143	CATATTTCCCCCAATCC TGT	CGGATCTCCATATGTACT TGTACA
62	D1Mit14	112	TTCCATCTACTGCTGTT TAGGG	TCTGCCTTCTCACATGAA CA
58	D1Wox27	150	CTGATTACCAGGTCACC TTAAG	TCTAACAGCTGTAGCAAC TGG
52	D4Mgh16	259	CAGGAGCTGTCTGGGA CTTC	GAACACTAGAGAAACTA GGCAGGC
55	D6Mit4	225	TCACAAGTTTGTGTGCC TGA	AAAGCAAGTTTTAGGATA GCAGG
56	D6Wox21	120	TTGAGAAGCGTTAAAA TATGTG	TTGGTTTCCAGGGTGAGA A
60	D7Wox2	180	TGTGGCAAGTACATAC ATCCC	CTCTACCTGCCTGGTCTA GC

Tm °C	Marker	Size (bp)	Left	Right
60	D9Mit1	130	ACAACTCCCATCTCTTG AGAGG	GCTTTCAAACACCACAGG GT
60	D10Mgh11	140	GGTGTAGGTTCGTCTGT CAGG	CGGTGCTCATAAAAGGGA AA
59	D10Wox2	192	CTTGGATGAAGAAGTC TCCAC	CAAAGACCCTTTTGAGAG AAC
54	D10Wox3	176	GAAGTCTTCACTTTTAC TTGTGG	GACCCTTTTGAGAGAACT TTTG
61	D11Mgh6	100	AACAGTCAAAAGAGAT ATCCAGGG	AAACAAATGATGTACATG CATACA
59	D11Rat17	150	GCATATGGGAGTTTTGC CTG	CCAGTTGCAGATGATTTC CA
54	D12Mgh3	124	GGATTGAGGGTGGGGT AAGT	TTCAACAACCACCTCACT TCC
54	D15Mgh2	148	TTCAGATTAGTATAGGC AGGGTCC	GAGACCCTCAACCTGTGC AT
52	D15Mgh3	146	AGACCCAGGGTAGGCA TTTT	GATTACAATTCTGTCCAA GTCACG
56	D16Wox1	103-122	CCTGGGAATTTCATTCT TGG	AGCTGTCCTCTGACCTTC ACA
57	D16Wox12	131	GCCACACTTGGTGATCT AGC	TATTGTCTGGGTTTGCTCT CT
58	D17Wox13	134	AGTAGACAGGAGTGGG AAGGA	CTCTTTGGGCAGCTTACA TT
59	D17Wox20	185	ATAATCCAATCAGGGC TTAAC	AGACACATTCACTTCCAG GTC
62	D18Wox18	149	CCAGAACGATTACCCTC ACC	CCTCAGGACCAGACACTA CG
60	D19Mit5	97	TGAGCCCTAGGTTCAAC ACC	ACAAAAGCTGCTAGGTTT GAGG
60	DXMit5	215	TGCTCACTTCACAACTG GCT	CCTTCTCCAAAGCACCAA AA
60	D13Mgh3	120	TGGGAACATCCATATC ATTCA	TGAGCCATTTGCAAAGAG G
60	D4Wox24	194	ACCCTAAGGCTCTGTCT CAAA	CTTTGGATAGTAATGAGT GCTTTG
59	D8Wox21	324	TACCGTTATCAATGAAA GAGTCTA	GATCTGAATACTTATGTG CCCTC
58	D9Wox20	107	GCTGTTGTCCTCAAATT TTCTC	GGTCTCAGAAGGTATACC CATAG
54	D13Mgh16	140	TCACAGAGACCATGGA GCAG	GACCCTTATTCTCTCCCTC CC
54	D20Wox5	259	GAAAAATACTTCCACA CACTAATG	AAAGTCAAGCCCTGGAGT G

Tm °C	Marker	Size (bp)	Left	Right
57	D4Got12	170	ACATCAACCCCATTAG ATTTCA	AACCTCATCCTCATCCAA AAAG
57	D15Mit3	200	GACCTGACCTGTTGTGG GAT	GTTGCTCTCTGGCCTCCTC
52	D1Mgh5	155	CCTTTGCTCTGAGCCTG G	AGAGAAAAAGAAAAGGG AAAACG
55	D1Wox32	188	GCTACTGCCTTGCCCTC A	TCACATTTTACCTGTAGTT GGAA
55	D1mit1	146	GGGGAAGTTTTAGGAA GTCCC	AGGGAATGAAAATACAA CACGC
50	D4Mgh7	145	GATCCAGCTCACATCTA ATCCC	CCAAATGCTCTTGCAGTC AA
52	D7Mgh5	229	TCCCAACTCTCCCTTAC CG	TGTCTTGGAAGAAAGAAA GAAGG
55	D8Mgh7	191	TGAAGAGTTTTACTGGG TAGCTCC	TGGACCAGGCAAGTTCTC TT
55	D9mit3	156	TGAGACTTGTATTCACT CCTCCC	CTATCCCTGTCTCTGTGTC TACCA
55	D9wox18	178	GCCAGATATAAGATGA TTAGTCTG	CCACAGTCATTGAGTTAT TGGT
55	D13Wox4	180	CCTGGACACTAATCCTA TCTTG	GGGTAGGTCTGAGGGAA GG
55	D16wox10	118	AGGCTTTGATTGCAGG AAG	AAAGAGCTGTCGTCCACA AC
55	D16mit1	164	GGCTTGTGTGGACACCT GTA	AAAGAGCAGGGAAGAGA CAGG
55	D18wox12	148	CACATGTTTACTTTCTA AGCATTTG	CCCCTCTTCTGGACTTCAT AG
55	D18wox16	152	TCACAATAAAAAACTC CTCCAAC	AGTCTGTGCCCTGTTCCC A
55	D19Wox2	129	GGTATGGGAGTAACAT GACCTC	GGACACATACAGTAAGCA CATGC
55	D19wox8	111	TGCCCGTCTCTGTTACT CAT	CAAGAACCCTGAGGCAAT AA
55	D20wox3	125	AGGAAATGGGTTTCAG TTCC	CAGGATTCTGTGGCAATC TG
55	Dxwox3	130	GATCGTCCAGCATCGTG G	GTTGGTGCTACTCAAGAT CGG
56	D3Mit7	128	TTCGAGAATATGTGGCT GCA	GTTAGGGAACACCGGTGA GG
60	D3Rat128	127	ACTTGAGTTGATGGCTT GGC	AGAGGATGCCTCTGAAGC AA
60	D3Rat133	130	GATTGCAGAATGACTG GCAT	ACCCTTTGCCTCCATTCTC T

Tm °C	Marker	Size (bp)	Left	Right
52	D3Rat114	131	CTCAATGCCTGCATCTG AAG	CAGGTGTAGCCTTCTCAC ACA
60	D3Rat59	170	ATCCCAGCACTGCATA AACC	AGGATGTCAGGAACGCA GAT
58	D3Rat35	154	GTAAGTGGCTCCAGTTT GGG	CCTGGGTTCGATTCCTAA CA
54	D3Rat94	160	GCTCAGCATGCATCTTC TTG	CAGTCTAGGCAACTGAGA CACTG
56	D3Rat30	162	CCCCAATCTTCATCTAA CCC	TGGGAGCAGAAGAATCTC TCA
57	D3Mgh15	165	GAAAGCAATGGCATCC TGAT	TATTATTGTGTATTTTGGG CATGC
58	D3Mgh14	124	GAAAGCAATGGCATCC TGAT	TATTATTGTGTATTTTGGG CATGC
58	D3Got83	125	CTCGCACTAAGAGGGC ACTG	GATCCACAATACTCACAT GTGAAAT
60	D3Mit4	124	GCAAAGAGATGCACAT CTGG	AAAAAACCAACCCCCTTC C
60	D3Wox19	145	TTCTACTTGGGGATTTC TTGAT	ACTTTGACGTTGAATGGT TGA
60	D3Got125	156	TACCTGAAATGCCCACC CT	CTGCCTCAGAAAATAAGG TGGA
60	D3Got141	151	CTTTTTGGGAAAAGCA AAAAGC	TCGATCTTAGAGCACACC ATG
59	D3Got129	130	CCACAAAAAAAGCATCC AAACA	GGAGAGAATCTACCAACT GTTGC
59	D3Mgh5	178	AGCCATGACATTGTCTT CTGG	GAACTTTTTGAATGGGAT AAAGAA
57	D3Got132	147	CACAAAAAACGTCCCTTT CCT	GATCACTGCACTCGTGTA TTGTTC
55	D3Got120	156	GATCTTATCTGCCTCTT T	ATCTGAACTCCATTGACT ACG
55	D3Got121	154	GGCCCTGCCTCAGAAA ATAA	CCCACCCTTAGGTTTCTTG TGT
60	D3Got141	121	CTTTTTGGGAAAAGCA AAAAGC	TCGATCTTAGAGCACACC ATG

APPENDIX VI

Cited Cardiac mass QTL

Chr No.	Start Pos.	Stop Pos.	*QTL	Flanking markers	LOD score	P-value
1	135159025	176894238	QTL 23	D1Mgh9, D1Mit2	4.6	0.0004
1	181664764	263910134	QTL35	D1Rat155, D1Mgh14	5.7	
1	87443392	153756953	QTL 16	D1Rat189, D1Rat158	2.7	
1	103228034	37184	QTL 32	D1Rat29, D1Rat188	5.2	
1	103228034	37184	QTL 36	D1Rat29, D1Rat188	4.1	
1	103228034	37184	QTL 32	D1Rat29, D1Rat188	5.2	
1	209484615	239484615	QTL 7	D1Rat73, D1Rat92	5.32	0.0001
2	146178185	35064	QTL 29	D2Mgh15, D2Rat64	3.50	
2	77461812	156192873	QTL 22	D2Mit6, D2Mgh7	4.3	0.0008
2	24474448	163154228	QTL 38	D2Rat182, D2Rat40	2	
2	24474448	163154228	QTL 39	D2Rat182, D2Rat40	2.26	
2	24474448	212168914	QTL 41	D2Rat182, D2Rat55	2.73	
2	24474448	212168914	QTL 42	D2Rat182, D2Rat55	2.82	
2	105274088	170210328	QTL 14	D2Mgh26, Ecf1a2	2.1	
3	21353078	51353078	QTL 8	D3Mgh7	7.03	0.0001
3	1	19010302	QTL 10	D3Mgh9	7.34	0.0001
3	26674019	6373336	QTL 43	D3Mit9, D3Mgh16	6.6	2.9E-08
3	26674019	6373336	QTL 46	D3Mit9, D3Mgh16	5.4	5.5E-06
3	26674019	6373336	QTL 48	D3Mit9, D3Mgh16	4	0.0001
3	21197575	35034292	QTL 13	D3Rat100, D3Mco16	2.5	

Chr No.	Start Pos.	Stop Pos.	*QTL	Flanking markers	LOD score	P-value
3	103497433	133497433	QTL 17	D3Rat160	2	
3	58879349	87777490	QTL 25	D3Rat27, D3Rat38	4.8	0.0001
3	21353078	51353078	QTL 8	D8Rat120, D8Rat149	7.03	0.0001
4	129019956	159019956	QTL 18	D4Rat195	2.6	
5	135083701	165083701	QTL 24	D5Rat173, D5Wox10	3.5	
6			QTL 47	D6Mgh4, D6Mit4	2.9	0.001
7	47266045	107884993	QTL 6	D7Rat136, D7Arb16	4.09	
7	47985908	125333398	QTL 27	D7Rat9, D7Rat107	3.45	
7	105547152	108809845	QTL 1	D7UIA1, D7Mco1	2.7	
7	47266045	107884993	QTL 6	D6Mit5, D6Mgh6	4.09	
8	98905540	126436679	QTL 19	D8Rat130, D8Rat3	2.6	
8	57427796	58611955	QTL 3	D8Rat149, D8Rat36	3.97	
8	74716950	36003	QTL 2	D8Rat159, D8Rat14	3.65	
8	103174717	106194717	QTL 40	D8Rat164, D8Mgh3	1.89	
8	29565716	103691902	QTL 30	D8Rat51, D8Mgh15	3.77	
9	77170798	105579863	QTL 53	D9Mco6, D9Uia6	3.3	0.0001
9	3587583	37414784	QTL 4	D9Rat101, D9Rat26	3.55	
9	24732014	54732014	QTL 11	D9Rat125	3.1	0.00089
9	12522363	37414784	QTL 20	D9Rat36, D9Rat26	3.9	
9	21568480	77454334	QTL 28	D9Rat70, D9Uia6	7.3	
9	77254082	105889541	QTL 21	D9Uia6, D9Mco6	2.7	
10	29975240	10466	QTL 31	D10Mgh11, D10Mit1	3.8461	
10	29975240	10466	QTL 44	D10Mgh6, D10Mgh1	4.8	$3.7x10^{-5}$

Chr No.	Start Pos.	Stop Pos.	*QTL	Flanking markers	LOD score	P-value
10	56944071	34813	QTL 33	D10Rat156, D10Rat16	2.8	
10	53806591	83806591	QTL 51	D10Wox11, D10Wox6	3	
10	23806740	53806740	QTL 50	D10Wox3, D10Wox11	6.6	
10	23806740	53806740	QTL 44	D10Wox3, D10Wox11	4.8	3.7E-05
12	28893568	46007684	QTL 5	D12Mgh5, D12Rat22	3.78	
12	28893568	46007684	QTL 5	D13Wox6	3.78	
13	28893568	46007684	QTL 45	D13Wox6	3.6	0.002
13	28893568	46007684	QTL 45	D13Wox6	3.6	0.002
17	9988754	35473	QTL 34	D17Rat2, D17Rat58	8.7	
17	76740345	92705174	QTL 26	D17Rat39, D17Rat52	3.71	
17	65811231	81723321	QTL 15	D17Wox9, D17Rat44	6.5	
19	1	21799962	QTL 9	D19Rat18	4.27	0.0001
19	1	21799962	QTL 12	D19Rat18	3.33	0.00053
19	1	21799962	QTL 9	D19Rat18	4.27	0.0001

*QTL number is arbitrarily assigned by Rat Genome Database.